

DISS. ETH NO. 22827

**QTL MAPPING OF IMPORTANT AGRICULTURAL AND LIFE HISTORY TRAITS
IN THE PLANT PATHOGENIC FUNGUS *ZYMOSEPTORIA TRITICI***

A thesis submitted to attain the degree of

DOCTOR OF SCIENCES of ETH ZURICH

(Dr. sc. ETH Zurich)

presented by

MARK HENRY LENDENMANN

MSc ETH Agr, ETH Zurich

Born May 17th 1980

Citizen of Zurich (ZH)

accepted on the recommendation of

Prof. Bruce A. McDonald, examiner

Dr. Daniel Croll, co-examiner

Prof. Edward J. Louis, co-examiner

2015

TABLE OF CONTENTS

SUMMARY	1
<hr/>	
ZUSAMMENFASSUNG	3
<hr/>	
CHAPTER 1	7
<hr/>	
General Introduction	
<hr/>	
CHAPTER 2	27
<hr/>	
Quantitative Trait Locus Mapping of Melanization in the Plant Pathogenic Fungus <i>Zymoseptoria tritici</i>	
<hr/>	
CHAPTER 3	69
<hr/>	
QTL Mapping of Fungicide Sensitivity Reveals Novel Genes and Pleiotropy with Melanization in the Pathogen <i>Zymoseptoria tritici</i>	
<hr/>	
CHAPTER 4	115
<hr/>	
QTL Mapping of Temperature Sensitivity Reveals Candidate Genes for Thermal Adaptation and Growth Morphology in the Plant Pathogenic Fungus <i>Zymoseptoria tritici</i>	
<hr/>	
CHAPTER 5	155
<hr/>	
General Conclusions and Outlook	
<hr/>	
ACKNOWLEDGEMENTS	165
<hr/>	
PUBLICATIONS	167
<hr/>	
CURRICULUM VITAE	169
<hr/>	
APPENDIX	171
<hr/>	

SUMMARY

The aim of this PhD study was the identification of novel genes as well as natural genetic variance and its effect on phenotypic variance in quantitative traits in the fungus *Zymoseptoria tritici*. *Z. tritici* is a wheat pathogen found worldwide, able to cause serious yield losses. Establishing the connection between genetic variance and phenotypic variance in natural populations is of great importance within the field evolutionary biology, allowing for better understanding of the potential of a population to adapt to changing environments. To decipher the genetic architecture of the traits of interest we used quantitative trait locus (QTL) mapping. This technique had never been applied to *Z. tritici* previously. QTL mapping was carried out upon progeny of two crosses obtained from four parental strains. Parental strains had been collected in naturally infected wheat fields in 1999 in Switzerland. Each of the two crosses provided ~260 progeny, which were genotyped and phenotyped for all the traits. We focused on five important, yet genetically poorly understood agricultural and life history traits: colony melanization, growth rate at two different temperatures (15°C and 22°C), fungicide sensitivity, temperature sensitivity and yeast/hyphae dimorphism.

To genotype the progeny we used restriction site associated DNA sequencing (RADseq). Through the usage of RADseq, a high-throughput next generation sequencing (NGS) technique, progeny sequences could be collected at a relative low cost, spanning the majority of the IPO323 reference genome (~90%). RADseq had never been applied to *Z. tritici* previously. This technique allowed the construction of two highly dense, high quality genetic maps. Parental strain sequences were obtained through full genome sequencing. To phenotype all progeny and parental strains we developed a novel Petri dish assay based on digital image analysis. Digital images were analyzed by applying a novel batch macro, which had been designed during this PhD. The macro allowed high-throughput yet very precise measurement of size and grey value composition of single spore colonies growing on axenic cultures.

For three out of the five traits (growth rate, fungicide and temperature sensitivity) their quantitative nature had been established previously to this study, however their genetic architecture had either not been investigated so far (growth rate, temperature sensitivity) or was still poorly understood (fungicides sensitivity). For the traits of melanization and the yeast/hyphae dimorphism neither their quantitative nature nor their genetic architecture had been studied previously. Our results confirmed the quantitative nature of the traits of growth rate, fungicide and temperature sensitivity. We newly showed that also melanization as well as the yeast/hyphae

dimorphism are of a quantitative nature in *Z. tritici*. We could resolve the genetic architecture of all the quantitative traits as well as elucidate their complexity through the mapping of multiple QTLs for each trait. On average ~32% of total phenotypic variance was explained by an average of 2.7 significant QTLs per trait. For the trait of melanization we identified a total of 12 unique QTLs over both crosses, eight containing novel melanization genes. The high marker density of our genetic maps provided very narrow confidence intervals for four QTLs, with as little as only one candidate gene in one particular case. The QTL with the highest LOD score (~32) contained the *PKS1* gene beside three other candidate genes. *PKS1*, a polyketide synthase gene, is known to play a role in the synthesis of dihydroxynaphthalene (DHN) melanin. We consider this finding as a confirmation of the functionality of our methods applied. We could show that melanization has a highly complex genetic architecture in *Z. tritici*. For fungicide sensitivity we mapped a total of three QTLs. The three QTLs were positioned on chromosomes that differed from the chromosome containing the target gene of azole fungicides. Our findings imply that other genes apart from the fungicide target site are of importance in contributing to fungicide sensitivity in *Z. tritici*. Additionally our results suggest the usage of a novel fungicide mixture due to evidence for pleiotropy among melanization and fungicide sensitivity. QTL mapping of temperature sensitivity provided evidence of the high osmolarity glycerol (HOG) pathway being important in *Z. tritici* for thermal adaptation.

Overall we mapped novel genes not previously associated with the studied traits as well as novel genes not previously associated with natural phenotypic variance for the trait of fungicide sensitivity. We conclude, that *Z. tritici* has a high evolutionary potential and thus is able to adapt rapidly to changing environments through selection acting upon standing genetic variation. We believe that this work and the findings made during this PhD are of importance for future control strategies of *Z. tritici* but also of other fungal plant, as well as animal and human pathogens.

ZUSAMMENFASSUNG

Das Hauptthema dieser Doktorarbeit war die Identifikation neuer Gene, sowie natürlicher genetischer Varianz und ihr Effekt auf phänotypische Varianz in quantitativen Merkmalen des Pilzes *Zymoseptoria tritici*. Bei *Z. tritici* handelt es sich um ein global verbreitetes Weizenpathogen, welches zu erheblichen Ertragsausfällen führen kann. Die Verknüpfung zwischen genetischer Varianz und phänotypischer Varianz in natürlichen Populationen ist von grosser Bedeutung auf dem Gebiet der Evolutionsbiologie, da sie zu einem besserem Verständnis des Adaptionspotentials einer Population innerhalb wechselnder Umweltbedingungen beiträgt. Wir verwendeten Quantitative Trait Locus (QTL) Mapping, um die genetischen Architektur der Merkmale von Interesse zu entschlüsseln. Diese Technik wurde noch nie an *Z. tritici* angewendet. QTL Mapping wurde auf die Nachkommen zweier Kreuzungen von vier Elternstämmen, welche im Jahr 1999 in natürlich infizierten Weizenfeldern in der Schweiz gesammelt wurden, angewendet. Für beide Kreuzungen wurden rund 260 Nachkommen gesammelt, welche genotypisiert, sowie auch bezüglich allen Merkmalen phänotypisiert wurden. Insgesamt wurden fünf wichtige, aber bis anhin genetisch schlecht verstandene landwirtschaftliche und Life-History Merkmale untersucht: Koloniemelanisierung, Wachstumsrate unter zwei verschiedenen Temperaturen (15°C und 22°C), Fungizidsensitivität, Temperatursensitivität und die Hefe/Hyphe Dimorphie.

Restriction Site Associated DNA Sequencing (RADseq) wurde verwendet um die Nachkommen zu genotypisieren. Mittels RADseq, ein Hochdurchsatzverfahren von Sequenzierung der nächsten Generation (NGS), konnten Sequenzdaten der Nachkommen zu tiefen Kosten gesammelt werden, wobei die Sequenzen den Grossteil (~90%) des Referenzgenoms von IPO323 abdeckten. RADseq wurde nie zuvor auf *Z. tritici* angewendet. Die Methode erlaubte die Konstruktion von zwei dichten, genetischen Karten von hoher Qualität. Sequenzdaten der Elternstämmen wurde durch das Sequenzieren ihres kompletten Genoms erworben. Für das Phänotypisieren aller Nachkommen sowie der Eltern wurde eine neue Petrischalenmethode entwickelt, basierend auf der Analyse digitaler Bilder. Die digitalen Bilder wurden analysiert mittels eines Makros, welches mehrere Bilder durch Stapelverarbeitung analysiert und speziell im Rahmen dieses Doktorates kreiert wurde. Das Makro erlaubte, trotz Hochdurchsatzverfahrens, eine sehr genaue Messung in Bezug auf Grösse und Grauwerten von Einzelsporkolonien, welche in einem keimfreien Umfeld wuchsen.

Die quantitative Eigenschaft von drei der fünf Merkmale (Wachstumsrate, Fungizid- und Temperatursensitivität) wurde bereits in vorangehenden Studien aufgezeigt, jedoch wurde ihre genetische Architektur entweder bis anhin nicht erforscht (Wachstumsrate, Temperatursensitivität) oder sie war nur teilweise entschlüsselt (Fungizidsensitivität). Weder die quantitative Eigenschaft noch die genetische Architektur von Melanisierung sowie der Hefe/Hyphe Dimorphie wurde zuvor untersucht. Unsere Resultate bestätigten die quantitative Eigenschaft der Merkmale Wachstumsrate, Fungizid- und Temperatursensitivität. Wir konnten zudem aufzeigen, dass sowohl Melanisierung wie auch die Hefe/Hyphe Dimorphie Merkmale von quantitativer Natur in *Z. tritici* sind. Mittels der Kartierung mehrerer QTLs war es uns möglich die genetische Architektur aller quantitativen Merkmale zu entschlüsseln sowie ihre Komplexität aufzuzeigen. Im Durchschnitt erklärten 2.7 QTLs pro Merkmal ein Mittel von ~32% der gesamten phenotypischen Varianz. Für das Merkmal Melanisierung identifizierten wir über beide Kreuzungen insgesamt 12 QTLs, acht davon enthielten neue Melanisierungsgene. Für vier QTLs ergab die hohe Markerdichte unserer genetischen Karten sehr schmale Vertrauensintervalle mit nur einem Kandidatengen in einem der vier QTLs. Das QTL mit dem höchsten LOD Wert (~32) enthielt das Gen *PKS1* nebst drei anderen Kandidatengenen. *PKS1*, eine Polyketid-Synthase, spielt eine wichtige Rolle in der Synthese von Dihydroxynaphthalene (DHN) Melanin. Wir betrachteten dieses Ergebnis als Bestätigung der Funktionalität unserer angewendeten Methoden. Wir vermochten zudem aufzuzeigen, dass dem Merkmal Melanisierung eine komplexe genetische Architektur in *Z. tritici* unterliegt. Für das Merkmal Fungizidsensitivität wurden drei QTLs identifiziert. Die drei QTLs befanden sich auf Chromosomen, welche sich vom Chromosom mit dem Zielgen der Azolefungizide unterschieden. Unsere Ergebnisse zeigen auf, dass auch andere Gene als das Fungizidzielgen einen substantziellen Beitrag zur Fungizidsensitivität in *Z. tritici* beisteuern. Aufgrund eines Pleiotropienachweises zwischen Melanisierung und Fungizidsensitivität empfehlen wir die Anwendung einer neuartigen Fungizidmischung. QTL Mapping von Temperatursensitivität ergab den Hinweis der Involvierung des high osmolarity glycerol (HOG) Signalweges in *Z. tritici* bezüglich thermaler Adaptation.

Insgesamt kartierten wir neue Gene, welche nie zuvor mit dem untersuchten Merkmal assoziiert wurden, sowie neue Gene, welche nicht zuvor mit natürlicher phänotypischer Varianz von Fungizidsensitivität in Verbindung gebracht wurden. Daraus schlussfolgern wir, dass *Z. tritici* ein hohes Evolutionspotential hat und somit in der Lage ist sich schnell an eine verändernde Umwelt anzupassen, indem Selektion auf bestehende genetische Variation wirkt. Wir glauben, dass diese

Arbeit und die erzielten Ergebnisse dieses Doktorates wichtig für künftige Kontrollstrategien von *Z. tritici*, aber auch von anderen pilzlichen Pflanzen-, sowie auch Tier- und Humanpathogenen sind.

CHAPTER 1

General Introduction

GENERAL INTRODUCTION

Importance of fungal plant pathogens in modern agriculture

Fungal plant pathogens have been colonizing plants in natural ecosystems since the emergence of their hosts. Additionally they have been challenging farmers since domestication of the first crop plants between 2000 to 12000 years BP (BALTER 2007) and are now a big concern for producers of various crops worldwide, causing substantial yield and quality loss of modern agricultural produce (PENNISI 2010; DEAN *et al.* 2012). A study from 2012 estimated the yield loss due to fungal and oomycete diseases upon five major crops (rice, wheat, maize, potato and soybean) to correspond to the equivalent of an amount able to provide food for up to 4'287 million people per year or 61.2% of the world's population (FISHER *et al.* 2012).

Fungal plant pathogens are heterotrophic organisms and rely on colonization of host organisms in order to survive. Over the long evolutionary time period of coexistence with their host, fungal plant pathogens have developed specific mechanisms for colonization and invasion. For example appressoria are specialized fungal structures used by different fungal plant pathogens for host colonization. These structures use mechanical force and/or enzymatic activity to breach the host cuticle (WILSON and TALBOT 2009). Rust fungi, obligate biotrophs from the order of Pucciniales, have developed a specialized infection structure known as haustorium. These structures are formed once within the host plant in order to form a tight bond between the fungus and the host cells. This bound allows for nutrient uptake from the host, while at the same time excreting molecules into the host in order to suppress its immune responses (GARNICA *et al.* 2014).

Host plants on the other hand have developed complex mechanical and biochemical strategies to defend themselves against fungal plant pathogens. For example they are able to detect fungal pathogens through resistance genes. These genes, also known as R-genes, encode proteins that are able to recognize fungal plant pathogens upon their invasion process (JONES and DANGL 2006). The recognition of the fungal pathogen triggers complex signaling cascades, which results in a hypersensitive response (HR) within the host tissue. The HR ultimately leads to programmed plant cell death (PCD) around the infected site and hinders the fungal pathogen from further progression (VAN DER BIEZEN and JONES 1998; McDOWELL and WOFFENDEN 2003). The understanding of how plants protect themselves against fungal pathogens helps to improve modern agriculture. For example breeders have been making use of these R-genes to protect crops against attacks of fungal

pathogens. Over the past 50 years the Green Revolution (GR) had contributed strongly in improving worldwide crop production due to newly gained scientific knowledge applied upon cultivar breeding (EVENSON and GOLLIN 2003; PINGALI 2012). One strategy, beside the breeding of dwarf-cultivars, was the incorporation of R genes into modern cultivars (PENNISI 2010).

Additionally to understanding how plants protect themselves from fungal pathogens, it is also of great importance for agricultural practices to understand the mechanisms of host colonization of fungal pathogens in more detail. This may help improve future control strategies and contribute to a more sustainable agriculture. As an example, R-genes have been overcome by fungal pathogens in the past, rendering the R-genes ineffective and crops more susceptible to the fungal pathogens. For example in 1998 a strain of *Puccinia graminis tritici*, the causal fungal agent of stem rust disease on wheat, was discovered in Uganda. This strain, now commonly known as Ug99, showed the ability to overcome the major resistance genes of wheat cultivars, which were bred during the beginning of the GR in the 1950s. Till 1998 these wheat cultivars had shown effective protection against stem rust. Ug99 as well as new strains, which have derived from Ug99, currently threaten the major wheat producing regions in the world, as 90% of the commercial wheat cultivars are susceptible to these strains (SINGH *et al.* 2011).

Many of our major crops today are protected from fungal pathogens through resistance cultivars using R-genes (PENNISI 2010). However as seen by examples mentioned earlier, fungal plant pathogens are able to overcome these host resistance mechanisms or the R-genes only provide partial resistance. Therefore the usage of antimicrobial compounds in modern agriculture, such as fungicides, is also important in controlling fungal plant pathogens (PENNISI 2010). However even for antimicrobial compounds history has shown that fungal pathogen populations can evolve rather quickly and develop resistance mechanisms against these compounds. Various examples of fungicide resistance emergence has been observed in recent years in different fungal pathogen populations, with emergence time down to as little as one year (GRIMMER *et al.* 2014). This is because modern agriculture and its corresponding practices impose a high selection pressure upon fungal plant pathogen populations. This high selection pressure for example originates in the usage of monocultures with only one cultivar growing in the fields or the frequent usage of only one fungicide containing one active agent. As a result populations evolve quicker in agricultural-ecosystems (agro-ecosystems) than in natural ecosystems (STAHL and BISHOP 2000; McDONALD and LINDE 2002; ZHAN *et al.* 2002b). Therefore understanding mechanisms of fungal plant pathogen

populations on how they adapt to a changing environment, especially through identification of the underlying genes involved, may help to deploy improved control strategies in the future. This is of great importance as future agriculture is challenged by changing climate, increasing human population and a higher energy demand. These challenges need to be met by increased productivity of the current agricultural land, while at the same time optimizing resource-efficiency (FOLEY *et al.* 2011).

The study system

Zymoseptoria tritici (syn. *Mycosphaerella graminicola*) is a heterothallic, hemibiotrophic filamentous ascomycete that causes *Septoria tritici* blotch (STB) disease on wheat (*Triticum aestivum*) leaves. The disease is found in all major wheat growing regions in the world, with more than 90% of global genetic diversity found within a single wheat field (ZHAN *et al.* 2003; ZHAN and McDONALD 2011). Under favorable conditions an epidemic of STB can significantly damage the host population and result in yield losses up to 30-50% (EYAL *et al.* 1987) beside negatively affecting grain quality (ARABI *et al.* 2007), both contributing to significant economic losses. This is especially the case in regions with humid and temperate climates such as Northwestern Europe. It therefore is not surprising that STB was recently recognized as the most yield reducing disease in European countries with intensive wheat production (JORGENSEN *et al.* 2014). Wheat is the third-most-produced global cereal and is grown on more land area than any other commercial crop in the world. In 2010 the global production ranged up to 653 million metric tons on a total area of 217 million hectares (FAO 2013). In this context controlling STB is of major importance for sustainable food production. Control of STB relies mainly on deployment of fungicides and to a lesser extent on resistant wheat cultivars (GOUEMAND *et al.* 2013), with annual fungicide costs in Europe ranging up to more than 400 million euros, while in the USA growers invest around 275 million dollars each year in fungicide applications (O'DRISCOLL *et al.* 2014). Additional control strategies include integrated pest management approaches, such as crop rotations and the usage of cultivar mixtures. These strategies however remain less effective or have a more negative impact on yields compared to the two main control strategies (GIGOT *et al.* 2013).

Different classes of fungicides with different mode of actions (e.g. quinone outside inhibitors (QoIs or commonly referred to as the strobilurins), demethylase inhibitors (DMIs) and succinate dehydrogenase inhibitors (SDHIs)) can be used to fight STB either singularly or in combination of

each other (<http://www.eurowheat.org>). However *Z. tritici* populations have shown an impressive capacity to rapidly evolve complete or partial resistance to these fungicides either observed in the field or mainly found *in vitro* under laboratory conditions (e.g. SDHI-resistance) (FRAAIJE *et al.* 2005; COOLS *et al.* 2007; TORRIANI *et al.* 2009; FRAAIJE *et al.* 2012; SCALLIET *et al.* 2012; COOLS and FRAAIJE 2013; ESTEP *et al.* 2014). This has led to the situation of certain fungicides not being effective in *Z. tritici* populations any more or the future usage of currently still effective fungicides being threatened. For example Qols have been used successfully to fight STB in the UK since 1997. However in 2002 a mutation in the cytochrome *b* gene (*cyt b*), caused by an amino acid change at position 143 from glycine to alanine (G143A), had emerged, rendering isolates resistant to Qols. This mutation has rapidly spread till 2004 through UK populations, resulting in a high field frequency (~90%). Therefore Qols today in the UK are only allowed in mixtures with DMIs, with a maximum of two applications per season in order to slow down resistance progression and therefore the fixation of this mutation in field populations. However in some UK populations nowadays resistance to Qols is so widespread that these fungicides are no longer effective, even in mixtures. The single mode of action of Qols coupled with the absence of a significant fitness penalty of the G143A mutation as well as the heavy usage of Qols in agriculture most likely lead to the wide spread of this resistance in UK populations (FRAAIJE *et al.* 2005; TORRIANI *et al.* 2009). Thus today's chemical control of STB relies heavily on the usage of DMIs, SDHI and protective multi-site inhibitors (e.g. chlorothalonil), which can be deployed in mixtures (O'DRISCOLL *et al.* 2014). However even some of the main DMIs are currently threatened. For example one of the main groups of DMI fungicides providing sufficient control, both protective and curative, against STB on wheat refers to the systemic azoles, more precisely imidazoles and triazoles. These chemical compounds inhibit P450 14 α -demethylase, an enzyme encoded by the gene *CYP51/ERG11* and involved in ergosterol in *Z. tritici* (COOLS and FRAAIJE 2008). Although the usage of these two azole classes has been widespread and frequently applied in European agriculture since their introduction in 1970 with a resulting high selection pressure, development of resistance to imidazoles and triazoles in *Z. tritici* populations has been seldom and of rather low impact, even though these fungicides have a single target site mechanism, like the Qols. This may be explained to some extent based on high costs associated with higher resistance found in laboratory strains (COOLS *et al.* 2013). Nevertheless in recent years a progression of more frequent resistant *Z. tritici* field strains has been noticed, threatening the future use of these two currently important azoles (COOLS *et al.* 2011). Therefore the reliance on the recently (2003)

introduced SDHIs is expected to increase in the future. However also for this class of fungicides their sustainability is already questionable, as they have a single-site mode of action and *in vitro* studies have shown that *Z. tritici* populations have the potential to generate resistance to SDHI rather quickly at low to no fitness cost (FRAAIJE *et al.* 2012; SCALLIET *et al.* 2012). Although substantial progress has been made in the recent years, the genetic basis as well as natural genetic variance affecting phenotypic variance of fungicide sensitivity in *Z. tritici* still remains elusive, especially with regards to multi-drug-resistance (MDR), (ZWIERS *et al.* 2002; STERGIOPOULOS *et al.* 2003; ZWIERS *et al.* 2003; ROOHPARVAR *et al.* 2007; ROOHPARVAR *et al.* 2008; COOLS and FRAAIJE 2013; COOLS *et al.* 2013). Regarding resistance breeding of the host so far up to 18 loci were identified in wheat to provide STB resistance and have been used in wheat breeding programs (ORTON *et al.* 2011; GHAFARY *et al.* 2012). However *Z. tritici* has already shown to be able to overcome host resistance rather quickly. For example *Z. tritici* populations have evolved to be virulent on the wheat cultivar 'Gene' just after 3 years of the introduction of the cultivar (COWGER *et al.* 2000).

The high evolutionary potential of *Z. tritici* is likely due to population characteristics favoring rapid evolution: *Z. tritici* undergoes regular cycles of recombination, shows high effective population sizes as well as high mutation rates and a high amount of gene flow (MCDONALD and LINDE 2002; ZHAN *et al.* 2003; ZHAN and MCDONALD 2004; STUKENBROCK and MCDONALD 2008). This potential coupled with a strong selection pressure imposed upon *Z. tritici* populations through modern agricultural practices, as well as the ability of *Z. tritici* populations to adapt at relatively low or even no fitness cost, are the main reasons that rendered the two main control methods not sustainable.

Z. tritici is on the verge of becoming a fungal model-organism due to substantial work that has been carried out in the past within the fields of population dynamics, molecular biology and evolutionary biology. *Z. tritici* has therefore recently been considered as one of the top ten fungal pathogens in molecular plant pathology, which takes into consideration its scientific as well as economic importance (DEAN *et al.* 2012). For example the evolutionary history of *Z. tritici* is one of the most intensively studied for any fungal pathogen. Earlier studies elucidated the center of diversity/origin of this pathogen to correspond to the Fertile Crescent, where it followed a host-tracking model. The center of origin was also the location where two progenitor species *Zymoseptoria pseudotritici* and *Zymoseptoria ardabiliae* were collected from wild grasses. These show lower levels of infection on domesticated wheat compared to *Z. tritici* (STUKENBROCK *et al.* 2007; STUKENBROCK and MCDONALD 2008; STUKENBROCK *et al.* 2011). Gene flow is high globally,

resulting in a worldwide panmixia (ZHAN *et al.* 2003) and the sexual cycle was shown to play an important role in evolutionary biology, including the production of novel alleles through intragenic recombination that encoded important phenotypes such as fungicide resistance (BRUNNER *et al.* 2008). The recently sequenced and annotated 39Mb reference genome, based upon the Dutch isolate IPO323 and conducted by the Joint Genome Institute (JGI), is amongst the best-assembled fungal genomes available. It contains a total of ~ 11,000 predicted genes and spans over 21 chromosomes sequenced from telomere to telomere, of which 13 are core chromosomes and eight are accessory chromosomes (ACs) (GOODWIN *et al.* 2011). However as this assembled genome still contains to a rather large extent incomplete gene models (14%), which lack a start and/or stop codon, recent attempts to improve the JGI annotations were conducted. This was done through the usage of transcript assemblies based on RNA-Seq data, homology searches and *ab initio* gene predictors, which allowed the additional annotation of 1200 not previously predicted gene models (GRANDAUBERT *et al.* 2015). The accuracy of predicted gene models is important for any “omics” analysis, such as for example comparative genomics, transcriptomics and proteomics. Nevertheless since the appearance of the fully annotated reference genome coupled with the recent emergence of new molecular tools, such as next generation sequencing (NGS), different studies have been able to conduct full genome investigations (MCDONALD *et al.* 2015).

The present study

The aim of this PhD study was the identification of novel genes as well as natural genetic variance and its effect on phenotypic variance in important agricultural and life history traits in the major fungal wheat pathogen *Z. tritici*. Establishing the connection between genetic variance and phenotypic variance in natural populations is of great importance within the field evolutionary biology, allowing for better understanding of the potential of a population to adapt to changing environments, as genetic variation is the raw material for selection to act upon and for evolutionary changes to occur within populations. To do so we used quantitative trait locus (QTL) mapping, a powerful forward genetics approach, which allows for deciphering of the genetic architecture of an adaptive, quantitative phenotype (MACKAY 2001), a topic which still remains elusive for various microscopic species, including *Z. tritici* (ELLISON *et al.* 2011). We investigated a total of five important agricultural and life history traits: colony melanization, growth rate at two different temperatures (15°C and 22°C), fungicide sensitivity, temperature sensitivity and dimorphism. In nature various

traits of medical, agricultural and evolutionary relevance are of a quantitative character, due to the involvement of multiple loci. Examples include blood pressure (MORRISON *et al.* 2014), milk production (OLSEN *et al.* 2011) and seed number (BROWN *et al.* 2010). We investigated colony melanization, as fungal melanization has been associated with pathogen virulence, antimicrobial resistance and protection against extreme temperatures (LARSSON and TJALVE 1979; BUTLER and DAY 1998; NOSANCHUK *et al.* 2000; IKEDA *et al.* 2003; MORRIS-JONES *et al.* 2003; YOUNGCHIM *et al.* 2004; MEDNICK *et al.* 2005; NOSANCHUK and CASADEVALL 2006; TABORDA *et al.* 2008; NGAMSKULRUNGROJ and MEYER 2009; LIAW *et al.* 2010). Growth rate is of importance as it may be directly related to pathogen fitness and is the basic measurement to establish the two relative traits of fungicide and temperature sensitivity. *Z. tritici* till today is mainly controlled by the application of fungicides, more precisely using azoles, one of the few classes of systemic fungicides still providing adequate control of STB in Europe (COOLS *et al.* 2007). We therefore used the azole ‘propiconazole’ to investigate the genetic architecture of fungicide sensitivity in *Z. tritici* and identify genes other than the well studied target site (Cyp51) of azole fungicides. Temperature sensitivity is a key component for a pathogen to expand into new climatic regions as well as to cope with climate change. The trait of dimorphism was studied, as its ecological importance in the life cycle of *Z. tritici* is not understood.

We justify the usage of QTL mapping upon these five traits in *Z. tritici* as follow: 1) NGS studies conducted so far upon *Z. tritici* (KELLNER *et al.* 2014; RUDD *et al.* 2015) focused strongly on identification of genes involved in pathogenicity, such as effector genes (JONES and DANGL 2006), but didn’t investigate other important agricultural traits, such as for example fungicide sensitivity. Further they only used one genotype in their experiments and therefore don’t investigate natural genetic diversity and its effects on phenotypic diversity within populations. For example Rudd and colleagues used an extensive deep RNA-Seq experiment, where gene expression profiles of the reference isolate IPO323 were compared over different time points *in planta* and in axenic cultures. They identified 115 putative effectors, which were differentially expressed, with a peak expression at 9 dpi. Knock-out (KO) studies upon five most likely candidates showed no phenotypic effect upon pathogenicity, illustrating the high redundancy present in *Z. tritici* (RUDD *et al.* 2015). 2) Other studies, which investigated the natural phenotypic variance of virulence as well as other traits in *Z. tritici* didn’t investigate the genetic architecture underlying these traits. For example Zhan and colleagues studied natural phenotypic variance of virulence and other important agricultural and life history traits (e.g. growth rate, fungicide and temperature sensitivity) in ~140 strains. These

strains were collected from 5 field populations in different parts of the world (Europe, North America, Western Asia and Australia). In the context of a $Q_{ST} - G_{ST}$ experiment they measured degrees of local adaptation using a set of neutral markers, but the study didn't allow association of genetic variance with phenotypic variance (ZHAN *et al.* 2005; ZHAN and McDONALD 2011). 3) Other studies investigated the natural genetic variance of loci involved in phenotypic variance, however to our knowledge this was only done for the trait of fungicide sensitivity with the focus only upon one locus, namely the target site of DMI fungicides. For example Cools and colleagues studied in European populations recently emerged, natural genetic variants of *CYP51*. Through sensitivity tests of *Saccharomyces cerevisiae* transformants the effect sizes of these variants could be tested. However these effect sizes weren't brought in relation with the overall phenotypic variance of fungicide sensitivity occurring in natural field populations and no additional loci were investigated (COOLS *et al.* 2011). 4) Various functional characterization studies using KO approaches on different genes have been conducted in *Z. tritici*. These studies found multiple interesting phenotypes even for traits different than virulence, such as for melanization, dimorphism, fungicide sensitivity and colony growth. However these studies didn't investigate natural genetic variance of the studied genes occurring in field populations and therefore neither investigated natural phenotypic variance (COUSIN *et al.* 2006; MEHRABI and KEMA 2006; MEHRABI *et al.* 2006a; MEHRABI *et al.* 2006b; MEHRABI *et al.* 2009; CHOI and GOODWIN 2011a; CHOI and GOODWIN 2011b; ORTON *et al.* 2011; GOHARI *et al.* 2014).

QTL mapping has advantages, but also disadvantages. Advantages are the following: The same mapping population, once it has been genotyped, can be investigated for multiple traits. Contrary to a genome-wide association study (GWAS) no population structure effects are present and therefore no population corrections are needed. QTL mapping allows mapping of rare alleles, through the crossing of parental strains with rare phenotypes, where rare alleles are assumed to be present. Only few markers are needed for a complete genome scan, however marker density is a crucial factor affecting confidence interval size. Disadvantages of QTL mapping are: QTL mapping will only detect genetic diversity present amongst the parental strains. Therefore if parents don't differ regarding a QTL genetically, no phenotypic association can be made. This makes QTL mapping highly cross and context specific. Additionally there are limitations in separating pleiotropic effects versus physically close genes (KOWALSKI *et al.* 1994; MORGAN and MACKAY 2006). QTL mapping has been used extensively in animals (GODDARD and HAYES 2009), including humans (FLINT and MACKAY 2009) and also plants (HOLLAND 2007), but very few QTL mapping studies have been reported for

filamentous fungi (FOULONGNE-ORIOU 2012). QTL mapping has never been applied to *Z. tritici*. QTL mapping in *Z. tritici* therefore may set the bases for future investigations in order to answer questions such as: How many loci are responsible for phenotypic variation in the trait of interest within populations and amongst population? What is the degree of additive effects compared to the degree of epistasis (allele – allele interactions between loci)? Which loci affect multiple traits (pleiotropic effects)? Which evolutionary forces have shaped a population in the past and how will a population react in the future upon changing environmental conditions?

References

- ARABI, M. I. E., M. JAWHAR and N. M. ALI, 2007 The effects of *Mycosphaerella graminicola* infection on wheat protein content and quality. *Cereal Research Communications* **35**: 81-88.
- BALTER, M., 2007 Seeking agriculture's ancient roots. *Science* **316**: 1830-1835.
- BROWN, R. N., R. E. BARKER, S. E. WARNKE, L. D. COOPER, L. A. BRILMAN *et al.*, 2010 Identification of quantitative trait loci for seed traits and floral morphology in a field-grown *Lolium perenne* x *Lolium multiflorum* mapping population. *Plant Breeding* **129**: 29-34.
- BRUNNER, P. C., F. L. STEFANATO and B. A. McDONALD, 2008 Evolution of the *CYP51* gene in *Mycosphaerella graminicola*: evidence for intragenic recombination and selective replacement. *Molecular Plant Pathology* **9**: 305-316.
- BUTLER, M. J., and A. W. DAY, 1998 Fungal melanins: a review. *Canadian Journal of Microbiology* **44**: 1115-1136.
- CHOI, Y.-E., and S. B. GOODWIN, 2011a Gene encoding a C-type cyclin in *Mycosphaerella graminicola* is involved in aerial mycelium formation, filamentous growth, hyphal swelling, melanin biosynthesis, stress response, and pathogenicity. *Molecular Plant-Microbe Interactions* **24**: 469-477.
- CHOI, Y.-E., and S. B. GOODWIN, 2011b *MVE1*, encoding the velvet gene product homolog in *Mycosphaerella graminicola*, is associated with aerial mycelium formation, melanin biosynthesis, hyphal swelling and light signaling. *Applied and Environmental Microbiology* **77**: 942-953.
- COOLS, H. J., and B. A. FRAAIJE, 2008 Are azole fungicides losing ground against Septoria wheat disease? Resistance mechanisms in *Mycosphaerella graminicola*. *Pest Management Science* **64**: 681-684.
- COOLS, H. J., and B. A. FRAAIJE, 2013 Update on mechanisms of azole resistance in *Mycosphaerella graminicola* and implications for future control. *Pest Management Science* **69**: 150-155.
- COOLS, H. J., B. A. FRAAIJE, T. P. BEAN, J. ANTONIW and J. A. LUCAS, 2007 Transcriptome profiling of the response of *Mycosphaerella graminicola* isolates to an azole fungicide using cDNA microarrays. *Molecular Plant Pathology* **8**: 639-651.
- COOLS, H. J., N. J. HAWKINS and B. A. FRAAIJE, 2013 Constraints on the evolution of azole resistance in plant pathogenic fungi. *Plant Pathology* **62**: 36-42.

- COOLS, H. J., J. G. L. MULLINS, B. A. FRAAIJE, J. E. PARKER, D. E. KELLY *et al.*, 2011 Impact of recently emerged sterol 14 alpha-demethylase (CYP51) variants of *Mycosphaerella graminicola* on azole fungicide sensitivity. *Applied and Environmental Microbiology* **77**: 3830-3837.
- COUSIN, A., R. MEHRABI, M. GUILLEROUX, M. DUFRESNE, T. VAN DER LEE *et al.*, 2006 The MAP kinase-encoding gene *MgFus3* of the non-appressorium phytopathogen *Mycosphaerella graminicola* is required for penetration and in vitro pycnidia formation. *Molecular Plant Pathology* **7**: 269-278.
- COWGER, C., M. E. HOFFER and C. C. MUNDT, 2000 Specific adaptation by *Mycosphaerella graminicola* to a resistant wheat cultivar. *Plant Pathology* **49**: 445-451.
- DEAN, R., J. A. L. VAN KAN, Z. A. PRETORIUS, K. E. HAMMOND-KOSACK, A. DI PIETRO *et al.*, 2012 The Top 10 fungal pathogens in molecular plant pathology (vol 13, pg 414, 2012). *Molecular Plant Pathology* **13**: 804-804.
- ELLISON, C. E., C. HALL, D. KOWBEL, J. WELCH, R. B. BREM *et al.*, 2011 Population genomics and local adaptation in wild isolates of a model microbial eukaryote. *Proceedings of the National Academy of Sciences of the United States of America* **108**: 2831-2836.
- ESTEP, L. K., S. F. F. TORRIANI, M. ZALA, N. P. ANDERSON, M. D. FLOWERS *et al.*, 2014 Emergence and early evolution of fungicide resistance in North American populations of *Zymoseptoria tritici*. *Plant Pathology* **na**: 1-11.
- EVENSON, R. E., and D. GOLLIN, 2003 Assessing the impact of the Green Revolution, 1960 to 2000. *Science* **300**: 758-762.
- EYAL, Z., A. L. SCHAREN, J. M. PRESCOTT and M. VAN GINKEL, 1987 The *Septoria* diseases of wheat: concepts and methods of disease management. Mexico, D.F.: CIMMYT.
- FAO, 2013 *FAO Statistical Yearbook 2013*, Food and agricultural organization of the United Nations. Rome, Italy.
- FISHER, M. C., D. A. HENK, C. J. BRIGGS, J. S. BROWNSTEIN, L. C. MADOFF *et al.*, 2012 Emerging fungal threats to animal, plant and ecosystem health. *Nature* **484**: 186-194.
- FLINT, J., and T. F. C. MACKAY, 2009 Genetic architecture of quantitative traits in mice, flies, and humans. *Genome Research* **19**: 723-733.
- FOLEY, J. A., N. RAMANKUTTY, K. A. BRAUMAN, E. S. CASSIDY, J. S. GERBER *et al.*, 2011 Solutions for a cultivated planet. *Nature* **478**: 337-342.

- FOULONGNE-ORIOU, M., 2012 Genetic linkage mapping in fungi: current state, applications, and future trends. *Appl Microbiol Biotechnol* **95**: 891-904.
- FRAAIJE, B. A., C. BAYON, S. ATKINS, H. J. COOLS, J. A. LUCAS *et al.*, 2012 Risk assessment studies on succinate dehydrogenase inhibitors, the new weapons in the battle to control Septoria leaf blotch in wheat. *Molecular Plant Pathology* **13**: 263-275.
- FRAAIJE, B. A., H. J. COOLS, J. FOUNTAINE, D. J. LOVELL, J. MOTTERAM *et al.*, 2005 Role of ascospores in further spread of QoI-resistant cytochrome b alleles (G143A) in field populations of *Mycosphaerella graminicola*. *Phytopathology* **95**: 933-941.
- GARNICA, D. P., A. NEMRI, N. M. UPADHYAYA, J. P. RATHJEN and P. N. DODDS, 2014 The ins and outs of rust haustoria. *Plos Pathogens* **10**: e1004329.
- GHAFFARY, S. M. T., J. D. FARIS, T. L. FRIESEN, R. G. F. VISSER, T. A. J. VAN DER LEE *et al.*, 2012 New broad-spectrum resistance to septoria tritici blotch derived from synthetic hexaploid wheat. *Theoretical and Applied Genetics* **124**: 125-142.
- GIGOT, C., S. SAINT-JEAN, L. HUBER, C. MAUMENE, M. LCONTE *et al.*, 2013 Protective effects of a wheat cultivar mixture against splash-dispersed septoria tritici blotch epidemics. *Plant Pathology* **62**: 1011-1019.
- GODDARD, M. E., and B. J. HAYES, 2009 Mapping genes for complex traits in domestic animals and their use in breeding programmes. *Nature Reviews Genetics* **10**: 381-391.
- GOHARI, A. M., R. MEHRABI, O. ROBERT, I. A. INCE, S. BOEREN *et al.*, 2014 Molecular characterization and functional analyses of *ZtWor1*, a transcriptional regulator of the fungal wheat pathogen *Zymoseptoria tritici*. *Molecular Plant Pathology* **15**: 394-405.
- GOODWIN, S. B., S. BEN M'BAREK, B. DHILLON, A. H. J. WITTENBERG, C. F. CRANE *et al.*, 2011 Finished genome of the fungal wheat pathogen *Mycosphaerella graminicola* reveals dispensome structure, chromosome plasticity, and stealth pathogenesis. *PLOS Genetics* **7**: e1002070.
- GOUEMAND, E., V. LAURENT, L. DUCHALAIS, S. M. T. GHAFFARY, G. H. J. KEMA *et al.*, 2013 Association mapping and meta-analysis: two complementary approaches for the detection of reliable *Septoria tritici* blotch quantitative resistance in bread wheat (*Triticum aestivum* L.). *Molecular Breeding* **32**: 563-584.
- GRANDAUBERT, J., A. BHATTACHARYYA and E. H. STUKENBROCK, 2015 RNA-seq based gene annotation and comparative genomics of four fungal grass pathogens in the genus *Zymoseptoria* identify

- novel orphan genes and species-specific invasions of transposable elements. *G3: Genes|Genomes|Genetics* **Early Online**: DOI: 10.1534/g1533.1115.017731.
- GRIMMER, M. K., F. VAN DEN BOSCH, S. J. POWERS and N. D. PAVELEY, 2014 Fungicide resistance risk assessment based on traits associated with the rate of pathogen evolution. *Pest Management Science* **71**: 207-215.
- HOLLAND, J. B., 2007 Genetic architecture of complex traits in plants. *Current Opinion in Plant Biology* **10**: 156-161.
- IKEDA, R., T. SUGITA, E. S. JACOBSON and T. SHINODA, 2003 Effects of melanin upon susceptibility of *Cryptococcus* to antifungals. *Microbiology and Immunology* **47**: 271-277.
- JONES, J. D. G., and J. L. DANGL, 2006 The plant immune system. *Nature* **444**: 323-329.
- JORGENSEN, L. N., M. S. HOVMOLLER, J. G. HANSEN, P. LASSEN, B. CLARK *et al.*, 2014 IPM strategies and their dilemmas including an introduction to www.eurowheat.org. *Journal of Integrative Agriculture* **13**: 265-281.
- KELLNER, R., A. BHATTACHARYYA, S. POPPE, T. Y. HSU, R. B. BREM *et al.*, 2014 Expression profiling of the wheat pathogen *Zymoseptoria tritici* reveals genomic patterns of transcription and host-specific regulatory programs. *Genome Biology and Evolution* **6**: 1353-1365.
- KOWALSKI, S. P., T. H. LAN, K. A. FELDMANN and A. H. PATERSON, 1994 QTL mapping of naturally-occurring variation in flowering time of *Arabidopsis thaliana*. *Molecular & General Genetics* **245**: 548-555.
- LARSSON, B., and H. TJALVE, 1979 Studies on the mechanism of drug-binding to melanin. *Biochemical Pharmacology* **28**: 1181-1187.
- LIAW, S. J., Y. L. LEE and P. R. HSUEH, 2010 Multidrug resistance in clinical isolates of *Stenotrophomonas maltophilia*: roles of integrons, efflux pumps, phosphoglucomutase (SpgM), and melanin and biofilm formation. *International Journal of Antimicrobial Agents* **35**: 126-130.
- MACKAY, T. F. C., 2001 The genetic architecture of quantitative traits. *Annual Review of Genetics* **35**: 303-339.
- MCDONALD, B. A., and C. LINDE, 2002 Pathogen population genetics, evolutionary potential, and durable resistance. *Annual Review of Phytopathology* **40**: 349-379.
- MCDONALD, M. C., B. A. MCDONALD and P. S. SOLOMON, 2015 Recent advances in the *Zymoseptoria tritici*-wheat interaction: insights from pathogenomics. *Frontiers in Plant Science* **6**: 1-5.

- McDOWELL, J. M., and B. J. WOFFENDEN, 2003 Plant disease resistance genes: recent insights and potential applications. *Trends in Biotechnology* **21**: 178-183.
- MEDNICK, A. J., J. D. NOSANCHUK and A. CASADEVALL, 2005 Melanization of *Cryptococcus neoformans* affects lung inflammatory responses during cryptococcal infection. *Infection and Immunity* **73**: 2012-2019.
- MEHRABI, R., S. BEN M'BAREK, T. A. J. VAN DER LEE, C. WAALWIJK, P. J. G. M. DE WIT *et al.*, 2009 G alpha and G beta proteins regulate the cyclic AMP pathway that is required for development and pathogenicity of the phytopathogen *Mycosphaerella graminicola*. *Eukaryotic Cell* **8**: 1001-1013.
- MEHRABI, R., and G. H. J. KEMA, 2006 Protein kinase A subunits of the ascomycete pathogen *Mycosphaerella graminicola* regulate asexual fructification, filamentation, melanization and osmosensing. *Molecular Plant Pathology* **7**: 565-577.
- MEHRABI, R., T. VAN DER LEE, C. WAALWIJK and G. H. J. KEMA, 2006a *MgSlr2*, a cellular integrity MAP kinase gene of the fungal wheat pathogen *Mycosphaerella graminicola*, is dispensable for penetration but essential for invasive growth. *Molecular Plant-Microbe Interactions* **19**: 389-398.
- MEHRABI, R., L.-H. ZWIERS, M. A. DE WAARD and G. H. J. KEMA, 2006b *MgHog1* regulates dimorphism and pathogenicity in the fungal wheat pathogen *Mycosphaerella graminicola*. *Molecular Plant-Microbe Interactions* **19**: 1262-1269.
- MORGAN, T. J., and T. F. C. MACKAY, 2006 Quantitative trait loci for thermotolerance phenotypes in *Drosophila melanogaster*. *Heredity* **96**: 232-242.
- MORRIS-JONES, R., S. YOUNGCHIM, B. L. GOMEZ, P. AISEN, R. J. HAY *et al.*, 2003 Synthesis of melanin-like pigments by *Sporothrix schenckii* in vitro and mammalian infection. *Infection and Immunity* **71**: 4026-4033.
- MORRISON, A. C., J. C. BIS, S.-J. HWANG, G. B. EHRET, T. LUMLEY *et al.*, 2014 Sequence analysis of six blood pressure candidate regions in 4,178 individuals: the cohorts for heart and aging research in genomic epidemiology (charge) targeted sequencing study. *Plos One* **9**: e109155.
- NGAMSKULRUNGROJ, P., and W. MEYER, 2009 Melanin production at 37 degrees C is linked to the high virulent *Cryptococcus gattii* Vancouver Island outbreak genotype VGIIa. *Australasian Mycologist* **28**: 9-14.

- NOSANCHUK, J. D., and A. CASADEVALL, 2006 Impact of melanin on microbial virulence and clinical resistance to antimicrobial compounds. *Antimicrobial Agents and Chemotherapy* **50**: 3519-3528.
- NOSANCHUK, J. D., A. L. ROSAS, S. C. LEE and A. CASADEVALL, 2000 Melanisation of *Cryptococcus neoformans* in human brain tissue. *Lancet* **355**: 2049-2050.
- O'DRISCOLL, A., S. KILDEA, F. DOOHAN, J. SPINK and E. MULLINS, 2014 The wheat–Septoria conflict: a new front opening up? *Trends in Plant Science* **19**: 602-610.
- OLSEN, H. G., B. J. HAYES, M. P. KENT, T. NOME, M. SVENDSEN *et al.*, 2011 Genome-wide association mapping in Norwegian Red cattle identifies quantitative trait loci for fertility and milk production on BTA12. *Animal Genetics* **42**: 466-474.
- ORTON, E. S., S. DELLER and J. K. M. BROWN, 2011 *Mycosphaerella graminicola*: from genomics to disease control. *Molecular Plant Pathology* **12**: 413-424.
- PENNISI, E., 2010 Armed and dangerous. *Science* **327**: 804-805.
- PINGALI, P. L., 2012 Green Revolution: Impacts, limits, and the path ahead. *Proceedings of the National Academy of Sciences* **109**: 12302-12308.
- ROOHPARVAR, R., A. HUSER, L.-H. ZWIERS and M. A. DE WAARD, 2007 Control of *Mycosphaerella graminicola* on wheat seedlings by medical drugs known to modulate the activity of ATP-binding cassette transporters. *Applied and Environmental Microbiology* **73**: 5011-5019.
- ROOHPARVAR, R., R. MEHRABI, J. G. M. VAN NISTELROOY, L.-H. ZWIERS and M. A. DE WAARD, 2008 The drug transporter *MgMfs1* can modulate sensitivity of field strains of the fungal wheat pathogen *Mycosphaerella graminicola* to the strobilurin fungicide trifloxystrobin. *Pest Management Science* **64**: 685-693.
- RUDD, J. J., K. KANYUKA, K. HASSANI-PAK, M. DERBYSHIRE, A. ANDONGABO *et al.*, 2015 Transcriptome and metabolite profiling of the infection cycle of *Zymoseptoria tritici* on wheat reveals a biphasic interaction with plant immunity involving differential pathogen chromosomal contributions and a variation on the hemibiotrophic lifestyle definition. *Plant physiology* **167**: 1158-1185.
- SCALLIET, G., J. BOWLER, T. LUKSCH, L. KIRCHHOFFER-ALLAN, D. STEINHAEUER *et al.*, 2012 Mutagenesis and functional studies with succinate dehydrogenase inhibitors in the wheat pathogen *Mycosphaerella graminicola*. *Plos One* **7**: e35429.

- SINGH, R. P., D. P. HODSON, J. HUERTA-ESPINO, Y. JIN, S. BHAVANI *et al.*, 2011 The emergence of Ug99 races of the stem rust fungus is a threat to world wheat production, pp. 465-481 in *Annual Review of Phytopathology, Vol 49*, edited by N. K. VANALFEN, G. BRUENING and J. E. LEACH.
- STAHL, E. A., and J. G. BISHOP, 2000 Plant-pathogen arms races at the molecular level. *Current Opinion in Plant Biology* **3**: 299-304.
- STERGIOPOULOS, I., J. G. M. VAN NISTELROOY, G. H. J. KEMA and M. A. DE WAARD, 2003 Multiple mechanisms account for variation in base-line sensitivity to azole fungicides in field isolates of *Mycosphaerella graminicola*. *Pest Management Science* **59**: 1333-1343.
- STUKENBROCK, E. H., S. BANKE, M. JAVAN-NIKKHAH and B. A. McDONALD, 2007 Origin and domestication of the fungal wheat pathogen *Mycosphaerella graminicola* via sympatric speciation. *Molecular Biology and Evolution* **24**: 398-411.
- STUKENBROCK, E. H., T. BATAILLON, J. Y. DUTHEIL, T. T. HANSEN, R. LI *et al.*, 2011 The making of a new pathogen: Insights from comparative population genomics of the domesticated wheat pathogen *Mycosphaerella graminicola* and its wild sister species. *Genome Research* **21**: 2157-2166.
- STUKENBROCK, E. H., and B. A. McDONALD, 2008 The origins of plant pathogens in agro-ecosystems. *Annual Review of Phytopathology* **46**: 75-100.
- TABORDA, C. P., M. B. DA SILVA, J. D. NOSANCHUK and L. R. TRAVASSOS, 2008 Melanin as a virulence factor of *Paracoccidioides brasiliensis* and other dimorphic pathogenic fungi: a minireview. *Mycopathologia* **165**: 331-339.
- TORRIANI, S. F. F., P. C. BRUNNER, B. A. McDONALD and H. SIEROTZKI, 2009 QoI resistance emerged independently at least 4 times in European populations of *Mycosphaerella graminicola*. *Pest Management Science* **65**: 155-162.
- VAN DER BIEZEN, E. A., and J. D. G. JONES, 1998 Plant disease-resistance proteins and the gene-for-gene concept. *Trends in Biochemical Sciences* **23**: 454-456.
- WILSON, R. A., and N. J. TALBOT, 2009 Under pressure: investigating the biology of plant infection by *Magnaporthe oryzae*. *Nat Rev Micro* **7**: 185-195.
- YOUNGCHIM, S., R. MORRIS-JONES, R. J. HAY and A. J. HAMILTON, 2004 Production of melanin by *Aspergillus fumigatus*. *Journal of Medical Microbiology* **53**: 175-181.

- ZHAN, J., C. C. LINDE, T. JURGENS, U. MERZ, F. STEINEBRUNNER *et al.*, 2005 Variation for neutral markers is correlated with variation for quantitative traits in the plant pathogenic fungus *Mycosphaerella graminicola*. *Molecular Ecology* **14**: 2683-2693.
- ZHAN, J., and B. A. McDONALD, 2004 The interaction among evolutionary forces in the pathogenic fungus *Mycosphaerella graminicola*. *Fungal Genetics and Biology* **41**: 590-599.
- ZHAN, J., and B. A. McDONALD, 2011 Thermal adaptation in the fungal pathogen *Mycosphaerella graminicola*. *Molecular Ecology* **20**: 1689-1701.
- ZHAN, J., C. C. MUNDT, M. E. HOFFER and B. A. McDONALD, 2002 Local adaptation and effect of host genotype on the rate of pathogen evolution: an experimental test in a plant pathosystem. *Journal of Evolutionary Biology* **15**: 634-647.
- ZHAN, J., R. E. PETTWAY and B. A. McDONALD, 2003 The global genetic structure of the wheat pathogen *Mycosphaerella graminicola* is characterized by high nuclear diversity, low mitochondrial diversity, regular recombination, and gene flow. *Fungal Genetics and Biology* **38**: 286-297.
- ZWIERS, L. H., I. STERGIOPOULOS, M. M. C. GIELKENS, S. D. GOODALL and M. A. DE WAARD, 2003 ABC transporters of the wheat pathogen *Mycosphaerella graminicola* function as protectants against biotic and xenobiotic toxic compounds. *Molecular Genetics and Genomics* **269**: 499-507.
- ZWIERS, L. H., I. STERGIOPOULOS, J. G. M. VAN NISTELROOY and M. A. DE WAARD, 2002 ABC transporters and azole susceptibility in laboratory strains of the wheat pathogen *Mycosphaerella graminicola*. *Antimicrobial Agents and Chemotherapy* **46**: 3900-3906.

CHAPTER 2

Quantitative Trait Locus Mapping of Melanization in the Plant Pathogenic Fungus *Zymoseptoria tritici*

Mark H. Lendenmann, Daniel Croll, Ethan L. Stewart and Bruce A. McDonald

Published online in G3-Genes Genomes Genetics (2014). DOI: 10.1534/g3.114.015289. Accepted 28.10.2014.

ABSTRACT

Melanin plays an important role in virulence and antimicrobial resistance in several fungal pathogens. The wheat pathogen *Zymoseptoria tritici* is important worldwide, but little is known about the genetic architecture of pathogenicity, including the production of melanin. Because melanin production can exhibit complex inheritance, we used quantitative trait locus (QTL) mapping in two crosses to identify the underlying genes. Restriction site associated DNA sequencing (RADseq) was used to genotype 263 (cross 1) and 261 (cross 2) progeny at ~8500 single nucleotide polymorphisms (SNP) and construct two dense linkage maps. We measured grey values, representing degrees of melanization, for single spore colonies growing on Petri dishes using a novel image processing approach that enabled high-throughput phenotyping. Because melanin production can be affected by stress, each offspring was grown in two stressful environments and one control environment. We detected six significant QTLs in cross 1 and nine in cross 2, with three QTLs shared between the crosses. Different QTLs were identified in different environments and at different colony ages. By obtaining complete genome sequences for the four parents and analyzing sequence variation in the QTL confidence intervals, we identified 16 candidate genes likely to affect melanization. One of these candidates was *PKS1*, a polyketide synthase gene known to play a role in the synthesis of dihydroxynaphthalene (DHN) melanin. Three candidate quantitative trait nucleotides (QTNs) were identified in *PKS1*. Many of the other candidate genes were not previously associated with melanization.

INTRODUCTION

Most fungi produce melanin pigments that are located mainly in their cell walls. Melanins are dark, often black, biological macromolecules composed of various types of phenolic or indolic monomers that often form complexes with proteins and carbohydrates. Proposed functions of fungal melanins include protection against irradiation, enzymatic lysis and extreme temperatures (BUTLER and DAY 1998). Melanin also plays an important role in virulence (NOSANCHUK *et al.* 2000; MORRIS-JONES *et al.* 2003; YOUNGCHIM *et al.* 2004; MEDNICK *et al.* 2005; NGAMSKULRUNGROJ and MEYER 2009) and resistance to antimicrobial compounds (LARSSON and TJALVE 1979; IKEDA *et al.* 2003; NOSANCHUK and CASADEVALL 2006; TABORDA *et al.* 2008; LIAW *et al.* 2010). Melanin is needed in appressoria to contain the high turgor pressure formed during penetration of the plant epidermis by fungal pathogens (HOWARD *et al.* 1991). Thus melanization plays an important role in fungal biology and in host-parasite interactions.

At least four melanins have been identified in fungi, and two of these, dihydroxynaphthalene (DHN) and dihydroxyphenylalanine (DOPA) melanin, have been subjected to intensive study. DHN melanin is considered to be the main fungal melanin. It is produced by a wide range of plant pathogenic fungi and is the best characterized fungal melanin, with a known biosynthetic pathway. The genetic basis of melanization can differ among fungi and the complexity in known melanin production pathways suggested that a quantitative trait locus (QTL) mapping approach would be useful to identify candidate genes (BUTLER and DAY 1998).

Zymoseptoria tritici (syn *Mycosphaerella graminicola*) is a heterothallic, hemibiotrophic filamentous ascomycete that causes the foliar disease Septoria tritici blotch on wheat worldwide. Under favorable conditions, yield losses can reach 30-50% (EYAL *et al.* 1987), especially in regions with humid and temperate climates such as north-western Europe. *Z. tritici* is currently one of the most important wheat pathogens in Europe (HARDWICK *et al.* 2001; O'DRISCOLL *et al.* 2014), however only eight genes involved in melanization have been investigated in *Z. tritici*. These eight genes encoded G proteins (MEHRABI *et al.* 2009), mitogen-activated protein kinases (MAPK) (COUSIN *et al.* 2006; MEHRABI *et al.* 2006a; MEHRABI *et al.* 2006b), a velvet protein (CHOI and GOODWIN 2011b) and a c-type cyclin (CHOI and GOODWIN 2011a). The G proteins and c-type cyclin had been associated with melanization in other filamentous fungi, but none of the eight genes were associated with a specific melanin biosynthetic pathway (BUTLER and DAY 1998). The effect of each gene on melanin production was validated using knockout mutants. Seven of the knockout mutants showed reduced virulence in addition to reduced melanization (COUSIN *et al.* 2006; MEHRABI *et al.* 2006a; MEHRABI *et*

al. 2006b; MEHRABI *et al.* 2009; CHOI and GOODWIN 2011b). The eighth knockout mutant exhibited increased melanization and reduced virulence (CHOI and GOODWIN 2011a). Lower melanization was correlated with higher sensitivity to azole fungicides in one of the mutants (MEHRABI *et al.* 2006a), but in another study a knock-out of a different gene (MEHRABI *et al.* 2006b) showed lower melanization as well as lower sensitivity to phenylpyrrole and dicarboximide fungicides. Hence, the typical pattern of higher melanization correlating with higher virulence and lower fungicide sensitivity is not clearly established in *Z. tritici*.

Melanization is likely a quantitative trait in *Z. tritici* because several genes were associated with the trait in other pathogenic fungi (TAKANO *et al.* 1995; ELIAHU *et al.* 2007; KARKOWSKA-KULETA *et al.* 2009; FUJIHARA *et al.* 2010; IPCHO *et al.* 2012; LIN *et al.* 2012; UPADHYAY *et al.* 2013) and some gene knockouts caused only reduced melanin production (KIMURA *et al.* 2001; PARISOT *et al.* 2002; SOLOMON *et al.* 2004; LIN *et al.* 2006; MEHRABI *et al.* 2009). We tested this hypothesis by using QTL mapping to determine the genetic architecture of melanization in *Z. tritici*. QTL mapping enables the identification and characterization of the chromosomal segments and corresponding genes that encode quantitative traits (MACKAY 2001). QTL mapping has been used extensively in animals (GODDARD and HAYES 2009), including humans (FLINT and MACKAY 2009) and also plants (HOLLAND 2007), but very few QTL mapping studies have been reported for filamentous fungi (FOULONGNE-ORIOU 2012). Although fungal melanin biosynthetic pathways were characterized in earlier studies, additional melanin genes were identified in recent studies (FUJIHARA *et al.* 2010; CHOI and GOODWIN 2011b; CHOI and GOODWIN 2011a) indicating that melanin biosynthetic pathways may be more complex than previously thought. QTL mapping was applied to fungal melanization in an earlier study with *Cryptococcus neoformans* (LIN *et al.* 2006), but this is the first QTL analysis of melanization in a fungal plant pathogen.

We used two mapping populations derived from four unique wild-type strains to identify QTLs involved in melanization. Because melanin production can be affected by stress (BUTLER and DAY 1998; HENSON *et al.* 1999; JACOBSON 2000), we exposed each offspring to two stressful environments, cold temperature and sub-lethal fungicide exposure, that could be compared to a control environment to determine whether temperature or fungicide stress would result in environment dependent QTLs. We chose a next generation sequencing (NGS) genotyping method called restriction site associated DNA sequencing (RADseq) to construct two highly dense genetic maps using single nucleotide polymorphism (SNP) markers covering most of the reference genome.

Phenotyping was based on high-throughput digital image processing to score the melanization of single spore colonies grown on solid media.

MATERIAL AND METHODS

Generation of mapping populations

Two crosses were made between four *Z. tritici* isolates. Isolate ST99CH3D1 (3D1: SRS383146) was crossed to ST99CH3D7 (3D7: SRS383147) and ST99CH1A5 (1A5: SRS383142) was crossed to ST99CH1E4 (1E4: SRS383143). All four parents were collected from naturally infected wheat fields in 1999 in Switzerland. The isolates were previously characterized phenotypically (ZHAN *et al.* 2002a) and genetically (ZHAN *et al.* 2002a; CROLL *et al.* 2013) and found to differ for virulence and several life history traits, including melanization. Crosses were performed by co-infecting wheat leaves using an established protocol (KEMA *et al.* 1996). Ascospores were collected, grown in vitro and stored on anhydrous silica gel and glycerol at -80°. Cross 3D1 x 3D7 produced 359 progeny and cross 1A5 x 1E4 produced 341 progeny.

Genotyping

We used restriction site associated DNA sequencing (RADseq) (BAIRD *et al.* 2008) to identify single nucleotide polymorphism (SNP) markers segregating in the progeny populations. RADseq SNPs in the parental strains were confirmed using complete parental genome sequences obtained earlier (CROLL *et al.* 2013). To construct libraries, spores were lyophilized and DNA was extracted using the DNeasy plant mini kit (Qiagen Inc., Switzerland). DNA was then quantified and standardized for all samples. 1.5 µg of genomic DNA per progeny was digested with the restriction enzyme *Pst*I. Libraries and pools were constructed following a modified RADseq protocol (ETTER *et al.* 2011). The main modification was to use Illumina TrueSeq compatible P2 adapters. Pools containing an average of 132 progeny were generated, with each pool consisting of 6 different P2 adapters. 22 P1 adapters with distinct inline barcodes were used to distinguish progeny DNA with an identical P2 adapter. Pools were sequenced on an Illumina HiSeq2000 in 100 bp paired-end mode.

Raw sequence reads were quality checked using the tool FastQC (Babraham Bioinformatics; Cambridge, UK). Reads were then quality trimmed with Trimmomatic v. 0.30 (LOHSE *et al.* 2012) by using the following settings upon phred + 33 quality scores: trailing = 3, slidingwindow = 20:5 and minlen = 50. Progeny reads were separated according to the P1 adapter using the FASTX-Toolkit v. 0.13 (Hannon Lab: http://hannonlab.cshl.edu/fastx_toolkit/links.html). Progeny reads were aligned individually against the IPO323 reference genome (assembly version MG2, Sept 2008) (GOODWIN *et al.* 2011) using the short-read aligner Bowtie 2 version 2.0.2 (LANGMEAD and SALZBERG 2012) to create progeny sequence alignment/map (sam) files. Default settings for a sensitive end-to-end alignment

were used (-D 15; -R 2; -L 22; -I S, 1,1.15). All four parental genome sequences (CROLL *et al.* 2013) were also aligned to the reference genome using identical trimming and assembly parameters. Parental and progeny sam files were converted into binary alignment/map files (bam) using SAMtools version 0.1.18 (LI *et al.* 2009). RADseq progeny aligned read data is available from the NCBI Short Read Archive under the BioProject accession numbers PRJNA256988 and PRJNA256991. SNPs were identified using the Genome Analysis Toolkit (GATK) version 2.6-4-g3e5ff60 (DEPRISTO *et al.* 2011) and VCFtools version 0.1.10 (<http://vcftools.sourceforge.net>). Initial SNP calling was performed in comparison to the reference genome using the GATK UnifiedGenotyper with a maximum alternative allele setting of 1. The sample-level was set to ploidy of 1 (haploid) using the sequence alignment/map files of progeny of one of the crosses combined with their respective parents. The genotype likelihood model was set to the SNP general ploidy model. Marker genotype SNP filtering was performed using GATK VariantFiltration, by setting the following filters for SNPs to pass: quality by depth ($QD \geq 5$), Fisher's Exact Test for strand bias ($FS \leq 60$), haplotype score ($HaplotypeScore \leq 10$), overall quality score ($QUAL \geq 1000$), lower and upper allele frequency ($AF_{lower} \geq 0.2$ and $AF_{upper} \leq 0.8$) and total number of alleles within each marker genotype ($AN \geq 60$). This filter excluded SNPs only called among the parental genomes. Progeny and parent genotypes were then filtered further using a phred-scaled genotype quality (GQ) setting of at least 30.

Genetic map construction and quality assessment

The construction of the linkage map was performed using R/qtl version 1.27-10 (ARENDS *et al.* 2010), a package of the open-source software R (R_CORE_TEAM 2012). A genotype matrix was constructed containing only progeny with a minimum of 45% of all SNPs genotyped. We further omitted any markers if less than 70% of the progeny were genotyped. Potential clones in the progeny populations were excluded by randomly selecting one progeny from a group of potential clones. Clones were defined as having at least 90% of SNP alleles in common. Adjacent non-recombining markers were reduced to retain only a single marker for each cluster of non-recombining markers. We excluded any markers showing significant evidence of non-Mendelian segregation (Chi-square test: $P < 0.1$), but no progeny genotypes matched the omission criteria for segregation distortion. Progeny genotypes were further investigated for evidence of genotyping errors ($error.prob < 0.01$). Markers with significant evidence for genotyping error in at least one progeny were excluded from

all progeny. NCBI Short Read Archive accession numbers for the retained progeny within each cross can be found in Table S1.

The genetic map was constructed by estimating the genetic distance amongst pairs of neighboring markers and translating recombination frequency into map distance (centiMorgans, cM). We checked for appropriate linkage group assignment, order and binary status among the retained markers by inspecting each genetic map for unusual inflation patterns. We constructed a plot of pairwise marker recombination fractions and LOD scores for tests of $r = \frac{1}{2}$ (heat map). A plot with a diagonal red line indicates a good assignment with consistent marker order and an absence of switched alleles. We compared the chromosome coverage of our linkage groups relative to the reference genome IPO323.

Phenotyping

Melanization was measured using a Petri dish assay combined with digital image analysis. Progeny of each cross were retrieved from long-term storage and grown on yeast malt sucrose (YMS) agar (4 g/L yeast extract, 4 g/L malt extract, 4 g/L sucrose, 50 mg/L kanamycin). Petri dishes were stored for approximately 4 days at 18°. 600 ul of sterile water was added to each plate and blastospores were gently scraped into the solution using a sterile glass slide. 450 ul of the highly concentrated spore suspension were then transferred into sterile 500 ul Eppendorf tubes and stored for no longer than 3 month at -20°. Spores of each offspring were taken from these tubes and diluted in sterile water to a concentration of 200 spores per ml using a haemocytometer. 500 µl of the spore suspension was spread across Petri plates containing potato dextrose agar (PDA, 4 g/L potato starch, 20 g/L dextrose, 15 g/L agar) using a sterile glass rod. Only single spore colonies were scored. An average of 20 colonies formed on each plate, but only nine individual colonies were scored on average because ~50 % of all colonies had fused with a neighboring colony. Each treatment produced the same average number of colonies.

Each progeny was exposed to two stress environments (cold temperature and sub-lethal fungicide concentration) and one control environment, with five technical repeats for each environment. The data point from a technical repeat was the average grey value from an average of nine colonies scored on one Petri dish. The control environment consisted of PDA plates growing at 22°. The cold-stress environment was PDA plates growing at 15°, while the fungicide-stress environment was PDA plates containing 0.75 ppm propiconazole (Syngenta, Basel, Switzerland) growing at 22°.

Following inoculation, Petri plates were dried for 30 min in a laminar flow cabinet and sealed using Parafilm. Plates were then randomized in a growth chamber set to a constant temperature with 70% humidity and no light. Plates were photographed at 8, 11 and 14 days post inoculation (dpi) for image analysis. These time points were chosen because they represented different colony ages and provided the largest phenotypic variance in preliminary experiments. This experimental design resulted in nine unique Environment-Colony-Age-Melanization (ECAM) phenotypes for each isolate, which we will refer to as ECAM phenotypes.

Digital images were captured through the Petri dish lid using standardized camera settings and lighting environments (see Table S2, Table S3, Figure S1). After images were acquired, Petri dishes were re-randomized and returned to the growth chamber for further colony growth and later image acquisition. Images were processed using a batch macro developed in the open-source software ImageJ (SCHNEIDER *et al.* 2012), enabling automated image analysis. The macro identified and scored individual colonies in the images (see File S1). Melanization was measured using average grey values of individual colonies. Grey values range from 0 to 255, with 0 representing black and 255 representing white (Figure 1). We used untransformed grey values as phenotypic values representing different degrees of colony melanization. We calculated broad-sense heritability (H^2) values (BURTON and DEVANE 1953) over means of the five technical repeats for each environment and colony age using a one-way ANOVA model in R (R_CORE_TEAM 2012). The melanization phenotypes for the retained progeny within each cross can be found in Table S4.

QTL mapping

QTL mapping was performed in R/qtl version 1.27-10 (ARENDS *et al.* 2010) using single marker analysis combined with interval mapping, resulting in simple interval mapping (SIM) analysis. The analysis was based on progeny mean values, calculated over the five technical repeats for each environment and colony age, so that nine different ECAM phenotypes were generated for each cross (three environments x three colony ages). Interval mapping improves on the marker regression method by estimating markers (pseudomarkers) in between true markers. For SIM analysis we used the EM algorithm. Significance thresholds were determined by permutating the marker data. We applied genome-wide permutations, with 1000 permutations for each ECAM phenotype. We considered only QTL peaks with LOD scores that provided P-values lower than 0.05. We used the reference IPO323 genome to convert cM positions of markers into base pair (bp) positions on the reference genome. For 95% confidence interval calculations we used Bayesian

credible intervals from SIM combined with the EM algorithm (MANICHAIKUL *et al.* 2006). Marker mean differences and the amount of variance explained by significant markers were calculated using true markers and not pseudomarkers. We assumed that our marker alleles were additive because we did not detect any significant epistasis.

Identification of candidate genes within QTL confidence intervals

To identify candidate genes within QTL confidence intervals, we first identified sequence variants amongst the parents in each cross by comparing their genome sequences, which had been previously aligned against the IPO323 reference genome. SNPs associated with synonymous and non-synonymous mutations were called using the GATK UnifiedGenotyper with a maximum alternative allele setting of 2. Filter settings in the GATK VariantFiltration were as follows: $QD \geq 5$, $FS \leq 60$, $HaplotypeScore \leq 10.0$, $QUAL \geq 100$, $AFlower \geq 0.2$, $AFupper \leq 0.8$ and $AN \geq 2$. For all other sequence variants we used default settings of the GATK tools (DEPRISTO *et al.* 2011). SNP and other sequence variation annotation results amongst the parental strains within each cross were obtained using the open-source tools SnpEff and SnpSift version 3.3h (CINGOLANI *et al.* 2012). Synonymous SNPs were not considered in further analyses. Genes without gene ontology annotations were described as having unknown functions. Genes were considered as candidate genes within a confidence interval if they contained at least one sequence variant within the boundaries of the confidence interval, excluding genes with no sequence variation or with only synonymous SNPs.

A total of 29 genes involved in fungal melanin biosynthesis have been described in the literature. Orthologs (Table S5) for each of these genes were identified in *Z. tritici* by performing a BlastP search in the NCBI non-redundant protein database (<http://www.ncbi.nlm.nih.gov>) and conducting phylogenetic analyses of the amino acid sequences using the maximum likelihood algorithm with default parameters in MEGA5 (TAMURA *et al.* 2011). All QTL confidence intervals were searched for presence of the identified orthologs, which were considered as candidate melanization genes.

RNA-Seq data were obtained for parent 3D7 as described earlier (BRUNNER *et al.* 2013). Briefly, RNA-Seq data were obtained during an in planta infection time course that included all major phases of the pathogen life cycle (ie biotrophic, necrotrophic and saprotrophic phases), including 3 biological repeats at 7, 13, and 56 days post inoculation (dpi). Reads per kilobase per million (RPKM) per gene values were calculated by normalizing the RNA reads and mapping them onto the reference genome. Significant differences in transcript abundances were calculated as

described earlier (BRUNNER *et al.* 2013). Transcription profiles were obtained for the orthologs to genes involved in melanin biosynthesis as well as candidate genes identified within QTL confidence intervals.

Amino acid differences in *PKS1* amongst parents 3D1 and 3D7

We identified synonymous and non-synonymous substitutions in the gene *PKS1* (ProteinID 96592) encoding a polyketide synthase that catalyzes the first step of the DHN melanin biosynthetic pathway. Sequence polymorphism was scored in a Swiss field population of 25 *Z. tritici* isolates. Nine of the 25 isolates, including the 4 parental strains, had their genomes sequenced in a previous study (CROLL *et al.* 2013), while complete genome sequences of 16 additional isolates (3A2, 3A4, 3A5, 3A6, 3A8, 3A10, 3B2, 3B4, 3C7, 3D3, 3D5, 3F1, 3F3, 3F4, 3G3 and 3H1) were obtained using the same methods for this study. SNPs amongst the isolates were called and filtered using the GATK tools (DEPRISTO *et al.* 2011) with similar settings as applied for the RADseq dataset. Introns as well as synonymous and non-synonymous SNPs were manually curated.

A BlastP search in the NCBI non-redundant protein database (<http://www.ncbi.nlm.nih.gov>) was performed to investigate sequence conservation amongst ascomycetes. The *PKS1* amino acid sequence of the *Z. tritici* reference genome isolate IPO323 was aligned against 10 ascomycetes, including *Pseudocercospora fijiensis*, *Cladosporium phlei*, *Elsinoe fawcettii*, *Leptosphaeria maculans*, *Alternaria alternata*, *Phaeosphaeria nodorum*, *Pyrenophora tritici-repentis*, *Magnaporthe oryzae*, *Neurospora crassa* and *Aspergillus nidulans*. The Pfam database was used to identify functional *PKS1* protein domains (FINN *et al.* 2014).

RESULTS

Genetic maps

We retained 263 unique progeny and 9745 SNP markers in the 3D1 x 3D7 cross. 96 progeny were excluded because of missing genotypes (18) or clonality (78). The quality filtered dataset in the 1A5 x 1E4 cross included 261 progeny and 7333 SNP markers. 80 progeny were excluded because of missing genotypes (14) or clonality (66). Table 1 and Table 2 summarize the results for each genetic map.

Marker density was high with an average genetic spacing of 0.44 cM, representing an average physical spacing of ~3600 bp between SNP markers in cross 3D1 x 3D7 and average spacing of 0.71 cM (~4700 bp) in cross 1A5 x 1E4. On average our genetic maps covered around 90% of the reference genome over both crosses. Figure 2 shows the genetic maps as well as plots of pairwise marker recombination fractions and LOD scores for tests of $r = 0.5$, which indicate a distorted diagonal red line for chromosome 13 in both crosses, indicating marker order inconsistencies. Chromosome 13 likely exhibits map inflation in both crosses, indicated by an unusual genetic length (Table 1, Table 2) and larger gaps on the genetic map (Figure 2).

The 8 smallest chromosomes (14 to 21) in the *Z. tritici* reference genome are accessory chromosomes (ACs) (GOODWIN *et al.* 2011) that often exhibit presence/absence polymorphisms (CROLL *et al.* 2013). In the 3D1 x 3D7 cross, the parental genome sequences revealed that ACs 14, 15, 18 and 21 were missing in one of the parents, hence only ACs 16, 17, 19 and 20 were mapped. In the 1A5 x 1E4 cross, AC 17 was missing in one of the parents and therefore only ACs 14, 15, 16, 18, 19, 20 and 21 were mapped.

Melanization is a quantitative trait that shows transgressive segregation

For both crosses over all three environments and all three colony ages, we found that melanization showed a continuous distribution consistent with a quantitative character (Figure S2, Figure S3). Many progeny had more extreme phenotypes than the parents, indicating transgressive segregation. The degree of melanization increased over time for most isolates in most environments, indicating that melanin concentration increases as colonies age.

Reaction norms over the three colony ages differed among the progeny in each cross, providing evidence for differential interactions between genotypes and environments over time. To illustrate this, we compared the two progeny showing the most extreme phenotypes at 14 dpi in one environment with their corresponding phenotypes in the other two environments (Figure S4,

Figure S5). In both crosses we found strong evidence for phenotype-by-environment interaction over all colony ages. Hence, we analyzed each colony age separately in the QTL analyses.

Comparison of mapped QTLs reveals unique and shared QTLs between the two crosses

We found six significant QTLs in cross 3D1 x 3D7 and nine significant QTLs in cross 1A5 x 1E4 (Figure 3, Table 3, Table 4). QTLs were considered to be different if the confidence intervals did not overlap. This approach was applied across environments and colony ages as well as within crosses and amongst crosses. Three QTLs were shared between the two crosses. Shared QTLs were further characterized based on the 3D1 x 3D7 cross. A detailed description of all significant QTLs found in both crosses is given in Table S6, Table S7, Table S8 and Table S9. No QTLs were found on accessory chromosomes.

Environment and colony age affect QTL mapping results

In both crosses we found environment-specific QTLs as well as QTLs that were shared across all environments. In cross 3D1 x 3D7, five QTLs were environment-specific and a QTL on chromosome 11 was found in all environments. In cross 1A5 x 1E4, six QTLs were environment-specific and three QTLs were found in all environments (Figure 3).

Colony age also affects QTL detection for some environments in both crosses. For example, in cross 3D1 x 3D7 the chromosome 5 QTL was found in colonies that were 11 and 14 days old, while the chromosome 8 QTL was found only in colonies that were 11 days old. In the 1A5 x 1E4 cross, the QTLs on chromosomes 5 and 8 were significant in colonies that were 11 and 14 days old, but the QTLs on chromosomes 6, 7 and 11 were found only in colonies that were 14 days old (Figure 3).

Genetic architecture of melanization in the two crosses

We found differences in the genetic architecture of melanization amongst the two crosses. On average, cross 3D1 x 3D7 had fewer (1.8) melanization QTLs for each colony age and environment than cross 1A5 x 1E4 (3.6). But the average total variance explained by the QTLs for each ECAM phenotype was similar (~35%) in both crosses. In cross 3D1 x 3D7 nearly half of the total phenotypic variance was explained by one QTL on chromosome 11, while in cross 1A5 x 1E4 a similar amount of variance was explained by six QTLs distributed across several chromosomes, suggesting a more

complex genetic basis of melanin production in cross 1A5 x 1E4 compared to cross 3D1 x 3D7 (Table 5).

Identification of candidate genes and orthologous genes related to melanization in QTL regions

A summary of the candidate genes found within each confidence interval for cross 3D1 x 3D7 and 1A5 x 1E4 is given in Table S8 and Table S9, respectively. On average we found ~190 candidate genes per confidence interval, with a minimum of one candidate gene (14 dpi, fungicide environment, 1A5 x 1E4) and a maximum of 1245 genes (8 dpi, control environment, 1A5 x 1E4). ~32% of the candidate genes found in a confidence interval had no known function and ~42% showed significant changes in transcript abundance across biotrophic, necrotrophic and saprotrophic stages in the life cycle. Eleven orthologs of the 29 genes described to be involved in melanin biosynthesis (Table S5) were identified as candidate genes in four of the 12 cross-specific QTL confidence intervals (Figure 3). Nine of the 29 orthologs were found in three of the QTLs in cross 3D1 x 3D7 and two were found in one of the QTLs in cross 1A5 x 1E4 (Table 6). These 11 orthologs encode two (*MgSlt2* and *MgFus3*) mitogen-activated protein kinases (MAPKs), one (*CLAP1*) copper-transporting ATPase, two (*LAC4* and *LAC8*) laccases, one (*PRF1*) prefolding chaperone, one (*PKS1*) polyketide synthase, one (*MgGpa1*) G alpha protein, as well as two (*PEX6* and *PEX13*) genes involved in peroxisome biosynthesis and one (*AYG2*) of an unknown function (Table S5). Three (*MgSlt2*, *MgFus3* and *MgGpa1*) of these 11 genes were associated with melanization in *Z. tritici* in earlier studies (COUSIN *et al.* 2006; MEHRABI *et al.* 2006a; MEHRABI *et al.* 2009), but the other 8 genes have not previously been associated with melanization in *Z. tritici*.

To narrow the search for candidate genes affecting melanization, we focused on major QTLs (LOD > 7.5) containing ≤ 30 candidate genes in their confidence intervals. We identified two confidence intervals meeting these criteria in each cross (Table 7). For cross 3D1 x 3D7, the QTL on chromosome 10 for the 11 dpi cold environment had 12 candidate genes and the QTL on chromosome 11 for the 8 dpi control environment had four candidate genes (Table S10, Figure 4). For cross 1A5 x 1E4, the QTL on chromosome 4 for the 14 dpi fungicide environment had one candidate gene and the QTL on chromosome 8 for the 11 dpi cold environment had 22 candidate genes (Table S11, Figure 4). Taking into account all of the available information (gene ontology, the predicted impact of observed sequence variation, the position of the QTL peak, gene expression) as shown in Table S10 and Table S11, we further narrowed the list down to eight high-priority

candidate genes in the 3D1 x 3D7 cross and eight high-priority candidate genes in the 1A5 x 1E4 cross, resulting in a total of 16 high-priority candidate genes over both crosses.

DISCUSSION

Genetic maps

The two genetic maps have very high marker density compared to other reported genetic maps in filamentous fungi (FOULONGNE-ORIOU 2012). The high marker density reflects the high degree of recombination in the mapping populations as well as the large number of markers provided by our genotyping method. Earlier genetic maps based on the genome reference isolate IPO323 (KEMA *et al.* 2002; WITTENBERG *et al.* 2009) were ~72% smaller than our genetic maps. We hypothesize that our maps are larger due to higher recombination resulting from larger numbers of offspring and more extensive chromosome coverage resulting from larger numbers of genetic markers. Our maps covered ~90% of the reference genome on average. Incomplete coverage can be explained by missing restriction sites or low quality mapping reads toward one or both telomeres of each chromosome. Other explanations include a lack of recombining polymorphic markers or lower polymorphism towards the telomeres. The ratio of physical distance to genetic distance was ~7.5 kb/cM for both crosses, comparable to the ratio of 8.1 kb/cM described in *Aspergillus nidulans* (CHRISTIANS *et al.* 2011).

The unusual genetic length (Table 1, Table 2) and larger gaps on the genetic map of chromosome 13 (Figure 2) are consistent with map inflation resulting from incorrect marker order, most likely due to inappropriate alignment of our illumina reads onto the reference genome. We hypothesize that this could be due to the presence of the mating type idiomorphs (WAALWIJK *et al.* 2002) on this chromosome, the occurrence of transposable elements or because of incorrect reference genome assembly. As chromosome 13 coverage was good (88% in cross 3D1 x 3D7 and 90% for cross 1A5 x 1E4) and no QTLs were found on this chromosome for either cross, this issue was not investigated further.

Melanization is a quantitative trait that is affected by environment and colony age

The finding that all ECAM phenotypes showed a continuous distribution (Figure S2, Figure S3) and high broad-sense heritability (74-95%; Figure S4 and Figure S5) in both crosses indicates that several genes are likely to contribute to the melanization phenotype in *Z. tritici*. We found 15 significant QTLs in total, with more than one significant QTL identified for 13 out of 18 ECAM phenotypes (Table 5). On average, a QTL contributed ~15% of the phenotypic variance observed in each cross. The pattern of transgressive segregation is also consistent with the hypothesis that melanization is a quantitative trait. Our findings stand in contrast to an earlier melanization mapping study (LIN *et al.*

2006) that identified only one significant QTL associated with several melanin phenotypes in a mapping population.

Our experimental design allowed us to investigate the effects of both colony age and environment on the melanization phenotype. We were able to demonstrate both colony age and environmental effects, as reflected by unique QTLs, within both mapping populations. These findings are consistent with the hypothesis that genes affecting melanization are differentially regulated in different environments and at different stages of colony development.

Unique QTLs and shared QTLs were identified by comparing QTLs of the two crosses

We identified three shared QTLs and nine QTLs that were unique to one of the crosses. For the three shared QTLs (found on chromosomes 1, 5 and 11), we compared the candidate genes found in the corresponding confidence intervals and found that more than 40% of the candidate genes in these confidence intervals were shared amongst the two crosses, suggesting that the shared QTLs are likely to be due to same source of genetic variance in each cross. Among the 15 identified QTLs, we postulate that the six QTLs in Table 8 are the most likely to be replicated in other QTL mapping studies, based on having a combination of high LOD scores (≥ 7) and being found at least twice over different colony ages and/or environments.

Identification of orthologs to genes involved in melanin biosynthesis within QTL intervals

All the previously identified orthologs of genes involved in melanin biosynthesis (Table S5) were expressed (≥ 2 RPKM), hence all of the orthologs could affect melanization in *Z. tritici*. Eleven of the 29 orthologs were found within four of the twelve cross-specific QTL confidence intervals (Table 6, Figure 3) identified in our analyses. We postulate that several of these known genes contributed to the melanization phenotypes in our crosses. Among the 11 orthologous candidates, three (*MgSlt2* (MEHRABI *et al.* 2006a), *MgGpa1* (SOLOMON *et al.* 2004; MEHRABI *et al.* 2009) and *MgFus3* (COUSIN *et al.* 2006)) were functionally validated in *Z. tritici* but none of these have been investigated as contributing to a quantitative character. The other 8 candidates have not yet been analyzed in *Z. tritici*, but our QTL analyses indicate that these genes may also affect melanization in *Z. tritici*. Following gene disruption, 8 of these 11 orthologous candidates exhibited a measurable change in mycelial melanization in vitro, and three (*PEX6*, *LAC4* and *LAC8*) affected melanization of appressoria but not mycelia in *Colletotrichum* spp (KIMURA *et al.* 2001; LIN *et al.* 2012). None of the

18 remaining orthologs were found as candidate genes in the 12 cross-specific QTL confidence intervals.

QTL confidence intervals contain both novel and known candidate genes affecting melanization

Three of the 16 high-priority candidate genes carried no GO annotation and thus have no known function. These candidates could represent novel transcription factors, enzymes or structural proteins that affect the melanization phenotype. The remaining 13 genes had gene ontology annotations. Seven of the 16 high-priority candidate genes showed significant changes in transcript abundance across biotrophic, necrotrophic and saprotrophic stages of the life cycle, consistent with expected changes in melanin production across the pathogen life cycle. Melanin production is expected to increase during the development of the black pycnidia that form early in the saprotrophic stage of the life cycle (EYAL *et al.* 1987).

Within three of the four major-effect QTL confidence intervals, none of the candidate genes is an ortholog of genes known to be involved in melanin biosynthesis, thus these represent novel candidates for genes affecting fungal melanization. Gene 92291 encodes a transcription factor and was the only candidate gene within the QTL confidence interval on chromosome 4. We hypothesize that this transcription factor regulates genes under fungicide stress because this QTL was found only in the fungicide environment.

The major-effect QTL on chromosome 11 contains three high-priority candidate genes and had the highest LOD score (32.2) amongst the 12 cross specific QTLs over both crosses (Table 3, Table 4). Two of the 3 genes were orthologous to genes known to be involved in melanin biosynthesis (Table S5), namely *PRF1* (Protein ID: 96591) and *PKS1* (Protein ID: 96592). The third gene (96588) is involved in zinc binding and was also considered a high-priority candidate because the melanin biosynthesis ortholog *CMR1* (ELIAHU *et al.* 2007) (Table S5) encodes a transcription factor with a zinc finger (TSUJI *et al.* 2000) and is located 28 kb upstream from 96588. We hypothesize that gene 96588 is involved in zinc homeostasis of *CMR1* and ultimately affects melanin biosynthesis. But our analyses of sequence diversity led us to conclude that *PKS1* is the major contributor to the phenotypic variance explained by the large effect QTL on chromosome 11.

Identification of a candidate QTN in *PKS1*

PKS1 is the polyketide synthase enzyme catalyzing the first step of DHN melanin synthesis through head-to-tail joining and cyclization of acetate molecules (TAKANO *et al.* 1995; BUTLER and DAY 1998) in

the DHN melanin biosynthetic pathway. *PKS1* carries three non-synonymous mutations amongst parents 3D1 and 3D7 while *PRF1* and 96588 contain 1 and 0 non-synonymous mutations, respectively (Table S10). The region on chromosome 11 containing *PKS1* comprises the main DHN melanin biosynthetic gene cluster. We interpret this finding as a validation of our QTL mapping approach to identify genes affecting melanization. DHN melanin, which is the best characterized melanin in fungi (BUTLER and DAY 1998), has so far not been studied in *Z. tritici* (Table S5). The identification of *PKS1* as a highly probable candidate gene within the QTL having the largest LOD score amongst the 12 cross-specific QTLs suggests that DHN melanin plays a major role in melanization in *Z. tritici*.

Three non-synonymous substitutions at amino acid positions 155, 884 and 1783 were found in *PKS1* amongst parents 3D1 and 3D7, but positions 884 and 1783 (Figure 5) were considered as more likely candidates to explain differences in melanization because position 155 was not in a functional domain and the alternative amino acids did not differ for polarity, acidity (TAYLOR 1986) or hydrophathy index (KYTE and DOOLITTLE 1982). Fifteen of the 25 field isolates had an alanine at position 884 while 10 isolates carried a valine at that position. At position 1783, only the 3D7 parent had a threonine residue while the other 24 isolates had a proline (Figure 5). Position 1783 was more conserved amongst ascomycetes than site 884, but neither site was located within an annotated functional domain of *PKS1* (Figure 5). The amino acid property changes were most striking for site 1783, because proline is nonpolar while threonine is polar. In addition, proline is unique among the 20 proteinogenic amino acids because its side group links to the amino group, often resulting in strong effects on protein secondary structure.

Based on these analyses of *PKS1* sequence polymorphism, we postulate that the non-synonymous mutation found at amino acid 1783 explains most of the phenotypic variance associated with the large-effect QTL on chromosome 11. If this is confirmed, then the associated SNP represents a quantitative trait nucleotide (QTN) (FRIDMAN *et al.* 2004) that explains the majority of the phenotypic variance in this cross. Functional validation will be needed to confirm this hypothesis.

ACKNOWLEDGMENTS

The research was supported by a grant from the Swiss National Science Foundation (31003A_134755). Technical help was provided by Michael Mielewczik and Tryggvi S. Stefansson. The RNA-Seq data was kindly provided by Stefano F. F. Torriani. We thank Marc-Henri Lebrun (UR BIOGER, INRA, France) for information on the annotation of melanin biosynthesis genes. RADseq libraries were constructed at the Genetic Diversity Centre (GDC) and sequenced in the Quantitative Genomics Facility at the Department of Biosystems Science and Engineering (D-BSSE) at the scientific central facilities of ETH Zurich.

REFERENCES

- ARENDS, D., P. PRINS, R. C. JANSEN and K. W. BROMAN, 2010 R/qtl: high-throughput multiple QTL mapping. *Bioinformatics* **26**: 2990-2992.
- BAIRD, N. A., P. D. ETTER, T. S. ATWOOD, M. C. CURREY, A. L. SHIVER *et al.*, 2008 Rapid SNP discovery and genetic mapping using sequenced rad markers. *PLOS One* **3**: e3376.
- BRUNNER, P. C., S. F. F. TORRIANI, D. CROLL, E. H. STUKENBROCK and B. A. McDONALD, 2013 Coevolution and life cycle specialization of plant cell wall degrading enzymes in a hemibiotrophic pathogen. *Molecular Biology and Evolution* **30**: 1337-1347.
- BURTON, G. W., and E. H. DEVANE, 1953 Estimating heritability in tall fescue (*Festuca-arundinacea*) from replicated clonal material. *Agronomy Journal* **45**: 478-481.
- BUTLER, M. J., and A. W. DAY, 1998 Fungal melanins: a review. *Canadian Journal of Microbiology* **44**: 1115-1136.
- CHOI, Y.-E., and S. B. GOODWIN, 2011a Gene encoding a C-type cyclin in *Mycosphaerella graminicola* is involved in aerial mycelium formation, filamentous growth, hyphal swelling, melanin biosynthesis, stress response, and pathogenicity. *Molecular Plant-Microbe Interactions* **24**: 469-477.
- CHOI, Y.-E., and S. B. GOODWIN, 2011b *MVE1*, encoding the velvet gene product homolog in *Mycosphaerella graminicola*, is associated with aerial mycelium formation, melanin biosynthesis, hyphal swelling and light signaling. *Applied and Environmental Microbiology* **77**: 942-953.
- CHRISTIANS, J. K., M. S. CHEEMA, I. A. VERGARA, C. A. WATT, L. J. PINTO *et al.*, 2011 Quantitative trait locus (QTL) mapping reveals a role for unstudied genes in *Aspergillus* virulence. *PLOS One* **6**: e19325.
- CINGOLANI, P., A. PLATTS, L. L. WANG, M. COON, N. TUNG *et al.*, 2012 A program for annotating and predicting the effects of single nucleotide polymorphisms, SnpEff: SNPs in the genome of *Drosophila melanogaster* strain w(1118); iso-2; iso-3. *Fly* **6**: 80-92.
- COUSIN, A., R. MEHRABI, M. GUILLEROUX, M. DUFRESNE, T. VAN DER LEE *et al.*, 2006 The MAP kinase-encoding gene *MgFus3* of the non-appressorium phytopathogen *Mycosphaerella graminicola* is required for penetration and in vitro pycnidia formation. *Molecular Plant Pathology* **7**: 269-278.

- CROLL, D., M. ZALA and B. A. McDONALD, 2013 Breakage-fusion-bridge cycles and large insertions contribute to the rapid evolution of accessory chromosomes in a fungal pathogen. *PLOS Genetics* **9**: e1003567.
- DEPRISTO, M. A., E. BANKS, R. POPLIN, K. V. GARIMELLA, J. R. MAGUIRE *et al.*, 2011 A framework for variation discovery and genotyping using next-generation DNA sequencing data. *Nature Genetics* **43**: 491-501.
- ELIAHU, N., A. IGBARIA, M. S. ROSE, B. A. HORWITZ and S. LEV, 2007 Melanin biosynthesis in the maize pathogen *Cochliobolus heterostrophus* depends on two mitogen-activated protein kinases, *Chk1* and *Mps1*, and the transcription factor *Cmr1*. *Eukaryotic Cell* **6**: 421-429.
- ETTER, P. D., S. BASSHAM, P. A. HOHENLOHE, E. A. JOHNSON and W. A. CRESKO, 2011 SNP discovery and genotyping for evolutionary genetics using RAD sequencing. *Methods in Molecular Biology* **772**: 157-178.
- EYAL, Z., A. L. SCHAREN, J. M. PRESCOTT and M. VAN GINKEL, 1987 The *Septoria* diseases of wheat: concepts and methods of disease management. Mexico, D.F.: CIMMYT.
- FINN, R. D., A. BATEMAN, J. CLEMENTS, P. COGGILL, R. Y. EBERHARDT *et al.*, 2014 Pfam: the protein families database. *Nucleic Acids Research* **42**: D222-D230.
- FLINT, J., and T. F. C. MACKAY, 2009 Genetic architecture of quantitative traits in mice, flies, and humans. *Genome Research* **19**: 723-733.
- FOULONGNE-ORIOU, M., 2012 Genetic linkage mapping in fungi: current state, applications, and future trends. *Appl Microbiol Biotechnol* **95**: 891-904.
- FRIDMAN, E., F. CARRARI, Y. S. LIU, A. R. FERNIE and D. ZAMIR, 2004 Zooming in on a quantitative trait for tomato yield using interspecific introgressions. *Science* **305**: 1786-1789.
- FUJIHARA, N., A. SAKAGUCHI, S. TANAKA, S. FUJII, G. TSUJI *et al.*, 2010 Peroxisome biogenesis factor *PEX13* is required for appressorium-mediated plant infection by the anthracnose fungus *Colletotrichum orbiculare*. *Molecular Plant-Microbe Interactions* **23**: 436-445.
- GODDARD, M. E., and B. J. HAYES, 2009 Mapping genes for complex traits in domestic animals and their use in breeding programmes. *Nature Reviews Genetics* **10**: 381-391.
- GOODWIN, S. B., S. BEN M'BAREK, B. DHILLON, A. H. J. WITTENBERG, C. F. CRANE *et al.*, 2011 Finished genome of the fungal wheat pathogen *Mycosphaerella graminicola* reveals dispensome structure, chromosome plasticity, and stealth pathogenesis. *PLOS Genetics* **7**: e1002070.
- HARDWICK, N. V., D. R. JONES and J. E. SLOUGH, 2001 Factors affecting diseases of winter wheat in England and Wales, 1989-98. *Plant Pathology* **50**: 453-462.

- HENSON, J. M., M. J. BUTLER and A. W. DAY, 1999 The dark side of the mycelium: Melanins of phytopathogenic fungi. *Annual Review of Phytopathology* **37**: 447-471.
- HOLLAND, J. B., 2007 Genetic architecture of complex traits in plants. *Current Opinion in Plant Biology* **10**: 156-161.
- HOWARD, R. J., M. A. FERRARI, D. H. ROACH and N. P. MONEY, 1991 Penetration of hard substrates by a fungus employing enormous turgor pressures. *Proceedings of the National Academy of Sciences of the United States of America* **88**: 11281-11284.
- HU, Y., X. HAO, J. LOU, P. ZHANG, J. PAN *et al.*, 2012 A PKS gene, *pks-1*, is involved in chaetoglobosin biosynthesis, pigmentation and sporulation in *Chaetomium globosum*. *Science China-Life Sciences* **55**: 1100-1108.
- IKEDA, R., T. SUGITA, E. S. JACOBSON and T. SHINODA, 2003 Effects of melanin upon susceptibility of *Cryptococcus* to antifungals. *Microbiology and Immunology* **47**: 271-277.
- IPCHO, S. V. S., J. K. HANE, E. A. ANTONI, D. AHREN, B. HENRISSAT *et al.*, 2012 Transcriptome analysis of *Stagonospora nodorum*: gene models, effectors, metabolism and pantothenate dispensability. *Molecular Plant Pathology* **13**: 531-545.
- JACOBSON, E. S., 2000 Pathogenic roles for fungal melanins. *Clinical Microbiology Reviews* **13**: 708-717.
- KARKOWSKA-KULETA, J., M. RAPALA-KOZIK and A. KOZIK, 2009 Fungi pathogenic to humans: molecular bases of virulence of *Candida albicans*, *Cryptococcus neoformans* and *Aspergillus fumigatus*. *Acta Biochimica Polonica* **56**: 211-224.
- KEMA, G. H. J., S. B. GOODWIN, S. HAMZA, E. C. P. VERSTAPPEN, J. R. CAVALETTO *et al.*, 2002 A combined amplified fragment length polymorphism and randomly amplified polymorphism DNA genetic linkage map of *Mycosphaerella graminicola*, the septoria tritici leaf blotch pathogen of wheat. *Genetics* **161**: 1497-1505.
- KEMA, G. H. J., E. C. P. VERSTAPPEN, M. TODOROVA and C. WAALWIJK, 1996 Successful crosses and molecular tetrad and progeny analyses demonstrate heterothallism in *Mycosphaerella graminicola*. *Current Genetics* **30**: 251-258.
- KIMURA, A., Y. TAKANO, I. FURUSAWA and T. OKUNO, 2001 Peroxisomal metabolic function is required for appressorium-mediated plant infection by *Colletotrichum lagenarium*. *Plant Cell* **13**: 1945-1957.
- KYTE, J., and R. F. DOOLITTLE, 1982 A simple method for displaying the hydropathic character of a protein. *Journal of Molecular Biology* **157**: 105-132.

- LANGFELDER, K., M. STREIBEL, B. JAHN, G. HAASE and A. A. BRAKHAGE, 2003 Biosynthesis of fungal melanins and their importance for human pathogenic fungi. *Fungal Genetics and Biology* **38**: 143-158.
- LANGMEAD, B., and S. L. SALZBERG, 2012 Fast gapped-read alignment with Bowtie 2. *Nature Methods* **9**: 357-U354.
- LARSSON, B., and H. TJALVE, 1979 Studies on the mechanism of drug-binding to melanin. *Biochemical Pharmacology* **28**: 1181-1187.
- LI, H., B. HANDSAKER, A. WYSOKER, T. FENNELL, J. RUAN *et al.*, 2009 The sequence alignment/map format and SAMtools. *Bioinformatics* **25**: 2078-2079.
- LIAW, S. J., Y. L. LEE and P. R. HSUEH, 2010 Multidrug resistance in clinical isolates of *Stenotrophomonas maltophilia*: roles of integrons, efflux pumps, phosphoglucomutase (SpgM), and melanin and biofilm formation. *International Journal of Antimicrobial Agents* **35**: 126-130.
- LIN, S. Y., S. OKUDA, K. IKEDA, T. OKUNO and Y. TAKANO, 2012 *LAC2* encoding a secreted laccase is involved in appressorial melanization and conidial pigmentation in *Colletotrichum orbiculare*. *Molecular Plant-Microbe Interactions* **25**: 1552-1561.
- LIN, X. R., J. C. HUANG, T. G. MITCHELL and J. HEITMAN, 2006 Virulence attributes and hyphal growth of *C. neoformans* are quantitative traits and the MAT alpha allele enhances filamentation. *PLOS Genetics* **2**: 1801-1814.
- LOHSE, M., A. M. BOLGER, A. NAGEL, A. R. FERNIE, J. E. LUNN *et al.*, 2012 RobiNA: a user-friendly, integrated software solution for RNA-Seq-based transcriptomics. *Nucleic Acids Research* **40**: W622-W627.
- MACKAY, T. F. C., 2001 The genetic architecture of quantitative traits. *Annual Review of Genetics* **35**: 303-339.
- MANICHAIKUL, A., J. DUPUIS, S. SEN and K. W. BROMAN, 2006 Poor performance of bootstrap confidence intervals for the location of a quantitative trait locus. *Genetics* **174**: 481-489.
- MEDNICK, A. J., J. D. NOSANCHUK and A. CASADEVALL, 2005 Melanization of *Cryptococcus neoformans* affects lung inflammatory responses during cryptococcal infection. *Infection and Immunity* **73**: 2012-2019.
- MEHRABI, R., S. BEN M'BAREK, T. A. J. VAN DER LEE, C. WAALWIJK, P. J. G. M. DE WIT *et al.*, 2009 G alpha and G beta proteins regulate the cyclic AMP pathway that is required for development and pathogenicity of the phytopathogen *Mycosphaerella graminicola*. *Eukaryotic Cell* **8**: 1001-1013.

- MEHRABI, R., T. VAN DER LEE, C. WAALWIJK and G. H. J. KEMA, 2006a *MgSlt2*, a cellular integrity MAP kinase gene of the fungal wheat pathogen *Mycosphaerella graminicola*, is dispensable for penetration but essential for invasive growth. *Molecular Plant-Microbe Interactions* **19**: 389-398.
- MEHRABI, R., L.-H. ZWIERS, M. A. DE WAARD and G. H. J. KEMA, 2006b *MgHog1* regulates dimorphism and pathogenicity in the fungal wheat pathogen *Mycosphaerella graminicola*. *Molecular Plant-Microbe Interactions* **19**: 1262-1269.
- MORRIS-JONES, R., S. YOUNGCHIM, B. L. GOMEZ, P. AISEN, R. J. HAY *et al.*, 2003 Synthesis of melanin-like pigments by *Sporothrix schenckii* in vitro and mammalian infection. *Infection and Immunity* **71**: 4026-4033.
- NGAMSKULRUNGROJ, P., and W. MEYER, 2009 Melanin production at 37 degrees C is linked to the high virulent *Cryptococcus gattii* Vancouver Island outbreak genotype VGIIa. *Australasian Mycologist* **28**: 9-14.
- NOSANCHUK, J. D., and A. CASADEVALL, 2006 Impact of melanin on microbial virulence and clinical resistance to antimicrobial compounds. *Antimicrobial Agents and Chemotherapy* **50**: 3519-3528.
- NOSANCHUK, J. D., A. L. ROSAS, S. C. LEE and A. CASADEVALL, 2000 Melanisation of *Cryptococcus neoformans* in human brain tissue. *Lancet* **355**: 2049-2050.
- O'DRISCOLL, A., S. KILDEA, F. DOOHAN, J. SPINK and E. MULLINS, 2014 The wheat–Septoria conflict: a new front opening up? *Trends in Plant Science* **19**: 602-610.
- PARISOT, D., M. DUFRESNE, C. VENEULT, R. LAUGE and T. LANGIN, 2002 *Clap1*, a gene encoding a copper-transporting ATPase involved in the process of infection by the phytopathogenic fungus *Colletotrichum lindemuthianum*. *Molecular Genetics and Genomics* **268**: 139-151.
- R_CORE_TEAM, 2012 R: A language and environment for statistical computing. R Foundation for Statistical Computing. Vienna, Austria. ISBN 3-900051-07-0, URL <http://www.R-project.org/>.
- SCHNEIDER, C. A., W. S. RASBAND and K. W. ELICEIRI, 2012 NIH Image to ImageJ: 25 years of image analysis. *Nature Methods* **9**: 671-675.
- SOLOMON, P. S., K. C. TAN, P. SANCHEZ, R. M. COOPER and R. P. OLIVER, 2004 The disruption of a G alpha subunit sheds new light on the pathogenicity of *Stagonospora nodorum* on wheat. *Molecular Plant-Microbe Interactions* **17**: 456-466.

- TABORDA, C. P., M. B. DA SILVA, J. D. NOSANCHUK and L. R. TRAVASSOS, 2008 Melanin as a virulence factor of *Paracoccidioides brasiliensis* and other dimorphic pathogenic fungi: a minireview. *Mycopathologia* **165**: 331-339.
- TAKANO, Y., Y. KUBO, K. SHIMIZU, K. MISE, T. OKUNO *et al.*, 1995 Structural-analysis of *PKS1*, a polyketide synthase gene involved in melanin biosynthesis in *Colletotrichum lagenarium*. *Molecular & General Genetics* **249**: 162-167.
- TAMURA, K., D. PETERSON, N. PETERSON, G. STECHER, M. NEI *et al.*, 2011 MEGA5: molecular evolutionary genetics analysis using maximum likelihood, evolutionary distance, and maximum parsimony methods. *Molecular Biology and Evolution* **28**: 2731-2739.
- TAYLOR, W. R., 1986 The classification of amino-acid conservation. *Journal of Theoretical Biology* **119**: 205-218.
- TSAI, H. F., M. H. WHEELER, Y. C. CHANG and K. J. KWON-CHUNG, 1999 A developmentally regulated gene cluster involved in conidial pigment biosynthesis in *Aspergillus fumigatus*. *Journal of Bacteriology* **181**: 6469-6477.
- TSUJI, G., Y. KENMOCHI, Y. TAKANO, J. SWEIGARD, L. FARRALL *et al.*, 2000 Novel fungal transcriptional activators, Cmr1p of *Colletotrichum lagenarium* and Pig1p of *Magnaporthe grisea*, contain Cys2His2 zinc finger and Zn(II)2Cys6 binuclear cluster DNA-binding motifs and regulate transcription of melanin biosynthesis genes in a developmentally specific manner. *Molecular Microbiology* **38**: 940-954.
- UPADHYAY, S., G. TORRES and X. LIN, 2013 Laccases Involved in 1,8-dihydroxynaphthalene melanin biosynthesis in *Aspergillus fumigatus* are regulated by developmental factors and copper homeostasis. *Eukaryotic Cell* **12**: 1641-1652.
- WAALWIJK, C., O. MENDES, E. C. P. VERSTAPPEN, M. A. DE WAARD and G. H. J. KEMA, 2002 Isolation and characterization of the mating-type idiomorphs from the wheat septoria leaf blotch fungus *Mycosphaerella graminicola*. *Fungal Genetics and Biology* **35**: 277-286.
- WITTENBERG, A. H. J., T. A. J. VAN DER LEE, S. BEN M'BAREK, S. B. WARE, S. B. GOODWIN *et al.*, 2009 Meiosis Drives Extraordinary Genome Plasticity in the Haploid Fungal Plant Pathogen *Mycosphaerella graminicola*. *Plos One* **4**.
- YOUNGCHIM, S., R. MORRIS-JONES, R. J. HAY and A. J. HAMILTON, 2004 Production of melanin by *Aspergillus fumigatus*. *Journal of Medical Microbiology* **53**: 175-181.

ZHAN, J., G. H. J. KEMA, C. WAALWIJK and B. A. McDONALD, 2002 Distribution of mating type alleles in the wheat pathogen *Mycosphaerella graminicola* over spatial scales from lesions to continents. Fungal Genetics and Biology **36**: 128-136.

Table 1 Genetic map summary for the cross between *Zymoseptoria tritici* isolates 3D1 and 3D7.

Chromosome	No. of markers	Average marker spacing (cM)	Genetic length covered by markers (cM)	Physical length covered by markers (kb)	Ratio of physical distance to genetic distance (kb/cM)	Percentage of reference genome covered by markers (%)
1	1906	0.299	569.3	5885	10.34	97
2	1129	0.338	381.7	3755	9.84	97
3	987	0.364	358.6	3409	9.51	97
4	811	0.355	287.9	2816	9.78	98
5	553	0.775	427.8	2730	6.38	95
6	775	0.357	276.1	2533	9.17	95
7	429	0.555	237.6	2574	10.83	97
8	836	0.317	264.5	2347	8.87	96
9	543	0.465	252.1	2075	8.23	97
10	149	1.386	205.2	1487	7.24	88
11	252	0.759	190.4	1522	7.99	94
12	365	0.55	200.2	1361	6.8	93
13	400	0.723	288.5	1044	3.62	88
16	48	0.792	37.2	455	12.24	75
17	192	0.501	95.8	439	4.59	75
19	173	0.48	82.5	470	5.69	85
20	197	0.51	99.9	429	4.29	91
Total	9745	0.437	4255.4	35331	Average 7.97	Average 92

Table 2 Genetic map summary for the cross between *Zymoseptoria tritici* isolates 1A5 and 1E4.

Chromosome	No. of markers	Average marker spacing (cM)	Genetic length covered by markers (cM)	Physical length covered by markers (kb)	Ratio of physical distance to genetic distance (kb/cM)	Percentage of reference genome covered by markers (%)
1	1336	0.612	817.5	5813	7.11	95
2	743	0.59	437.8	3712	8.48	96
3	695	0.738	512.5	3419	6.67	98
4	494	0.796	392.5	2806	7.15	97
5	504	0.753	378.7	2657	7.02	93
6	468	0.769	359.2	2495	6.95	93
7	522	0.725	377.7	2574	6.82	97
8	528	0.591	311.6	2329	7.47	95
9	421	0.699	293.7	2056	7.00	96
10	366	0.711	259.4	1634	6.30	97
11	212	0.975	205.7	1521	7.40	94
12	95	0.743	69.8	515	7.38	35
13	263	1.038	272	1069	3.93	90
14	55	1.314	71	620	8.74	80
15	160	0.797	126.7	509	4.01	80
16	29	1.297	36.3	434	11.96	71
18	43	1.348	56.6	492	8.70	86
19	113	0.877	98.2	494	5.03	90
20	106	0.76	79.8	398	4.99	84
21	180	0.192	34.4	279	8.10	68
Total	7333	0.708	5191.3	35827	Average 7.06	Average 87

Table 3 Positions and effects of the six cross-specific QTLs identified in cross 3D1 x 3D7.

Environment	Colony age (dpi)	QTL peak marker ^a	Chromosome	Estimated position of peaking marker (cM)	Estimated position of peaking marker (kb)	LOD score at peak	P-value	Mean 3D1 allele (grey value)	Mean 3D7 allele (grey value)	Mean difference	Allele effect ^b	Percentage of variance explained by QTL (%)	Estimated position of proximal marker (kb) ^c	Estimated position of distal marker (kb) ^c	Bayes confidence interval length (kb)
Cold	8	12_143193	12	5.74	143	4.85	0.002	134.56	129.28	5.27	3D1	9.2	29	305	276
Cold	11	8_1250811	8	140.32	1251	4.07	0.01	101.72	112.39	10.66	3D7	7.1	897	2228	1332
Cold	11	c10.loc108 (p)	10	108.13	649	9.55	< 0.001	116.28	100.17	16.11	3D1	15.6	634	673	39
Control	8	c11.loc82 (p)	11	82.06	581	32.2	< 0.001	118	93.73	24.27	3D1	39.2	560	603	43
Control	11	5_871061	5	157.26	871	4.38	0.003	74.99	85.47	10.48	3D7	7.5	449	2799	2350
Fungicide	14	1_1740191	1	193.5	1740	3.64	0.014	64.87	73.03	8.16	3D7	6.3	1063	4267	3203

^a A (p) indicates that a pseudomarker provided the highest LOD score. In all other cases a true marker provided the highest LOD score.

^b 3D7 indicates that the parental 3D7 allele provided the higher phenotypic mean then the parental 3D1 allele, while 3D1 indicates that the parental 3D1 allele provided the higher phenotypic mean then the parental 3D7 allele.

^c Markers flanking Bayes confidence interval.

Table 4 Positions and effects of the six cross-specific QTLs identified in cross 1A5 x 1E4.

Environment	Colony age (dpi)	QTL peak marker ^a	Chromosome	Estimated position of peaking marker (cM)	Estimated position of peaking marker (kb)	LOD score at peak	P-value	Mean 1A5 allele (grey values)	Mean 1E4 allele (grey values)	Mean difference	Allele effect ^b	Percentage of variance explained by QTL (%)	Estimated position of proximal marker (kb) ^c	Estimated position of distal marker (kb) ^c	Bayes confidence interval length (kb)
Cold	8	c3.loc208 (p)	3	208.04	1301	8.52	< 0.001	133.71	138.79	5.08	1E4	12.1	869	1749	880
Cold	11	8_429575	8	58.42	430	7.65	< 0.001	117.28	103.6	13.68	1A5	12.8	348	446	99
Cold	14	7_841106	7	181.47	841	4.01	0.014	103.42	93.3	10.13	1A5	7	428	1893	1464
Cold	8	c2.loc226 (p)	2	226.07	1699	10	< 0.001	139.11	133.43	5.69	1A5	17	1646	1819	173
Fungicide	14	c4.loc54 (p)	4	54.04	420	9.47	< 0.001	92.37	111.73	19.36	1E4	16.2	417	426	9
Fungicide	14	6_2299166	6	289.62	2299	3.56	0.027	108.33	96	12.33	1A5	6.2	1166	2438	1272

^a A (p) indicates that a pseudomarker provided the highest LOD score. In all other cases a true marker provided the highest LOD score.

^b 1E4 indicates that the parental 1E4 allele provided the higher phenotypic mean then the parental 1A5 allele, while 1A5 indicates that the parental 1A5 allele provided the higher phenotypic mean then the parental 1E4 allele.

^c Markers flanking Bayes confidence interval.

Table 5 Phenotypic contributions and distribution of all significant QTLs.

Cross ^a	Environment	Colony age (dpi)	Chromosomes with QTL	Allele effect ^b	Total percentage of variance explained by QTL(s) (%)	Number of significant QTLs
3D1 x 3D7 °	Cold	8	10, 12	3D1(2)	22.8	2
3D1 x 3D7 °	Cold	11	8, 10, 11	3D1(2), 3D7(1)	30.1	3
3D1 x 3D7	Control	8	11	3D1(1)	39.2	1
3D1 x 3D7 °	Control	11	5, 11	3D1(1), 3D7(1)	45.7	2
3D1 x 3D7 °	Control	14	5, 11	3D1(1), 3D7(1)	36.5	2
3D1 x 3D7	Fungicide	8	11	3D1(1)	45.8	1
3D1 x 3D7	Fungicide	11	11	3D1(1)	30.4	1
3D1 x 3D7 °	Fungicide	14	1, 2	3D1(1), 3D7(1)	33.5	2
					Average:	Average:
					35.5	1.8
1A5 x 1E4 °	Cold	8	1, 2, 3	1A5(1), 1E4(2)	35.4	3
1A5 x 1E4 °	Cold	11	1, 2, 5, 8	1A5(3), 1E4(1)	43.6	4
1A5 x 1E4 °	Cold	14	1, 3, 5, 7, 8	1A5(4), 1E4(1)	45.9	5
1A5 x 1E4 °	Control	8	1, 2	1A5(2)	18.1	2
1A5 x 1E4	Control	11	1	1E4(1)	10.9	1
1A5 x 1E4 °	Control	14	1, 3, 4, 5, 11	1A5(1), 1E4(4)	42.4	5
1A5 x 1E4 °	Fungicide	8	2, 4	1A5(1), 1E4(1)	25.2	2
1A5 x 1E4 °	Fungicide	11	1, 2, 3, 4	1A5(1), 1E4(3)	40.6	4
1A5 x 1E4 °	Fungicide	14	1, 2, 3, 4, 6, 11	1A5(3), 1E4(3)	55.5	6
					Average:	Average:
					35.3	3.6

^a A ° refers to ECAM phenotypes with at least two significant QTLs, while no ° refers to ECAM phenotypes with only one significant QTL.

^b 3D7/1E4 indicates that the parental 3D7/1E4 allele provided the higher phenotypic mean contribution than the parental 3D1/1A5 allele, while 3D1/1A5 indicates that the parental 3D1/1A5 allele provided the higher phenotypic mean contribution than the parental 3D7/1E4 allele. The number within brackets following the parental allele indicates the number of significant QTLs.

Table 6 Genes associated with melanization that were identified as candidate genes within the 6 cross-specific QTLs in each cross.

Cross	Environment	Colony age (dpi)	LOD score at peak	Chromosome	Estimated position of peaking marker (kb)	Estimated position of proximal marker (kb) ^a	Estimated position of distal marker (kb) ^a	Orthologs to genes involved in melanin biosynthesis found ^b
3D1 x 3D7	Cold	8	4.85	12	143	29	305	/
3D1 x 3D7	Cold	11	4.07	8	1251	897	2228	/
3D1 x 3D7	Cold	11	9.55	10	649	634	673	/
3D1 x 3D7	Control	8	32.2	11	581	560	603	<i>PRF1, PKS1</i>
3D1 x 3D7	Control	11	4.38	5	871	449	2799	<i>PEX13, LAC4, LAC8</i>
3D1 x 3D7	Fungicide	14	3.64	1	1740	1063	4267	<i>MgSlit2, CLAP1, MgGpa1, PEX6</i>
1A5 x 1E4	Cold	8	8.52	3	1301	869	1749	/
1A5 x 1E4	Cold	11	7.65	8	430	348	446	/
1A5 x 1E4	Cold	14	4.01	7	841	428	1893	/
1A5 x 1E4	Cold	8	10	2	1699	1646	1819	/
1A5 x 1E4	Fungicide	14	9.47	4	420	417	426	/
1A5 x 1E4	Fungicide	14	3.56	6	2299	1166	2438	<i>MgFus3, AYG2</i>

^a Markers flanking Bayes confidence interval.

^b Orthologs to genes involved in melanin biosynthesis found as candidate genes in Bayes confidence interval.

Table 7 Large-effect QTL intervals containing ≤ 30 candidate genes.

Cross	Environment	Colony age (dpi)	Chromosome	Estimated position of peaking marker (kb)	LOD score at peak	P-value	Estimated position of proximal marker (kb) ^a	Estimated position of distal marker flanking (kb) ^a	Bayes confidence interval length (kb)	Number of sequence variations ^b	Number of genes ^b	Number of genes affected by sequence variations ^b	Percentage of total genes affected by sequence variations (%) ^b	Number of sequence variation affected genes with unknown function ^b	Percentage of total sequence variation affected genes with unknown function (%) ^b
3D1 x 3D7	Cold	11	10	649	9.55	< 0.001	634	673	39	59	15	12	80	2	17
3D1 x 3D7	Control	8	11	581	32.2	< 0.001	560	603	43	8	14	4	29	0	0
1A5 x 1E4	Fungicide	14	4	420	9.47	< 0.001	417	426	9	7	2	1	50	0	0
1A5 x 1E4	Cold	11	8	430	7.65	< 0.001	348	446	99	132	27	22	81	9	41

^a Markers flanking Bayes confidence interval.

^b Numbers refer to within Bayes confidence interval.

Table 8 Most reproducible QTLs in the two crosses.

Cross	Environment	Colony age (dpi)	Chromosome	LOD score at peak	P-value	Number of peaks confirming the QTL out of a possible 9
3D1 x 3D7	Cold	11	10	9.55	< 0.001	2
3D1 x 3D7	Control	8	11	32.2	< 0.001	7
1A5 x 1E4	Cold	8	3	8.52	< 0.001	5
1A5 x 1E4	Cold	11	8	7.65	< 0.001	2
1A5 x 1E4	Cold	8	2	10	< 0.001	6
1A5 x 1E4	Fungicide	14	4	9.47	< 0.001	4

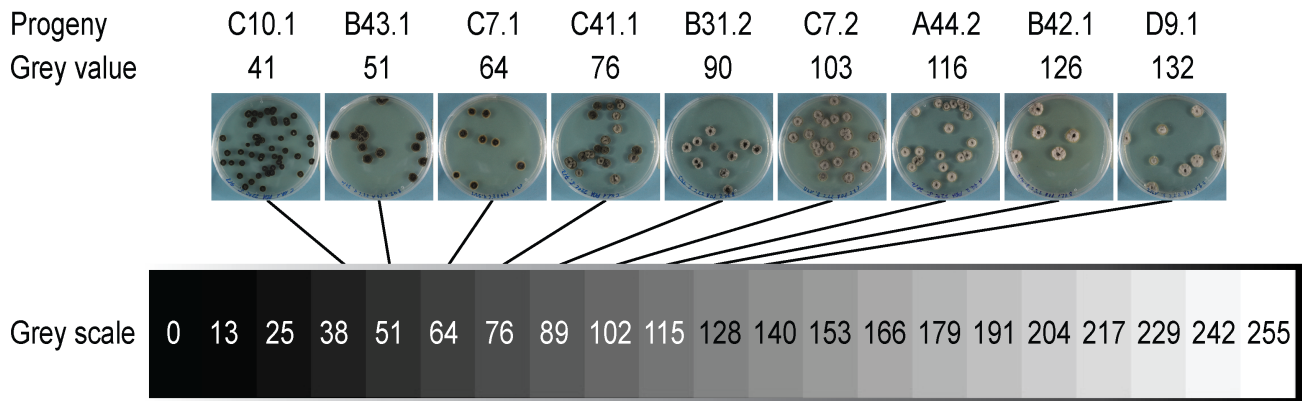


Figure 1 Colony melanization was measured by digital image analyses of grey scale values ranging from 0 (black) to 255 (white). Images from the control environment at 14 dpi for representative progeny from the cross 1A5 x 1E4 are positioned onto the scale to illustrate the different degrees of melanization observed in the crosses. Each image is labeled with the corresponding progeny name (top) and the corresponding grey value (bottom) as measured in the images. The grey values shown represent the full phenotypic variance found under the control environment at 14 dpi in the progeny from the cross 1A5 x 1E4.

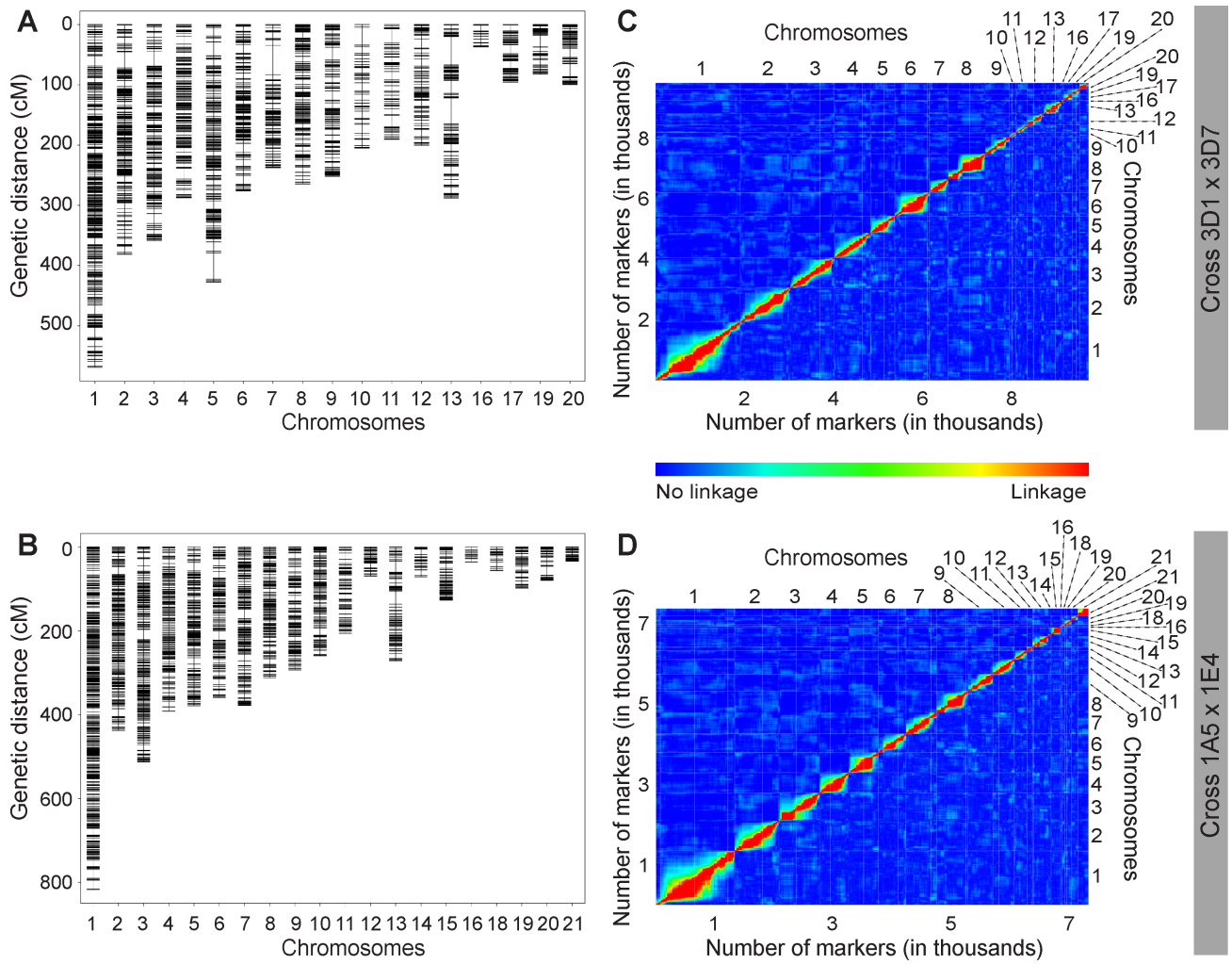


Figure 2 (A, B) Genetic maps and (C, D) pairwise linkage comparisons of markers for each cross (Top: 3D1 x 3D7; Bottom: 1A5 x 1E4). (C, D) Within the pairwise linkage comparison plot marker-pairwise recombination fractions are shown in the upper left triangle and LOD scores for tests of $r = \frac{1}{2}$ are shown in the lower right triangle. Red corresponds to a large LOD or a small recombination fraction, while blue is the reverse. Thus red indicates linkage, whilst blue indicates no linkage.

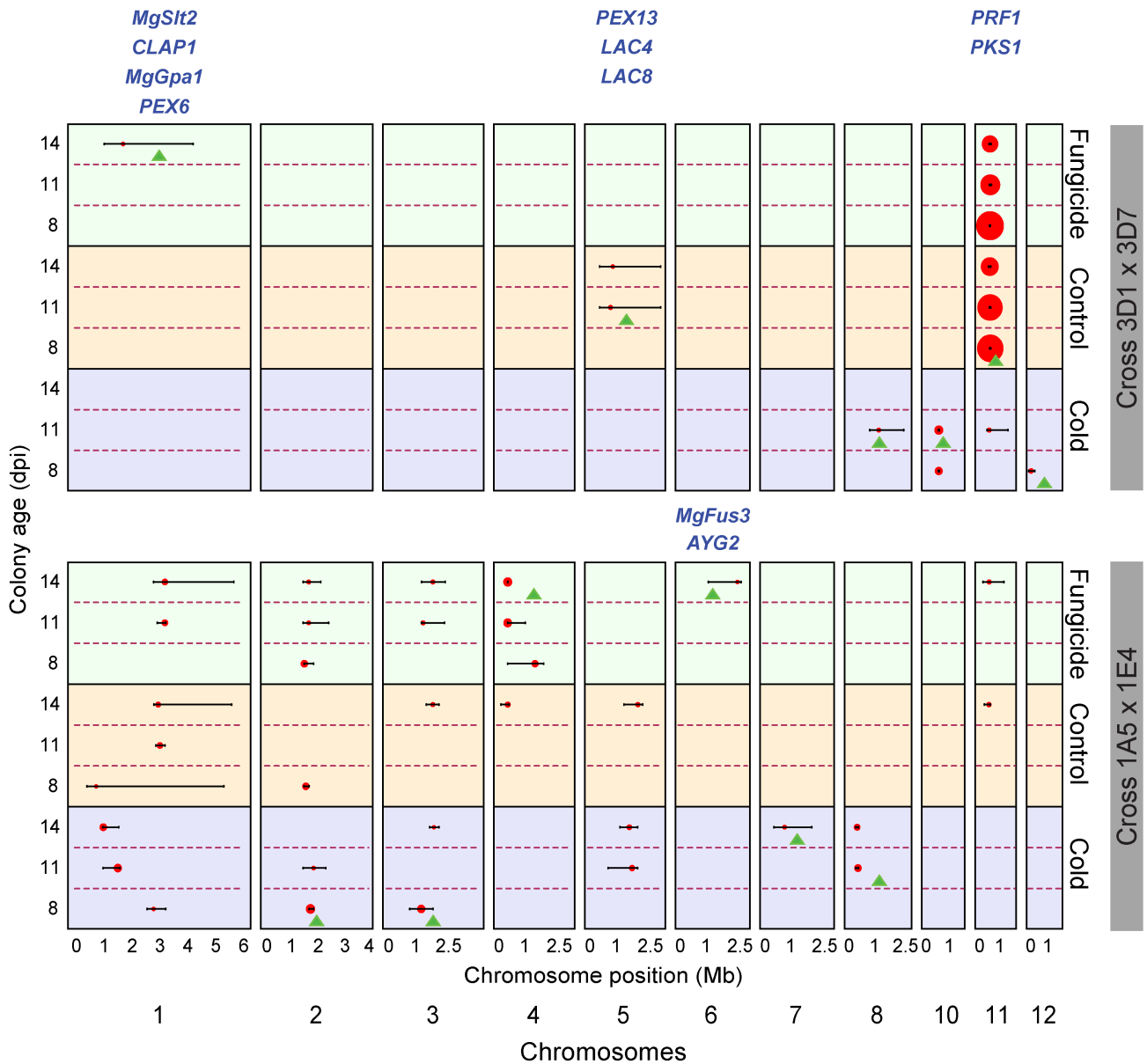


Figure 3 QTL peaks (red dots) and associated confidence intervals for all significant QTLs detected in the experiment. Cross 3D1 x 3D7 is shown in the upper half and cross 1A5 x 1E4 is shown in the lower half of the figure. Environments are color-coded: green = fungicide stress environment; orange = control environment; purple = cold stress environment. Colony age increases within each environment from the bottom up. The different sizes of red dots represent the relative size of the associated LOD scores. The 12 cross-specific QTLs are marked with a green triangle. Orthologs involved in melanin biosynthesis found within 12 cross-specific QTL confidence intervals as candidate genes are indicated with names in blue positioned above the corresponding chromosome. Chromosome sizes are presented in mega base pairs (Mb).

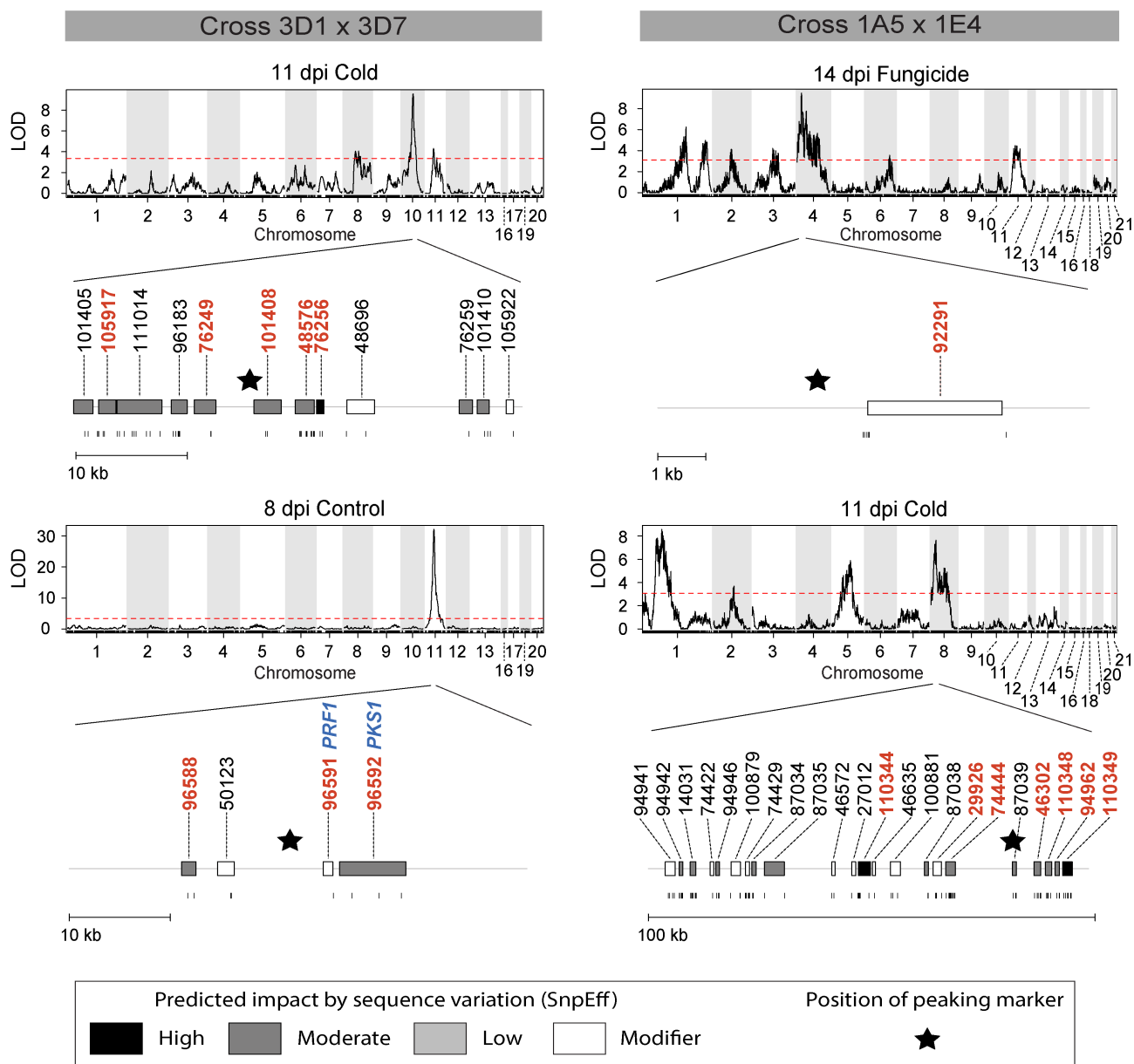
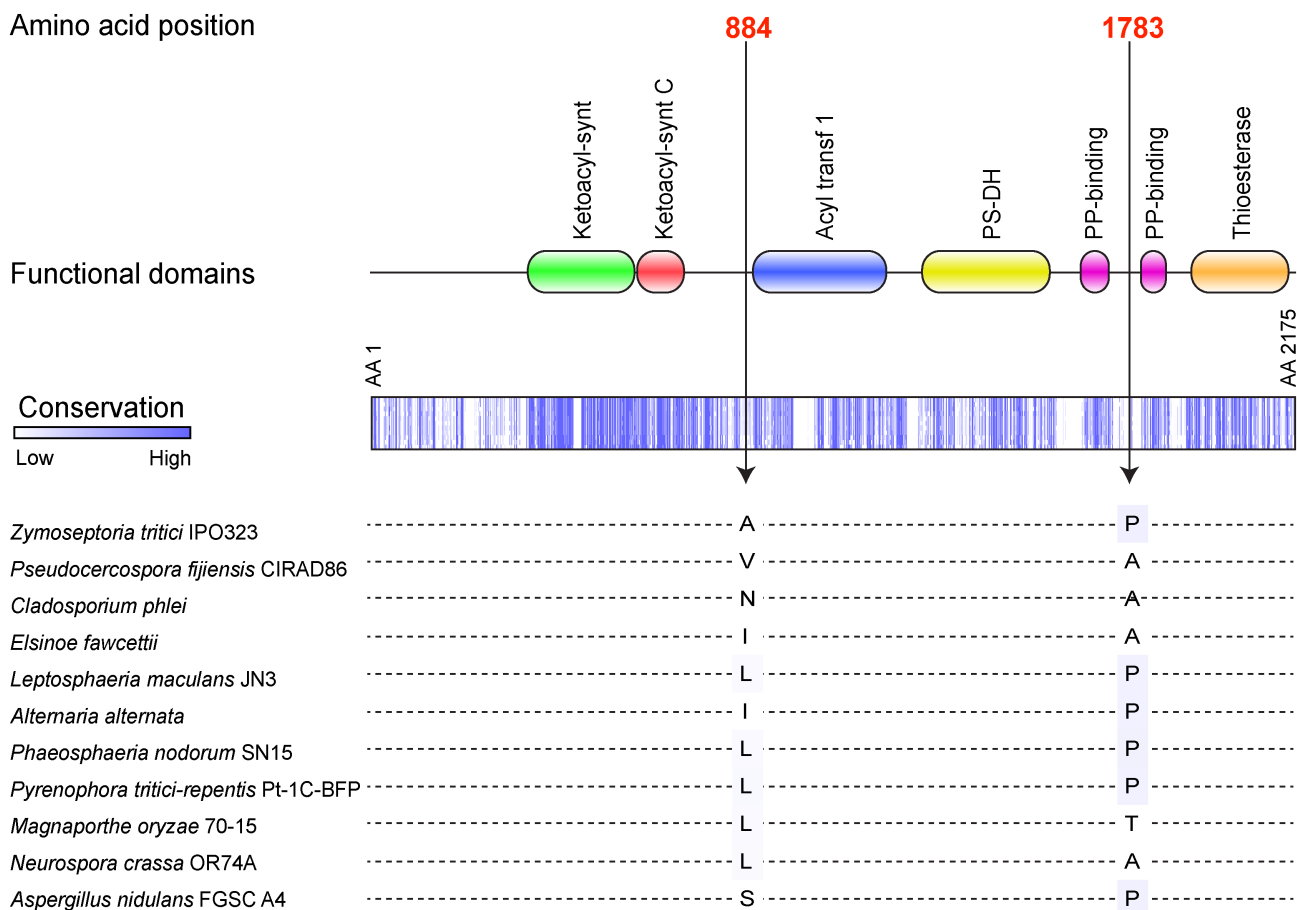


Figure 4 LOD plots from the single marker interval mapping (SIM) analysis over all chromosomes for the phenotypes that provided the peaks with confidence interval containing the smallest number (≤ 30) of candidate genes. The horizontal dashed red line in the LOD plots represents the significance threshold ($p = 0.05$) obtained by 1000 genome-wide permutations. Below each LOD plot is the confidence interval (grey line) for the peak with the fewest candidate genes (gene bars), which are positioned within the confidence interval. The genes are color coded according to the predicted impact by SnpEff of the observed sequence variation (white = modifier, light grey = low (no case within the confidence interval shown), grey = moderate, black= high) and labeled with their protein ID just above the gene bars. Below the gene bars are vertical lines, representing the position of each sequence variant within a gene. The asterisk symbol represents the position of the peaking marker within the confidence interval. Orthologs to genes involved in melanin biosynthesis found as candidate genes within the confidence interval are represented by their name in blue, just above the corresponding protein ID. High-priority candidate genes are colored in red.

Parent 3D1 amino acid	Alanine (A)	Proline (P)
Polarity / hydrophathy index / acidity	nonpolar / 1.8 / neutral	nonpolar / - 1.6 / neutral

Parent 3D7 amino acid	Valine (V)	Threonine (T)
Polarity / hydrophathy index / acidity	nonpolar / 4.2 / neutral	polar / - 0.7 / neutral

Amino acid position



Frequency among 25 *Z. tritici* field isolates

15 A vs. 10 V

24 P vs. 1 T

Figure 5 PKS1 amino acid alterations between parent 3D1 and 3D7 and a schematic diagram of the entire PKS1 gene (2175 amino acids). The two investigated amino acid alterations at position 884 and 1783 are indicated on the gene, showing their positions relative to the predicted functional domain sites. The lower panel shows polymorphisms present among 11 ascomycetes as well as 25 genetically distinct *Z. tritici* field isolates from Switzerland.

SUPPORTING MATERIAL

All supplementary files for this chapter are available online. Please refer to:
www.g3journal.org/content/early/2014/10/29/g3.114.015289/suppl/DC1

CHAPTER 3

QTL Mapping of Fungicide Sensitivity Reveals Novel Genes and Pleiotropy with Melanization in the Pathogen *Zymoseptoria tritici*

Mark H. Lendenmann, Daniel Croll and Bruce A. McDonald

Published online in Fungal Genetics and Biology (2015). DOI: 10.1016/j.fgb.2015.05.001. Accepted 04.05.2015.

ABSTRACT

A major problem associated with the intensification of agriculture is the emergence of fungicide resistance. Azoles are ergosterol biosynthesis inhibitors that have been widely used in agriculture and medicine since the 1970s, leading to emergence of increasingly resistant fungal populations. The known genetic mechanisms underlying lower azole sensitivity include mutations affecting the *CYP51* gene that encodes the target protein, but in many cases azole resistance is a more complex trait with an unknown genetic basis. We used quantitative trait locus (QTL) mapping to identify genes affecting azole sensitivity in two crosses of *Zymoseptoria tritici*, the most damaging wheat pathogen in Europe. Restriction site associated DNA sequencing (RADseq) was used to genotype 263 (cross 1) and 261 (cross 2) progeny at ~8500 single nucleotide polymorphisms (SNP) and construct two dense linkage maps. Azole sensitivity was assessed using high-throughput digital image analysis of colonies growing on Petri dishes with or without the fungicide propiconazole. We identified three QTLs for azole sensitivity, including two that contained novel fungicide sensitivity genes. One of these two QTLs contained only 16 candidate genes, among which four most likely candidates were identified. The third QTL contained *ERG6*, encoding another protein involved in ergosterol biosynthesis. Known genes in QTLs affecting colony growth included *CYP51* and *PKS1*, a gene affecting melanization in *Z. tritici*. *PKS1* showed compelling evidence for pleiotropy, with a rare segregating allele that increased melanization while decreasing growth rate and propiconazole sensitivity. This study resolved the genetic architecture of an important agricultural trait and led to identification of novel genes that are likely to affect azole sensitivity in *Z. tritici*. It also provided insight into fitness costs associated with lowered azole sensitivity and suggests a novel fungicide mixture strategy.

INTRODUCTION

One consequence of intensification of agriculture is an increase in fungicide use worldwide. Concomitant with increased fungicide use has been the often-rapid emergence of resistance against most classes of fungicides used in agricultural ecosystems. In some cases, entire fungicide classes are no longer effective as a result of resistance evolution (ANDERSON 2005; BRENT and HOLLOMON 2007; DEISING *et al.* 2008). The genetic basis of resistance is well known for some fungicide classes (BRENT and HOLLOMON 2007) but for other fungicides, including the ergosterol biosynthesis inhibitors commonly used in both agriculture and medicine, resistance generally has a complex genetic architecture that is poorly understood (COOLS and FRAAIJE 2013; COOLS *et al.* 2013).

The imidazole and triazole fungicides inhibit P450 14 α -demethylase, a key enzyme involved in ergosterol biosynthesis and encoded by *CYP51/ERG11* (COOLS and FRAAIJE 2008). Known mechanisms for resistance to azole fungicides include 1) sterol biosynthesis alterations (JOSEPHHORNE *et al.* 1995), 2) mutations and 3) elevated expression of the *CYP51* gene that encodes the targeted protein (COOLS *et al.* 2011; COOLS *et al.* 2012) as well as 4) reduction of fungicide concentration in the fungal cell due to increased active efflux, due to increased expression of genes encoding membrane transporters, such as ATP-binding cassette (ABC) transporters and major facilitators (ZWIERS *et al.* 2002; STERGIOPOULOS *et al.* 2003; ZWIERS *et al.* 2003; ROOHPARVAR *et al.* 2007). These mechanisms can act alone or in combination to produce resistant strains (HIGGINS 2007; COOLS *et al.* 2013). Azole sensitivity appears to be a polygenic trait in many fungi (COOLS *et al.* 2013).

QTL mapping enables the identification and characterization of chromosomal segments affecting quantitative traits, leading ultimately to the genes and quantitative trait nucleotides (QTNs) encoding these traits (MACKAY 2001). QTL mapping provides a powerful and unbiased forward genetic approach to determine the genetic architecture of fungicide sensitivity and identify novel mechanisms contributing to fungicide resistance. Because the known azole sensitivity mechanisms and underlying genes are unable to fully explain the phenotypic variance observed in natural field populations of plant pathogens (ZWIERS *et al.* 2002; STERGIOPOULOS *et al.* 2003; ZWIERS *et al.* 2003; COOLS *et al.* 2007; COOLS and FRAAIJE 2013; COOLS *et al.* 2013), we used QTL mapping to seek novel genes involved in azole sensitivity. To our knowledge this is the first study to use QTL mapping to identify molecular determinants of fungicide sensitivity in a filamentous ascomycete.

Zymoseptoria tritici is a globally distributed pathogen that causes Septoria tritici blotch (STB) on wheat. It is the most damaging wheat pathogen in Europe (JORGENSEN *et al.* 2014). *Z. tritici* has

shown an impressive capacity to rapidly evolve resistance to fungicides (FRAAIJE *et al.* 2005; COOLS *et al.* 2007; TORRIANI *et al.* 2009; COOLS and FRAAIJE 2013; ESTEP *et al.* 2014). This high evolutionary potential is likely due to the regular cycles of recombination, high effective population sizes and high gene flow associated with field populations of this pathogen (McDONALD and LINDE 2002; ZHAN *et al.* 2003; ZHAN and McDONALD 2004; STUKENBROCK and McDONALD 2008). Control relies mainly on deployment of fungicides and resistant wheat cultivars. However, a lack of commercially viable STB-resistant wheat cultivars has led to a heavy reliance on fungicides in Europe. The azoles are one of the few classes of systemic fungicides still providing adequate control of STB in Europe (COOLS *et al.* 2007). Although azoles have been widely and intensively used in European agriculture since their introduction in 1970, resistance to imidazoles and triazoles was slow to develop and was not considered important in *Z. tritici* until recently. The slow emergence of resistance may reflect high fitness costs associated with lower azole sensitivity (COOLS *et al.* 2013). The current strategy to manage azole resistance is to mix azoles with succinate dehydrogenase inhibitors and/or multisite inhibitors (O'DRISCOLL *et al.* 2014).

We used two mapping populations derived from four Swiss wild-type strains to identify QTLs involved in azole sensitivity. Candidate genes and candidate QTNs within 95% QTL confidence intervals were identified based on complete genome sequences available for all four parents. We coupled restriction site associated DNA sequencing (RADseq) with high-throughput digital image analysis to identify QTLs affecting growth and fungicide sensitivity in both crosses. We showed that fungicide sensitivity in *Z. tritici* is a quantitative trait affected by several genes in addition to the *CYP51* gene that encodes the azole target site, which until now has been the primary explanation for the quantitative nature of this trait (COOLS and FRAAIJE 2013; COOLS *et al.* 2013). We also gained novel insight into pathogen fitness costs associated with resistance.

MATERIAL AND METHODS

Mapping populations, genotyping, genetic maps, gene expression

Methods used for mapping and gene expression were described earlier (BRUNNER *et al.* 2013; LENDENMANN *et al.* 2014). Briefly, two crosses were made between four *Z. tritici* isolates. Isolate ST99CH3D1 (3D1: SRS383146) was crossed to ST99CH3D7 (3D7: SRS383147) and ST99CH1A5 (1A5: SRS383142) was crossed to ST99CH1E4 (1E4: SRS383143). Cross 3D1 x 3D7 produced 359 progeny and cross 1A5 x 1E4 produced 341 progeny. We used restriction site associated DNA sequencing (RADseq) (BAIRD *et al.* 2008) to identify segregating single nucleotide polymorphism (SNP) markers. RADseq SNPs in the parental strains were confirmed using parental genome sequences (CROLL *et al.* 2013). The linkage map was constructed using R/qtl version 1.27-10 (ARENDS *et al.* 2010). RNA-Seq data were obtained for parent 3D7 as described earlier (BRUNNER *et al.* 2013). Transcription profiles were obtained for all genes associated with azole sensitivity as well as candidate genes identified within QTL confidence intervals. NCBI Short Read Archive accession numbers for the retained progeny within each cross can be found in Table S1.

Phenotyping

Fungicide sensitivity was measured using a growth rate assay on Petri plates. Methods used to produce spores and spore suspensions and to inoculate plates were described earlier (LENDENMANN *et al.* 2014). Growth rates of all isolates (progeny and parents) were measured on potato dextrose agar (PDA, 4 g/L potato starch, 20 g/L dextrose, 15 g/L agar) plates either amended or without a fungicide. The amended plates contained 0.75 mg/L (= 0.75 ppm) propiconazole (Syngenta, Basel, Switzerland). After inoculation, plates were sealed with Parafilm and randomized in a growth chamber set to 22°C with 70% humidity and no light. Plates were photographed at 8, 11 and 14 days post inoculation (dpi) for digital image analysis. Images were captured through the Petri dish lid using standardized camera settings and lighting environments described earlier (LENDENMANN *et al.* 2014). After image capture, Petri dishes were re-randomized and returned to the growth chamber for further incubation and later image acquisition. Digital images were processed using a batch macro developed in the open-source software ImageJ (SCHNEIDER *et al.* 2012). Image analysis identified and scored individual colonies in the images, avoiding any fused colonies. Individual colonies were measured for area (mm²) as well as grey values, which represent degrees of melanization (LENDENMANN *et al.* 2014).

Five technical repeats (= five Petri plates) were conducted for each isolate. The data point from a technical repeat was the average colony area or grey value from an average of nine single spore colonies scored per Petri dish and colony age. The average colony area of the five technical repeats was calculated for each treatment and colony age. We calculated broad-sense heritability (H^2) (BURTON and DEVANE 1953) based on area means of the five technical repeats for both treatments at each colony age using a one-way ANOVA model in R (R_CORE_TEAM 2012). Based on previous studies of filamentous fungi that showed a linear increase of colony radius over time (TRINCI 1969; TRINCI 1971; FEDOROVA *et al.* 2008), we used a linear model to calculate the radial growth rate for each isolate in both treatments. The average colony radius for each isolate and colony age was calculated by dividing the average colony area by π and taking the square root. The radial growth rate (mm day^{-1}) for each isolate was measured by plotting the colony radius over time and applying a general linear model using Pearson's correlation coefficient in R. The slope of the regression line is the radial growth rate. The average fit (r^2) of the model was higher than 99% across both crosses and treatments, indicating that the linear model was appropriate to calculate radial growth rate (Figure S1). Fungicide sensitivity was calculated by dividing the radial growth rate measured on the fungicide-amended media by the radial growth rate measured for the fungicide-free control. This experimental design resulted in two traits based on absolute values (radial growth rate in the presence and absence of fungicide) and one trait based on a relative value (relative growth rate coefficient = fungicide sensitivity). All three traits were used in the QTL analysis. The absolute and relative phenotypes for the retained progeny within each cross can be found in Table S2.

QTL mapping

QTL mapping was based on simple interval mapping (SIM) analysis. Significant logarithm of odds (LOD) values were calculated by applying 1000 genome-wide permutations. Only significant QTL peaks with LOD scores that provided P-values lower than 0.05 were considered in further analyses. The reference IPO323 genome (GOODWIN *et al.* 2011) was used to convert cM positions of markers into base pair (bp) positions on the reference genome. 95% confidence intervals were calculated using Bayesian credible intervals (MANICHAIKUL *et al.* 2006). A more detailed description of QTL mapping methods was provided earlier (LENDENMANN *et al.* 2014).

Our experimental design included both radial growth rate and colony melanization (LENDEMANN *et al.* 2014). Since melanization was associated with resistance to antimicrobial compounds (LARSSON and TJALVE 1979; BUTLER and DAY 1998; IKEDA *et al.* 2003; NOSANCHUK and CASADEVALL 2006; TABORDA *et al.* 2008; LIAW *et al.* 2010), pleiotropy amongst the traits growth rate, fungicide sensitivity and melanization was investigated by overlapping full SIM genome scans and conducting linear regressions amongst these traits using a general linear model in R with Pearson's correlation coefficient. Marker allele effects were calculated using R/qtl to confirm the linear regressions.

Sterol 14 α -demethylase CYP51 gene characterization

The azole propiconazole inhibits sterol 14 α -demethylase, an enzyme essential for the biosynthesis of mycoosterols. This enzyme is encoded by *CYP51* (Protein ID: 110231, Joint Genome Institute), which is also called *CYP74* and *ERG11*. Current knowledge on azole resistance in *Z. tritici* (COOLS *et al.* 2013) indicates that resistance mechanisms are due mainly to amino acid alterations within Cyp51 (COOLS and FRAAIJE 2013) or insertions within the *CYP51* promoter that lead to overexpression (COOLS *et al.* 2012). *CYP51* sequence polymorphisms amongst the parents were identified using parental Illumina resequencing reads (CROLL *et al.* 2013). Reads were aligned to the reference genome using the short-read aligner Bowtie 2 version 2.0.2 (LANGMEAD and SALZBERG 2012). Sequence variants were identified using the Genome Analysis Toolkit (GATK) version 2.6-4-g3e5ff60 (DEPRISTO *et al.* 2011). SNPs associated with synonymous and non-synonymous mutations were called using the GATK UnifiedGenotyper with a maximum alternative allele setting of two. Filter settings in the GATK VariantFiltration were as follows: QD \geq 5, FS \leq 60, HaplotypeScore \leq 10.0, QUAL \geq 100, AFlower \geq 0.2, AFupper \leq 0.8 and AN \geq 2. For all other sequence variants we used default settings of the GATK tools. Sequence variants were annotated using the open-source tools SnpEff and SnpSift (Version 3.3h) (CINGOLANI *et al.* 2012). The *CYP51* promoter region as well as codon deletions were investigated using a *de novo* assembly for each parent that was aligned to the reference genome (TORRIANI *et al.* 2011).

We used ARMS-PCR (YE *et al.* 2001) to differentiate parental *CYP51* alleles in the progeny of cross 3D1 x 3D7 using the following primers: 3D7_SNP_Forward: 5'-CTCGGAGTCTTGCAAGTTGC-3'; 3D1_SNP_Reverse: 5'-GTCATGGCCACTAACAGGC-3'; 3D7_GENE_Reverse: 5'-TCTTGGAGGAGTTCGTCTTG-3'; 3D1_GENE_Forward: 5'-GGAAAAGTGAAGGACGTCAA-3'. PCR

conditions were as follows: 10 min at 96°C for initial denaturation followed by 36 cycles of 45 s denaturation at 96°C, 30 s annealing at 57°C and 45 s extension at 72°C. The final extension step was set for 10 min at 72°C. Primers were designed to generate either a 360 bp or a 635 bp amplicon depending on which parental allele was present in the offspring. This allowed identification of a SNP positioned at 950 bp within the *CYP51* gene. The PCR products were loaded onto 1% agarose gels, stained with ethidium bromide and scored visually. We used a one-way ANOVA model to calculate the phenotypic variance explained by this marker, as well as a Wilcoxon rank-sum test to address significant mean differences between the marker alleles in R (R_CORE_TEAM 2012).

Identification of candidate genes within QTL confidence intervals

Methods used to identify candidate genes within QTL confidence intervals were described earlier (LENDEMANN *et al.* 2014). All QTL confidence intervals were screened for 24 genes already associated with azole sensitivity (Table S3). These known genes included genes encoding the ergosterol biosynthesis pathway in *Z. tritici* (COOLS *et al.* 2007; COOLS *et al.* 2012; COOLS and FRAAIJE 2013), as well as genes associated with transmembrane transport, respiration and transcriptional regulation. These genes were identified based on differences in gene expression amongst strains differing in fungicide sensitivity, up-regulation of transcriptional activity in the presence of fungicide (STERGIOPOULOS *et al.* 2003; COOLS *et al.* 2007) or validated by yeast transformation or knock-out (KO) studies (ZWIERS *et al.* 2002; ROOHPARVAR *et al.* 2007).

In addition to the 24 known genes we scanned QTL confidence intervals for novel candidate genes associated with hypothesized fungicide sensitivity functions, including sterol biosynthesis, respiration, drug resistance, ABC transporters, drug transporters, drug efflux, major facilitators and transcription factors. These candidates were identified using corresponding search terms in the reference IPO323 genome (GOODWIN *et al.* 2011). We searched for genes associated with ABC transporters and major facilitators as these genes are known to be involved in fungicide sensitivity in other fungi (PEREA *et al.* 2001; TENREIRO *et al.* 2002; TENREIRO *et al.* 2005), as well as azole sensitivity in *Z. tritici* (ZWIERS *et al.* 2002; ZWIERS *et al.* 2003; ROOHPARVAR *et al.* 2007). Genes associated with respiration were also taken into account. Although the effect of azoles on mitochondrial functions has not yet been clearly established, an association was made between ergosterol biosynthesis and mitochondrial respiration (DAUM *et al.* 1998).

Phenotypic comparisons of important allele combinations

We compared fungicide sensitivity phenotypes among progeny of the 3D1 x 3D7 cross according to the four allele combinations found for the ARMS-PCR marker located within *CYP51* and the *PKS1* marker (RADseq marker 11_535446). The four allelic combinations were as follows: *CYP51LS-PKS1LS*, *CYP51LS-PKS1HS*, *CYP51HS-PKS1LS* and *CYP51HS-PKS1HS*, where LS was the allele associated with lower mean sensitivity and HS was the allele associated with higher mean sensitivity. Among the 263 progeny, 64 were *CYP51LS-PKS1LS*, 56 were *CYP51LS-PKS1HS*, 55 were *CYP51HS-PKS1LS* and 45 were *CYP51HS-PKS1HS*. 43 progeny were not included in this analysis because of missing data. We used a Kruskal-Wallis rank sum test to model the overall effects of the different allele combinations. To investigate significant mean differences ($p \leq 0.05$) amongst groups of allele combinations, we conducted pairwise comparisons of the different allele combinations using Tukey's honest significant differences test.

RESULTS

The genetic architecture of azole sensitivity

Broad-sense heritability (H^2) for the colony average area was high (>70%) for both crosses and treatments, indicating low environmental variance amongst the 5 technical repeats (Figure S1). For both crosses we found that all three traits showed a continuous distribution consistent with a quantitative character. Many progeny had more extreme phenotypes than the parents, consistent with transgressive segregation (Figure S2).

QTLs were considered different if their confidence intervals did not overlap. For the fungicide sensitivity trait, we identified one significant QTL in cross 3D1 x 3D7 and two QTLs in cross 1A5 x 1E4, with each QTL located on a different chromosome (Figure 1, Figure 2, Table 1 and Table 2). For growth rate in the presence or absence of propiconazole, we identified three QTLs in cross 3D1 x 3D7 and three QTLs in cross 1A5 x 1E4 (Table 1 and Table 2). The confidence intervals overlapped for a QTL on chromosome 2 in both crosses (Table S4 and Table S5), suggesting that one QTL may be shared in the two crosses. No QTLs were found on accessory chromosomes. The variance for each trait explained by the significant QTLs averaged ~24% in both crosses (Table 3). A detailed description of all significant QTLs is presented in Tables S4, S5, S6 and S7.

Identification and characterization of candidate genes within QTL confidence intervals

We investigated all annotated genes within each QTL 95% confidence interval, excluding all genes that lacked sequence variation or with only synonymous SNPs. A summary of the number of candidate genes found for cross 3D1 x 3D7 is given in Table S6. Table S7 summarizes the number of candidate genes found in cross 1A5 x 1E4. On average we found ~170 candidate genes per confidence interval, with a minimum of 16 candidate genes (chromosome 8, fungicide sensitivity, cross 1A5 x 1E4, Table 4) and a maximum of 327 genes (chromosome 4, growth rate fungicide present, 1A5 x 1E4). On average ~40% of the candidate genes had no known function (Table S6 and Table S7).

In cross 3D1 x 3D7 (Figure 1, Table 1) we found two candidate genes (Table 5) among the 24 genes already associated with azole sensitivity (Table S3). These two genes encode the Erg6 and Cyp51 proteins involved in the ergosterol biosynthesis pathway. *ERG6* (Protein ID 70113) encodes a sterol C-24 methyltransferase catalyzing the conversion of zymosterol to fecosterol. *CYP51* (Protein ID 110231) encodes a sterol 14 α -demethylase converting lanosterol to 4,4"-dimethyl cholesta-

8,14,24-triene-3-beta-ol (COOLS *et al.* 2007). Cyp51 is a known target enzyme of the triazole class of fungicides, including propiconazole. None of the 24 azole sensitivity-associated genes were found in the five QTLs mapped in cross 1A5 x 1E4 (Figure 2, Table 2), but each QTL confidence interval contained other candidate genes potentially associated with fungicide sensitivity (Table 5).

To further narrow the search for candidate genes having a large effect on fungicide sensitivity we focused on major QTLs (LOD > 7.0) containing \leq 30 candidate genes in their confidence intervals. We identified one confidence interval associated with the fungicide sensitivity trait on chromosome 8 in cross 1A5 x 1E4. This QTL contains a total of 16 candidate genes (Table S7), none of which has been previously associated with azole sensitivity in *Z. tritici* (Table 5). This QTL was therefore subjected to more detailed investigation (Table 4, Figure 3).

Identification of CYP51 as a candidate gene within the chromosome 7 QTL confidence interval

Among the 24 genes associated with azole sensitivity (Table S3), *CYP51* (Protein ID 110231) is the only gene which has been extensively studied to determine the effects of sequence variants in *Z. tritici* (COOLS and FRAAIJE 2013). Because *CYP51* emerged as a candidate gene in a mapped QTL confidence interval (chromosome 7, growth rate fungicide present) in cross 3D1 x 3D7 (Table 5), we intensively investigated sequence variants amongst the parents for this gene. The 3D7 parent carried an amino acid substitution (V136A) previously associated with decreased azole sensitivity (LEROUX *et al.* 2007; COOLS *et al.* 2011). The 3D1 parent carried two amino acid substitutions (L50S and N513K) hypothesized to decrease azole sensitivity, though no clear effect was established in *Z. tritici* (COOLS and FRAAIJE 2013) (Table 6). A recent study (COOLS *et al.* 2012) showed that a 120 bp insertion within the predicted *CYP51* promoter region, which starts at 83 bp upstream from the start codon, reduced azole sensitivity. In the region 450 bp upstream from the start of *CYP51* we found a 1 bp insertion at 72 bp upstream in 3D7 and an 8 bp insertion at 89 bp upstream in 3D1. The corresponding sequences of the 1A5 x 1E4 parents were identical to the reference genome isolate IPO323. Based on these findings, we hypothesized that the quantitative trait nucleotide (QTN) at amino acid position 136 found amongst the parents 3D1 and 3D7 is the main source of phenotypic variance mapped on chromosome 7. V136A without the presence of Δ Y459/G460 codon deletions was shown to be lethal (COOLS and FRAAIJE 2013; COOLS *et al.* 2013). The Δ Y459/G460 deletions are common in modern *Z. tritici* populations, associated with lower azole sensitivity (BRUNNER *et al.* 2008; COOLS *et al.* 2010), and were found in all four parents (Table 6).

Because none of the RADseq markers fell directly within the *CYP51* gene, we used an ARMS-PCR SNP marker positioned within *CYP51* at 257 kb from the peaking marker of the QTL confidence interval on chromosome 7 and 543 bp from the non-synonymous SNP causing the V136A mutation (Table 1) to model all three traits in the 3D1 x 3D7 cross. Among the 263 assayed progeny, we found 113 alleles from 3D1 and 148 alleles from 3D7, with insufficient amplification from two offspring. The *CYP51* SNP marker explained 6% ($p < 0.01$) of the phenotypic variance in growth rate on media with fungicide, but <2% of the variance for growth rate on media without fungicide ($p < 0.05$) or the fungicide sensitivity trait ($p > 0.05$) (Table 7).

Evidence for pleiotropy on chromosome 11 in cross 3D1 x 3D7

Because melanization has been associated with fungicide resistance (BUTLER and DAY 1998; NOSANCHUK and CASADEVALL 2006; TABORDA *et al.* 2008), we sought evidence for pleiotropy by comparing genome scans as well as conducting correlation analysis amongst traits. Based on our earlier finding that the *PKS1* gene (Protein ID 96592) is the most likely candidate explaining the melanization QTL in cross 3D1 x 3D7 on chromosome 11 (LENDEMANN *et al.* 2014), we hypothesized a pleiotropic effect with the fungicide sensitivity trait. We compared melanization at 11 dpi in the presence or absence of fungicide to growth rate in the presence or absence of fungicide as well as fungicide sensitivity (Figure 4). 11 dpi was chosen for the melanization trait over the other two colony ages (8 and 14 dpi) because it had the highest LOD scores per QTL, indicating the lowest environmental variance at this colony age. The RADseq marker 11_535446, positioned on chromosome 11 at base pair position 535446, is closest to the *PKS1* gene, which carried a putative QTN at amino acid position 1783 (LENDEMANN *et al.* 2014). Thus the 11_535446 marker was used to model for allele effects (Figure 4, Table 8). We found QTL peak overlaps on chromosome 11 including the 11_535446 marker for all traits, accounting for $\geq 5.3\%$ of phenotypic variance (Table 8) as well as significant allelic correlations in cross 3D1 x 3D7. Neither significant linear correlation nor QTL peak overlaps were found amongst the traits in cross 1A5 x 1E4, indicating that other melanization QTLs did not affect fungicide sensitivity (Figure 4).

Phenotypic comparisons of *CYP51* and *PKS1* allele combinations

The four possible combinations of the *CYP51* and *PKS1* alleles explained 6% of the total phenotypic variance of the fungicide sensitivity trait, with the factor 'allele combinations' significant at $p = 0.01$.

The LS-LS allele combination had the highest mean phenotype, the HS-HS combination had the lowest mean and the LS-HS combinations were intermediate for the fungicide sensitivity trait. Mean differences between the two extreme allele combinations (LS-LS vs. HS-HS) were significant ($p = 0.02$) (Figure S3).

DISCUSSION

We used QTL mapping to show that azole sensitivity in *Z. tritici* is a complex trait. Genes not previously associated with azole sensitivity were identified and showed a larger contribution to azole sensitivity than known mutations in *CYP51*. We also found compelling evidence for pleiotropy between azole sensitivity and melanization.

QTLs associated with radial growth rate in the absence of fungicide likely represent genes affecting overall growth of filamentous fungi, including genes involved in respiration, cell wall and membrane synthesis and integrity, hyphal elongation, nutrient uptake and turn-over, biosynthesis of essential amino acids and cell homeostasis. Because we used sublethal fungicide concentrations, QTLs associated with radial growth rate in the presence of fungicide likely include these genes affecting overall growth as well as genes that are activated under fungicide stress (e.g. stress signaling pathways (HAYES *et al.* 2014)) and genes which compensate for the toxic effects associated with the fungicide, by interfering with binding of the fungicide to its target or by activating alternative biosynthetic pathways). Propiconazole is known to inhibit the 14 α -demethylase enzyme encoded by *CYP51*, thus impairing ergosterol biosynthesis, affecting membrane integrity and slowing hyphal growth. Any genes encoding substances that mitigate the effects associated with inhibiting the Cyp51 protein could lie within the fungicide-related QTLs identified in our crosses. Earlier studies (ZWIERS *et al.* 2002; STERGIOPOULOS *et al.* 2003; ZWIERS *et al.* 2003; ROOHPARVAR *et al.* 2007; COOLS *et al.* 2011; COOLS *et al.* 2012; COOLS and FRAAIJE 2013) indicated that mutations affecting Cyp51 structure and expression or increased efflux by membrane transporters are the main mechanisms of resistance against imidazoles and triazoles in *Z. tritici*. Increased efflux is effective for many fungicides and may lead to multidrug resistance (MDR). These mechanisms may also act in combination (HIGGINS 2007; COOLS *et al.* 2013). We hypothesize that each of these mechanisms affect not only fungicide sensitivity, but also cell membrane integrity and cross-membrane transport of inorganic ions, sugars, amino acids, proteins and complex polysaccharides. Hence, these mechanisms affect cell homeostasis (HIGGINS 2001; HIGGINS 2007) and may ultimately explain the phenotypic variance in our mapping populations for growth in both the presence and absence of fungicide.

Comparisons of the genome scans in both mapping populations revealed that all fungicide sensitivity QTLs are associated with QTLs affecting colony growth in the absence of fungicide (Figure 1, Figure 2). This pattern suggests that genes affecting growth rates have a significant impact on

fungicide sensitivity, with faster growth associated with greater sensitivity, indicating a trade-off between growth rate and fungicide sensitivity. Costs associated with fungicide resistance have been widely reported (Anderson, 2005), including in *Z. tritici* (COOLS *et al.* 2013). We hypothesize that slower growth leads to lower ergosterol demand per unit of time, allowing slower growing isolates to be less affected by a sublethal azole dose than faster growing isolates. Other QTLs were uniquely associated with growth in the presence of fungicide, including the QTLs on chromosome 7 in cross 3D1 x 3D7 and on chromosome 10 in cross 1A5 x 1E4. These patterns are consistent with an increase in phenotypic variance amongst the progeny in the mapping populations triggered by the presence of the fungicide. Thus these QTLs may represent genes involved in stress signaling pathways activated by the presence of toxic compounds (HAYES *et al.* 2014) or genes that are differentially regulated in the presence of toxins (HAWKINS *et al.* 2014). However neither of these QTLs were significantly associated with fungicide sensitivity in either cross.

Unique QTLs and shared QTLs were identified by comparing QTLs of the two crosses

We identified one QTL shared amongst the two crosses and seven QTLs that were unique to one of the crosses. For the shared QTL found on chromosome 2 (Table 1, Table 2), we compared the candidate genes found in the corresponding confidence intervals and found that more than 55% of the candidate genes in these confidence intervals were shared, suggesting that the shared QTL could be due to the same gene(s) in each cross. None of the 24 genes associated with azole sensitivity (Table S3) were found within this shared QTL (Table 5). However five genes hypothesized to function in fungicide sensitivity were shared within this QTL (Table 9). We hypothesized that the phenotypic variance mapped to this QTL was due to at least one of these five genes, potentially resulting from shared genetic variation in the two crosses. This hypothesis was supported by the observation that the chromosome 2 QTL behaved the same way in both crosses, with the QTL found for both of the growth rate traits, but not for the fungicide sensitivity trait. We tested this hypothesis by searching for non-synonymous mutations shared amongst the two crosses within these five genes. Two (Protein ID: 84542 and 55137) of the five genes had only non-synonymous mutations that were unique to one cross and were not investigated further, but ~60% of the non-synonymous mutations found in the other three genes (Protein ID: 68128, 108045 and 36282) were shared in both crosses. After taking into account the allele effects associated with the peaking markers in each cross (Table 1, Table 2), only gene 108045 carried shared non-synonymous

mutations consistent with the allele effects shown in both crosses. We thus postulated that gene 108045 is responsible for the chromosome 2 QTL mapped in both crosses.

Gene 108045 encodes a putative ATP-binding cassette (ABC) transporter. ABC transporters are membrane-bound and regulate uptake or efflux of specific compounds by ATP hydrolysis. They exhibit a wide range of substrate specificities (HIGGINS 2001), with known substrates including fungicides, plant metabolites, antibiotics and mycotoxins in *Z. tritici* (ZWIERS *et al.* 2003). ABC transporters are associated with multidrug resistance (MDR) in prokaryotes as well as eukaryotes, including fungi (HIGGINS 2007). Transmembrane transport was shown to be a major source of azole resistance in *Candida albicans* associated with up-regulation of multidrug efflux transporters, including ABC transporters (PEREA *et al.* 2001). ABC transporters were also associated with membrane integrity in *Saccharomyces cerevisiae* (MAHE *et al.* 1996) and were proposed to play a role in membrane integrity of *Z. tritici* (ZWIERS *et al.* 2003). We hypothesize that gene 108045 is involved mainly in membrane integrity in our crosses because it was not associated with a fungicide sensitivity QTL, suggesting it does not directly impact fungicide sensitivity. This hypothesis is supported by findings of an earlier study which found that complementation of *S. cerevisiae* with the ABC transporter *MgAtr5* from *Z. tritici* did not increase resistance to propiconazole, while other ABC transporters did, indicating that some ABC transporters do not affect drug resistance (ZWIERS *et al.* 2003). The RPKM mean value associated with gene 108045 was low and constant (1.0 at 13 dpi; Table 9), suggesting that this is a housekeeping gene expressed at a constant low level throughout the fungal life cycle.

Identification and characterization of candidate genes within QTL confidence intervals

We found only two (Protein ID: 70113 and 110231) of the 24 genes already associated with azole sensitivity (Table S3) within the identified QTL confidence intervals as candidate genes (Table 5). We postulate that both of these genes contributed to the QTLs mapped on the two chromosomes, but each confidence interval contained more than 100 candidate genes and it was not possible to exclude the possibility that other genes in these QTLs contributed to the traits. However, because one of these genes was *CYP51*, encoding a well known target of propiconazole, and because one of the parents carried a mutation (V136A) known to affect azole sensitivity (Table 6), we consider it likely that this gene is the main source of phenotypic variance mapped on chromosome 7 in cross 3D1 x 3D7. Neither of the fungicide sensitivity QTLs mapped in cross 1A5 x 1E4 contained any of the

24 known genes (Table S3), indicating these QTLs contained completely novel fungicide sensitivity genes.

Two QTL confidence intervals on chromosomes 8 and 11 were less than 160 kb in length and contained fewer than 40 candidate genes. We postulate that *PKS1* (Protein ID: 96592), a polyketide synthase involved in synthesis of dihydroxynaphthalene (DHN) melanin, is the gene responsible for the QTL on chromosome 11 in cross 3D1 x 3D7. In this case we have evidence for pleiotropy because *PKS1* was also implicated in a QTL associated with melanization in a previous study (LENDENMANN *et al.* 2014). The chromosome 8 QTL involved in fungicide sensitivity in cross 1A5 x 1E4 had a narrow 95% confidence interval of 88 kb containing only 16 candidate genes, among which we identified four high-priority candidates (Table 4).

The four high-priority candidate genes on chromosome 8 (Table 4) were chosen based on the following criteria: Gene 27012 encodes a protein involved in membrane-bound phospholipid biosynthesis and could represent an alternative pathway that compensates for lost ergosterol production under azole stress, reestablishing membrane integrity. Genes 110344 and 110349 both contain frame shift mutations in one of the parents, with a high resulting impact on their encoded proteins suggested by SnpEff. Gene 74444 contains 10 non-synonymous mutations, representing the highest number of non-synonymous mutations among the 16 candidate genes. Future functional validation, e.g. using knockouts and allele swaps, will be needed to determine if any of these candidate genes explains this QTL.

Identification of CYP51 as a candidate gene within the chromosome 7 QTL confidence interval

We have several lines of evidence indicating that *CYP51* is responsible for the chromosome 7 QTL affecting growth rate in the presence of fungicide in cross 3D1 x 3D7. 1) *CYP51* is a known target of azoles and plays a key role in biosynthesis of ergosterol (COOLS *et al.* 2007). 2) The 3D7 parent carries the V136A substitution known to decrease azole sensitivity (LEROUX *et al.* 2007; COOLS *et al.* 2011). 3) Progeny carrying the alanine at position 136 show lower average propiconazole sensitivity than progeny carrying a valine. 4) The ARMS-PCR marker lying within *CYP51* explained a large fraction of the phenotypic variance for all three traits (Table 7). Taken together, these findings indicate that the V136A substitution in *CYP51* is a likely QTN responsible for the mapped QTL on chromosome 7 in cross 3D1 x 3D7. Though the genome scan revealed a visible peak at the same position for the growth rate in absence of the fungicide (Figure 1), this peak did not reach the

significance threshold. But the ARMS-PCR assay detected a significant effect associated with fungal growth in both the presence and absence of fungicide (Table 7). These findings suggest that the V136A substitution affects growth rates in the presence or absence of fungicides, with more pronounced growth differences in the presence of fungicide. Surprisingly, the alanine variant was associated with faster growth in both presence and absence of the fungicide, suggesting that there was no fitness cost associated with the V136A mutation in our mapping population. Although it is often found that drug resistance mutations impose a fitness cost (ANDERSON 2005), our findings suggest that the V136A mutation, which is lethal in the absence of a $\Delta Y459/G460$ deletion (COOLS and FRAAIJE 2013), shows an opposite pattern. The absence of a fitness cost associated with azole resistance was documented earlier (COWEN *et al.* 2001; ANDERSON *et al.* 2003), but we are not aware of other examples where the resistance mutations accelerated growth in the absence of the fungicide. However we recognize that *in planta* growth rates may differ compared to what we observed on PDA.

We hypothesize that *CYP51* did not generate a significant QTL for the fungicide sensitivity trait because other QTLs (namely, the chromosome 3 and 11 QTLs) made a larger contribution to the overall phenotypic variance in this cross. Overall we interpret the identification of a QTN in *CYP51* as a validation of our QTL mapping strategy, increasing our confidence that the other QTLs identified in these crosses also contain genes likely to significantly affect growth rate and/or fungicide sensitivity.

Indication for pleiotropy on chromosome 11 in cross 3D1 x 3D7

Our analyses indicate that *PKS1*, in particular the postulated QTN at amino acid position 1783 (LENDEMANN *et al.* 2014), is the source of phenotypic variance in the chromosome 11 QTL for four traits, including melanization, growth rate in the presence or absence of fungicide, and fungicide sensitivity (Figure 4, Table 8). This is consistent with a pleiotropic effect as follows: the 3D7 *PKS1* allele increases melanization, leads to slower growth in both the presence and absence of fungicide, but decreases fungicide sensitivity (Figure 5), indicating a fungicide resistance trade-off (ANDERSON *et al.* 2003). This pattern follows the general paradigm that fungal isolates with greater melanization are less sensitive to fungicides (BUTLER and DAY 1998; NOSANCHUK and CASADEVALL 2006; TABORDA *et al.* 2008), with the underlying mechanism thought to be direct binding of melanin to the fungicide (NOSANCHUK and CASADEVALL 2006). Although the involvement of *PKS1* in DHN melanin biosynthesis

and the association between melanin and fungicide resistance was already established (BUTLER and DAY 1998; HU *et al.* 2012), we are not aware of previous work finding a direct association between *PKS1* and fungicide resistance in a filamentous ascomycete. We postulate that mutations in *PKS1* may explain the emergence of azole resistance in other ascomycete fungi. This finding also suggests a novel disease control strategy for *Z. tritici* and other fungi, namely deployment of fungicide mixtures containing both azoles and DHN melanin inhibitors (e.g. tricyclazole and pyroquilon). In this mixture strategy, the function of the melanin inhibitor is not fungicidal, but rather to reduce melanin production and thus lessen the amount of melanin available to inhibit the activity of the azole component of the mixture. For fungi like *Z. tritici* that show significant variation in melanization among field populations (D. Croll, B.A. McDonald, unpublished), we expect that this mixture would be most effective in populations producing high levels of DHN melanin.

Genetic architecture of fungicide sensitivity

The finding that all three traits (radial growth rate in the presence and absence of fungicide and fungicide sensitivity) showed a continuous distribution and exhibited transgressive segregation in both crosses indicates that several genes are likely contributing to each trait. We identified a total of 9 significant QTLs distributed across 7 different chromosomes, with more than one significant QTL identified for all traits except fungicide sensitivity in cross 3D1 x 3D7 (Table 3). On average, each QTL explained 9.8% of the trait variance, with the largest additive effect being 34.5% of the total phenotypic variance explained by the three QTLs affecting growth rate in the absence of fungicide (Table 3). The genome scans revealed several additional peaks that were below the significance threshold (Figure 1 and Figure 2). This leads us to predict that additional QTLs will be revealed in future studies that include a greater number of markers and a larger number of offspring.

In cross 3D1 x 3D7 we found that approximately half of the progeny grew faster on PDA amended with fungicide compared to PDA without fungicide (Figure S2). This phenomenon was observed in previous studies using sublethal fungicide concentrations (TOUBIARAHME *et al.* 1995; KENYON *et al.* 1997; RAMIREZ *et al.* 2004) but it could not be explained. We hypothesized that this pattern reflected additive effects of independently assorting alleles that neutralized the effects of propiconazole at the low concentration used in the experiment. We tested this hypothesis by focusing on the large effect alleles at the *CYP51* and *PKS1* loci associated with growth rate QTLs in

the presence of propiconazole. We found that progeny carrying the V136A low sensitivity (LS) allele of *CYP51* and the P1783T LS allele of *PKS1* grew, on average, significantly faster in the presence of propiconazole than progeny carrying the alternative high sensitivity (HS) alleles. LS:HS offspring had, on average, intermediate growth rates, though their mean growth rates suggest that the *PKS1* contribution was greater than the *CYP51* contribution (Figure S3). The overall pattern is consistent with an additive effect for these loci whereby one contributing LS allele was sufficient to mostly neutralize the effect of propiconazole and two LS alleles were sufficient to completely neutralize its toxic properties at the tested concentration. We propose that earlier observations of strains that grow faster in the presence of sublethal fungicide concentrations also reflect additive effects among loci that neutralize the toxicity of the fungicide.

For the trait fungicide sensitivity, we compared the mean differences and the amount of phenotypic variance explained by the three QTLs mapped on chromosomes 2, 3 and 8 in both crosses (Figure 1, Figure 2, Table 1 and Table 2) versus the mean differences and the amount of variance explained by *CYP51* and *PKS1* (Table 7 and Table 8). This comparison revealed an overall larger contribution, reflected as larger mean differences and higher amounts of variance explained (Table 1, Table 2, Table 7 and Table 8), for the three mapped QTLs than for *CYP51* or *PKS1*. This comparison suggests that these significant QTLs are worthy of additional investigation to determine how they affect azole sensitivity.

Study limitations

We recognize that interpretations of our results are limited by the study design. The QTLs were identified in an *in vitro* context using a single environment. Other QTLs and allele effects might be identified *in planta*, in different growth media or at different fungicide concentrations. We did not directly quantify the relevant gene products, such as ergosterol or melanin, to validate our hypotheses. Additional studies will be needed to differentiate among competing hypotheses and determine if mixtures of azoles and inhibitors of melanin biosynthesis can be effective in practice. In spite of these limitations, we consider our findings to be robust and a good illustration of the potential for QTL mapping to identify the genetic determinants of quantitative traits in fungi.

ACKNOWLEDGMENTS

The research was supported by a grant from the Swiss National Science Foundation (31003A_134755). Technical assistance was provided by Ethan L. Stewart, Michael Mielewczik and Tryggvi S. Stefansson. The RNA-Seq data was kindly provided by Stefano F. F. Torriani. RADseq libraries were constructed at the Genetic Diversity Centre (GDC) and sequenced in the Quantitative Genomics Facility at the Department of Biosystems Science and Engineering (D-BSSE) at the scientific central facilities of ETH Zurich.

REFERENCES

- ANDERSON, J. B., 2005 Evolution of antifungal-drug resistance: Mechanisms and pathogen fitness. *Nature Reviews Microbiology* **3**: 547-556.
- ANDERSON, J. B., C. SIRJUSINGH, A. B. PARSONS, C. BOONE, C. WICKENS *et al.*, 2003 Mode of selection and experimental evolution of antifungal drug resistance in *Saccharomyces cerevisiae*. *Genetics* **163**: 1287-1298.
- ARENDS, D., P. PRINS, R. C. JANSEN and K. W. BROMAN, 2010 R/qtl: high-throughput multiple QTL mapping. *Bioinformatics* **26**: 2990-2992.
- BAIRD, N. A., P. D. ETTER, T. S. ATWOOD, M. C. CURREY, A. L. SHIVER *et al.*, 2008 Rapid SNP discovery and genetic mapping using sequenced rad markers. *PLOS One* **3**: e3376.
- BRENT, K. J., and D. W. HOLLOMON, 2007 Fungicide resistance in crop pathogens: how can it be managed? FRAC Monograph No. 1 (2nd edition). Croplife International, Brussels, Belgium. (http://www.frac.info/frac/publication/ahang/FRAC_Mono1_2007_100dpi.pdf).
- BRUNNER, P. C., F. L. STEFANATO and B. A. McDONALD, 2008 Evolution of the *CYP51* gene in *Mycosphaerella graminicola*: evidence for intragenic recombination and selective replacement. *Molecular Plant Pathology* **9**: 305-316.
- BRUNNER, P. C., S. F. F. TORRIANI, D. CROLL, E. H. STUKENBROCK and B. A. McDONALD, 2013 Coevolution and life cycle specialization of plant cell wall degrading enzymes in a hemibiotrophic pathogen. *Molecular Biology and Evolution* **30**: 1337-1347.
- BURTON, G. W., and E. H. DEVANE, 1953 Estimating heritability in tall fescue (*Festuca-arundinacea*) from replicated clonal material. *Agronomy Journal* **45**: 478-481.
- BUTLER, M. J., and A. W. DAY, 1998 Fungal melanins: a review. *Canadian Journal of Microbiology* **44**: 1115-1136.
- CINGOLANI, P., A. PLATTS, L. L. WANG, M. COON, N. TUNG *et al.*, 2012 A program for annotating and predicting the effects of single nucleotide polymorphisms, SnpEff: SNPs in the genome of *Drosophila melanogaster* strain w(1118); iso-2; iso-3. *Fly* **6**: 80-92.
- COOLS, H. J., C. BAYON, S. ATKINS, J. A. LUCAS and B. A. FRAAIJE, 2012 Overexpression of the sterol 14 alpha-demethylase gene (*MgCYP51*) in *Mycosphaerella graminicola* isolates confers a novel azole fungicide sensitivity phenotype. *Pest Management Science* **68**: 1034-1040.

- COOLS, H. J., and B. A. FRAAIJE, 2008 Are azole fungicides losing ground against Septoria wheat disease? Resistance mechanisms in *Mycosphaerella graminicola*. *Pest Management Science* **64**: 681-684.
- COOLS, H. J., and B. A. FRAAIJE, 2013 Update on mechanisms of azole resistance in *Mycosphaerella graminicola* and implications for future control. *Pest Management Science* **69**: 150-155.
- COOLS, H. J., B. A. FRAAIJE, T. P. BEAN, J. ANTONIW and J. A. LUCAS, 2007 Transcriptome profiling of the response of *Mycosphaerella graminicola* isolates to an azole fungicide using cDNA microarrays. *Molecular Plant Pathology* **8**: 639-651.
- COOLS, H. J., N. J. HAWKINS and B. A. FRAAIJE, 2013 Constraints on the evolution of azole resistance in plant pathogenic fungi. *Plant Pathology* **62**: 36-42.
- COOLS, H. J., J. G. L. MULLINS, B. A. FRAAIJE, J. E. PARKER, D. E. KELLY *et al.*, 2011 Impact of recently emerged sterol 14 alpha-demethylase (CYP51) variants of *Mycosphaerella graminicola* on azole fungicide sensitivity. *Applied and Environmental Microbiology* **77**: 3830-3837.
- COOLS, H. J., J. E. PARKER, D. E. KELLY, J. A. LUCAS, B. A. FRAAIJE *et al.*, 2010 Heterologous expression of mutated eburicol 14 alpha-Demethylase (CYP51) proteins of *Mycosphaerella graminicola* to assess effects on azole fungicide sensitivity and intrinsic protein function. *Applied and Environmental Microbiology* **76**: 2866-2872.
- COWEN, L. E., L. M. KOHN and J. B. ANDERSON, 2001 Divergence in fitness and evolution of drug resistance in experimental populations of *Candida albicans*. *Journal of Bacteriology* **183**: 2971-2978.
- CROLL, D., M. ZALA and B. A. McDONALD, 2013 Breakage-fusion-bridge cycles and large insertions contribute to the rapid evolution of accessory chromosomes in a fungal pathogen. *PLOS Genetics* **9**: e1003567.
- DAUM, G., N. D. LEES, M. BARD and R. DICKSON, 1998 Biochemistry, cell biology and molecular biology of lipids of *Saccharomyces cerevisiae*. *Yeast* **14**: 1471-1510.
- DEISING, H. B., S. REIMANN and S. F. PASCHOLATI, 2008 Mechanisms and significance of fungicide resistance. *Brazilian Journal of Microbiology* **39**: 286-295.
- DEPRISTO, M. A., E. BANKS, R. POPLIN, K. V. GARIMELLA, J. R. MAGUIRE *et al.*, 2011 A framework for variation discovery and genotyping using next-generation DNA sequencing data. *Nature Genetics* **43**: 491-501.

- ESTEP, L. K., S. F. F. TORRIANI, M. ZALA, N. P. ANDERSON, M. D. FLOWERS *et al.*, 2014 Emergence and early evolution of fungicide resistance in North American populations of *Zymoseptoria tritici*. *Plant Pathology* **na**: 1-11.
- FEDOROVA, N. D., N. KHALDI, V. S. JOARDAR, R. MAITI, P. AMEDEO *et al.*, 2008 Genomic islands in the pathogenic filamentous fungus *Aspergillus fumigatus*. *PLOS Genetics* **4**: e1000046.
- FRAAIJE, B. A., H. J. COOLS, J. FOUNTAINE, D. J. LOVELL, J. MOTTERAM *et al.*, 2005 Role of ascospores in further spread of QoI-resistant cytochrome b alleles (G143A) in field populations of *Mycosphaerella graminicola*. *Phytopathology* **95**: 933-941.
- GOODWIN, S. B., S. BEN M'BAREK, B. DHILLON, A. H. J. WITTENBERG, C. F. CRANE *et al.*, 2011 Finished genome of the fungal wheat pathogen *Mycosphaerella graminicola* reveals dispensome structure, chromosome plasticity, and stealth pathogenesis. *PLOS Genetics* **7**: e1002070.
- HAWKINS, N. J., H. J. COOLS, H. SIEROTZKI, M. W. SHAW, W. KNOGGE *et al.*, 2014 Paralog Re-Emergence: A Novel, Historically Contingent Mechanism in the Evolution of Antimicrobial Resistance. *Molecular Biology and Evolution* **31**: 1793-1802.
- HAYES, B. M. E., M. A. ANDERSON, A. TRAVEN, N. L. VAN DER WEERDEN and M. R. BLEACKLEY, 2014 Activation of stress signalling pathways enhances tolerance of fungi to chemical fungicides and antifungal proteins. *Cellular and Molecular Life Sciences* **71**: 2651-2666.
- HIGGINS, C. F., 2001 ABC transporters: physiology, structure and mechanism - an overview. *Research in Microbiology* **152**: 205-210.
- HIGGINS, C. F., 2007 Multiple molecular mechanisms for multidrug resistance transporters. *Nature* **446**: 749-757.
- HU, Y., X. HAO, J. LOU, P. ZHANG, J. PAN *et al.*, 2012 A PKS gene, *pks-1*, is involved in chaetoglobosin biosynthesis, pigmentation and sporulation in *Chaetomium globosum*. *Science China-Life Sciences* **55**: 1100-1108.
- IKEDA, R., T. SUGITA, E. S. JACOBSON and T. SHINODA, 2003 Effects of melanin upon susceptibility of *Cryptococcus* to antifungals. *Microbiology and Immunology* **47**: 271-277.
- JORGENSEN, L. N., M. S. HOVMOLLER, J. G. HANSEN, P. LASSEN, B. CLARK *et al.*, 2014 IPM strategies and their dilemmas including an introduction to www.eurowheat.org. *Journal of Integrative Agriculture* **13**: 265-281.

- JOSEPHHORNE, T., N. J. MANNING, D. HOLLOMON and S. L. KELLY, 1995 Defective sterol delta(5(6))desaturase as a cause of azole resistance in *Ustilago maydis*. *Fems Microbiology Letters* **127**: 29-34.
- KENYON, D. M., G. R. DIXON and S. HELFER, 1997 The repression and stimulation of growth of *Erysiphe* sp. on *Rhododendron* by fungicidal compounds. *Plant Pathology* **46**: 425-431.
- LANGMEAD, B., and S. L. SALZBERG, 2012 Fast gapped-read alignment with Bowtie 2. *Nature Methods* **9**: 357-U354.
- LARSSON, B., and H. TJALVE, 1979 Studies on the mechanism of drug-binding to melanin. *Biochemical Pharmacology* **28**: 1181-1187.
- LENDENMANN, M. H., D. CROLL, E. L. STEWART and B. A. McDONALD, 2014 Quantitative trait locus mapping of melanization in the plant pathogenic fungus *Zymoseptoria tritici*. *G3-Genes Genomes Genetics* **4**: 2519-2533.
- LEROUX, P., C. ALBERTINI, A. GAUTIER, M. GREDT and A.-S. WALKER, 2007 Mutations in the *CYP51* gene correlated with changes in sensitivity to sterol 14 alpha-demethylation inhibitors in field isolates of *Mycosphaerelia graminicola*. *Pest Management Science* **63**: 688-698.
- LIAW, S. J., Y. L. LEE and P. R. HSUEH, 2010 Multidrug resistance in clinical isolates of *Stenotrophomonas maltophilia*: roles of integrons, efflux pumps, phosphoglucosyltransferase (SpgM), and melanin and biofilm formation. *International Journal of Antimicrobial Agents* **35**: 126-130.
- MACKAY, T. F. C., 2001 The genetic architecture of quantitative traits. *Annual Review of Genetics* **35**: 303-339.
- MAHE, Y., Y. LEMOINE and K. KUHLER, 1996 The ATP binding cassette transporters *Pdr5* and *Sng5* of *Saccharomyces cerevisiae* can mediate transport of steroids in vivo. *Journal of Biological Chemistry* **271**: 25167-25172.
- MANICHAIKUL, A., J. DUPUIS, S. SEN and K. W. BROMAN, 2006 Poor performance of bootstrap confidence intervals for the location of a quantitative trait locus. *Genetics* **174**: 481-489.
- MCDONALD, B. A., and C. LINDE, 2002 Pathogen population genetics, evolutionary potential, and durable resistance. *Annual Review of Phytopathology* **40**: 349-379.
- NOSANCHUK, J. D., and A. CASADEVALL, 2006 Impact of melanin on microbial virulence and clinical resistance to antimicrobial compounds. *Antimicrobial Agents and Chemotherapy* **50**: 3519-3528.

- O'DRISCOLL, A., S. KILDEA, F. DOOHAN, J. SPINK and E. MULLINS, 2014 The wheat–Septoria conflict: a new front opening up? *Trends in Plant Science* **19**: 602-610.
- PEREA, S., J. L. LOPEZ-RIBOT, W. R. KIRKPATRICK, R. K. MCATEE, R. A. SANTILLAN *et al.*, 2001 Prevalence of molecular mechanisms of resistance to azole antifungal agents in *Candida albicans* strains displaying high-level fluconazole resistance isolated from human immunodeficiency virus-infected patients. *Antimicrobial Agents and Chemotherapy* **45**: 2676-2684.
- R_CORE_TEAM, 2012 R: A language and environment for statistical computing. R Foundation for Statistical Computing. Vienna, Austria. ISBN 3-900051-07-0, URL <http://www.R-project.org/>.
- RAMIREZ, M. L., S. CHULZE and N. MAGAN, 2004 Impact of environmental factors and fungicides on growth and deoxinivalenol production by *Fusarium graminearum* isolates from Argentinian wheat. *Crop Protection* **23**: 117-125.
- ROOHPARVAR, R., M. A. DE WAARD, G. H. J. KEMA and L.-H. ZWIERS, 2007 MgMfs1, a major facilitator superfamily transporter from the fungal wheat pathogen *Mycosphaerella graminicola*, is a strong protectant against natural toxic compounds and fungicides. *Fungal Genetics and Biology* **44**: 378-388.
- SCHNEIDER, C. A., W. S. RASBAND and K. W. ELICEIRI, 2012 NIH Image to ImageJ: 25 years of image analysis. *Nature Methods* **9**: 671-675.
- STERGIOPOULOS, I., J. G. M. VAN NISTELROOY, G. H. J. KEMA and M. A. DE WAARD, 2003 Multiple mechanisms account for variation in base-line sensitivity to azole fungicides in field isolates of *Mycosphaerella graminicola*. *Pest Management Science* **59**: 1333-1343.
- STUKENBROCK, E. H., and B. A. McDONALD, 2008 The origins of plant pathogens in agro-ecosystems. *Annual Review of Phytopathology* **46**: 75-100.
- TABORDA, C. P., M. B. DA SILVA, J. D. NOSANCHUK and L. R. TRAVASSOS, 2008 Melanin as a virulence factor of *Paracoccidioides brasiliensis* and other dimorphic pathogenic fungi: a minireview. *Mycopathologia* **165**: 331-339.
- TENREIRO, S., P. A. NUNES, C. A. VIEGAS, M. S. NEVES, M. C. TEIXEIRA *et al.*, 2002 *AQR1* gene (ORF *YNL065w*) encodes a plasma membrane transporter of the major facilitator superfamily that confers resistance to short-chain monocarboxylic acids and quinidine in *Saccharomyces cerevisiae*. *Biochemical and Biophysical Research Communications* **292**: 741-748.
- TENREIRO, S., R. C. VARGAS, M. C. TEIXEIRA, C. MAGNANI and I. SA-CORREIA, 2005 The yeast multidrug transporter Qdr3 (Ybr043c): localization and role as a determinant of resistance to quinidine,

- barban, cisplatin, and bleomycin. *Biochemical and Biophysical Research Communications* **327**: 952-959.
- TORRIANI, S. F. F., P. C. BRUNNER, B. A. McDONALD and H. SIEROTZKI, 2009 QoI resistance emerged independently at least 4 times in European populations of *Mycosphaerella graminicola*. *Pest Management Science* **65**: 155-162.
- TORRIANI, S. F. F., E. H. STUKENBROCK, P. C. BRUNNER, B. A. McDONALD and D. CROLL, 2011 Evidence for extensive recent intron transposition in closely related fungi. *Current Biology* **21**: 2017-2022.
- TOUBIARAHME, H., D. E. ALIHAIMOUD, G. BARRAULT and L. ALBERTINI, 1995 Effect of four fungicides on barley net blotch caused by *Drechslera teres*. *Journal of Phytopathology* **143**: 335-339.
- TRINCI, A. P. J., 1969 A kinetic study of growth of *Aspergillus nidulans* and other fungi. *Journal of General Microbiology* **57**: 11-24.
- TRINCI, A. P. J., 1971 Influence of width of peripheral growth zone on radial growth rate of fungal colonies on solid media. *Journal of General Microbiology* **67**: 325-344.
- YE, S., S. DHILLON, X. KE, A. R. COLLINS and I. N. M. DAY, 2001 An efficient procedure for genotyping single nucleotide polymorphisms. *Nucleic Acids Res.* **29**: art. no.-e88.
- ZHAN, J., and B. A. McDONALD, 2004 The interaction among evolutionary forces in the pathogenic fungus *Mycosphaerella graminicola*. *Fungal Genetics and Biology* **41**: 590-599.
- ZHAN, J., R. E. PETTWAY and B. A. McDONALD, 2003 The global genetic structure of the wheat pathogen *Mycosphaerella graminicola* is characterized by high nuclear diversity, low mitochondrial diversity, regular recombination, and gene flow. *Fungal Genetics and Biology* **38**: 286-297.
- ZWIERS, L. H., I. STERGIOPOULOS, M. M. C. GIELKENS, S. D. GOODALL and M. A. DE WAARD, 2003 ABC transporters of the wheat pathogen *Mycosphaerella graminicola* function as protectants against biotic and xenobiotic toxic compounds. *Molecular Genetics and Genomics* **269**: 499-507.
- ZWIERS, L. H., I. STERGIOPOULOS, J. G. M. VAN NISTELROOY and M. A. DE WAARD, 2002 ABC transporters and azole susceptibility in laboratory strains of the wheat pathogen *Mycosphaerella graminicola*. *Antimicrobial Agents and Chemotherapy* **46**: 3900-3906.

Table 1 Positions and effects of the four QTLs identified in cross 3D1 x 3D7.

Trait	Chromosome	Estimated position of peaking marker (cM)	Estimated position of peaking marker (kb)	LOD score at peak	P-value	Mean 3D1 allele (growth rate/fungicide sensitivity)	Mean 3D7 allele (growth rate/fungicide sensitivity)	Mean difference	Allele effect ^a	Percentage of variance explained by QTL (%)	Estimated position of proximal marker (kb) ^b	Estimated position of distal marker (kb) ^b	Bayes confidence interval length (kb)
Growth rate fungicide present	2	119.04	906	4.67	0.003	0.375	0.42	0.045	3D7	8.5	747	1826	1079
Fungicide sensitivity	3	269.05	2914	4.71	0.003	1.024	0.95	0.074	3D1	8.6	2220	3096	876
Growth rate fungicide present	7	130.62	1191	4.41	0.004	0.375	0.418	0.043	3D7	8.3	1078	1607	529
Growth rate fungicide absent	11	78.07	538	10.38	< 0.001	0.452	0.376	0.076	3D1	17.9	435	592	157

^a 3D1 indicates that the 3D1 parent allele provided a higher phenotypic mean than the 3D7 parent allele. 3D7 indicates that the 3D7 parent allele provided a higher phenotypic mean than the 3D1 parent allele.

^b Markers flanking the 95% Bayes confidence interval of the associated QTL.

Table 2 Positions and effects of the five QTLs identified in cross 1A5 x 1E4.

Trait	Chromosome	Estimated position of peaking marker (cM)	Estimated position of peaking marker (kb)	LOD score at peak	P-value	Mean 1A5 allele (growth rate/fungicide sensitivity)	Mean 1E4 allele (growth rate/fungicide sensitivity)	Mean difference	Allele effect ^a	Percentage of variance explained by QTL (%)	Estimated position of proximal marker (kb) ^b	Estimated position of distal marker (kb) ^b	Bayes confidence interval length (kb)
Growth rate fungicide absent	2	188.41	1372	3.71	0.023	0.418	0.365	0.053	1A5	6.5	1122	1829	707
Fungicide sensitivity	2	424.07	3584	3.56	0.027	0.614	0.539	0.075	1A5	5.9	3413	3778	365
Growth rate fungicide absent	4	234.90	1312	6.77	<0.001	0.357	0.427	0.07	1E4	11.6	508	1728	1220
Fungicide sensitivity	8	51.59	388	7.29	<0.001	0.636	0.528	0.108	1A5	12.7	375	463	88
Growth rate fungicide present	10	154.62	1060	3.73	0.013	0.226	0.205	0.021	1A5	6.6	292	1220	928

^a 1A5 indicates that the 1A5 parent allele provided a higher phenotypic mean than the 1E4 parent allele. 1E4 indicates that the 1E4 parent allele provided a higher phenotypic mean than the 1A5 parent allele.

^b Markers flanking the 95% Bayes confidence interval of the associated QTL.

Table 3 Genetic architecture of each trait for both crosses.

Trait	Chromosome with a QTL	Allele effect ^a	Total % variance explained by QTL(s)	Number of significant QTLs	Confirmation of transgressive segregation	Cross
Growth rate fungicide present	2, 7, 11	3D1(1), 3D7(2)	30.1	3	Yes	3D1 x 3D7
Growth rate fungicide absent	2, 3, 11	3D1(1), 3D7(2)	34.5	3	Yes	
Fungicide sensitivity	3	3D1(1)	8.6	1	No	
			Average 24.4	Average 2.3		
Growth rate fungicide present	2, 4, 10	1A5(2), 1E4(1)	24.4	3	Yes	1A5 x 1E4
Growth rate fungicide absent	2, 4, 8	1A5(1), 1E4(2)	27.7	3	Yes	
Fungicide sensitivity	2, 8	1A5(2)	18.6	2	No	
			Average 23.6	Average 2.6		

^a 3D7/1E4 indicates that the parental 3D7/1E4 allele provided the higher phenotypic mean contribution than the parental 3D1/1A5 allele, while 3D1/1A5 indicates that the parental 3D1/1A5 allele provided the higher phenotypic mean contribution than the parental 3D7/1E4 allele. The number within brackets following the parental allele indicates the number of significant QTLs.

Table 4 Genes within a chromosome 8 fungicide sensitivity QTL confidence interval containing ≤ 30 candidate genes for cross 1A5 x 1E4, excluding genes with no sequence variation or with only synonymous SNPs.

Protein ID ^a	Gene ontology Name	Gene ontology biological process	Gene ontology cellular component	Gene ontology molecular function	Number of Non-Syn SNPs ^b	Number of other sequence variations ^{b,c}	Additional information	Highest RPKM mean ^d	RPKM Stdv
87035	DNA binding	transcription, DNA-dependent; response to DNA damage stimulus	membrane	DNA binding; ATP binding; helicase activity	0	1 downstream (m)	Homolog of <i>Saccharomyces cerevisiae</i> INO80, a Swi2/Snf2-related ATPase that forms a large complex, containing actin and several actin-related proteins, that has chromatin remodeling activity and 3' to 5' DNA helicase activity in vitro	36.0 (13 dpi)	6.0
46572 [#]	Not Available	Not Available	Not Available	Not Available	0	1 upstream (m), 1 intron (m)	/	107.2 (7 dpi) [*]	18.9
27012 [°]	phospholipid biosynthetic process	phospholipid biosynthetic process	membrane	phosphotransferase activity, for other substituted phosphate groups	0	2 upstream (m)	Putative CDP-alcohol phosphatidyltransferase. Shows some sequence similarity to cardiolipin synthase. Predicted signal peptide. Predicted membrane localization.	10.0 (7 dpi)	5.5
110344 [°]	Not Available	nuclear mRNA cis splicing, via spliceosome; mRNA transport;	nuclear cap binding complex	RNA cap binding	4 (M)	1 downstream (m), 2 frameshift (H), 1 intron (m)	/	48.6 (13 dpi) [*]	5.2

46635	nucleus	nuclear mRNA splicing, via spliceosome; cellular bud site selection	U2 snRNP	Not Available	0	2 intron (m)	/	69.2 (7 dpi)	25.6
100881	protein kinase activity	protein phosphorylation; serine family amino acid metabolic process	Not Available	ATP binding; protein serine/threonine kinase activity	0	3 intron (m), 1 UTR5 Prime (m)	Name: GSK3 (serine/threonine protein kinase, CMGC family, glycogen synthase kinase subfamily)	180.8 (13 dpi) *	51.8
87038	Not Available	Not Available	Not Available	nucleotide binding	2 (M)	0	/	1.1 (7 dpi)	1.8
29926	Not Available	Not Available	Not Available	Not Available	0	1 upstream (m), 6 intron (m)	/	31.7 (13 dpi) *	3.2
74444 °	tRNA processing	mitochondrial tRNA wobble uridine modification	mitochondrion	flavin adenine dinucleotide binding	10 (M)	2 intron (m)	/	31.5 (7 dpi)	9.5
87039	Not Available	Not Available	membrane	Not Available	3 (M)	0	/	0 (No Specific Day)	0.0
46302	protein kinase activity	protein phosphorylation; serine family amino acid metabolic process	Not Available	ATP binding; protein serine/threonine kinase activity;	4 (M)	4 downstream (m), 2 intron (m)	/	21.6 (13 dpi)	2.0

110348	nucleic acid binding	DNA catabolic process	Not Available	endonuclease activity; nucleic acid binding	7 (M)	0	/	4.5 (7 dpi)	4.5
94962	Not Available	Not Available	Not Available	Not Available	3 (M)	0	/	13.0 (7 dpi) *	7.7
110349 °	Not Available	Not Available	Not Available	Not Available	9 (M)	3 frameshift (H), 3 intron (m)	putative secreted protein unknown function, probably unique to <i>Z. tritici</i>	11.8 (7 dpi)	8.3
74453	hydrolase activity, hydrolyzing O-glycosyl compounds	carbohydrate metabolic process	Not Available	hydrolase activity, hydrolyzing O-glycosyl compounds	1 (M)	0	/	8.8 (7 dpi)	6.3
94965	Not Available	Not Available	Not Available	Not Available	6 (M)	0	/	11.6 (13 dpi)	2.5

^a A # Indicates the QTL peak is positioned closest to this gene or within the gene. A ° Indicates candidate genes with a higher likelihood of contributing to fungicide sensitivity compared to unmarked candidate genes. A § Indicates genes in *Z. tritici* known to be involved in fungicide sensitivity (Table S3).

^b The letter within brackets following the number of a specific sequence polymorphism refers to the likely impact of the sequence polymorphism according to SnpEff. H=high, M=moderate, L=low, m=modifier.

^c Other sequence variations include codon change plus insertion/deletion, codon insertion/deletion, 100 bp upstream or downstream, frameshift, intron, splice site acceptor/donor, start gained/lost, stop gained/lost, untranslated regions (UTR).

^d We chose a RKPM value of 2 as an expression threshold. A * Indicates significant changes in transcript abundances over time in planta.

Table 5 Summary of candidate genes associated with fungicide sensitivity found within QTL confidence intervals.

Cross	Trait	LOD score at peak	Chromosome	Estimated position of peaking marker (kb)	Estimated position of proximal marker (kb) ^a	Estimated position of distal marker (kb) ^a	Number of genes affected by sequence variations ^b	Candidate genes associated with azole sensitivity ^{b,c}	Number of candidate genes associated with functions connected to fungicide sensitivity ^a	Number of candidate genes associated with functions of transcription factor ^b
3D1 x 3D7	Growth rate fungicide present	4.67	2	906	747	1826	245	/	Respiration (1), Drug resistance (1), ABC transport (7), Drug transport (1), Major facilitator (3)	22
	Fungicide sensitivity	4.71	3	2914	2220	3096	224	70113 (S)	Sterol biosynthesis (1), Respiration (4), Drug resistance (2), Major facilitator (5)	20
	Growth rate fungicide present	4.41	7	1191	1078	1607	112	110231 (S)	ABC transport (1), Major facilitator (1)	8
	Growth rate fungicide absent	10.38	11	538	435	592	35	/	Major facilitator (1)	1
1A5 x 1E4	Growth rate fungicide absent	3.71	2	1372	1122	1829	165	/	ABC transport (4), Drug transport (1), Major facilitator (2)	14
	Fungicide sensitivity	3.56	2	3584	3413	3778	75	/	Sterol biosynthesis (1), Respiration (1), ABC transport (1), Major facilitator (1)	6
	Growth rate fungicide absent	6.77	4	1312	508	1728	256	/	Sterol biosynthesis (3), Respiration (2), Respiration (1), ABC transport (5), Drug transport (1), Major facilitator (2)	33
	Fungicide sensitivity	7.29	8	388	375	463	16	/	/	1
	Growth rate fungicide present	3.73	10	1060	292	1220	253	/	Sterol biosynthesis (1), Respiration (5), Respiration (2), ABC transport (3), Drug transport (1), Major facilitator (6)	25

^a Markers flanking the 95% Bayes confidence interval of the associated QTL.

^b Information refers to number of genes within the 95% Bayes confidence interval of the associated QTL.

^c The number refers to the protein ID (JGI) with further gene information found in Table S3. The letter in brackets refers to one of the three functional categories (Sterol biosynthesis (S), mitochondrial electron transport chain (R), transporter (T)) as specified in Table S3.

^d The number of candidate genes is given in brackets following the function search terms.

Table 6 Cyp51 (Protein ID: 110231) variation amongst the parents of each cross.

Parents and wild-type (wt) isolates	Amino acid alteration and position			
	L50S ¹⁾	V136A ²⁾	ΔY459/G460 ³⁾	N513K ¹⁾
3D1 ⁴⁾	S	V	Δ	K
3D7 ⁴⁾	L	A	Δ	N
1A5 ⁵⁾	L	V	Δ	N
1E4 ⁵⁾	L	V	Δ	N
IPO323 (wt)	L	V	Y459/G460	N

¹⁾ No clear effect on *Z. tritici* isolate azole sensitivity (COOLS and FRAAIJE 2013).

²⁾ Common in modern *Z. tritici* populations and clearly associated with contrasting effects on azole sensitivity. Found in combination with changes at Y459 – Y461 (COOLS and FRAAIJE 2013).

³⁾ Common in modern *Z. tritici* populations. Decreased azole sensitivity when expressed in *Saccharomyces cerevisiae* (COOLS and FRAAIJE 2013).

⁴⁾ Additional sequence variations found amongst parents 3D1 and 3D7: 1 downstream and 2 upstream.

⁵⁾ No additional sequence variations found amongst parents 1A5 and 1E4.

Table 7 Summary of CYP51 ARMS-PCR marker modeling for the three traits in cross 3D1 x 3D7.

Trait	Mean 3D1 allele (growth rate/fungicide sensitivity)	Mean 3D7 allele (growth rate/fungicide sensitivity)	Mean difference	Allele effect ^a	Percentage of variance explained by PCR marker (%)	P-value
Growth rate fungicide present	0.38	0.42	0.04	3D7	6.2	< 0.01
Growth rate fungicide absent	0.39	0.42	0.03	3D7	1.9	0.01 - 0.05
Fungicide sensitivity	0.98	1.00	0.02	3D7	1.2	> 0.05

^a 3D1 indicates that the 3D1 parent allele provided a higher phenotypic mean than the 3D7 parent allele. 3D7 indicates that the 3D7 parent allele provided a higher phenotypic mean than the 3D1 parent allele.

Table 8 Summary of allele effects for RADseq marker 11_535446 in cross 3D1 x 3D7.

Trait	Mean 3D1 allele (growth rate/fungicide sensitivity)	Mean 3D7 allele (growth rate/fungicide sensitivity)	Mean difference	Allele effect ^a	Percentage of variance explained by QTL (%)
Melanization fungicide present	96.826	75.054	21.772	3D1	32.6
Melanization fungicide absent	93.697	69.233	24.464	3D1	39.9
Growth rate fungicide present	0.428	0.375	0.053	3D1	12.1
Growth rate fungicide absent	0.452	0.376	0.076	3D1	18.4
Fungicide sensitivity	0.956	1.015	0.059	3D7	5.3

^a 3D1 indicates that the 3D1 parent allele provided a higher phenotypic mean than the 3D7 parent allele. 3D7 indicates that the 3D7 parent allele provided a higher phenotypic mean than the 3D1 parent allele.

Table 9 Shared candidate genes with hypothesized fungicide sensitivity functions within the shared QTL found on chromosome 2.

Protein ID	Fungicide sensitivity associated function	Number of Non-Syn SNPs ^{a,c}	Number of other sequence variations ^{a,c,d}	Number of Non-Syn SNPs ^{b,c}	Number of other sequence variations ^{b,c,d}	Additional information	Highest RPKM mean ^e	RPKM Stdv
68128	Drug transport	5 (M)	2 downstream (m)	7 (M)	0	P450 with unknown function. Comparison with characterized P450s did not yield highly significant matches. This model is 32% identical to a P450 that is part of an ergot-like cluster in <i>A. fumigatus</i> and 28% identical to a P450 that is part the ergot gene cluster in <i>C. purpurea</i> . Similarities with these P450s were found by multiple seq alignment and NJ cluster analysis.	372.1 (56 dpi) [*]	23.1
84542	Major facilitator	3 (M)	1 frame shift (H), 1 intron (m)	0	4 upstream (m), 1 intron (m)	/	8.6 (56 dpi) [*]	1.8
55137	ABC transport	5 (M)	2 upstream (m)	0	1 upstream (m)	/	23.9 (13 dpi)	0.8
108045	ABC transport	12 (M)	1 downstream (m), 1 upstream (m), 4 intron (m)	13 (M)	2 downstream (m), 1 upstream (m), 9 intron (m)	Putative ABC transporter, ABC-C family, MRP type. TC3.A.1.208. These transporters mainly transport conjugated compounds and can be involved in metal resistance.	1.0 (13 dpi)	0.4
36282	Major facilitator	8 (M)	1 frame shift (H), 4 intron (m)	4 (M)	1 upstream (m)	/	0 (No Specific Day)	0.0

^a Data applies to parents 3D1 and 3D7

^b Data applies to parents 1A5 and 1E4

^c The letter within brackets following the number of a specific sequence polymorphism refers to the likely impact of the sequence polymorphism according to SnpEff. H=high, M=moderate, L=low, m=modifier.

^d Other sequence variations include codon change plus insertion/deletion, codon insertion/deletions, 100 bp upstream or downstream, frameshift, intron, splice site acceptor/donor, start gained/lost, stop gained/lost, untranslated regions (UTR).

^e We chose a RPKM value of 2 as an expression threshold. A * Indicates significant changes in transcript abundances over time in planta.

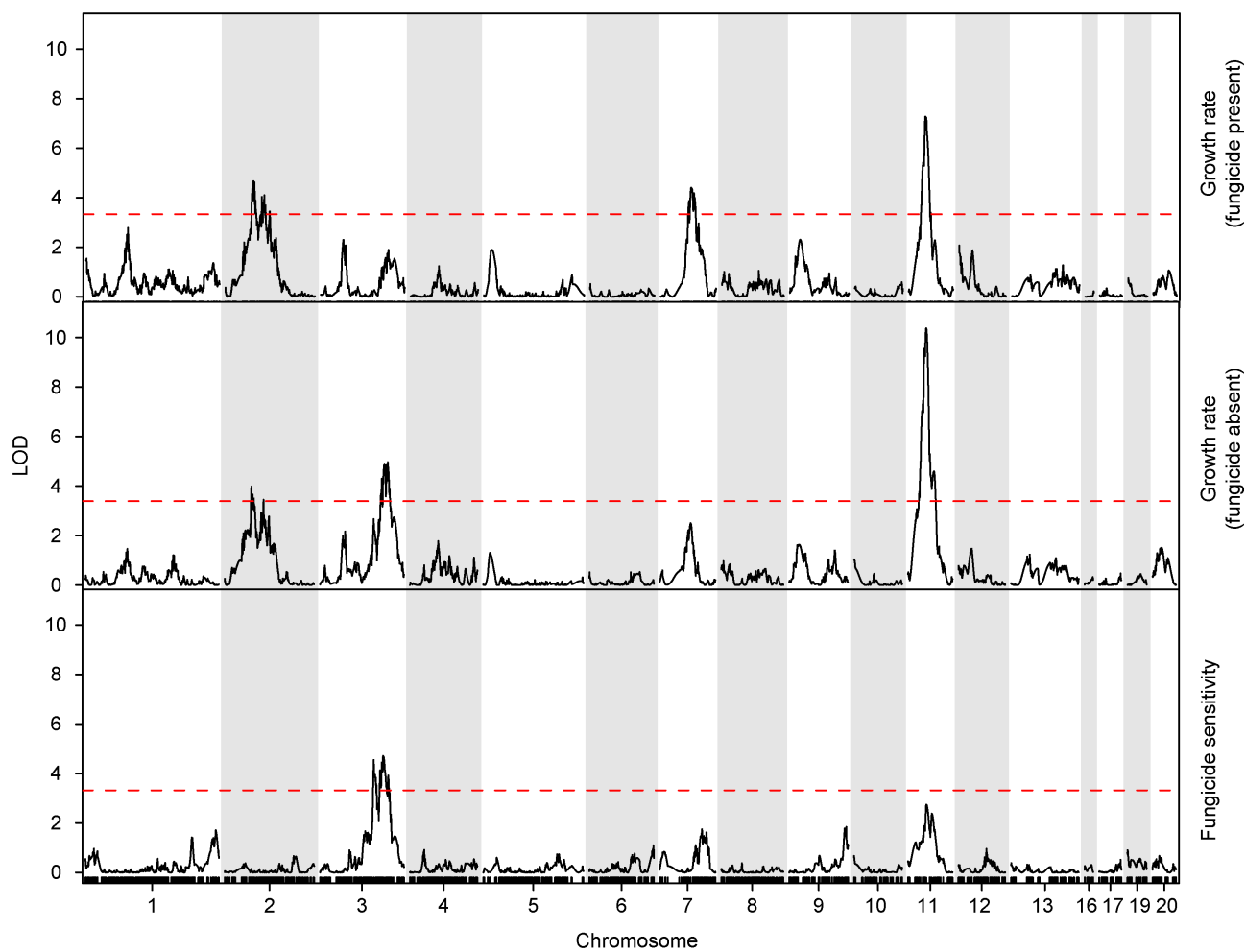


Figure 1 LOD plots from single marker interval mapping (SIM) analysis over all chromosomes for growth rate with and without fungicide and fungicide sensitivity for cross 3D1 x 3D7. The dashed horizontal red line represents the significance threshold ($p = 0.05$) obtained using 1000 genome-wide permutations.

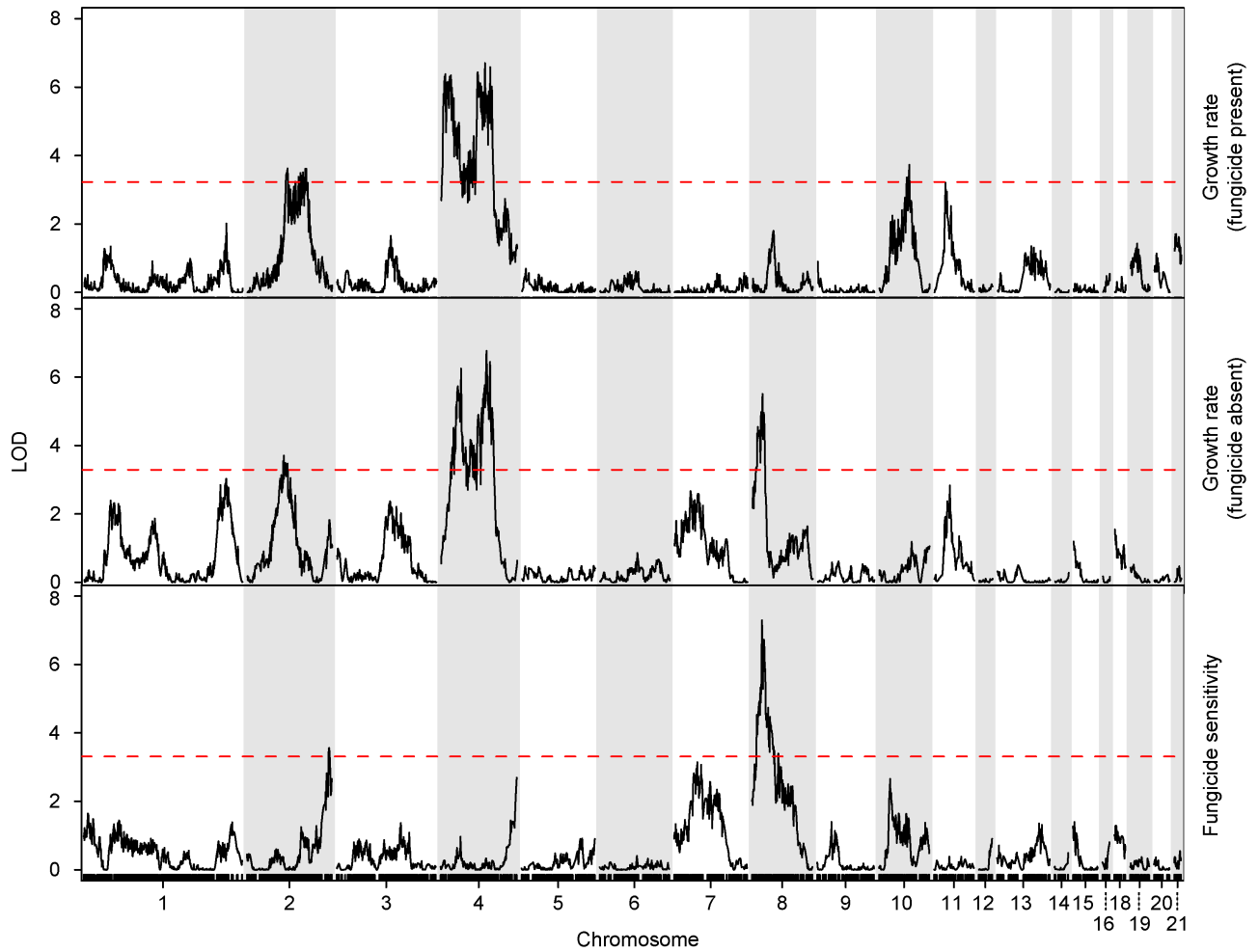


Figure 2 LOD plots from single marker interval mapping (SIM) analysis over all chromosomes for growth rate with and without fungicide and fungicide sensitivity for cross 1A5 x 1E4. The dashed horizontal red line represents the significance threshold ($p = 0.05$) obtained using 1000 genome-wide permutations.

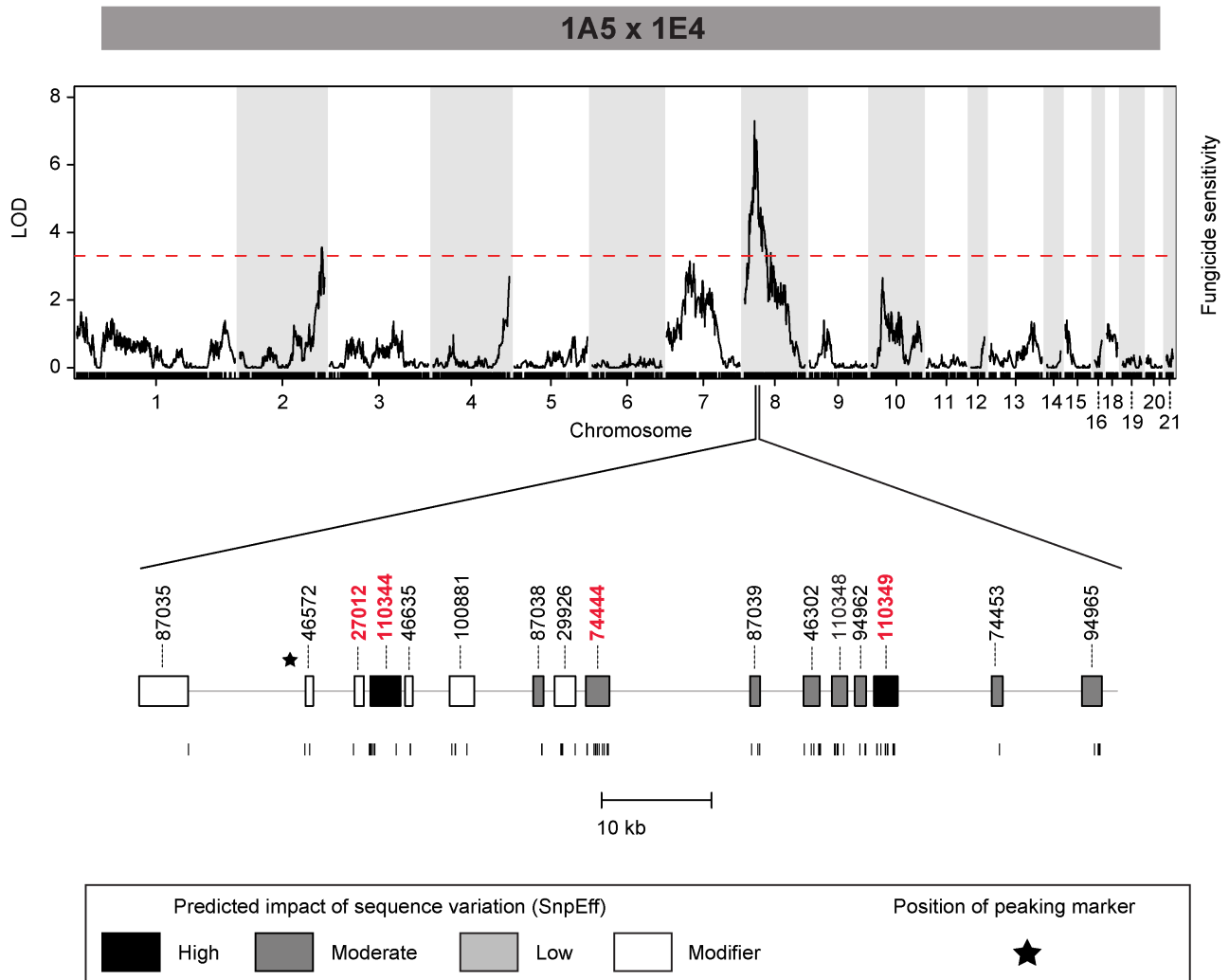


Figure 3 LOD plot from the single marker interval mapping (SIM) analysis over all chromosomes for the fungicide sensitivity QTL with a 95% confidence interval containing the smallest number (≤ 30) of candidate genes. The horizontal dashed red line shows the significance threshold ($p = 0.05$) obtained by 1000 genome-wide permutations. The relative positions of the candidate genes in the 95% confidence interval of the Chromosome 8 QTL are shown below the LOD plot. The genes are color coded according to the predicted impact by SnEff of the observed sequence variation (white = modifier, grey = moderate, black= high) and labeled with their protein ID. Below the gene bars are vertical lines showing the position of each sequence variant within each gene. The asterisk symbol represents the position of the peaking marker within the confidence interval. Highest likelihood candidate genes are colored in red.

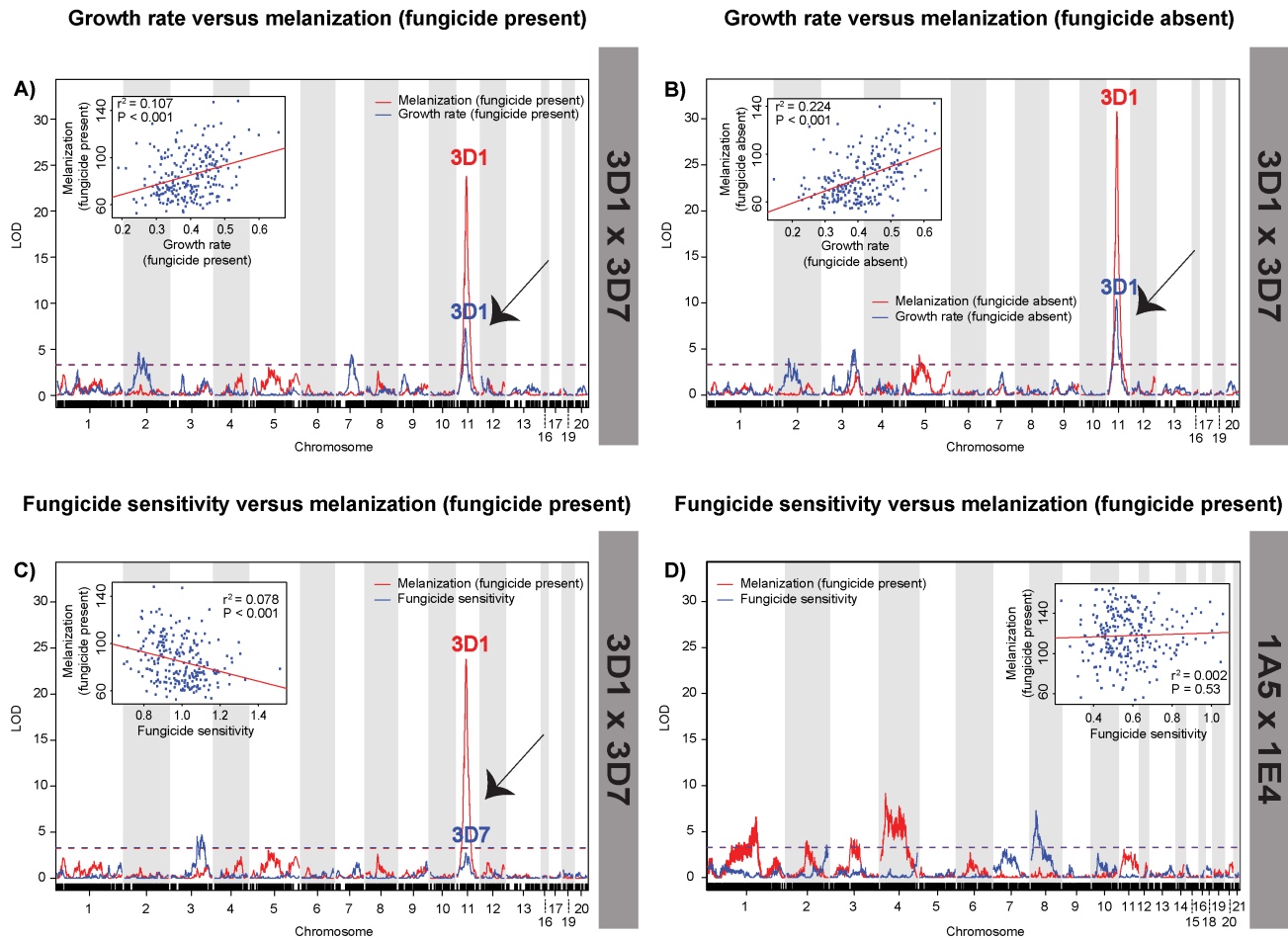


Figure 4 Evidence for pleiotropy among melanization, growth rate, and fungicide sensitivity for the chromosome 11 QTL in cross 3D1 x 3D7. Melanization is represented by grey values (LENDENMANN *et al.* 2014). The 3D7 allele that increases melanization also slows growth in the presence (Panel A) or absence (Panel B) of fungicide and decreases azole sensitivity (Panel C). No pleiotropic effect was observed in cross 1A5 x 1E4 (Panel D). Each panel shows a full genome scan LOD overlap plot based on single marker interval mapping (SIM) analysis, with traits separated by colors (red = melanization trait, blue = growth rate/fungicide sensitivity trait). Horizontal lines in the LOD plots represent the color-coded significance thresholds ($p = 0.05$) obtained with 1000 genome-wide permutations. Each panel includes the corresponding linear correlation plot amongst the two traits. The name above each QTL peak indicates which parental allele provided the higher phenotypic mean. Arrows point to the QTL peaks of interest.

Cross 3D1 x 3D7

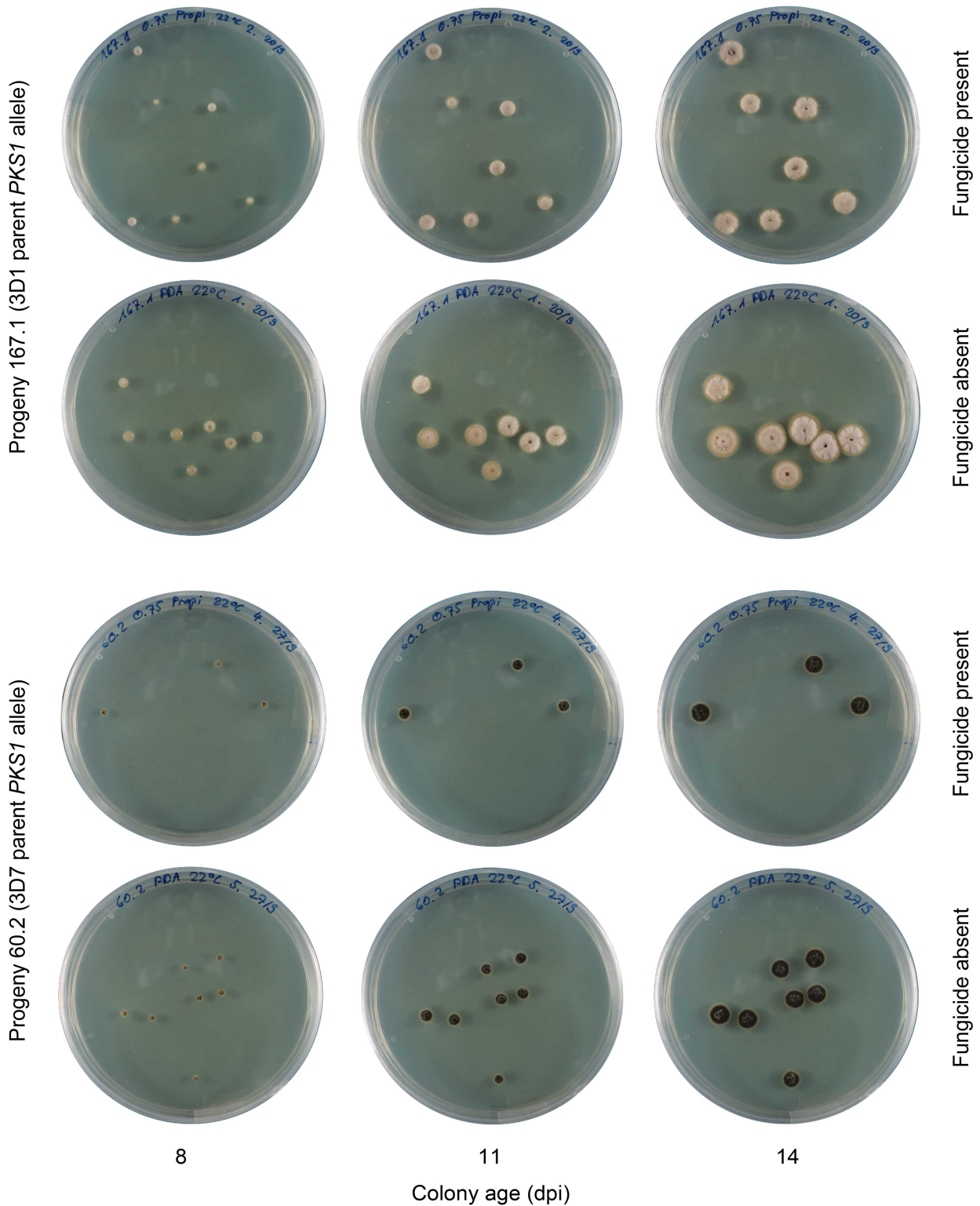


Figure 5 Illustration of the *PKS1* allele effects using two progeny (60.2 and 167.1) from cross 3D1 x 3D7. Progeny 60.2 (3D7 parent *PKS1* allele) shows increased melanization, slower growth in both the presence and absence of fungicide, and decreased fungicide sensitivity compared to the progeny 167.1 (3D1 parent *PKS1* allele).

SUPPORTING MATERIAL

All supplementary files for this chapter are available online. Please refer to:

www.sciencedirect.com/science/article/pii/S1087184515000973

CHAPTER 4

QTL Mapping of Temperature Sensitivity Reveals Candidate Genes for Thermal Adaptation and Growth Morphology in the Plant Pathogenic Fungus *Zymoseptoria tritici*

Mark H. Lendenmann, Daniel Croll, Javier Palma-Guerrero, Ethan L. Stewart and Bruce A. McDonald

Manuscript in preparation

ABSTRACT

Different thermal environments impose strong, differential selection on populations, leading to local adaptation, but the genetic basis of thermal adaptation is poorly understood. We used quantitative trait locus (QTL) mapping in the fungal wheat pathogen *Zymoseptoria tritici* to study the genetic architecture of thermal adaptation and identify candidate genes. Four wild-type strains originating from the same thermal environment were crossed to generate two mapping populations with 263 (cross 3D1 x 3D7) and 261 (cross 1A5 x 1E4) progeny. Restriction site associated DNA sequencing (RADseq) was used to genotype 9745 (cross 3D1 x 3D7) and 7333 (cross 1A5 x 1E4) single nucleotide polymorphism (SNP) markers segregating within the mapping population. Temperature sensitivity was assessed using digital image analysis of colonies growing at two different temperatures. We identified four QTLs for temperature sensitivity, with unique QTLs found in each cross. One QTL had a LOD score >11 and contained only six candidate genes, including *PBS2*, encoding a mitogen-activated protein kinase kinase associated with low temperature tolerance in *Saccharomyces cerevisiae*. This and other QTLs showed evidence for pleiotropy amongst growth rate, melanization and growth morphology, suggesting that many traits can be correlated with thermal adaptation in fungi. Our findings show that thermal adaptation has a complex genetic architecture and that populations of *Z. tritici* harbor standing genetic variation for thermal adaptation. We therefore conclude that *Z. tritici* populations have a potential to rapidly adapt to climatic changes as well as expand into new climatic regions.

INTRODUCTION

Temperature has a strong effect on many life history traits, including growth, development and reproduction (ANGILLETTA *et al.* 2006; DE JONG and VAN DER HAVE 2009). This is especially true for ectotherms, such as fungi, whose internal temperature directly reflects the surrounding environment (ANGILLETTA JR *et al.* 2002). Many species show a broad geographical distribution that includes a wide array of thermal environments where mean annual temperatures can differ by more than 10°C (e.g. (BUWALDA *et al.* 1998; RODRIGUES *et al.* 2008; ZHAN and McDONALD 2011; STEFANSSON *et al.* 2013)). Most organisms also require the capacity to tolerate local temperature environments that can fluctuate greatly on an hourly, daily, seasonal, and yearly basis. Two general strategies for adapting to different thermal environments are phenotypic plasticity and genetic differentiation (DYBDAHL and KANE 2005; KNIES *et al.* 2006; YAMORI *et al.* 2010). Phenotypic plasticity is an individual-based response that refers to the ability of the same genotype to produce different phenotypes in different environments (DE JONG and VAN DER HAVE 2009). For example, most organisms grow faster with increasing temperature up to an organism-specific optimal growth temperature (HU *et al.* 2012). Over generations, selection pressure for different temperature optima and growth rates can lead to changes in the genetic architecture of temperature adaptation. For example, non-synonymous substitutions can generate protein isoforms that differ for thermal stability and/or optimized function at different temperatures (SCHOVILLE *et al.* 2012). In a population, genetic diversity for thermal adaptation can be maintained by antagonistic pleiotropy (genetic trade-offs), in which an allele that has optimal function at one temperature exhibits maladaptation at a different temperature (FIELDS 2001). A better understanding of the genetic basis of thermal adaptation is likely to provide insight into the ability of species to adapt to global climate change (AUSTIN 2007).

Various pathogenic fungi are globally distributed and adapted to a wide range of thermal environments (FISHER *et al.* 2012). For mammalian fungal pathogens, a key adaptation to cause disease is the ability to grow at the host's body temperature (often exceeding 35°C; (ROBERT *et al.* 2015). For *Saccharomyces cerevisiae*, an opportunistic fungal pathogen, the ability to grow at high temperatures allows clinical strains to grow in immunodeficient humans (McCUSKER *et al.* 1994). The psychrophilic fungus *Pseudogymnoascus destructans*, causal agent of bat white nose syndrome, infects bats only during hibernation when their body temperature is low (BLEHERT *et al.* 2009; HOYT *et al.* 2015). The pathogenic fungus *Metarhizium robertsii* is widely used as a biological control

agent for insect pests in agriculture, but because *M. robertsii* is not well adapted to high temperatures, some insects can resist infection by elevating their body temperature or basking in sunlight (DE CRECY *et al.* 2009).

Thermal adaptation is also important for plant pathogenic fungi. Before 2000, the wheat stripe rust pathogen *Puccinia striiformis f. sp. tritici* caused epidemics only in cooler wheat growing regions. After 2000, two new clonal lineages of the pathogen able to cause epidemics in warmer climates emerged, allowing the pathogen to expand into previously unfavorable environments (MILUS *et al.* 2009; MBOUP *et al.* 2012). In the globally distributed barley pathogen *Rhynchosporium commune*, there was evidence for local adaptation to grow at higher temperatures (22°C), a key adaptation that may have enabled the global emergence of a pathogen that originated in the cold climate of Scandinavia (ZAFFARANO *et al.* 2006; LINDE *et al.* 2009; STEFANSSON *et al.* 2013). The virulence of a fungal population can be affected by an interaction between temperature and the host/parasite genotypes (LAINE 2008; BRYNER and RIGLING 2011).

In some cases the fungi grow saprophytically as filamentous hyphae outside their host, then undergo a morphological transformation to yeast-like growth after infecting their host. This is mainly the case for pathogens of mammals and insects such as *Blastomyces dermatitidis* and *Metarhizium robertsii*. These morphological switches enhance pathogenicity by facilitating dispersal within the host and enabling evasion of host immune responses (NADAL *et al.* 2008; GAUTHIER 2015). In other cases the switch is in the opposite direction, which is mainly the case for plant pathogens (e.g. *Ustilago maydis*), where yeast-like growth is observed outside the host and filamentous growth is observed within the host. For several fungal pathogens (eg. *Talaromyces marneffe* (BOYCE and ANDRIANOPOULOS 2013)), a change in temperature triggers a switch in growth morphology (GAUTHIER 2015).

Fungi use several mechanisms to cope with changing temperatures, including the induction or upregulation of proteins related to thermal-stress (i.e. heat shock proteins (HSPs) (FEDER and HOFMANN 1999)), changes in cellular composition (i.e. activation of the high-osmolarity glycerol (HOG) pathway resulting in glycerol accumulation in cells (PANADERO *et al.* 2006)) and adjustments in membrane fluidity (i.e. lipid saturation in cell membranes (LEACH and COWEN 2014)). Little is known regarding the genetic basis of how fungi tolerate different temperatures. The majority of research upon this topic has been conducted in yeasts and is oriented around the regulation of HSPs (FEDER and HOFMANN 1999; LEACH and COWEN 2014). HSPs are regulated through the heat shock

transcription factor (Hsf1), which has been extensively studied in *S. cerevisiae* (SORGER and PELHAM 1988; NICHOLLS *et al.* 2009). QTL mapping of high-temperature growth (Htg) in the progeny of a cross between a heat tolerant clinical strain of *S. cerevisiae* and a heat sensitive strain isolated from a rotting fig identified four linked genes involved in Htg, but none of these genes had a function known to affect thermal adaptation (STEINMETZ *et al.* 2002; SINHA *et al.* 2008). A bulk segregant analysis applied to yeast populations (EHRENREICH *et al.* 2010) identified 21 QTLs associated with Htg in a cross of a heat tolerant North American oak tree strain and a heat sensitive West African palm wine strain (PARTS *et al.* 2011). A transcriptome analysis of 48 *Neurospora crassa* isolates from subtropical and tropical environments identified two genes involved in thermal adaptation, including an MRH4-like RNA helicase (ELLISON *et al.* 2011). Despite the progress illustrated by these studies, many gaps remain in our understanding of the genetic mechanisms underlying thermal adaptation in fungi (ROBERT *et al.* 2015).

Zymoseptoria tritici (syn *Mycosphaerella graminicola*) is the fungal pathogen causing Septoria tritici blotch (STB), currently the most damaging wheat disease in Europe (JORGENSEN *et al.* 2014; O'DRISCOLL *et al.* 2014). *Z. tritici* is a dimorphic fungus that can grow either as filamentous hyphae or yeast-like budding cells when grown *in vitro* (NADAL *et al.* 2008). The pathogen is found in wheat-growing areas worldwide covering a wide range of temperature regimes (EYAL *et al.* 1987; JORGENSEN *et al.* 2014; O'DRISCOLL *et al.* 2014); (ZHAN and McDONALD 2011)). An earlier study that included 138 *Z. tritici* strains sampled from diverse thermal environments on three continents found evidence for thermal adaptation and concluded that most of the thermal adaptation was due to genetic differentiation rather than phenotypic plasticity (ZHAN and McDONALD 2011). Here we sought to determine the genetic architecture of thermal adaptation and identify candidate genes based on QTL mapping of temperature sensitivity in wild-type strains sampled from the same thermal environment. This approach allowed us to identify and characterize genetic polymorphisms segregating within populations (FRANKS and HOFFMANN 2012; ROBERT *et al.* 2015). Knowledge about co-occurring genetic variants conferring different levels of thermal adaptation allows us to predict how a population will be able to adapt to climate change. To determine the genetic architecture of thermal adaptation in *Z. tritici*, we used restriction site associated DNA sequencing (RADseq) for genotyping, coupled with high-throughput digital image analysis to measure growth rates under two temperatures (15°C and 22°C). We used QTL mapping to determine the genetic architecture of natural variation for temperature sensitivity and identify QTLs and their associated chromosomal

segments. Comparisons of complete genome sequences of parental isolates allowed us to identify polymorphism in candidate genes within the QTLs that affect thermal adaptation.

MATERIAL AND METHODS

Mapping population, genotyping, genetic mapping, gene expression

Methods used for genetic mapping and gene expression were described earlier (BRUNNER *et al.* 2013; LENDENMANN *et al.* 2014; LENDENMANN *et al.* 2015). Briefly, four Swiss wild-type strains were used to create two mapping populations, following an established protocol (KEMA *et al.* 1996). The mapping populations were composed of 263 [ST99CH3D1 (3D1: SRS383146) X ST99CH3D7 (3D7: SRS383147)] and 261 [ST99CH1A5 (1A5: SRS383142) X ST99CH1E4 (1E4: SRS383143)] retained progeny. Table S1 contains the NCBI Short Read Archive accession numbers for the retained progeny of each cross. Restriction site associated DNA sequencing (RADseq) (BAIRD *et al.* 2008) generated more than 7000 single nucleotide polymorphism (SNP) markers for each cross. Resequencing of all four parents (CROLL *et al.* 2013) allowed identification of the retained RADseq SNPs in the parents and candidate genes responsible for the observed QTLs. R/qtl version 1.27-10 (ARENDS *et al.* 2010) was used to construct two dense genetic maps (LENDENMANN *et al.* 2014). Candidate genes within QTL confidence intervals were characterized for their transcriptional profile, using RNA-Seq data from an *in planta* virulence time course assay (BRUNNER *et al.* 2013).

Phenotyping

Radial growth rates (mm day^{-1}) (TRINCI 1971; LENDENMANN *et al.* 2015) of single spore colonies grown at two temperatures (15°C and 22°C) and observed over three time points (8, 11 and 14 days post inoculation (dpi)) were used to calculate temperature sensitivity. Plate inoculation procedures and digital image analyses in ImageJ (SCHNEIDER *et al.* 2012) were described earlier (LENDENMANN *et al.* 2014). Isolates were grown in Petri plates on potato dextrose agar (PDA, 4 g/L potato starch, 20 g/L dextrose, 15 g/L agar) and placed at constant 15°C or 22°C with 70% humidity in the dark. Temperature sensitivity for each isolate was calculated as the radial growth rate at 22°C divided by the radial growth rate at 15°C. Two absolute value traits (radial growth rate at 15°C and 22°C) and one relative value trait (relative growth rate coefficient = temperature sensitivity) were calculated for each isolate and used for QTL analysis. The 22°C growth rate trait of this study was called growth rate (fungicide absent) in an earlier investigation mapping QTLs involved in fungicide sensitivity (LENDENMANN *et al.* 2015).

In addition to growth rate, two growth morphologies were scored for each strain. Though *Z. tritici* is considered a filamentous fungus that grows mainly as hyphae, a yeast-like morphology is

often observed in culture on rich media, suggesting that *Z. tritici* is dimorphic (MEHRABI and KEMA 2006; MEHRABI *et al.* 2006b; NADAL *et al.* 2008). To determine if the yeast/hyphae dimorphism can be mapped, we conducted a visual inspection of the digital images to classify the colonies of each isolate as either hyphal or yeast-like. Three people (ML, JP, ES) independently classified each isolate using all five technical replicates at 11 dpi for both temperatures. 11 dpi was chosen because the colonies were too small to make an accurate visual scoring at 8 dpi, while classifications at 14 dpi gave the same result. Progeny that exhibited only yeast-like colonies were scored as '0', whereas progeny exhibiting at least two hyphal colonies on a Petri dish were scored as '1' (Figure S1). Only progeny with identical classifications from all three scorers were included in this analysis. At 15°C, >98% of the progeny with a consensus score in cross 1A5 x 1E4 grew with a yeast-like morphology (binary value '0': 247 progeny / binary value '1': 3 progeny), hence this treatment was not included in the analysis. The binary counts were as follows: cross 3D1 x 3D7 at 22°C binary value '0': 111 progeny / binary value '1': 90 progeny; at 15°C binary value '0': 186 progeny / binary value '1': 52 progeny; cross 1A5 x 1E4 at 22°C binary value '0': 104 progeny / binary value '1': 33 progeny. Table S2 shows the absolute and relative phenotypes as well as the yeast/hyphae scores for the retained progeny of each cross.

QTL mapping

Simple interval mapping (SIM) was used for QTL analysis performed in R/qtl version 1.27-10 (ARENDS *et al.* 2010) using R (R_CORE_TEAM 2012). A binary model was applied for the yeast/hyphae dimorphism phenotype. 1000 genome-wide permutations were used to calculate the significant logarithm of odds (LOD) threshold. In addition to SIM, a multiple QTL model combined with interval mapping was used to evaluate two QTLs present on the same chromosome. Further analyses considered only QTLs that showed P-values lower than 0.05. Bayesian credible intervals (MANICHAIKUL *et al.* 2006) were used to calculate 95% confidence intervals for each QTL. Genetic positions (centiMorgans, cM) of markers were converted into physical positions (base pair, bp) by using the reference IPO323 genome (GOODWIN *et al.* 2011). QTLs were assumed to be different if their confidence intervals did not overlap. More detailed information on methods used for QTL mapping were described earlier (LENDENMANN *et al.* 2014).

Single spore colonies were also scored for their degree of melanization (LENDENMANN *et al.* 2014). Because melanin has been associated with protection against extreme temperatures as well

as fungicide resistance (BUTLER and DAY 1998; NOSANCHUK and CASADEVALL 2006; TABORDA *et al.* 2008), we investigated pleiotropy amongst the traits growth rate, temperature sensitivity and melanization (11dpi), but also looked for evidence of pleiotropic effects amongst temperature and fungicide sensitivity. This analysis was conducted by overlapping full SIM genome scans and using linear regression amongst the traits based on a general linear model in R with Pearson's correlation coefficient. Regression analysis between the yeast/hyphae dimorphism and growth rate at each temperature was conducted using a one-way ANOVA to calculate the phenotypic variance explained by the yeast/hyphae dimorphism phenotypes upon growth rate. A t-test was used to compare mean differences between the two morphologies in R. Marker allele effects were calculated using R/qtl to confirm the linear regressions.

Identification of candidate genes within QTL confidence intervals

Resequenced parents of each cross were aligned against the IPO323 reference genome and sequence variants were called and annotated using the open-source tools SnpEff and SnpSift version 3.3h (CINGOLANI *et al.* 2012). Synonymous SNPs were omitted from any further investigation. A gene was considered a candidate for explaining the QTL if it contained at least one sequence variant within the boundaries of the 95% confidence interval. More details regarding methods used to identify candidate genes within QTL confidence intervals were provided earlier (LENDENMANN *et al.* 2014). Because heat shock proteins play an important role in maintaining cellular functions under thermal stress (FEDER and HOFMANN 1999), a hypergeometric test was used to determine whether there was a significant enrichment of proteins with an InterPro domain classified as heat-shock proteins (HSPs) within the QTL 95% confidence intervals (Table 1 and Table 2). The QTL confidence intervals (Table 1 and Table 2) were also investigated for the presence of HSPs as candidate genes.

RESULTS

Genetic architecture of temperature sensitivity

The general linear model of growth rate based on radial development of colonies over time provided an average fit (r^2) higher than 98% across both crosses and treatments (Figure S2), justifying the method used to measure growth rate for each isolate. The growth rate and temperature sensitivity phenotypes showed a continuous distribution consistent with a quantitative trait in both crosses. Transgressive segregation was found for all traits, with many progeny showing more extreme phenotypes than their parents (Figure S3). The high broad-sense heritability ($H^2 > 80\%$) found for average colony area indicates a low environmental variance amongst the 5 technical repeats (Figure S2).

For the temperature sensitivity phenotype, one significant QTL was found in cross 3D1 x 3D7 and three were found in cross 1A5 x 1E4. These four QTLs were on chromosomes 1, 2, 4 and 10 with LOD values ranging from 4.3 to 11.8 (Figure 1, Figure 2, Table 1 and Table 2). For the absolute value phenotypes, cross 3D1 x 3D7 had four growth rate QTLs on chromosomes 2, 3, 7 and 11 and cross 1A5 x 1E4 had two growth rate QTLs on chromosomes 5 and 8 (Table 1 and Table 2). There was a confidence interval overlap between the two crosses for the QTLs on chromosome 2, suggesting a shared QTL. This QTL overlap was already described in a previous study (LENDENMANN *et al.* 2015). On average, ~30% of total variance was explained by the significant QTLs for each trait in both crosses (Table 3). No significant QTLs were mapped on the accessory chromosomes.

QTLs associated with the yeast/hyphae dimorphism

For the yeast/hyphae dimorphism phenotype we considered QTLs to be different if their confidence intervals did not overlap. In cross 3D1 x 3D7 we mapped five significant QTLs distributed on chromosomes 1, 3, 7 and 11 (Figure S4, Table S3 and Table S4), with two QTLs on chromosome 3 (Table S3). In cross 1A5 x 1E4 two significant QTLs were identified on chromosomes 7 and 11 (Figure S5, Table S5 and Table S6). Both of these QTLs overlapped with QTLs of cross 3D1 x 3D7, suggesting these QTLs were shared in the two crosses (Table S3 and Table S5).

Identification and characterization of candidate genes within QTL confidence intervals

All annotated genes within each QTL 95% confidence interval were investigated to identify candidate genes affecting each trait. We excluded from consideration all genes that lacked

sequence variation or that possessed only synonymous SNPs. For cross 3D1 x 3D7 a summary of the candidate genes for each trait is shown in Table S7 and Table S4. Table S8 and Table S6 summarize the candidate genes for cross 1A5 x 1E4.

On average, we found ~200 candidate genes per confidence interval, with a minimum of six candidate genes (chromosome 10, temperature sensitivity, cross 3D1 x 3D7) and a maximum of 1382 candidate genes (chromosome 1, growth rate (15°C), cross 1A5 x 1E4). On average ~40% of the candidate genes had no known function (Table S7, Table S8, Table S4 and Table S6). There was no evidence for enrichment of HSPs in the QTL confidence intervals relative to the rest of the genome. But some HSPs were among the candidate genes found within the QTL confidence intervals (Table 1 and Table 2).

A more detailed investigation was conducted on the three major QTLs ($LOD \geq 4.5$) containing ≤ 30 candidate genes in narrow confidence intervals (< 85 kb). The chromosome 10 QTL associated with temperature sensitivity in cross 3D1 x 3D7 had a LOD score of 11.8 and contained only six candidate genes (Table S7). The chromosome 1 and 3 QTLs associated with the yeast/hyphae dimorphism at 15°C in cross 3D1 x 3D7 contained 15 candidate genes each (Table S4) with LOD scores of 4.5 and 10.2, respectively. The lists of candidate genes associated with each QTL are summarized in Table 4, Table S9, Table S10, Figure 3 and Figure 4.

Evidence for pleiotropy

In a previous study (LENDENMANN *et al.* 2015), we described a shared QTL on chromosome 11 for melanization at 22°C, growth rate at 22°C and fungicide sensitivity in cross 3D1 x 3D7. We hypothesized that a rare mutation in *PKS1* (Protein ID 96592) found in the 3D7 parent was responsible for this pleiotropy (LENDENMANN *et al.* 2014). In this study we found evidence for pleiotropy between melanization and growth at 15°C following the same pattern described earlier (LENDENMANN *et al.* 2015), namely the *PKS1* allele that increases melanization also slows growth at 15°C. But there was no evidence for pleiotropy between melanization and temperature sensitivity associated with the chromosome 11 QTL in cross 3D1 x 3D7 (Figure 5). On the other hand, we found strong evidence for pleiotropy amongst melanization at 15°C, growth at 15°C and temperature sensitivity based on a shared chromosome 10 QTL in cross 3D1 x 3D7. This QTL displayed the following pattern: the 3D7 allele that increases melanization also accelerates growth at 15°C and decreases temperature sensitivity. There was some evidence for pleiotropy amongst melanization

and temperature sensitivity in cross 1A5 x 1E4 due to a shared chromosome 2 QTL and there were significant correlations between melanization and growth at 15°C for QTLs on chromosomes 5 and 8 (Figure 5). In both crosses we found no evidence for pleiotropy amongst temperature sensitivity and fungicide sensitivity (Figure S6).

The QTL peaks for the yeast/hyphae dimorphism overlapped with growth rate QTLs on chromosomes 3, 7, 10 and 11, providing evidence for pleiotropy in both crosses. There also was a strong correlation between growth rate and the yeast/hyphae dimorphism. In both crosses the allele associated with faster growth was also associated with filamentous growth (Table S11, Table S3, Table S5, Table S12, Figure S7 and Figure S8), with >17% of the total growth rate variance explained by the yeast/hyphae dimorphism and significant ($P < 0.001$) mean differences between the growth rates of the two morphologies (Figure S7 and Figure S8). On the other hand, QTLs on chromosomes 1, 2, 4 and 8 did not overlap between the yeast/hyphae dimorphism and growth rate, indicating that growth morphology is not the sole determinant of growth rate (Figure S7 and Figure S8). For example, in cross 3D1 x 3D7 there is a significant QTL for the yeast/hyphae dimorphism at 15°C on chromosome 1, but there is no growth rate QTL at this position, whereas there is a significant QTL for growth rate at 15°C on chromosome 2, but no corresponding QTL for the yeast/hyphae dimorphism (Figure S7, Panel B).

DISCUSSION

Genetic architecture of temperature sensitivity

The temperature sensitivity (TS) phenotype we used to measure thermal adaptation reflects differences in growth rates at two temperatures. Strains with a TS = 1 are “generalists” that grow at the same rate at both temperatures. Strains with TS > 1 grow faster at the higher temperature and strains with TS < 1 grow faster at the lower temperature. Strains that grow quickly at both temperatures (i.e. high growth rates and TS ≈ 1) exhibit the greatest degree of thermal tolerance. Although the temperature sensitivity phenotypes of the parental strains used in both crosses were similar, the progeny from these parents exhibited a variance in temperature sensitivity comparable to the variance measured in natural field populations from around the world (ZHAN and McDONALD 2011), indicating that the parents carried a high degree of genetic diversity for this trait. This finding also illustrates the potential for recombination to generate novel combinations of alleles that can affect thermal adaptation, providing a mechanism for a rapid evolutionary response to change in temperature. The presence of several visible but non-significant peaks on the genome scans, coupled with the finding that <50% of the total phenotypic variance was explained by the significant QTLs leads us to predict that additional QTLs will be revealed in future studies that include a greater number of markers and a larger number of offspring.

All four TS QTLs had allele means >1, indicating faster growth at 22°C than at 15°C. An earlier analysis of Swiss populations of *Z. tritici* found many isolates with a TS < 1, consistent with adaptation to growth at lower temperatures (ZHAN and McDONALD 2011). These findings suggest that genes involved in adaptation to cooler temperatures were not variable in the four Swiss parents. Among the six additional mapped growth rate QTLs, the four on chromosomes 2, 3, 8 and 11 exhibit phenotypic plasticity, with parental alleles showing different growth rate mean values at 15°C and 22°C. These QTLs could harbor alleles involved in adaptation to local environments (e.g. specifically adapted to warmer or colder climates), as *Z. tritici* populations have the ability to adapt to local conditions (ZHAN and McDONALD 2011). On the other hand the QTLs mapped for temperature sensitivity carry alleles involved in adaptation to temperature fluctuations (e.g. diurnal and seasonal) that will occur across a broad array of environments. This could be tested through additional experiments such as a genome wide association studies (GWAS) upon populations from different climates or QTL mapping upon a mapping population derived from parents of different climates. We found no evidence for antagonistic pleiotropy (genetic trade-offs), but we postulate

that testing our mapping population under more extreme temperatures (>22°C and <15°) could reveal such effects.

The finding of different TS QTLs in the two crosses likely reflects differences in the alleles found in the parents and suggests either a defective pathway, the same pathway or different pathways. These findings may also reflect different selective processes underlying thermal adaptation. In cross 3D1 x 3D7, the TS QTL on chromosome 10 was due mainly to a significant growth QTL exhibited in the 15°C environment. This may represent an adaptation to cooler temperatures that could ultimately contribute to greater success in sexual reproduction because the sexual cycle occurs mainly during the cooler seasons of Spring and Fall (PONOMARENKO *et al.* 2011). In cross 1A5 x 1E4 the significant TS QTLs on chromosomes 2 and 4 were due mainly to growth QTLs exhibited in the 22°C environment. Pathogen strains that grow faster at warmer temperatures are likely to be favored during the asexual phase of reproduction that occurs during the Summer (PONOMARENKO *et al.* 2011), as *in vitro* growth could be positively correlated with *in planta* growth and pathogen fitness (e.g. reproductive fitness and/or spore output). Hence, the genes affecting growth rate can have a significant impact on temperature sensitivity, with both slower growth (cross 3D1 x 3D7) and faster growth (cross 1A5 x 1E4) associated with greater temperature sensitivity, as shown by the allele effects. The finding of temperature-specific QTLs within the same cross suggest that proteins of different allele variants are better adapted to one temperature and maladapted to another temperature or that genes are differentially regulated at the two temperatures, a known mechanism for thermal tolerance (SCHOVILLE *et al.* 2012).

QTLs associated with the yeast/hyphae dimorphism

Several fungal pathogens of mammals, insects and plants are known to possess a yeast/hyphae dimorphism that can be triggered by a variety of environmental signals, increasing adaptation of the pathogen to their local environment. Temperature is a major trigger for mammalian dimorphic fungal pathogens, whereas exposure to hemolymph triggers the switch from hyphal to yeast growth for dimorphic insect pathogens. Yeast-like growth in animal hosts is associated with many factors that increase pathogenicity, including dispersal within the host, altered cell wall composition that may affect recognition by host immune systems and production of proteins or toxins that alter host behavior (GAUTHIER 2015). However the switch from filamentous to yeast-like growth isn't necessarily a mechanism for thermal adaptation. Knock-out (KO) studies of the dimorphism-

regulating kinase 1 (*DRK1*) in *Blastomyces dermatitidis* and *Histoplasma capsulatum* illustrated that these pathogens were still able to grow at the elevated temperature of the mammalian host, but only as filamentous hyphae, rendering the pathogens avirulent (NEMECEK *et al.* 2006). In the dimorphic insect pathogen *Metarhizium robertsii* deletion of the *MAD1* gene reduced the production of yeast-like cells, resulting in lower virulence (WANG and ST. LEGER 2007).

We identified 7 QTLs associated with the yeast/hyphae dimorphism, with 2 of these QTLs shared between the crosses. On average, ~35% of the overall variation in growth morphology was explained by these QTLs. These findings indicate that the yeast/hyphae dimorphism is inherited as a quantitative trait in *Z. tritici*. The yeast/hyphae dimorphism QTLs correlate with the growth QTLs, indicating pleiotropic effects. QTL alleles associated with faster growth were also associated with filamentous growth in both crosses. We assume morphology being the causality for the observed correlation, however the situation could also be the other way around. For example morphology could be a threshold trait, which is triggered through growth. Our results further indicate that growth rate is not determined solely by the colony morphology, as we found three growth QTLs that were not associated with the dimorphism phenotype. In *Z. tritici* the switch between morphologies can be induced *in vitro* by changing from a nutrient-rich medium, which favors yeast-like growth, to a poor medium that favors hyphal growth (MEHRABI and KEMA 2006; MEHRABI *et al.* 2006b). We found that temperature significantly affected dimorphism in our mapping populations, with more progeny exhibiting hyphal growth at 22°C compared to 15°C. The finding that higher temperatures favor hyphal growth in *Z. tritici* was described previously in gene KO studies using the genome reference isolate IPO323 (MEHRABI and KEMA 2006). While diverse environmental signals can affect dimorphism, the main signaling pathways appear well conserved, with the cAMP-dependent protein kinase A (PKA) and mitogen-activated protein kinase (MAPK) pathways (NADAL *et al.* 2008) playing major roles. In *Z. tritici* both of these pathways were shown to affect the dimorphism phenotype (COUSIN *et al.* 2006; MEHRABI and KEMA 2006; MEHRABI *et al.* 2006a; MEHRABI *et al.* 2006b; GOHARI *et al.* 2014). It is not known if the yeast-like morphology plays any role in the natural history of *Z. tritici*. Filamentous growth is obvious during all phases of its life cycle, including biotrophic, necrotrophic and saprophytic phases of growth and development, but a yeast-like morphology has never been reported *in planta*. *Z. tritici* forms filamentous germ tubes on the leaf surface in order to penetrate leaf stomata and then grows as hyphae among the host mesophyll cells (MEHRABI and KEMA 2006; NADAL *et al.* 2008). While it is not clear why lower temperatures would favor a yeast-like

morphology, we speculate that yeast-like growth may offer an advantage during competition with other microbes in rotting plant material during the winter, but it is equally plausible that this morphology has no adaptive function and is simply a relic of ancestors that exhibited yeast-like growth as part of their natural history. In the dimorphic basidiomycete *Ustilago maydis* that causes corn smut, haploid yeast cells excrete pheromones that allow recognition of the opposite mating type, leading to induction of the filamentous stage that enables fusion (plasmogamy) of two haploid isolates. This fusion leads to the formation of an infectious filamentous dikaryon that penetrates the plant cuticle and invades the host tissue (NADAL *et al.* 2008). Irregardless of the purpose of the yeast phase in *Z. tritici*, our findings illustrate that *Z. tritici* offers a new model for elucidating the mechanisms responsible for the yeast/hyphal dimorphism in fungi.

Identification and characterization of candidate genes within QTL confidence intervals

After taking into account gene ontology, the predicted impact of observed sequence variation, the position of the QTL peak, and gene expression, we narrowed the six candidate genes in the 3D1 x 3D7 chromosome 10 TS QTL down to two high-priority candidates (Protein ID: 76249 and 101408). The mitogen-activated protein kinase kinase (MAPKK, Gene 76249) and transmembrane transporter (Gene 101408) were selected based on proximity to the peaking marker, as well as observed sequence variation and its predicted impact.

Earlier gene disruption studies in the IPO323 reference strain identified 10 genes (*MgTpk2*, *MgGpa1*, *MgGpa3*, *MgGpb1*, *MCC1*, *MVE1*, *MgSlt2*, *MgHog1*, *MgFus3* and *ZtWor1*) that affected the yeast/hyphae growth morphology (COUSIN *et al.* 2006; MEHRABI and KEMA 2006; MEHRABI *et al.* 2006a; MEHRABI *et al.* 2006b; MEHRABI *et al.* 2009; CHOI and GOODWIN 2011a; CHOI and GOODWIN 2011b; GOHARI *et al.* 2014). We did not find any of these genes in the 95% confidence intervals of the dimorphism QTLs identified in our study, indicating that our QTL mapping approach identified novel gene candidates associated with the yeast/hyphae dimorphism in *Z. tritici*.

Among the 15 candidate genes found in the 3D7 x 3D1 chromosome 1 QTL for the yeast/hyphae dimorphism at 15°C, we identified three high-priority candidate genes (Protein ID: 32213, 88642 and 88644). Gene 32213, encoding an ABC transporter, was selected due to its proximity to the peaking marker. Gene 88642, with unknown function, contains a sequence variant predicted to have a high impact. Gene 88644 encodes a Ca²⁺/calmodulin-dependent protein kinase (CaMK), part of a kinase family involved in various signaling cascades. This candidate was selected

due to its cellular function, but also based on the 13 non-synonymous substitutions found amongst the parents, as well as a splice site acceptor sequence variant that is predicted to have a high impact on protein function. In the dimorphic ascomycete *Sporothrix schenckii*, CaMKs were shown to be involved in the dimorphism (VALLE-AVILES *et al.* 2007). Hence we consider gene 88644 as the most likely candidate to explain this chromosome 1 QTL.

The 3D7 x 3D1 chromosome 3 QTL for the yeast/hyphae (15°C) dimorphism contained three high priority candidate genes (Protein ID: 38371, 56742 and 79974). Gene 38371 encodes a peptidase that was selected based on its proximity to the peaking marker. Gene 79974 was chosen because it contained a frame shift mutation expected to have a high impact. Gene 56742 encodes a guanine nucleotide exchange factor (GEF), a family of proteins involved in various intracellular signaling pathways. Among these, we consider the GEF as the most likely candidate because a GEF was shown to be involved in dimorphism in *Ustilago maydis* (MULLER *et al.* 2003). This gene contains a downstream modifier in the 3' UTR region. The role of the UTR regions on the regulation of mRNA translation is well known, and mutations on these regions can affect protein translation rates (WILKIE *et al.* 2003). According to this, the SNP at the 3' UTR of 56742 could affect its translation, altering the levels of this protein and ultimately its activity, affecting the morphological switch.

Evidence for pleiotropy

The MAPKK candidate gene (JGI ID: 76249 (MgPbs2)) in the chromosome 10 TS QTL of cross 3D1 x 3D7 is the ortholog of the *S. cerevisiae* gene *PBS2*. Pbs2 phosphorylates the Hog1 protein (a mitogen-activated protein kinase (MAPK)) in *S. cerevisiae* as well as *Aspergillus nidulans* (PANADERO *et al.* 2006; DURAN *et al.* 2010), hence we postulate that MgPbs2 phosphorylates the Hog1 ortholog in *Z. tritici*. *HOG1* is part of the high osmolarity glycerol (HOG) pathway that is induced upon osmotic stress. Recent studies indicate that other stress responses, including thermal and acid stress, are also governed by the HOG pathway (PANADERO *et al.* 2006). We conclude that the chromosome 10 TS QTL reflects the HOG pathway and that MgPbs2 is responsible for the chromosome 10 TS QTL observed in the 3D1 x 3D7 cross, indicating that natural sequence variation in genes involved in signaling can play a major role in thermal adaptation in fungal populations. This is based on earlier findings. A mutant study (MEHRABI *et al.* 2006b) of the *Z. tritici* ortholog *HOG1*, MgHog1 (JGI ID: 76502), found higher melanization associated with greater hyphal growth as well as larger colony sizes and suggests the same phenotypic pattern as the allele effects identified in the

chromosome 10 TS QTL. The HOG pathway provides a mechanism for thermal adaptation that is activated under cold stress in *S. cerevisiae*, which accumulates glycerol that contributes to protection against freezing (PANADERO *et al.* 2006). In *Aspergillus fumigatus* the HOG pathway is also thought to affect the fluidity of plasma membranes providing protection under thermal stress (Ji *et al.* 2012). Changes in cell membrane fluidity are considered to be a common mechanism for microorganisms to adapt to changing temperatures (LEACH and COWEN 2014). Many of the chromosome 10 QTL pleiotropic effects in this study were observed at 15°C but not at 22°C. This suggests that *PBS2*, and the HOG pathway, may be induced at lower temperatures in *Z. tritici*, providing a plausible mechanism to explain phenotypic plasticity.

Pleiotropy also explains the shared QTL peak on chromosome 11 in cross 3D1 x 3D7 for melanization (11 dpi), growth rate and the yeast/hyphae dimorphism for both temperatures (LENDENMANN *et al.* 2014). In this case we hypothesize that *PKS1*, in particular the postulated quantitative trait nucleotide (QTN) at amino acid position 1783 (LENDENMANN *et al.* 2014) is the source of the observed trait variance. This hypothesis is supported by analyses showing that the RADseq marker closest to the *PKS1* gene explains >7% of the variance for each of these traits.

Conclusions

We elucidated the genetic architecture of thermal adaptation in a pathogenic fungus and identified multiple QTLs as well as candidate genes underlying this trait. To our knowledge this is the first study to use QTL mapping to identify genes involved in thermal adaptation in a plant pathogen. Our findings suggest that thermal adaptation in *Z. tritici* involves not only changes in growth rate, but also morphological adaptations, including degree of melanization and changes in growth morphology. This suggests that *Z. tritici* has evolved many strategies for thermal adaptation, in part explaining its global distribution across a wide temperature range and leading us to predict that it will adapt rapidly to global warming. Future investigations aiming to functionally validate the candidate genes responsible for the mapped QTLs are underway. Additional population genetic diversity studies are needed to analyze the variation for these genes found in global populations and may further elucidate the potential of *Z. tritici* to adapt to changes in temperature. These studies may form the foundation for understanding the potential response of fungal pathogens to global warming.

ACKNOWLEDGMENTS

The research was supported by a grant from the Swiss National Science Foundation (31003A_134755). Technical assistance was provided by Tryggvi S. Stefansson. The RNA-Seq data was kindly provided by Stefano F. F. Torriani. RADseq libraries were constructed at the Genetic Diversity Centre (GDC) and sequenced in the Quantitative Genomics Facility at the Department of Biosystems Science and Engineering (D-BSSE) at the scientific central facilities of ETH Zurich.

REFERENCES

- ANGILLETTA, MICHAEL J., CHRISTOPHER E. OUFIERO and ADAM D. LEACHÉ, 2006 Direct and indirect effects of environmental temperature on the evolution of reproductive strategies: an information-theoretic approach. *The American Naturalist* **168**: E123-E135.
- ANGILLETTA JR, M. J., P. H. NIEWIAROWSKI and C. A. NAVAS, 2002 The evolution of thermal physiology in ectotherms. *Journal of Thermal Biology* **27**: 249-268.
- ARENDS, D., P. PRINS, R. C. JANSEN and K. W. BROMAN, 2010 R/qtl: high-throughput multiple QTL mapping. *Bioinformatics* **26**: 2990-2992.
- AUSTIN, M., 2007 Species distribution models and ecological theory: a critical assessment and some possible new approaches. *Ecological Modelling* **200**: 1-19.
- BAIRD, N. A., P. D. ETTER, T. S. ATWOOD, M. C. CURREY, A. L. SHIVER *et al.*, 2008 Rapid SNP discovery and genetic mapping using sequenced rad markers. *PLOS One* **3**: e3376.
- BLEHERT, D. S., A. C. HICKS, M. BEHR, C. U. METEYER, B. M. BERLOWSKI-ZIER *et al.*, 2009 Bat white-nose syndrome: an emerging fungal pathogen? *Science* **323**: 227.
- BOYCE, K. J., and A. ANDRIANOPOULOS, 2013 morphogenetic circuitry regulating growth and development in the dimorphic pathogen *Penicillium marneffeii*. *Eukaryotic Cell* **12**: 154-160.
- BRUNNER, P. C., S. F. F. TORRIANI, D. CROLL, E. H. STUKENBROCK and B. A. McDONALD, 2013 Coevolution and life cycle specialization of plant cell wall degrading enzymes in a hemibiotrophic pathogen. *Molecular Biology and Evolution* **30**: 1337-1347.
- BRYNER, S. F., and D. RIGLING, 2011 temperature-dependent genotype-by-genotype interaction between a pathogenic fungus and its hyperparasitic virus. *American Naturalist* **177**: 65-74.
- BUTLER, M. J., and A. W. DAY, 1998 Fungal melanins: a review. *Canadian Journal of Microbiology* **44**: 1115-1136.
- BUWALDA, F., B. EVELEENS and R. WERTWIJN, 1998 Ornamental crops tolerate large temperature fluctuations: a potential for more efficient greenhouse heating strategies, pp. 141-150 in *Acta of Horticulture*, edited by M. BODSON.
- CHOI, Y.-E., and S. B. GOODWIN, 2011a Gene encoding a C-type cyclin in *Mycosphaerella graminicola* is involved in aerial mycelium formation, filamentous growth, hyphal swelling, melanin biosynthesis, stress response, and pathogenicity. *Molecular Plant-Microbe Interactions* **24**: 469-477.

- CHOI, Y.-E., and S. B. GOODWIN, 2011b *MVE1*, encoding the velvet gene product homolog in *Mycosphaerella graminicola*, is associated with aerial mycelium formation, melanin biosynthesis, hyphal swelling and light signaling. *Applied and Environmental Microbiology* **77**: 942-953.
- CINGOLANI, P., A. PLATTS, L. L. WANG, M. COON, N. TUNG *et al.*, 2012 A program for annotating and predicting the effects of single nucleotide polymorphisms, SnpEff: SNPs in the genome of *Drosophila melanogaster* strain w(1118); iso-2; iso-3. *Fly* **6**: 80-92.
- COUSIN, A., R. MEHRABI, M. GUILLEROUX, M. DUFRESNE, T. VAN DER LEE *et al.*, 2006 The MAP kinase-encoding gene *MgFus3* of the non-appressorium phytopathogen *Mycosphaerella graminicola* is required for penetration and in vitro pycnidia formation. *Molecular Plant Pathology* **7**: 269-278.
- CROLL, D., M. ZALA and B. A. McDONALD, 2013 Breakage-fusion-bridge cycles and large insertions contribute to the rapid evolution of accessory chromosomes in a fungal pathogen. *PLOS Genetics* **9**: e1003567.
- DE CRECY, E., S. JARONSKI, B. LYONS, T. J. LYONS and N. O. KEYHANI, 2009 Directed evolution of a filamentous fungus for thermotolerance. *Bmc Biotechnology* **9**: 1-11.
- DE JONG, G., and T. M. VAN DER HAVE, 2009 Temperature dependence of development rate, growth rate and size: from biophysics to adaptation. In: *Phenotypic plasticity of insects: mechanisms and consequences* (eds Whitman D.W., Ananthakrishnan T.N.), pp. 461-526. Science Publishers Inc., Plymouth, UK.
- DURAN, R., J. W. CARY and A. M. CALVO, 2010 Role of the osmotic stress regulatory pathway in morphogenesis and secondary metabolism in filamentous fungi. *Toxins* **2**: 367-381.
- DYBDAHL, M. F., and S. L. KANE, 2005 Adaptation vs. phenotypic plasticity in the success of a clonal invader. *Ecology* **86**: 1592-1601.
- EHRENREICH, I. M., N. TORABI, Y. JIA, J. KENT, S. MARTIS *et al.*, 2010 Dissection of genetically complex traits with extremely large pools of yeast segregants. *Nature* **464**: 1039-1042.
- ELLISON, C. E., C. HALL, D. KOWBEL, J. WELCH, R. B. BREM *et al.*, 2011 Population genomics and local adaptation in wild isolates of a model microbial eukaryote. *Proceedings of the National Academy of Sciences of the United States of America* **108**: 2831-2836.
- EYAL, Z., A. L. SCHAREN, J. M. PRESCOTT and M. VAN GINKEL, 1987 The *Septoria* diseases of wheat: concepts and methods of disease management. Mexico, D.F.: CIMMYT.

- FEDER, M. E., and G. E. HOFMANN, 1999 Heat-shock proteins, molecular chaperones, and the stress response: evolutionary and ecological physiology. *Annual Review of Physiology* **61**: 243-282.
- FIELDS, P. A., 2001 Review: Protein function at thermal extremes: balancing stability and flexibility. *Comparative Biochemistry and Physiology a-Molecular and Integrative Physiology* **129**: 417-431.
- FISHER, M. C., D. A. HENK, C. J. BRIGGS, J. S. BROWNSTEIN, L. C. MADOFF *et al.*, 2012 Emerging fungal threats to animal, plant and ecosystem health. *Nature* **484**: 186-194.
- FRANKS, S. J., and A. A. HOFFMANN, 2012 Genetics of climate change adaptation. *Annual Review of Genetics* **46**: 185-208.
- GAUTHIER, G. M., 2015 Dimorphism in fungal pathogens of mammals, plants, and insects. *PLOS Pathogens* **11**: e1004608-e1004608.
- GOHARI, A. M., R. MEHRABI, O. ROBERT, I. A. INCE, S. BOEREN *et al.*, 2014 Molecular characterization and functional analyses of *ZtWor1*, a transcriptional regulator of the fungal wheat pathogen *Zymoseptoria tritici*. *Molecular Plant Pathology* **15**: 394-405.
- GOODWIN, S. B., S. BEN M'BAREK, B. DHILLON, A. H. J. WITTENBERG, C. F. CRANE *et al.*, 2011 Finished genome of the fungal wheat pathogen *Mycosphaerella graminicola* reveals dispensable structure, chromosome plasticity, and stealth pathogenesis. *PLOS Genetics* **7**: e1002070.
- HOYT, J. R., T. L. CHENG, K. E. LANGWIG, M. M. HEE, W. F. FRICK *et al.*, 2015 Bacteria Isolated from Bats Inhibit the Growth of *Pseudogymnoascus destructans*, the Causative Agent of White-Nose Syndrome. *PLOS One* **10**: e0121329.
- HU, Y., X. HAO, J. LOU, P. ZHANG, J. PAN *et al.*, 2012 A PKS gene, *pks-1*, is involved in chaetoglobosin biosynthesis, pigmentation and sporulation in *Chaetomium globosum*. *Science China-Life Sciences* **55**: 1100-1108.
- JI, Y., F. YANG, D. MA, J. ZHANG, Z. WAN *et al.*, 2012 HOG-MAPK signaling regulates the adaptive responses of *Aspergillus fumigatus* to thermal stress and other related stress. *Mycopathologia* **174**: 273-282.
- JORGENSEN, L. N., M. S. HOVMOLLER, J. G. HANSEN, P. LASSEN, B. CLARK *et al.*, 2014 IPM strategies and their dilemmas including an introduction to www.eurowheat.org. *Journal of Integrative Agriculture* **13**: 265-281.

- KEMA, G. H. J., E. C. P. VERSTAPPEN, M. TODOROVA and C. WAALWIJK, 1996 Successful crosses and molecular tetrad and progeny analyses demonstrate heterothallism in *Mycosphaerella graminicola*. *Current Genetics* **30**: 251-258.
- KNIES, J. L., R. IZEM, K. L. SUPLER, J. G. KINGSOLVER and C. L. BURCH, 2006 The genetic basis of thermal reaction norm evolution in lab and natural phage populations. *PLOS Biology* **4**: 1257-1264.
- LAINE, A.-L., 2008 Temperature-mediated patterns of local adaptation in a natural plant-pathogen metapopulation. *Ecology Letters* **11**: 327-337.
- LEACH, M., and L. COWEN, 2014 To Sense or die: mechanisms of temperature sensing in fungal pathogens. *Current Fungal Infection Reports* **8**: 185-191.
- LENDENMANN, M. H., D. CROLL and B. A. McDONALD, 2015 QTL mapping of fungicide sensitivity reveals novel genes and pleiotropy with melanization in the pathogen *Zymoseptoria tritici*. *Fungal Genetics and Biology* **80**: 53-67.
- LENDENMANN, M. H., D. CROLL, E. L. STEWART and B. A. McDONALD, 2014 Quantitative trait locus mapping of melanization in the plant pathogenic fungus *Zymoseptoria tritici*. *G3-Genes Genomes Genetics* **4**: 2519-2533.
- LINDE, C. C., M. ZALA and B. A. McDONALD, 2009 Molecular evidence for recent founder populations and human-mediated migration in the barley scald pathogen *Rhynchosporium secalis*. *Molecular Phylogenetics and Evolution* **51**: 454-464.
- MANICHAIKUL, A., J. DUPUIS, S. SEN and K. W. BROMAN, 2006 Poor performance of bootstrap confidence intervals for the location of a quantitative trait locus. *Genetics* **174**: 481-489.
- MBOUP, M., B. BAHRI, M. LECONTE, C. DE VALLAVIEILLE-POPE, O. KALTZ *et al.*, 2012 Genetic structure and local adaptation of European wheat yellow rust populations: the role of temperature-specific adaptation. *Evolutionary Applications* **5**: 341-352.
- MCCUSKER, J. H., K. V. CLEMONS, D. A. STEVENS and R. W. DAVIS, 1994 Genetic characterization of pathogenic *Saccharomyces cerevisiae* isolates. *Genetics* **136**: 1261-1269.
- MEHRABI, R., S. BEN M'BAREK, T. A. J. VAN DER LEE, C. WAALWIJK, P. J. G. M. DE WIT *et al.*, 2009 G alpha and G beta proteins regulate the cyclic AMP pathway that is required for development and pathogenicity of the phytopathogen *Mycosphaerella graminicola*. *Eukaryotic Cell* **8**: 1001-1013.

- MEHRABI, R., and G. H. J. KEMA, 2006 Protein kinase A subunits of the ascomycete pathogen *Mycosphaerella graminicola* regulate asexual fructification, filamentation, melanization and osmosensing. *Molecular Plant Pathology* **7**: 565-577.
- MEHRABI, R., T. VAN DER LEE, C. WAALWIJK and G. H. J. KEMA, 2006a *MgSlt2*, a cellular integrity MAP kinase gene of the fungal wheat pathogen *Mycosphaerella graminicola*, is dispensable for penetration but essential for invasive growth. *Molecular Plant-Microbe Interactions* **19**: 389-398.
- MEHRABI, R., L.-H. ZWIERS, M. A. DE WAARD and G. H. J. KEMA, 2006b *MgHog1* regulates dimorphism and pathogenicity in the fungal wheat pathogen *Mycosphaerella graminicola*. *Molecular Plant-Microbe Interactions* **19**: 1262-1269.
- MILUS, E. A., K. KRISTENSEN and M. S. HOVMOLLER, 2009 Evidence for Increased Aggressiveness in a Recent Widespread Strain of *Puccinia striiformis* f. sp. *tritici* Causing Stripe Rust of Wheat. *Phytopathology* **99**: 89-94.
- MULLER, P., J. D. KATZENBERGER, G. LOUBRADOU and R. KAHMANN, 2003 Guanyl nucleotide exchange factor *Sql2* and *Ras2* regulate filamentous growth in *Ustilago maydis*. *Eukaryotic Cell* **2**: 609-617.
- NADAL, M., M. D. GARCIA-PEDRAJAS and S. E. GOLD, 2008 Dimorphism in fungal plant pathogens. *Fems Microbiology Letters* **284**: 127-134.
- NEMECEK, J. C., M. WUTHRICH and B. S. KLEIN, 2006 Global control of dimorphism and virulence in fungi. *Science* **312**: 583-588.
- NICHOLLS, S., M. D. LEACH, C. L. PRIEST and A. J. P. BROWN, 2009 Role of the heat shock transcription factor, *Hsf1*, in a major fungal pathogen that is obligately associated with warm-blooded animals. *Molecular Microbiology* **74**: 844-861.
- NOSANCHUK, J. D., and A. CASADEVALL, 2006 Impact of melanin on microbial virulence and clinical resistance to antimicrobial compounds. *Antimicrobial Agents and Chemotherapy* **50**: 3519-3528.
- O'DRISCOLL, A., S. KILDEA, F. DOOHAN, J. SPINK and E. MULLINS, 2014 The wheat–Septoria conflict: a new front opening up? *Trends in Plant Science* **19**: 602-610.
- PANADERO, J., C. PALLOTTI, S. RODRIGUEZ-VARGAS, F. RANDEZ-GIL and J. A. PRIETO, 2006 A downshift in temperature activates the high osmolarity glycerol (HOG) pathway, which determines freeze tolerance in *Saccharomyces cerevisiae*. *Journal of Biological Chemistry* **281**: 4638-4645.

- PARTS, L., F. A. CUBILLOS, J. WARRINGER, K. JAIN, F. SALINAS *et al.*, 2011 Revealing the genetic structure of a trait by sequencing a population under selection. *Genome Research* **21**: 1131-1138.
- PONOMARENKO, A., S. B. GOODWIN and G. H. J. KEMA, 2011 Septoria tritici blotch (STB) of wheat. The Plant Health Instructor. DOI:10.1094/PHI-I-2011-0407-01.
- R_CORE_TEAM, 2012 R: A language and environment for statistical computing. R Foundation for Statistical Computing. Vienna, Austria. ISBN 3-900051-07-0, URL <http://www.R-project.org/>.
- ROBERT, V., G. CARDINALI and A. CASADEVALL, 2015 Distribution and impact of yeast thermal tolerance permissive for mammalian infection. *BMC Biology* **13**: 1-14.
- RODRIGUES, D. F., N. IVANOVA, Z. HE, M. HUEBNER, J. ZHOU *et al.*, 2008 Architecture of thermal adaptation in an *Exiguobacterium sibiricum* strain isolated from 3 million year old permafrost: a genome and transcriptome approach. *Bmc Genomics* **9**: 1-17.
- SCHNEIDER, C. A., W. S. RASBAND and K. W. ELICEIRI, 2012 NIH Image to ImageJ: 25 years of image analysis. *Nature Methods* **9**: 671-675.
- SCHOVILLE, S. D., F. S. BARRETO, G. W. MOY, A. WOLFF and R. S. BURTON, 2012 Investigating the molecular basis of local adaptation to thermal stress: population differences in gene expression across the transcriptome of the copepod *Tigriopus californicus*. *Bmc Evolutionary Biology* **12**.
- SINHA, H., L. DAVID, R. C. PASCON, S. CLAUDER-MUENSTER, S. KRISHNAKUMAR *et al.*, 2008 Sequential elimination of major-effect contributors Identifies additional quantitative trait loci conditioning high-temperature growth in yeast. *Genetics* **180**: 1661-1670.
- SORGER, P. K., and H. R. B. PELHAM, 1988 Yeast heat shock factor is an essential DNA-binding protein that exhibits temperature-dependent phosphorylation. *Cell* **54**: 855-864.
- STEFANSSON, T. S., B. A. McDONALD and Y. WILLI, 2013 Local adaptation and evolutionary potential along a temperature gradient in the fungal pathogen *Rhynchosporium commune*. *Evolutionary Applications* **6**: 524-534.
- STEINMETZ, L. M., H. SINHA, D. R. RICHARDS, J. I. SPIEGELMAN, P. J. OEFNER *et al.*, 2002 Dissecting the architecture of a quantitative trait locus in yeast. *Nature* **416**: 326-330.
- TABORDA, C. P., M. B. DA SILVA, J. D. NOSANCHUK and L. R. TRAVASSOS, 2008 Melanin as a virulence factor of *Paracoccidioides brasiliensis* and other dimorphic pathogenic fungi: a minireview. *Mycopathologia* **165**: 331-339.
- TRINCI, A. P. J., 1971 Influence of width of peripheral growth zone on radial growth rate of fungal colonies on solid media. *Journal of General Microbiology* **67**: 325-344.

- VALLE-AVILES, L., S. VALENTIN-BERRIOS, R. R. GONZALEZ-MENDEZ and N. R.-D. VALLE, 2007 Functional, genetic and bioinformatic characterization of a calcium/calmodulin kinase gene in *Sporothrix schenckii*. *Bmc Microbiology* **7**: 1-12.
- WANG, C., and R. J. ST. LEGER, 2007 The MAD1 adhesin of *Metarhizium anisopliae* links adhesion with blastospore production and virulence to insects, and the MAD2 adhesin enables attachment to plants. *Eukaryotic Cell* **6**: 808-816.
- WILKIE, G. S., K. S. DICKSON and N. K. GRAY, 2003 Regulation of mRNA translation by 5' and 3'-UTR-binding factors. *Trends in Biochemical Sciences* **28**: 182-188.
- YAMORI, W., K. NOGUCHI, K. HIKOSAKA and I. TERASHIMA, 2010 Phenotypic plasticity in photosynthetic temperature acclimation among crop species with different cold tolerances. *Plant Physiology* **152**: 388-399.
- ZAFFARANO, P. L., B. A. McDONALD, M. ZALA and C. C. LINDE, 2006 Global hierarchical gene diversity analysis suggests the Fertile Crescent is not the center of origin of the barley scald pathogen *Rhynchosporium secalis*. *Phytopathology* **96**: 941-950.
- ZHAN, J., and B. A. McDONALD, 2011 Thermal adaptation in the fungal pathogen *Mycosphaerella graminicola*. *Molecular Ecology* **20**: 1689-1701.

Table 1 Positions and effects of the five temperature sensitivity associated QTLs identified in cross 3D1 x 3D7.

Trait	Chromosome	Estimated position of peaking marker (cM)	Estimated position of peaking marker (kb)	LOD score at peak	P-value	Mean 3D1 allele (growth rate/temperature sensitivity)	Mean 3D7 allele (growth rate/temperature sensitivity)	Mean difference	Allele effect ^a	Percentage of variance explained by QTL (%)	Estimated position of proximal marker (kb) ^b	Estimated position of distal marker (kb) ^b	Bayes confidence interval length (kb)	Heat-shock protein candidate genes (Gene ID) ^c
Growth rate (15°C)	2	189.12	1805	4.89	0.001	0.301	0.347	0.046	3D7	9.2	837	1833	996	68169, 90664
Growth rate (22°C)	3	289.38	3078	4.97	0.002	0.384	0.438	0.054	3D7	9.2	2781	3107	326	/
Growth rate (15°C)	7	121.17	1115	3.95	0.008	0.304	0.345	0.041	3D7	7.5	943	1205	262	/
Temperature sensitivity	10	106.13	644	11.8	<0.001	1.416	1.199	0.217	3D1	16.6	631	651	20	/
Growth rate (22°C)	11	78.07	538	10.38	<0.001	0.452	0.376	0.076	3D1	17.9	435	592	157	111223

^a 3D1 indicates that the 3D1 parent allele provided a higher phenotypic mean than the 3D7 parent allele. 3D7 indicates that the 3D7 parent allele provided a higher phenotypic mean than the 3D1 parent allele.

^b Markers flanking the 95% Bayes confidence interval of the associated QTL.

^c Data refer to within the 95% Bayes confidence interval.

Table 2 Positions and effects of the five temperature sensitivity associated QTLs identified in cross 1A5 x 1E4.

Trait	Chromosome	Estimated position of peaking marker (cM)	Estimated position of peaking marker (kb)	LOD score at peak	P-value	Mean 1A5 allele (growth rate/temperature sensitivity)	Mean 1E4 allele (growth rate/temperature sensitivity)	Mean difference	Allele effect ^a	Percentage of variance explained by QTL (%)	Estimated position of proximal marker (kb) ^b	Estimated position of distal marker (kb) ^b	Bayes confidence interval length (kb)	Heat-shock protein candidate genes (Gene ID) ^c
Temperature sensitivity	1	368.54	2216	5.66	< 0.001	1.281	1.127	0.154	1A5	9.9	2076	2324	248	/
Temperature sensitivity	2	193.42	1428	4.31	0.005	1.265	1.129	0.136	1A5	7.7	396	3516	3120	29054, 68169, 90664, 68653, 99310
Temperature sensitivity	4	222.25	1188	4.26	0.006	1.129	1.264	0.135	1E4	7.6	421	1863	1442	108995, 109019, 99959
Growth rate (15°C)	5	244.14	1909	4.81	0.002	0.311	0.348	0.037	1E4	7.5	1420	2786	1366	72449, 104628, 42499
Growth rate (15°C)	8	181.03	1506	6.77	< 0.001	0.304	0.349	0.045	1E4	11.5	364	1802	1437	/

^a 1A5 indicates that the 1A5 parent allele provided a higher phenotypic mean than the 1E4 parent allele. 1E4 indicates that the 1E4 parent allele provided a higher phenotypic mean than the 1A5 parent allele.

^b Markers flanking the 95% Bayes confidence interval of the associated QTL.

^c Data refer to within the 95% Bayes confidence interval.

Table 3 Genetic architecture of each trait for both crosses.

Trait	Chromosome with a QTL	Allele effect ^a	Total % variance explained by QTL(s)	Number of significant QTLs	Confirmation of transgressive segregation	Cross
Growth rate (22°C)	2, 3, 11	3D1(1), 3D7(2)	34.5	3	Yes	3D1 x 3D7
Growth rate (15°C)	2, 3, 7, 10, 11	3D1(1), 3D7(4)	48.2	5	Yes	
Temperature sensitivity	10	3D1(1)	16.6	1	No	
			Average 33.1	Average 3		
Growth rate (22°C)	2, 4, 8	1A5(1), 1E4(2)	27.7	3	Yes	1A5 x 1E4
Growth rate (15°C)	1, 5, 8	1E4(3)	25.2	3	No	
Temperature sensitivity	1, 2, 4	1A5(2), 1E4(1)	25.2	3	Yes	
			Average 26.0	Average 3		

Table 4 Genes within the chromosome 10 temperature sensitivity QTL confidence interval containing ≤ 30 candidate genes for cross 3D1 x 3D7, excluding genes with no sequence variation or with only synonymous SNPs.

Protein ID ^a	Gene ontology name	Gene ontology biological process	Gene ontology cellular component	Gene ontology molecular function	Number of Non-Syn SNPs ^b	Number of other sequence variations ^{b c}	Additional information	Highest RPKM mean ^d	RPKM Stdv
101405	catalytic activity	acetyl-CoA metabolic process; acetate metabolic process; pyruvate metabolic process	cytosol; mitochondrion; acetate CoA-transferase complex	acetate CoA-transferase activity; acetyl-CoA hydrolase activity	4 (M)	0	/	71.4 (13 dpi)	17.4
105917	5-methyltetrahydropteroyltriglutamate-homocysteine S-methyltransferase activity	methionine biosynthetic process; methylation	Not described	5-methyltetrahydropteroyltriglutamate-homocysteine S-methyltransferase activity	3 (M)	2 upstream (m), 1 UTR5 Prime (m)	/	148.0 (7 dpi)	24.0
111014	proteolysis	proteolysis	Not described	serine-type peptidase activity	7 (M)	2 intron (m), 1 UTR5 Prime (m)	/	49.8 (7 dpi)	43.3
96183	Not described	Not described	Not described	Not described	5 (M)	2 intron (m)	/	0 (No specific day)	0.0
76249 [#]	protein kinase activity	protein phosphorylation; serine family amino acid metabolic process	Not described	ATP binding; protein serine/threonine kinase activity	3 (M)	0	Name: MgPbs2 (Hypothetical MAP kinase kinase (MAPKK) involved in the osmosensing signal-transduction pathway, activated under severe osmotic stress)	139.2 (7 dpi) [*]	31.8

101408 °	integral to membrane	transmembrane transport	integral to membrane	Not described	2 (M)	0	Transporter - auxin efflux carrier-like with six predicted transmembrane regions	168.0 (56 dpi) *	24.3
----------	----------------------	-------------------------	----------------------	---------------	-------	---	--	------------------	------

^a A # Indicates the QTL peak is positioned closest to this gene or within the gene. A ° Indicates candidate genes with a higher likelihood of contributing to temperature sensitivity compared to unmarked candidate genes.

^b The letter within brackets following the number of a specific sequence polymorphism refers to the likely impact of the sequence polymorphism according to SnpEff. H=high, M=moderate, L=low, m=modifier.

^c Other sequence variations include codon change plus insertion/deletion, codon insertion/deletion, 100 bp upstream or downstream, frameshift, intron, splice site acceptor/donor, start gained/lost, stop gained/lost, untranslated regions (UTR).

^d A * Indicates significant changes in transcript abundances over time in planta.

Table 5 Summary of allele effects for RADseq marker 11_535446 (*PKS1*) in cross 3D1 x 3D7 modeled upon growth rate, melanization and the yeast/hyphae dimorphism.

Trait ^a	Mean 3D1 allele (growth rate/melanization/dimorphism)	Mean 3D7 allele (growth rate/melanization/dimorphism)	Mean difference	Allele effect ^b	Percentage of variance explained by QTL (%)
Melanization (22°C)	93.697	69.233	24.464	3D1	39.9
Melanization (15°C)	113.281	102.192	11.089	3D1	7.4
Growth rate (22°C)	0.452	0.376	0.076	3D1	18.4
Growth rate (15°C)	0.355	0.301	0.054	3D1	12.6
Yeast/hyphae (22°C)	0.721	0.228	0.493	3D1	22
Yeast/hyphae (15°C)	0.357	0.103	0.254	3D1	8.8

^a Melanization values are from 11 dpi scores.

^b 3D1 indicates that the 3D1 parent allele provided a higher phenotypic mean than the 3D7 parent allele. 3D7 indicates that the 3D7 parent allele provided a higher phenotypic mean than the 3D1 parent allele.

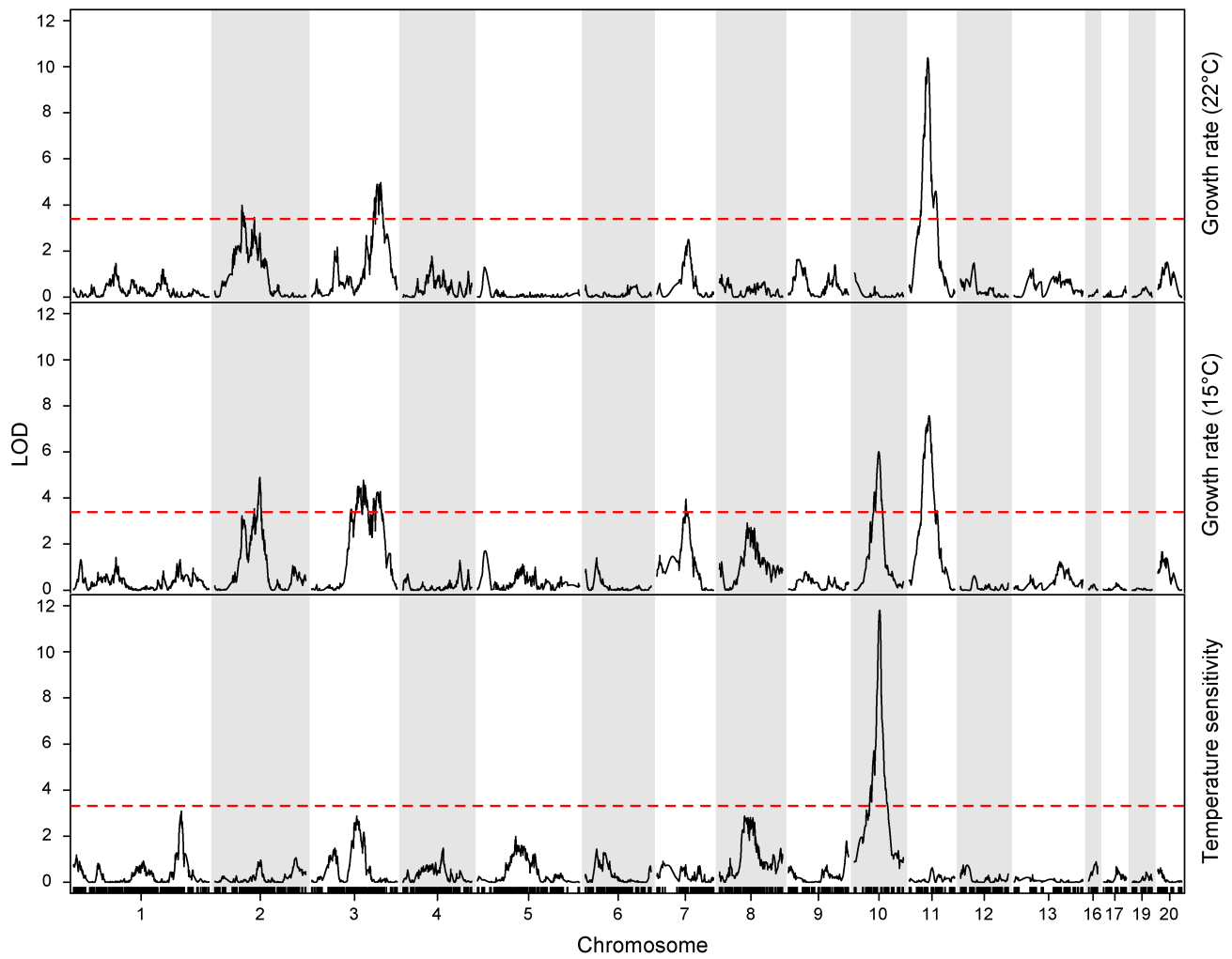


Figure 1 LOD plots from single marker interval mapping (SIM) analysis over all chromosomes for growth rate at 15°C and 22°C as well as temperature sensitivity for cross 3D1 x 3D7. The dashed horizontal red line represents the significance threshold ($p = 0.05$) obtained using 1000 genome-wide permutations.

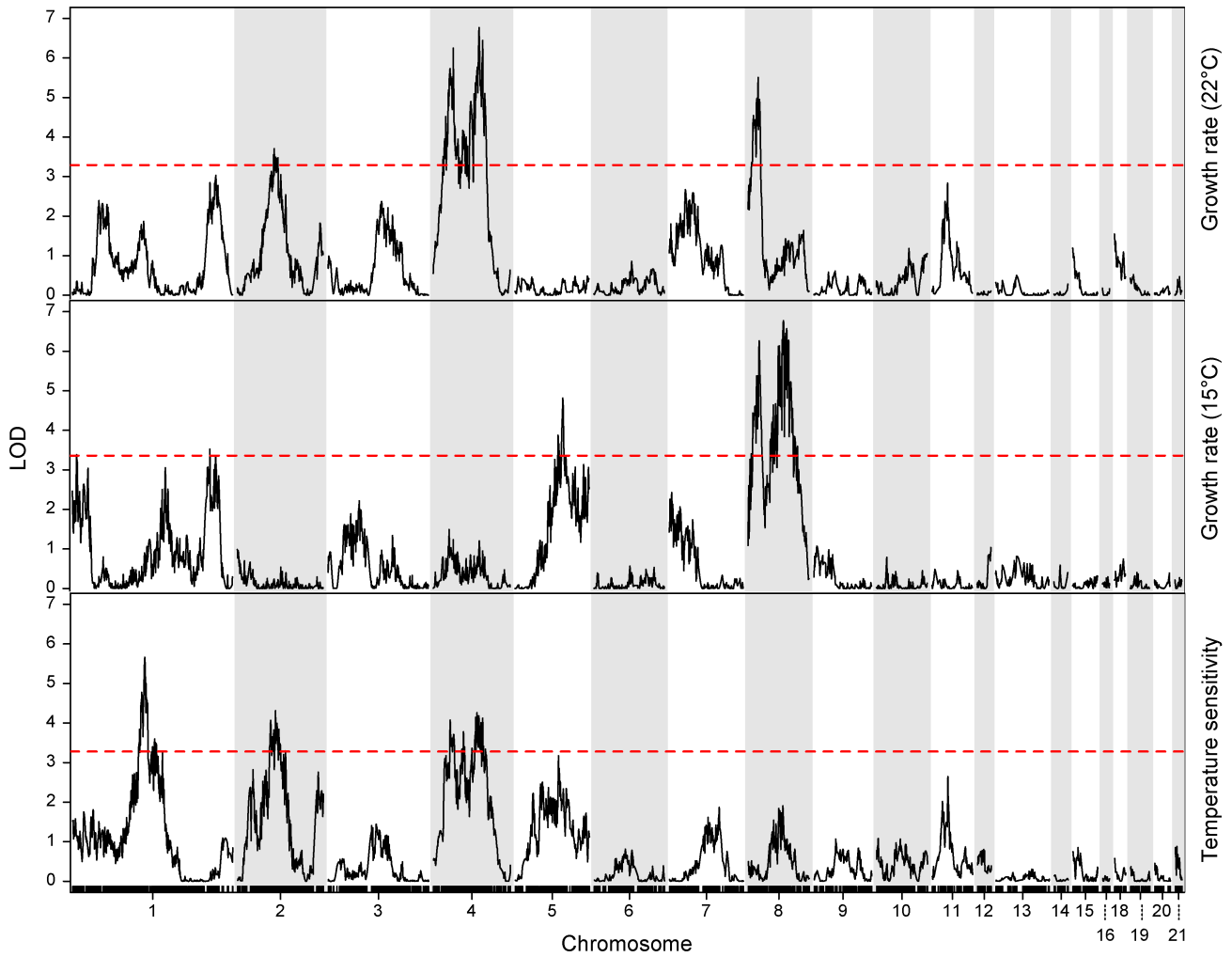


Figure 2 LOD plots from single marker interval mapping (SIM) analysis over all chromosomes for growth rate at 15°C and 22°C as well as temperature sensitivity for cross 1A5 x 1E4. The dashed horizontal red line represents the significance threshold ($p = 0.05$) obtained using 1000 genome-wide permutations.

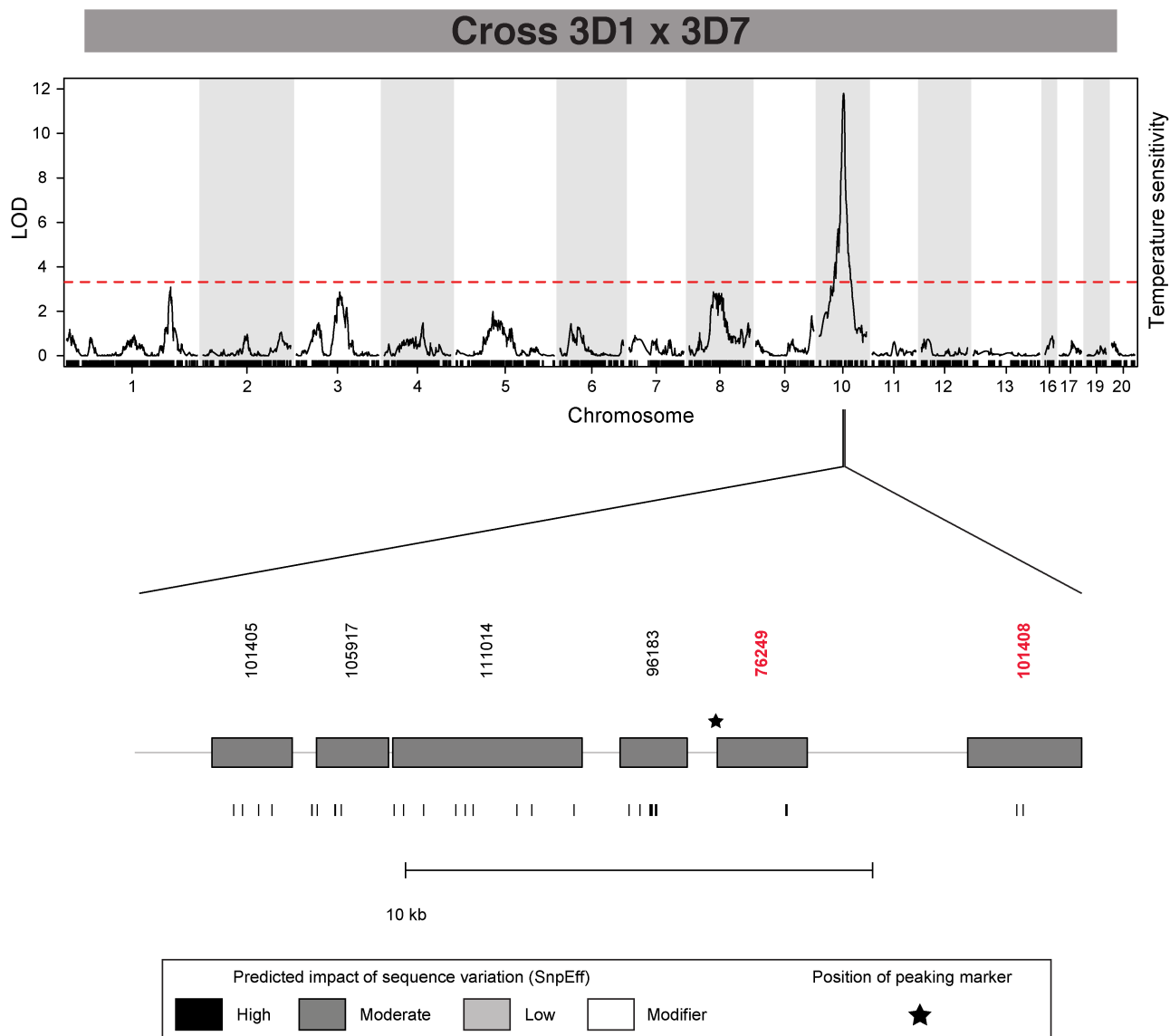


Figure 3 LOD plot from the single marker interval mapping (SIM) analysis over all chromosomes for the temperature sensitivity QTL with a 95% confidence interval containing the smallest number (≤ 30) of candidate genes. The horizontal dashed red line shows the significance threshold ($p = 0.05$) obtained by 1000 genome-wide permutations. The relative positions of the candidate genes in the 95% Bayes confidence interval of the Chromosome 10 QTL are shown below the LOD plot. The genes are color coded according to the predicted impact by SnPEff of the observed sequence variation (grey = moderate) and labeled with their protein ID. Below the gene bars are vertical lines showing the position of each sequence variant within each gene. The asterisk symbol represents the position of the peaking marker within the confidence interval. Highest likelihood candidate genes are colored in red (76249: a mitogen-activated protein kinase kinase (MAPKK), 101408: a transmembrane transporter).

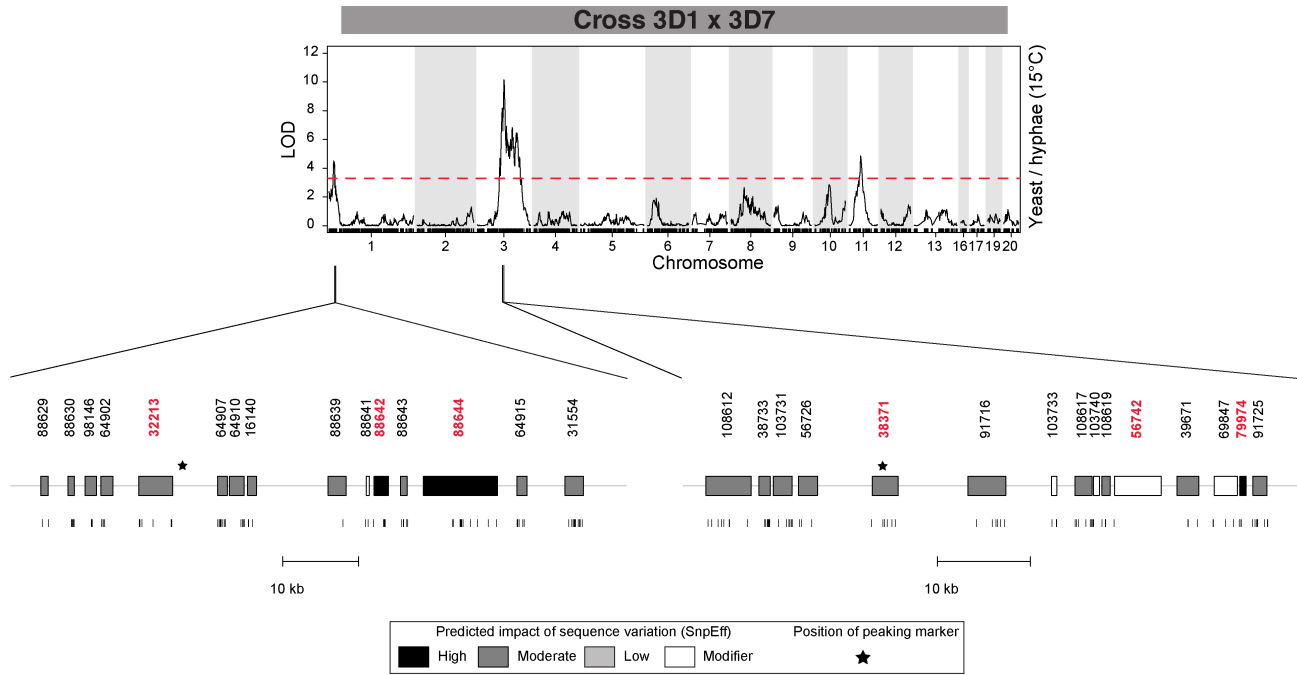


Figure 4 LOD plot from the single marker interval mapping (SIM) analysis over all chromosomes for the yeast/hyphae (15°C) dimorphism QTL with a 95% confidence interval containing the smallest number (≤ 30) of candidate genes. The horizontal dashed red line shows the significance threshold ($p = 0.05$) obtained by 1000 genome-wide permutations. The relative positions of the candidate genes in the 95% Bayes confidence interval of the Chromosome 1 and 3 QTLs are shown below the LOD plot. The genes are color-coded according to the predicted impact by SnpEff of the observed sequence variation (grey = moderate) and labeled with their protein ID. Below the gene bars are vertical lines showing the position of each sequence variant within each gene. The asterisk symbol represents the position of the peaking marker within the confidence interval. Highest likelihood candidate genes are colored in red (32213: an ABC transporter, 88642: unknown function, 88644: Ca²⁺/calmodulin-dependent protein kinase (CaMK), 38371: peptidase, 56742: guanine nucleotide exchange factor (GEF), 79974: unknown function).

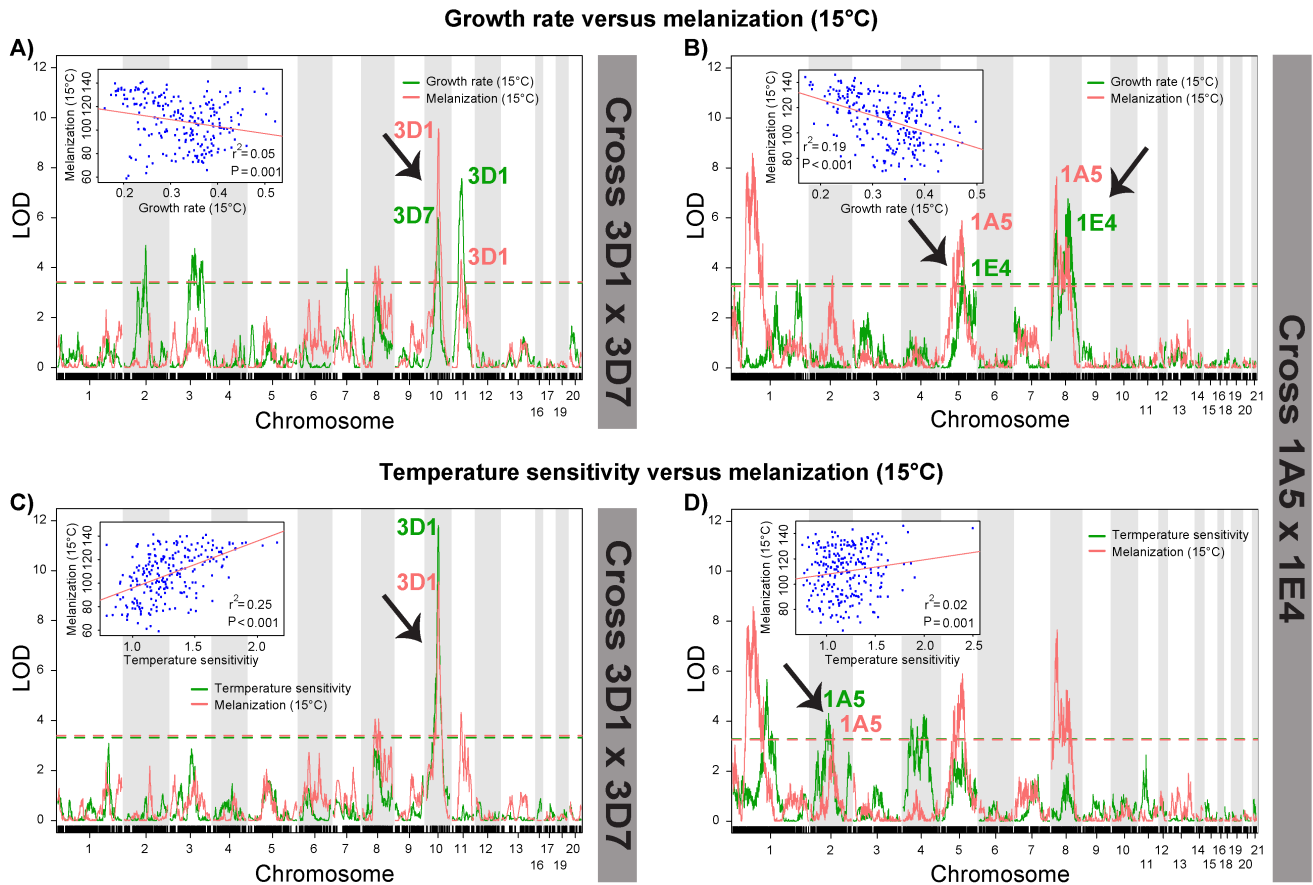


Figure 5 Evidence for pleiotropy amongst melanization, growth rate at 15°C, and temperature sensitivity for the chromosome 10 QTL in cross 3D1 x 3D7. Melanization is represented by grey values (11 dpi), with lower values indicating higher melanization (LENDENMANN *et al.* 2014). The 3D7 allele that increases melanization also accelerates growth at 15°C (Panel A) and decreases temperature sensitivity (Panel C). Contrary to cross 3D1 x 3D7, panel B and D, which show corresponding full genome scan overlaps to panel A and C for cross 1A5 x 1E4, indicate no clear pleiotropy amongst the three traits melanization, growth rate, and temperature sensitivity in cross 1A5 x 1E4. Each panel shows a full genome scan LOD overlap plot based on single marker interval mapping (SIM) analysis, with traits separated by colors (red = melanization trait, green = growth rate at 15°C/temperature sensitivity trait). Horizontal lines in the LOD plots represent the color-coded significance thresholds ($p = 0.05$) obtained with 1000 genome-wide permutations. Each panel includes the corresponding linear correlation plot amongst the two traits. The name above each QTL peak indicates which parental allele provided the higher phenotypic mean. Arrows point to the QTL peaks that could explain the observed positive or negative correlation amongst the two traits.

SUPPORTING MATERIAL

The supplementary information is provided in the appendix section starting from page 171.

CHAPTER 5

General Conclusions and Outlook

GENERAL CONCLUSIONS AND OUTLOOK

Depicting the quantitative nature of traits of interest by showing different degrees of phenotypes within natural populations is an important premise for QTL mapping, as only these traits can be mapped. Previous studies upon *Z. tritici* had shown for some of our traits of interest, that these are of a quantitative nature within natural field populations. This was the case for the traits of growth rate, temperature sensitivity (ZHAN and McDONALD 2011) as well as fungicide sensitivity upon azole fungicides (ZHAN *et al.* 2005; COOLS *et al.* 2011; COOLS and FRAAIJE 2013). However for growth rate and temperature sensitivity the genetic architecture in *Z. tritici* had never been investigated before and for fungicide sensitivity the genetic architecture was still poorly understood (ZWIERS *et al.* 2002; STERGIPOULOS *et al.* 2003; ZWIERS *et al.* 2003; COOLS *et al.* 2007; COOLS and FRAAIJE 2013; COOLS *et al.* 2013). Melanization and the yeast/hyphae dimorphism had not been previously shown to be of a quantitative nature in *Z. tritici* populations. As QTL mapping can be highly cross dependent, we used two mapping populations in order to provide a higher resolution of the genetic architecture of the traits. Overall we mapped for each of the investigated traits multiple significant QTL. Over both crosses and all traits on average ~32% of total phenotypic variance was explained by an average of 2.7 significant QTLs per trait, with a maximum of 55% of total phenotypic variance explained through 6 QTLs for the melanization trait. We found a continuous distribution of phenotypes as well as transgressive segregation, a phenomenon of progeny showing more extreme phenotypes than the parental strains, in all our traits. Overall these findings confirm that all our investigated traits are of a quantitative nature in *Z. tritici* populations with a complex genetic architecture. We therefore conclude, that *Z. tritici* populations are unlikely to be genetically limited to adapt to changing environments.

An additional goal to mapping significant QTLs was the identification of candidate genes as well as candidate quantitative trait nucleotides (QTNs). High-throughput genotyping, using restriction site associated DNA sequencing (RADseq), was applied to the progeny of both mapping populations, in order to obtain recombining, single nucleotide polymorphism (SNP) markers. RADseq is a time and cost efficient next generation sequencing (NGS) technique, providing less coverage than full genome sequencing but at a lower cost per individual (BAIRD *et al.* 2008). RADseq had never been applied to *Z. tritici* before, but had already been successfully used in other filamentous ascomycetes, such as *Neurospora crassa* (BAIRD *et al.* 2008). We could show that this molecular approach was feasible within *Z. tritici* through the adaptation of an existing protocol

(ETTER *et al.* 2011). We postulate that our adapted protocol could be further used in studies upon *Z. tritici* for example within the field of population genetics or GWAS (PETERSON *et al.* 2012). In our study we coupled RADseq with high quality SNP filtering, which allowed the construction of a high quality, highly dense genetic map for both mapping populations. The two genetic maps in our study have very high marker density compared to other reported genetic maps in filamentous fungi (FOULONGNE-ORIOU 2012). This high marker density is due to large numbers of progeny as well as high genome coverage. Earlier genetic maps based on the genome reference isolate IPO323 (KEMA *et al.* 2002; WITTENBERG *et al.* 2009) were ~72% smaller than our genetic maps. We conclude that our maps are larger due to extensive chromosome coverage of the RADseq markers. Additionally we developed a high-throughput yet very precise measurement of size and grey value composition of single spore colonies grown on Petri dishes. This was achieved through the development of a macro in the open-source software ImageJ (SCHNEIDER *et al.* 2012), which runs in batch mode and thus enables automated analysis of multiple digital images in one go (LENDENMANN *et al.* 2014). This macro, due to its precise and reproducible measurements at a high-throughput level, could be of great importance for future *in vitro* studies upon *Z. tritici* but also other pathogens. The macro had already been successfully applied without any further adaptations to another plant pathogen in our lab, namely the barley pathogen *Rhynchosporium commune*. The highly dense genetic maps coupled with precise phenotypic measurements resulted for some of our mapped QTLs in very narrow confidence intervals and therefore low amount of candidate genes. Over all traits investigated a total of eight significant QTLs contained ≤ 30 candidate genes within their confidence intervals, with as little as one candidate gene found in a specific case (LENDENMANN *et al.* 2014). Two of these confidence intervals contained a candidate gene providing high evidence of being the source of phenotypic variance mapped, due to the involvement of their orthologs in the traits in other filamentous fungi. The five other QTLs contained novel genes, not previously associated with the traits. The novel candidates provide the basis for future functional validation studies, e.g. using knockouts and allele swaps.

For the trait of melanization we identified a total of 12 unique QTLs over both crosses. Eight of these 12 QTLs contained novel genes not previously associated with melanization in fungi. Four melanization QTLs had confidence intervals containing ≤ 22 candidate genes. In one particular case the confidence interval stretched over only 9 kb with only one, novel candidate gene. Another of these four QTLs had a very high LOD score (~32) and contained the *PKS1* gene beside three other

candidate genes. *PKS1*, a polyketide synthase gene, is known to play a role in the synthesis of dihydroxynaphthalene (DHN) melanin. Through inter- and intra-species analysis of the *PKS1* gene, we gained evidence of a non-synonymous mutation representing the QTN within the mapped QTL. We consider the mapping of *PKS1* as a confirmation of the functionality of our methods and could show that melanization has a highly complex genetic architecture in *Z. tritici*. For fungicide sensitivity the majority of previous *Z. tritici* studies haven been focusing on the phenotypic effects of natural genetic diversity of the target gene (*CYP51*) of azole fungicides. We mapped a total of three QTLs for this trait. The three QTLs were positioned on chromosomes that differed from the chromosome containing the target gene. Two of these three QTLs covered novel fungicide sensitivity candidate genes, with one of them containing only 16 candidate genes. Our findings imply that other genes apart from the fungicide target site are of importance in contributing to the quantitative trait of fungicide sensitivity in *Z. tritici*. We also found compelling evidence for pleiotropy among melanization and fungicide sensitivity, with higher degrees of melanization associated with lesser fungicide sensitivity. As melanin appears to be a fungicide resistant factor, we suggest a novel disease control strategy to control *Z. tritici* in the field, namely deployment of fungicide mixtures containing both fungicides and melanin inhibitors (e.g. tricyclazole and pyroquilon). These mixtures could counteract the ability of melanin to inhibit the activity of fungicides. QTL mapping of temperature sensitivity provided a strong peak with a high LOD score (~12) containing six candidate genes. One of these candidate genes was *PBS2*, encoding a mitogen-activated protein kinase kinase and associated with low temperature tolerance in *Saccharomyces cerevisiae* as a part of the high osmolarity glycerol (HOG) pathway (PANADERO *et al.* 2006). Our results suggest that the HOG pathway is important in *Z. tritici* for thermal adaptation. Our results further show a complex genetic architecture of growth and temperature sensitivity in *Z. tritici*. We therefore conclude for thermal adaptation that distribution of this species is most likely not genetically limited and evolution under changing climate can occur rapidly. The trait of dimorphism has received very little attention in *Z. tritici* so far. We could show that this trait is of a quantitative nature in *Z. tritici*, with QTLs correlating strongly with growth QTLs, potentially suggesting that the dimorphism trait may be a threshold trait, which is triggered by growth.

We found no significant QTLs on the accessory chromosomes (ACs, chromosomes 14 to 21), which were present within both parental strains. These chromosomes are also considered as dispensable chromosomes, as they have been shown to be lost in certain individuals, with no

obvious phenotypic effect. The *Z. tritici* ACs represent the biggest number of ACs known in filamentous fungi and span a size of ~4.6Mb (MEHRABI *et al.* 2007; GOODWIN *et al.* 2011). Unlike in other fungal species, such as *Nectria haematococca* or *Fusarium oxysporum f. sp. lycopersici*, where pathogenicity factors have been attributed to the ACs (MIAO *et al.* 1991; COLEMAN *et al.* 2009; MA *et al.* 2010), their function in *Z. tritici* is till today of an unknown nature. However earlier studies show evidence in ACs harboring virulence genes due to the finding of genes being under accelerated evolution, containing protein patterns associated with a role in pathogenicity and showing differential expression between *in planta* and axenic culture (STUKENBROCK *et al.* 2010; GOODWIN *et al.* 2011; KELLNER *et al.* 2014). Possible explanations for not mapping any QTLs on the ACs in this study are the following: 1. Genes on the ACs are not involved in any of the studied phenotypes. 2. Parental strains are monomorph regarding accessory chromosome genes. 3. The allele effect sizes are too small to be detected under the current statistical power of the study.

In addition to simple interval mapping (SIM) we used a multiple QTL model combined with interval mapping to evaluate the presence of at least two QTLs on the same chromosome (data not shown here nor in any of the previous chapters). This was done for peaks, which showed a visible double peak behavior in the SIM full genome scans. All the peaks investigated showed evidence for at least two QTLs present on the same chromosome. These findings suggest more QTLs to be at state in both crosses than initially detected using SIM and may explain to a certain extent, why the majority (>85%) of the SIM QTLs, that underwent double-peak investigation, have a rather large confidence interval (>1000 kb), as two QTLs on the same chromosome unavoidably stretch the confidence interval. We postulate that this additional analysis could further help in narrowing down candidate genes due to obtaining more narrow confidence intervals under the multiple QTL model compared to SIM confidence intervals. However the confidence intervals obtained through the multiple QTL model need to be viewed with some caution, as their performance in the context of multiple QTLs on the same chromosome is not well understood (ARENDS *et al.* 2010).

Overall we would like to conclude that QTL mapping has been successfully applied for the first time upon *Z. tritici*. To our knowledge this PhD represents the first forward genetics study applied upon *Z. tritici* associating natural genetic variance with phenotypic variance for all investigated traits. We were able to resolve the genetic architecture for different traits, important in agriculture but also in the life history of the wheat pathogen *Z. tritici*. Our findings show that all investigated traits have a complex genetic architecture and that populations of *Z. tritici* harbor

standing genetic variation for selection to act upon. We therefore conclude that *Z. tritici* populations have a potential to rapidly adapt to environmental changes. The identified QTLs confirm genes but also identified novel genes not previously associated with the studied traits. This work sets the fundament for future QTL mapping studies in *Z. tritici*, where fine-mapping could be performed through the incorporation of additional progeny or the current mapping populations could be used to investigate additional phenotypes. We believe that this work and the findings made during this PhD are of importance for future control strategies of *Z. tritici* but also of other fungal plant, as well as animal and human pathogens.

References

- ARENDS, D., P. PRINS, R. C. JANSEN and K. W. BROMAN, 2010 R/qtl: high-throughput multiple QTL mapping. *Bioinformatics* **26**: 2990-2992.
- BAIRD, N. A., P. D. ETTER, T. S. ATWOOD, M. C. CURREY, A. L. SHIVER *et al.*, 2008 Rapid SNP discovery and genetic mapping using sequenced rad markers. *PLOS One* **3**: e3376.
- COLEMAN, J. J., S. D. ROUNSLEY, M. RODRIGUEZ-CARRES, A. KUO, C. C. WASMANN *et al.*, 2009 The genome of *Nectria haematococca*: contribution of supernumerary chromosomes to gene expansion. *Plos Genetics* **5**: e1000618.
- COOLS, H. J., and B. A. FRAAIJE, 2013 Update on mechanisms of azole resistance in *Mycosphaerella graminicola* and implications for future control. *Pest Management Science* **69**: 150-155.
- COOLS, H. J., B. A. FRAAIJE, T. P. BEAN, J. ANTONIW and J. A. LUCAS, 2007 Transcriptome profiling of the response of *Mycosphaerella graminicola* isolates to an azole fungicide using cDNA microarrays. *Molecular Plant Pathology* **8**: 639-651.
- COOLS, H. J., N. J. HAWKINS and B. A. FRAAIJE, 2013 Constraints on the evolution of azole resistance in plant pathogenic fungi. *Plant Pathology* **62**: 36-42.
- COOLS, H. J., J. G. L. MULLINS, B. A. FRAAIJE, J. E. PARKER, D. E. KELLY *et al.*, 2011 Impact of recently emerged sterol 14 alpha-demethylase (CYP51) variants of *Mycosphaerella graminicola* on azole fungicide sensitivity. *Applied and Environmental Microbiology* **77**: 3830-3837.
- ETTER, P. D., S. BASSHAM, P. A. HOHENLOHE, E. A. JOHNSON and W. A. CRESKO, 2011 SNP discovery and genotyping for evolutionary genetics using RAD sequencing. *Methods in Molecular Biology* **772**: 157-178.
- FOULONGNE-ORIOU, M., 2012 Genetic linkage mapping in fungi: current state, applications, and future trends. *Appl Microbiol Biotechnol* **95**: 891-904.
- GOODWIN, S. B., S. BEN M'BAREK, B. DHILLON, A. H. J. WITTENBERG, C. F. CRANE *et al.*, 2011 Finished genome of the fungal wheat pathogen *Mycosphaerella graminicola* reveals dispensome structure, chromosome plasticity, and stealth pathogenesis. *PLOS Genetics* **7**: e1002070.
- KELLNER, R., A. BHATTACHARYYA, S. POPPE, T. Y. HSU, R. B. BREM *et al.*, 2014 Expression profiling of the wheat pathogen *Zymoseptoria tritici* reveals genomic patterns of transcription and host-specific regulatory programs. *Genome Biology and Evolution* **6**: 1353-1365.
- KEMA, G. H. J., S. B. GOODWIN, S. HAMZA, E. C. P. VERSTAPPEN, J. R. CAVALETTO *et al.*, 2002 A combined amplified fragment length polymorphism and randomly amplified polymorphism DNA

- genetic linkage map of *Mycosphaerella graminicola*, the septoria tritici leaf blotch pathogen of wheat. *Genetics* **161**: 1497-1505.
- LENDENMANN, M. H., D. CROLL, E. L. STEWART and B. A. McDONALD, 2014 Quantitative trait locus mapping of melanization in the plant pathogenic fungus *Zymoseptoria tritici*. *G3-Genes Genomes Genetics* **4**: 2519-2533.
- MA, L.-J., H. C. VAN DER DOES, K. A. BORKOVICH, J. J. COLEMAN, M.-J. DABOUSSI *et al.*, 2010 Comparative genomics reveals mobile pathogenicity chromosomes in *Fusarium*. *Nature* **464**: 367-373.
- MEHRABI, R., M. TAGA and G. H. J. KEMA, 2007 Electrophoretic and cytological karyotyping of the foliar wheat pathogen *Mycosphaerella graminicola* reveals many chromosomes with a large size range. *Mycologia* **99**: 868-876.
- MIAO, V. P., S. F. COVERT and H. D. VANETTEN, 1991 A fungal gene for antibiotic-resistance on a dispensable ("B") chromosome. *Science* **254**: 1773-1776.
- PANADERO, J., C. PALLOTTI, S. RODRIGUEZ-VARGAS, F. RANDEZ-GIL and J. A. PRIETO, 2006 A downshift in temperature activates the high osmolarity glycerol (HOG) pathway, which determines freeze tolerance in *Saccharomyces cerevisiae*. *Journal of Biological Chemistry* **281**: 4638-4645.
- PETERSON, B. K., J. N. WEBER, E. H. KAY, H. S. FISHER and H. E. HOEKSTRA, 2012 Double Digest RADseq: An Inexpensive Method for De Novo SNP Discovery and Genotyping in Model and Non-Model Species. *Plos One* **7**: e37135.
- SCHNEIDER, C. A., W. S. RASBAND and K. W. ELICEIRI, 2012 NIH Image to ImageJ: 25 years of image analysis. *Nature Methods* **9**: 671-675.
- STERGIOPOULOS, I., J. G. M. VAN NISTELROOY, G. H. J. KEMA and M. A. DE WAARD, 2003 Multiple mechanisms account for variation in base-line sensitivity to azole fungicides in field isolates of *Mycosphaerella graminicola*. *Pest Management Science* **59**: 1333-1343.
- STUKENBROCK, E. H., F. G. JORGENSEN, M. ZALA, T. T. HANSEN, B. A. McDONALD *et al.*, 2010 Whole-genome and chromosome evolution associated with host adaptation and speciation of the wheat pathogen *Mycosphaerella graminicola*. *Plos Genetics* **6**: e1001189.
- WITTENBERG, A. H. J., T. A. J. VAN DER LEE, S. BEN M'BAREK, S. B. WARE, S. B. GOODWIN *et al.*, 2009 Meiosis Drives Extraordinary Genome Plasticity in the Haploid Fungal Plant Pathogen *Mycosphaerella graminicola*. *Plos One* **4**: e5863.

- ZHAN, J., C. C. LINDE, T. JURGENS, U. MERZ, F. STEINEBRUNNER *et al.*, 2005 Variation for neutral markers is correlated with variation for quantitative traits in the plant pathogenic fungus *Mycosphaerella graminicola*. *Molecular Ecology* **14**: 2683-2693.
- ZHAN, J., and B. A. McDONALD, 2011 Thermal adaptation in the fungal pathogen *Mycosphaerella graminicola*. *Molecular Ecology* **20**: 1689-1701.
- ZWIERS, L. H., I. STERGIOPOULOS, M. M. C. GIELKENS, S. D. GOODALL and M. A. DE WAARD, 2003 ABC transporters of the wheat pathogen *Mycosphaerella graminicola* function as protectants against biotic and xenobiotic toxic compounds. *Molecular Genetics and Genomics* **269**: 499-507.
- ZWIERS, L. H., I. STERGIOPOULOS, J. G. M. VAN NISTELROOY and M. A. DE WAARD, 2002 ABC transporters and azole susceptibility in laboratory strains of the wheat pathogen *Mycosphaerella graminicola*. *Antimicrobial Agents and Chemotherapy* **46**: 3900-3906.

ACKNOWLEDGEMENTS

I am very grateful to many people for their support during my PhD. In particular I would like to thank:

- Prof. Bruce A. McDonald for his great mentorship, for the opportunity to work on this project in a wonderful research group, for letting me drive and manage my projects, for the chance to attend several international meetings to present my work and most of all, for being a great boss.
- Dr. Daniel Croll for all the amazing help and valuable contribution he provided along my PhD in various fields (experimental design, statistics, bioinformatics, scientific writing, results discussion, etc.). You are a brilliant scientist and an amazing person and a huge inspiration to me.
- Prof. Edward J. Louis for agreeing to be a co-examiner. Thank you for your time.
- Ethan for all the great collaborations and insights. Working with you has been a huge pleasure. Many thanks as well for the organization of various social events.
- Tryggvi, my trusted officemate. Many thanks for all the great chats and musical inputs.
- Everybody in the ETH Plant Pathology group for all the support. This group is amazing. Special thanks to:
 - The whole A-floor gang (Fanny, Farhan, Parvathy, Megan, Rebecca and Ethan) for being wonderful work companions.
 - Stefano, Andrea, Michele and Javi for the long discussions and lots of laughs.
 - Sandra and Uli for all their administrative help.
 - Marcello for tolerating my random question invasion regarding laboratory work.
 - Jana and Joana for the beautiful ski weekends at their lovely mountain retreats.
 - Tina and Elizabeth for all the cleaning of laboratory materials and the delicious strawberry jam.

- All the people, who helped with the vast amount of phenotyping: Fanny, Tryggvi, Francesca, Renato and especially Fabienne and Viktor. You guys made phenotyping fun.
- Norbert and Michael for providing me with a kick-start regarding digital image analysis.
- The ETH staff of the Genetic Diversity Centre (GDC) and the Quantitative Genomics Facility for all their laboratory support.
- The Swiss National Science Foundation for founding this work.
- My family, friends and loved ones for all their huge support and love.
- André for being a wonderful roomie and all-around amazing person. Thanks for picking me up when I didn't have the strength.

PUBLICATIONS

Published work

- M.H. Lendenmann, D. Croll and B.A. McDonald. 2015. QTL mapping of fungicide sensitivity reveals novel genes and pleiotropy with melanization in the pathogen *Zymoseptoria tritici*. *Fungal Genetics and Biology*, 80:53-67.
- M.H. Lendenmann, D. Croll, E.L. Stewart and B.A. McDonald. 2014. Quantitative trait locus mapping of melanization in the plant pathogenic fungus *Zymoseptoria tritici*. *G3-Genes Genomes Genetics*, 4: 2519-2533.
- M.H. Lendenmann, C. Thonar, R.L. Barnard, Y. Salmon, R.A. Werner, E. Frossard and J. Jansa. 2011. Symbiont identity matters: carbon and phosphorus fluxes between *Medicago truncatula* and different arbuscular mycorrhizal fungi. *Mycorrhiza* 21: 689-702.

Unpublished work

- M.H. Lendenmann, D. Croll, J. Palma-Guerrero, E.L. Stewart and B.A. McDonald. QTL mapping of temperature sensitivity reveals candidate genes for thermal adaptation and growth morphology in the plant pathogenic fungus *Zymoseptoria tritici*. Manuscript in preparation.
- D. Croll, M.H. Lendenmann, E.L. Stewart and B.A. McDonald. Fine-scale recombination maps of the fungal pathogen *Zymoseptoria tritici* reveal intra-specific variation in recombination hotspot locations. Submitted to *Genetics* 05.05.2015.
- E.L. Stewart, D. Croll, M.H. Lendenmann, J. Palma-Guerrero, F.E. Hartmann and B. A. McDonald. QTL mapping reveals novel virulence genes in the plant pathogen *Zymoseptoria tritici*. Manuscript in preparation.

Awards

- Genetics society of America poster award. Fungal genetics meeting, Pacific Grove (USA). March 17-22, 2015.

Selected presentations

- Fungal genetics conference at Asilomar, Pacific Grove (USA). March 17-22, 2015. Poster
- Dothideomycetes comparative genomics workshop at Asilomar, Pacific Grove (USA). March 17, 2015. Talk
- *Zymoseptoria tritici* research community meeting, Exeter (UK). September 11-12, 2014. Talk
- Population genomics meeting: Fungi as models, Orsay (France). April 22, 2014. Talk
- European conference on fungal genetics, Seville (Spain). March 23-27, 2014. Poster
- Dothideomycetes workshop, Seville (Spain). March 23, 2014. Talk
- Genetic diversity center symposium, Zürich (Switzerland). January 30, 2014. Talk
- Zürich mycology symposium, Zürich (Switzerland). January 24, 2014. Talk
- *Zymoseptoria tritici* European workshop, Rothamsted (UK). August 5-6, 2013. Talk

CURRICULUM VITAE

Mark Henry Lendenmann

Born 17th May, 1980. Citizen of Switzerland

2015- Doctor of Science (PhD)

ETH Zurich

Plant Pathology Group: Institute of Integrative Biology

Title of thesis: QTL mapping of important agricultural and life history traits in the plant pathogenic fungus *Zymoseptoria tritici*

Advisor: Prof. Bruce A. McDonald

2009 – Teaching Certificate

ETH Zurich

2008 - Diploma Agricultural Engineering (equivalent to Master of Science (MSc))

M.Sc. Plant sciences

ETH Zurich

Title of thesis: Symbiont identity matters: carbon and phosphorus fluxes between *Medicago truncatula* and different arbuscular mycorrhizal fungi.

Advisors: Dr. Cécile Thonar, Dr. Jan Jansa and Prof. Emmanuel Frossard

APPENDIX

The appendix contains the supplementary information for the chapter 4, as this chapter isn't published yet.

Table S1 BioProject and sample accession numbers for the quality filtered retained progeny used in the QTL analysis for each of the two crosses.

Cross	Retained progeny for QTL analysis	NCBI BioProject accession	NCBI SRA sample accession
3D1 x 3D7	1.1	PRJNA256988	SRS670337
3D1 x 3D7	1.2	PRJNA256988	SRS670339
3D1 x 3D7	10.1	PRJNA256988	SRS670338
3D1 x 3D7	100.1	PRJNA256988	SRS670340
3D1 x 3D7	100.2	PRJNA256988	SRS670342
3D1 x 3D7	101.2	PRJNA256988	SRS670344
3D1 x 3D7	102.1	PRJNA256988	SRS670345
3D1 x 3D7	102.2	PRJNA256988	SRS670346
3D1 x 3D7	103.1	PRJNA256988	SRS670347
3D1 x 3D7	104.1	PRJNA256988	SRS670349
3D1 x 3D7	104.2	PRJNA256988	SRS670350
3D1 x 3D7	105.1	PRJNA256988	SRS670351
3D1 x 3D7	105.2	PRJNA256988	SRS670352
3D1 x 3D7	106.1	PRJNA256988	SRS670353
3D1 x 3D7	106.2	PRJNA256988	SRS670355
3D1 x 3D7	107.1	PRJNA256988	SRS670354
3D1 x 3D7	108.1	PRJNA256988	SRS670356
3D1 x 3D7	108.2	PRJNA256988	SRS670358
3D1 x 3D7	109.1	PRJNA256988	SRS670359
3D1 x 3D7	109.2	PRJNA256988	SRS670360
3D1 x 3D7	11.1	PRJNA256988	SRS670361
3D1 x 3D7	11.2	PRJNA256988	SRS670362
3D1 x 3D7	110.1	PRJNA256988	SRS670363
3D1 x 3D7	110.2	PRJNA256988	SRS670365
3D1 x 3D7	111.2	PRJNA256988	SRS670367
3D1 x 3D7	112.1	PRJNA256988	SRS670366
3D1 x 3D7	113.1	PRJNA256988	SRS670369
3D1 x 3D7	113.2	PRJNA256988	SRS670370
3D1 x 3D7	114.1	PRJNA256988	SRS670371
3D1 x 3D7	114.2	PRJNA256988	SRS670372
3D1 x 3D7	115.1	PRJNA256988	SRS670373
3D1 x 3D7	116.1	PRJNA256988	SRS670375
3D1 x 3D7	116.2	PRJNA256988	SRS670376
3D1 x 3D7	117.1	PRJNA256988	SRS670378
3D1 x 3D7	117.2	PRJNA256988	SRS670377
3D1 x 3D7	118.1	PRJNA256988	SRS670380
3D1 x 3D7	118.2	PRJNA256988	SRS670379

3D1 x 3D7	119.1	PRJNA256988	SRS670381
3D1 x 3D7	119.2	PRJNA256988	SRS670382
3D1 x 3D7	12.1	PRJNA256988	SRS670383
3D1 x 3D7	120.1	PRJNA256988	SRS670385
3D1 x 3D7	120.2	PRJNA256988	SRS670386
3D1 x 3D7	121.2	PRJNA256988	SRS670388
3D1 x 3D7	122.1	PRJNA256988	SRS670389
3D1 x 3D7	123.1	PRJNA256988	SRS670391
3D1 x 3D7	125.1	PRJNA256988	SRS670395
3D1 x 3D7	126.1	PRJNA256988	SRS670397
3D1 x 3D7	127.1	PRJNA256988	SRS670398
3D1 x 3D7	127.2	PRJNA256988	SRS670399
3D1 x 3D7	128.1	PRJNA256988	SRS670400
3D1 x 3D7	128.2	PRJNA256988	SRS670401
3D1 x 3D7	129.2	PRJNA256988	SRS670403
3D1 x 3D7	13.1	PRJNA256988	SRS670404
3D1 x 3D7	130.1	PRJNA256988	SRS670406
3D1 x 3D7	131.1	PRJNA256988	SRS670408
3D1 x 3D7	133.1	PRJNA256988	SRS670413
3D1 x 3D7	134.1	PRJNA256988	SRS670414
3D1 x 3D7	135.2	PRJNA256988	SRS670418
3D1 x 3D7	136.1	PRJNA256988	SRS670417
3D1 x 3D7	137.1	PRJNA256988	SRS670419
3D1 x 3D7	137.2	PRJNA256988	SRS670420
3D1 x 3D7	138.1	PRJNA256988	SRS670421
3D1 x 3D7	139.2	PRJNA256988	SRS670423
3D1 x 3D7	14.1	PRJNA256988	SRS670425
3D1 x 3D7	141.1	PRJNA256988	SRS670429
3D1 x 3D7	142.1	PRJNA256988	SRS670430
3D1 x 3D7	142.2	PRJNA256988	SRS670431
3D1 x 3D7	143.1	PRJNA256988	SRS670432
3D1 x 3D7	144.1	PRJNA256988	SRS670434
3D1 x 3D7	145.1	PRJNA256988	SRS670437
3D1 x 3D7	145.2	PRJNA256988	SRS670436
3D1 x 3D7	146.1	PRJNA256988	SRS670438
3D1 x 3D7	146.2	PRJNA256988	SRS670440
3D1 x 3D7	147.1	PRJNA256988	SRS670439
3D1 x 3D7	148.1	PRJNA256988	SRS670443
3D1 x 3D7	149.1	PRJNA256988	SRS670444
3D1 x 3D7	149.2	PRJNA256988	SRS670445

3D1 x 3D7	15.1	PRJNA256988	SRS670446
3D1 x 3D7	15.2	PRJNA256988	SRS670447
3D1 x 3D7	150.1	PRJNA256988	SRS670448
3D1 x 3D7	150.2	PRJNA256988	SRS670449
3D1 x 3D7	151.1	PRJNA256988	SRS670452
3D1 x 3D7	152.1	PRJNA256988	SRS670451
3D1 x 3D7	152.2	PRJNA256988	SRS670453
3D1 x 3D7	154.1	PRJNA256988	SRS670456
3D1 x 3D7	154.2	PRJNA256988	SRS670458
3D1 x 3D7	155.1	PRJNA256988	SRS670457
3D1 x 3D7	156.1	PRJNA256988	SRS670461
3D1 x 3D7	157.1	PRJNA256988	SRS670462
3D1 x 3D7	158.1	PRJNA256988	SRS670464
3D1 x 3D7	158.2	PRJNA256988	SRS670465
3D1 x 3D7	159.1	PRJNA256988	SRS670466
3D1 x 3D7	16.1	PRJNA256988	SRS670468
3D1 x 3D7	160.1	PRJNA256988	SRS670470
3D1 x 3D7	160.2	PRJNA256988	SRS670471
3D1 x 3D7	161.1	PRJNA256988	SRS670472
3D1 x 3D7	161.2	PRJNA256988	SRS670473
3D1 x 3D7	162.1	PRJNA256988	SRS670474
3D1 x 3D7	162.2	PRJNA256988	SRS670475
3D1 x 3D7	163.1	PRJNA256988	SRS670476
3D1 x 3D7	164.1	PRJNA256988	SRS670478
3D1 x 3D7	164.2	PRJNA256988	SRS670479
3D1 x 3D7	165.1	PRJNA256988	SRS670480
3D1 x 3D7	165.2	PRJNA256988	SRS670481
3D1 x 3D7	166.1	PRJNA256988	SRS670482
3D1 x 3D7	167.1	PRJNA256988	SRS670484
3D1 x 3D7	167.2	PRJNA256988	SRS670485
3D1 x 3D7	168.1	PRJNA256988	SRS670486
3D1 x 3D7	169.1	PRJNA256988	SRS670487
3D1 x 3D7	169.2	PRJNA256988	SRS670488
3D1 x 3D7	17.2	PRJNA256988	SRS670492
3D1 x 3D7	170.1	PRJNA256988	SRS670491
3D1 x 3D7	170.2	PRJNA256988	SRS670493
3D1 x 3D7	171.1	PRJNA256988	SRS670494
3D1 x 3D7	172.1	PRJNA256988	SRS670496
3D1 x 3D7	173.1	PRJNA256988	SRS670498
3D1 x 3D7	174.1	PRJNA256988	SRS670499

3D1 x 3D7	174.2	PRJNA256988	SRS670501
3D1 x 3D7	175.1	PRJNA256988	SRS670502
3D1 x 3D7	176.2	PRJNA256988	SRS670505
3D1 x 3D7	177.2	PRJNA256988	SRS670507
3D1 x 3D7	178.1	PRJNA256988	SRS670508
3D1 x 3D7	179.1	PRJNA256988	SRS670510
3D1 x 3D7	179.2	PRJNA256988	SRS670511
3D1 x 3D7	18.1	PRJNA256988	SRS670512
3D1 x 3D7	18.2	PRJNA256988	SRS670513
3D1 x 3D7	180.1	PRJNA256988	SRS670514
3D1 x 3D7	180.2	PRJNA256988	SRS670515
3D1 x 3D7	181.1	PRJNA256988	SRS670516
3D1 x 3D7	181.2	PRJNA256988	SRS670518
3D1 x 3D7	182.1	PRJNA256988	SRS670517
3D1 x 3D7	183.1	PRJNA256988	SRS670520
3D1 x 3D7	184.1	PRJNA256988	SRS670521
3D1 x 3D7	185.1	PRJNA256988	SRS670522
3D1 x 3D7	19.1	PRJNA256988	SRS670524
3D1 x 3D7	19.2	PRJNA256988	SRS670525
3D1 x 3D7	2.1	PRJNA256988	SRS670526
3D1 x 3D7	20.1	PRJNA256988	SRS670528
3D1 x 3D7	20.2	PRJNA256988	SRS670529
3D1 x 3D7	21.1	PRJNA256988	SRS670530
3D1 x 3D7	21.2	PRJNA256988	SRS670531
3D1 x 3D7	22.1	PRJNA256988	SRS670532
3D1 x 3D7	22.2	PRJNA256988	SRS670533
3D1 x 3D7	23.1	PRJNA256988	SRS670534
3D1 x 3D7	23.2	PRJNA256988	SRS670536
3D1 x 3D7	24.1	PRJNA256988	SRS670535
3D1 x 3D7	24.2	PRJNA256988	SRS670537
3D1 x 3D7	25.1	PRJNA256988	SRS670538
3D1 x 3D7	26.1	PRJNA256988	SRS670540
3D1 x 3D7	26.2	PRJNA256988	SRS670541
3D1 x 3D7	27.1	PRJNA256988	SRS670542
3D1 x 3D7	28.1	PRJNA256988	SRS670544
3D1 x 3D7	29.1	PRJNA256988	SRS670545
3D1 x 3D7	3.1	PRJNA256988	SRS670547
3D1 x 3D7	3.2	PRJNA256988	SRS670548
3D1 x 3D7	30.1	PRJNA256988	SRS670550
3D1 x 3D7	31.1	PRJNA256988	SRS670551

3D1 x 3D7	32.1	PRJNA256988	SRS670553
3D1 x 3D7	33.1	PRJNA256988	SRS670555
3D1 x 3D7	34.1	PRJNA256988	SRS670557
3D1 x 3D7	34.2	PRJNA256988	SRS670559
3D1 x 3D7	35.1	PRJNA256988	SRS670558
3D1 x 3D7	35.2	PRJNA256988	SRS670560
3D1 x 3D7	36.1	PRJNA256988	SRS670561
3D1 x 3D7	37.1	PRJNA256988	SRS670564
3D1 x 3D7	37.2	PRJNA256988	SRS670563
3D1 x 3D7	38.1	PRJNA256988	SRS670565
3D1 x 3D7	39.1	PRJNA256988	SRS670567
3D1 x 3D7	4.1	PRJNA256988	SRS670569
3D1 x 3D7	4.2	PRJNA256988	SRS670570
3D1 x 3D7	40.1	PRJNA256988	SRS670572
3D1 x 3D7	40.2	PRJNA256988	SRS670571
3D1 x 3D7	41.1	PRJNA256988	SRS670573
3D1 x 3D7	41.2	PRJNA256988	SRS670575
3D1 x 3D7	42.1	PRJNA256988	SRS670574
3D1 x 3D7	42.2	PRJNA256988	SRS670576
3D1 x 3D7	43.1	PRJNA256988	SRS670577
3D1 x 3D7	44.1	PRJNA256988	SRS670580
3D1 x 3D7	45.1	PRJNA256988	SRS670581
3D1 x 3D7	46.1	PRJNA256988	SRS670583
3D1 x 3D7	46.2	PRJNA256988	SRS670584
3D1 x 3D7	47.1	PRJNA256988	SRS670585
3D1 x 3D7	48.1	PRJNA256988	SRS670587
3D1 x 3D7	48.2	PRJNA256988	SRS670588
3D1 x 3D7	49.1	PRJNA256988	SRS670589
3D1 x 3D7	49.2	PRJNA256988	SRS670590
3D1 x 3D7	5.1	PRJNA256988	SRS670591
3D1 x 3D7	5.2	PRJNA256988	SRS670592
3D1 x 3D7	50.1	PRJNA256988	SRS670593
3D1 x 3D7	51.1	PRJNA256988	SRS670596
3D1 x 3D7	51.2	PRJNA256988	SRS670595
3D1 x 3D7	52.1	PRJNA256988	SRS670597
3D1 x 3D7	52.2	PRJNA256988	SRS670598
3D1 x 3D7	53.2	PRJNA256988	SRS670600
3D1 x 3D7	54.1	PRJNA256988	SRS670601
3D1 x 3D7	55.1	PRJNA256988	SRS670604
3D1 x 3D7	55.2	PRJNA256988	SRS670603

3D1 x 3D7	56.1	PRJNA256988	SRS670605
3D1 x 3D7	56.2	PRJNA256988	SRS670606
3D1 x 3D7	57.1	PRJNA256988	SRS670607
3D1 x 3D7	57.2	PRJNA256988	SRS670609
3D1 x 3D7	58.1	PRJNA256988	SRS670608
3D1 x 3D7	59.1	PRJNA256988	SRS670611
3D1 x 3D7	59.2	PRJNA256988	SRS670612
3D1 x 3D7	6.1	PRJNA256988	SRS670614
3D1 x 3D7	60.2	PRJNA256988	SRS670613
3D1 x 3D7	61.1	PRJNA256988	SRS670615
3D1 x 3D7	62.1	PRJNA256988	SRS670617
3D1 x 3D7	62.2	PRJNA256988	SRS670618
3D1 x 3D7	63.1	PRJNA256988	SRS670619
3D1 x 3D7	64.1	PRJNA256988	SRS670621
3D1 x 3D7	65.1	PRJNA256988	SRS670623
3D1 x 3D7	66.1	PRJNA256988	SRS670624
3D1 x 3D7	67.1	PRJNA256988	SRS670626
3D1 x 3D7	68.1	PRJNA256988	SRS670629
3D1 x 3D7	68.2	PRJNA256988	SRS670630
3D1 x 3D7	69.1	PRJNA256988	SRS670631
3D1 x 3D7	69.2	PRJNA256988	SRS670633
3D1 x 3D7	7.1	PRJNA256988	SRS670632
3D1 x 3D7	70.1	PRJNA256988	SRS670635
3D1 x 3D7	71.2	PRJNA256988	SRS670636
3D1 x 3D7	72.1	PRJNA256988	SRS670637
3D1 x 3D7	72.2	PRJNA256988	SRS670638
3D1 x 3D7	73.1	PRJNA256988	SRS670639
3D1 x 3D7	74.1	PRJNA256988	SRS670641
3D1 x 3D7	75.1	PRJNA256988	SRS670644
3D1 x 3D7	75.2	PRJNA256988	SRS670643
3D1 x 3D7	76.1	PRJNA256988	SRS670646
3D1 x 3D7	76.2	PRJNA256988	SRS670645
3D1 x 3D7	77.1	PRJNA256988	SRS670647
3D1 x 3D7	78.1	PRJNA256988	SRS670650
3D1 x 3D7	79.1	PRJNA256988	SRS670651
3D1 x 3D7	8.1	PRJNA256988	SRS670653
3D1 x 3D7	8.2	PRJNA256988	SRS670654
3D1 x 3D7	80.1	PRJNA256988	SRS670655
3D1 x 3D7	80.2	PRJNA256988	SRS670656
3D1 x 3D7	82.1	PRJNA256988	SRS670659

3D1 x 3D7	82.2	PRJNA256988	SRS670660
3D1 x 3D7	83.1	PRJNA256988	SRS670661
3D1 x 3D7	83.2	PRJNA256988	SRS670662
3D1 x 3D7	84.1	PRJNA256988	SRS670663
3D1 x 3D7	84.2	PRJNA256988	SRS670664
3D1 x 3D7	86.2	PRJNA256988	SRS670668
3D1 x 3D7	87.1	PRJNA256988	SRS670669
3D1 x 3D7	88.1	PRJNA256988	SRS670672
3D1 x 3D7	89.1	PRJNA256988	SRS670674
3D1 x 3D7	89.2	PRJNA256988	SRS670673
3D1 x 3D7	9.1	PRJNA256988	SRS670675
3D1 x 3D7	90.1	PRJNA256988	SRS670677
3D1 x 3D7	91.2	PRJNA256988	SRS670679
3D1 x 3D7	92.1	PRJNA256988	SRS670680
3D1 x 3D7	93.1	PRJNA256988	SRS670682
3D1 x 3D7	93.2	PRJNA256988	SRS670683
3D1 x 3D7	94.1	PRJNA256988	SRS670685
3D1 x 3D7	94.2	PRJNA256988	SRS670684
3D1 x 3D7	95.1	PRJNA256988	SRS670686
3D1 x 3D7	95.2	PRJNA256988	SRS670687
3D1 x 3D7	96.1	PRJNA256988	SRS670688
3D1 x 3D7	96.2	PRJNA256988	SRS670689
3D1 x 3D7	97.1	PRJNA256988	SRS670690
3D1 x 3D7	97.2	PRJNA256988	SRS670691
3D1 x 3D7	98.1	PRJNA256988	SRS670693
3D1 x 3D7	99.1	PRJNA256988	SRS670694
1A5 x 1E4	A1.1	PRJNA256991	SRS670696
1A5 x 1E4	A10.1	PRJNA256991	SRS670697
1A5 x 1E4	A11.1	PRJNA256991	SRS670699
1A5 x 1E4	A11.2	PRJNA256991	SRS670700
1A5 x 1E4	A12.2	PRJNA256991	SRS670701
1A5 x 1E4	A13.1	PRJNA256991	SRS670702
1A5 x 1E4	A13.2	PRJNA256991	SRS670704
1A5 x 1E4	A14.1	PRJNA256991	SRS670705
1A5 x 1E4	A14.2	PRJNA256991	SRS670706
1A5 x 1E4	A16.1	PRJNA256991	SRS670707
1A5 x 1E4	A16.2	PRJNA256991	SRS670708
1A5 x 1E4	A17.1	PRJNA256991	SRS670709
1A5 x 1E4	A18.1	PRJNA256991	SRS670711
1A5 x 1E4	A18.2	PRJNA256991	SRS670712

1A5 x 1E4	A19.1	PRJNA256991	SRS670713
1A5 x 1E4	A2.2	PRJNA256991	SRS670716
1A5 x 1E4	A21.1	PRJNA256991	SRS670717
1A5 x 1E4	A21.2	PRJNA256991	SRS670718
1A5 x 1E4	A22.1	PRJNA256991	SRS670720
1A5 x 1E4	A22.2	PRJNA256991	SRS670719
1A5 x 1E4	A23.1	PRJNA256991	SRS670722
1A5 x 1E4	A23.2	PRJNA256991	SRS670721
1A5 x 1E4	A24.1	PRJNA256991	SRS670723
1A5 x 1E4	A24.2	PRJNA256991	SRS670724
1A5 x 1E4	A25.1	PRJNA256991	SRS670725
1A5 x 1E4	A25.2	PRJNA256991	SRS670726
1A5 x 1E4	A26.1	PRJNA256991	SRS670727
1A5 x 1E4	A26.2	PRJNA256991	SRS670728
1A5 x 1E4	A28.1	PRJNA256991	SRS670729
1A5 x 1E4	A29.1	PRJNA256991	SRS670731
1A5 x 1E4	A3.1	PRJNA256991	SRS670733
1A5 x 1E4	A3.2	PRJNA256991	SRS670734
1A5 x 1E4	A30.1	PRJNA256991	SRS670735
1A5 x 1E4	A30.2	PRJNA256991	SRS670736
1A5 x 1E4	A31.1	PRJNA256991	SRS670738
1A5 x 1E4	A32.1	PRJNA256991	SRS670739
1A5 x 1E4	A33.1	PRJNA256991	SRS670741
1A5 x 1E4	A33.2	PRJNA256991	SRS670742
1A5 x 1E4	A35.2	PRJNA256991	SRS670744
1A5 x 1E4	A36.1	PRJNA256991	SRS670745
1A5 x 1E4	A37.1	PRJNA256991	SRS670747
1A5 x 1E4	A38.1	PRJNA256991	SRS670749
1A5 x 1E4	A39.1	PRJNA256991	SRS670751
1A5 x 1E4	A39.2	PRJNA256991	SRS670752
1A5 x 1E4	A4.1	PRJNA256991	SRS670753
1A5 x 1E4	A40.1	PRJNA256991	SRS670755
1A5 x 1E4	A40.2	PRJNA256991	SRS670756
1A5 x 1E4	A41.1	PRJNA256991	SRS670757
1A5 x 1E4	A42.1	PRJNA256991	SRS670760
1A5 x 1E4	A42.2	PRJNA256991	SRS670759
1A5 x 1E4	A43.1	PRJNA256991	SRS670762
1A5 x 1E4	A43.2	PRJNA256991	SRS670761
1A5 x 1E4	A44.1	PRJNA256991	SRS670763
1A5 x 1E4	A44.2	PRJNA256991	SRS670765

1A5 x 1E4	A45.1	PRJNA256991	SRS670766
1A5 x 1E4	A45.2	PRJNA256991	SRS670764
1A5 x 1E4	A46.1	PRJNA256991	SRS670767
1A5 x 1E4	A46.2	PRJNA256991	SRS670768
1A5 x 1E4	A47.1	PRJNA256991	SRS670769
1A5 x 1E4	A47.2	PRJNA256991	SRS670770
1A5 x 1E4	A48.1	PRJNA256991	SRS670771
1A5 x 1E4	A49.1	PRJNA256991	SRS670773
1A5 x 1E4	A5.1	PRJNA256991	SRS670775
1A5 x 1E4	A50.2	PRJNA256991	SRS670778
1A5 x 1E4	A51.2	PRJNA256991	SRS670779
1A5 x 1E4	A53.2	PRJNA256991	SRS670781
1A5 x 1E4	A54.1	PRJNA256991	SRS670780
1A5 x 1E4	A54.2	PRJNA256991	SRS670782
1A5 x 1E4	A55.1	PRJNA256991	SRS670783
1A5 x 1E4	A55.2	PRJNA256991	SRS670784
1A5 x 1E4	A57.1	PRJNA256991	SRS670785
1A5 x 1E4	A59.1	PRJNA256991	SRS670787
1A5 x 1E4	A59.2	PRJNA256991	SRS670788
1A5 x 1E4	A6.1	PRJNA256991	SRS670789
1A5 x 1E4	A60.1	PRJNA256991	SRS670791
1A5 x 1E4	A60.2	PRJNA256991	SRS670792
1A5 x 1E4	A62.1	PRJNA256991	SRS670793
1A5 x 1E4	A62.2	PRJNA256991	SRS670794
1A5 x 1E4	A63.1	PRJNA256991	SRS670795
1A5 x 1E4	A63.2	PRJNA256991	SRS670796
1A5 x 1E4	A64.1	PRJNA256991	SRS670797
1A5 x 1E4	A66.1	PRJNA256991	SRS670799
1A5 x 1E4	A66.2	PRJNA256991	SRS670800
1A5 x 1E4	A8.1	PRJNA256991	SRS670801
1A5 x 1E4	A9.1	PRJNA256991	SRS670803
1A5 x 1E4	A9.2	PRJNA256991	SRS670804
1A5 x 1E4	B1.1	PRJNA256991	SRS670805
1A5 x 1E4	B1.3	PRJNA256991	SRS670807
1A5 x 1E4	B10.1	PRJNA256991	SRS670808
1A5 x 1E4	B10.2	PRJNA256991	SRS670809
1A5 x 1E4	B11.1	PRJNA256991	SRS670811
1A5 x 1E4	B12.1	PRJNA256991	SRS670812
1A5 x 1E4	B13.2	PRJNA256991	SRS670815
1A5 x 1E4	B14.1	PRJNA256991	SRS670816

1A5 x 1E4	B15.1	PRJNA256991	SRS670818
1A5 x 1E4	B16.1	PRJNA256991	SRS670821
1A5 x 1E4	B16.2	PRJNA256991	SRS670820
1A5 x 1E4	B17.1	PRJNA256991	SRS670823
1A5 x 1E4	B17.2	PRJNA256991	SRS670824
1A5 x 1E4	B18.1	PRJNA256991	SRS670822
1A5 x 1E4	B18.2	PRJNA256991	SRS670826
1A5 x 1E4	B19.1	PRJNA256991	SRS670827
1A5 x 1E4	B19.2	PRJNA256991	SRS670825
1A5 x 1E4	B20.1	PRJNA256991	SRS670828
1A5 x 1E4	B20.2	PRJNA256991	SRS670829
1A5 x 1E4	B21.1	PRJNA256991	SRS670830
1A5 x 1E4	B22.1	PRJNA256991	SRS670831
1A5 x 1E4	B22.2	PRJNA256991	SRS670832
1A5 x 1E4	B23.1	PRJNA256991	SRS670833
1A5 x 1E4	B24.1	PRJNA256991	SRS670835
1A5 x 1E4	B24.2	PRJNA256991	SRS670836
1A5 x 1E4	B25.1	PRJNA256991	SRS670837
1A5 x 1E4	B26.1	PRJNA256991	SRS670839
1A5 x 1E4	B27.1	PRJNA256991	SRS670840
1A5 x 1E4	B28.1	PRJNA256991	SRS670842
1A5 x 1E4	B28.2	PRJNA256991	SRS670843
1A5 x 1E4	B29.1	PRJNA256991	SRS670844
1A5 x 1E4	B3.1	PRJNA256991	SRS670846
1A5 x 1E4	B30.1	PRJNA256991	SRS670847
1A5 x 1E4	B31.1	PRJNA256991	SRS670849
1A5 x 1E4	B31.2	PRJNA256991	SRS670850
1A5 x 1E4	B32.1	PRJNA256991	SRS670852
1A5 x 1E4	B32.2	PRJNA256991	SRS670851
1A5 x 1E4	B33.1	PRJNA256991	SRS670853
1A5 x 1E4	B33.2	PRJNA256991	SRS670854
1A5 x 1E4	B34.2	PRJNA256991	SRS670857
1A5 x 1E4	B35.1	PRJNA256991	SRS670856
1A5 x 1E4	B35.2	PRJNA256991	SRS670858
1A5 x 1E4	B37.1	PRJNA256991	SRS670859
1A5 x 1E4	B37.3	PRJNA256991	SRS670861
1A5 x 1E4	B38.1	PRJNA256991	SRS670862
1A5 x 1E4	B39.1	PRJNA256991	SRS670864
1A5 x 1E4	B39.2	PRJNA256991	SRS670865
1A5 x 1E4	B4.1	PRJNA256991	SRS670867

1A5 x 1E4	B4.2	PRJNA256991	SRS670868
1A5 x 1E4	B40.2	PRJNA256991	SRS670869
1A5 x 1E4	B41.1	PRJNA256991	SRS670870
1A5 x 1E4	B42.1	PRJNA256991	SRS670871
1A5 x 1E4	B42.2	PRJNA256991	SRS670872
1A5 x 1E4	B42.3	PRJNA256991	SRS670873
1A5 x 1E4	B43.1	PRJNA256991	SRS670874
1A5 x 1E4	B44.1	PRJNA256991	SRS670876
1A5 x 1E4	B45.1	PRJNA256991	SRS670878
1A5 x 1E4	B45.2	PRJNA256991	SRS670879
1A5 x 1E4	B46.1	PRJNA256991	SRS670880
1A5 x 1E4	B46.2	PRJNA256991	SRS670881
1A5 x 1E4	B48.1	PRJNA256991	SRS670883
1A5 x 1E4	B48.2	PRJNA256991	SRS670884
1A5 x 1E4	B49.1	PRJNA256991	SRS670885
1A5 x 1E4	B50.1	PRJNA256991	SRS670886
1A5 x 1E4	B50.2	PRJNA256991	SRS670888
1A5 x 1E4	B51.1	PRJNA256991	SRS670890
1A5 x 1E4	B7.1	PRJNA256991	SRS670891
1A5 x 1E4	B9.1	PRJNA256991	SRS670895
1A5 x 1E4	B9.2	PRJNA256991	SRS670896
1A5 x 1E4	C1.1	PRJNA256991	SRS670897
1A5 x 1E4	C1.2	PRJNA256991	SRS670898
1A5 x 1E4	C10.1	PRJNA256991	SRS670899
1A5 x 1E4	C11.1	PRJNA256991	SRS670901
1A5 x 1E4	C12.1	PRJNA256991	SRS670903
1A5 x 1E4	C12.2	PRJNA256991	SRS670904
1A5 x 1E4	C13.1	PRJNA256991	SRS670905
1A5 x 1E4	C14.1	PRJNA256991	SRS670907
1A5 x 1E4	C16.1	PRJNA256991	SRS670908
1A5 x 1E4	C16.2	PRJNA256991	SRS670910
1A5 x 1E4	C16.3	PRJNA256991	SRS670911
1A5 x 1E4	C17.1	PRJNA256991	SRS670912
1A5 x 1E4	C19.1	PRJNA256991	SRS670914
1A5 x 1E4	C2.1	PRJNA256991	SRS670917
1A5 x 1E4	C2.2	PRJNA256991	SRS670919
1A5 x 1E4	C20.1	PRJNA256991	SRS670918
1A5 x 1E4	C20.2	PRJNA256991	SRS670920
1A5 x 1E4	C21.1	PRJNA256991	SRS670921
1A5 x 1E4	C21.2	PRJNA256991	SRS670922

1A5 x 1E4	C22.1	PRJNA256991	SRS670923
1A5 x 1E4	C22.2	PRJNA256991	SRS670924
1A5 x 1E4	C23.1	PRJNA256991	SRS670925
1A5 x 1E4	C23.2	PRJNA256991	SRS670926
1A5 x 1E4	C24.1	PRJNA256991	SRS670927
1A5 x 1E4	C24.2	PRJNA256991	SRS670929
1A5 x 1E4	C25.1	PRJNA256991	SRS670928
1A5 x 1E4	C26.1	PRJNA256991	SRS670931
1A5 x 1E4	C27.1	PRJNA256991	SRS670933
1A5 x 1E4	C27.2	PRJNA256991	SRS670934
1A5 x 1E4	C28.1	PRJNA256991	SRS670935
1A5 x 1E4	C28.2	PRJNA256991	SRS670936
1A5 x 1E4	C29.2	PRJNA256991	SRS670938
1A5 x 1E4	C3.1	PRJNA256991	SRS670939
1A5 x 1E4	C3.2	PRJNA256991	SRS670940
1A5 x 1E4	C30.1	PRJNA256991	SRS670941
1A5 x 1E4	C30.2	PRJNA256991	SRS670942
1A5 x 1E4	C31.1	PRJNA256991	SRS670943
1A5 x 1E4	C32.1	PRJNA256991	SRS670946
1A5 x 1E4	C32.2	PRJNA256991	SRS670947
1A5 x 1E4	C33.1	PRJNA256991	SRS670948
1A5 x 1E4	C33.2	PRJNA256991	SRS670949
1A5 x 1E4	C34.1	PRJNA256991	SRS670950
1A5 x 1E4	C34.2	PRJNA256991	SRS670951
1A5 x 1E4	C35.1	PRJNA256991	SRS670952
1A5 x 1E4	C36.1	PRJNA256991	SRS670954
1A5 x 1E4	C38.1	PRJNA256991	SRS670956
1A5 x 1E4	C38.2	PRJNA256991	SRS670957
1A5 x 1E4	C4.1	PRJNA256991	SRS670958
1A5 x 1E4	C4.2	PRJNA256991	SRS670959
1A5 x 1E4	C41.1	PRJNA256991	SRS670960
1A5 x 1E4	C41.2	PRJNA256991	SRS670961
1A5 x 1E4	C42.1	PRJNA256991	SRS670962
1A5 x 1E4	C42.2	PRJNA256991	SRS670963
1A5 x 1E4	C44.1	PRJNA256991	SRS670964
1A5 x 1E4	C44.2	PRJNA256991	SRS670965
1A5 x 1E4	C45.1	PRJNA256991	SRS670966
1A5 x 1E4	C45.2	PRJNA256991	SRS670967
1A5 x 1E4	C48.1	PRJNA256991	SRS670968
1A5 x 1E4	C48.2	PRJNA256991	SRS670969

1A5 x 1E4	C49.1	PRJNA256991	SRS670970
1A5 x 1E4	C5.1	PRJNA256991	SRS670972
1A5 x 1E4	C5.2	PRJNA256991	SRS670973
1A5 x 1E4	C51.1	PRJNA256991	SRS670974
1A5 x 1E4	C51.2	PRJNA256991	SRS670975
1A5 x 1E4	C52.1	PRJNA256991	SRS670976
1A5 x 1E4	C53.1	PRJNA256991	SRS670977
1A5 x 1E4	C54.1	PRJNA256991	SRS670979
1A5 x 1E4	C55.1	PRJNA256991	SRS670981
1A5 x 1E4	C55.2	PRJNA256991	SRS670982
1A5 x 1E4	C56.1	PRJNA256991	SRS670983
1A5 x 1E4	C56.2	PRJNA256991	SRS670985
1A5 x 1E4	C57.1	PRJNA256991	SRS670986
1A5 x 1E4	C57.2	PRJNA256991	SRS670987
1A5 x 1E4	C59.2	PRJNA256991	SRS670989
1A5 x 1E4	C6.1	PRJNA256991	SRS670990
1A5 x 1E4	C60.1	PRJNA256991	SRS670992
1A5 x 1E4	C60.2	PRJNA256991	SRS670993
1A5 x 1E4	C61.1	PRJNA256991	SRS670994
1A5 x 1E4	C61.2	PRJNA256991	SRS670995
1A5 x 1E4	C62.1	PRJNA256991	SRS670996
1A5 x 1E4	C62.2	PRJNA256991	SRS670997
1A5 x 1E4	C63.1	PRJNA256991	SRS670998
1A5 x 1E4	C7.1	PRJNA256991	SRS671000
1A5 x 1E4	C7.2	PRJNA256991	SRS671001
1A5 x 1E4	C8.1	PRJNA256991	SRS671002
1A5 x 1E4	CR4_A1.1	PRJNA256991	SRS671004
1A5 x 1E4	CR4_A2.1	PRJNA256991	SRS671006
1A5 x 1E4	CR4_A2.2	PRJNA256991	SRS671007
1A5 x 1E4	CR4_A3.1	PRJNA256991	SRS671010
1A5 x 1E4	CR4_A3.2	PRJNA256991	SRS671012
1A5 x 1E4	CR4_A4.1	PRJNA256991	SRS671015
1A5 x 1E4	D1.1	PRJNA256991	SRS671014
1A5 x 1E4	D1.2	PRJNA256991	SRS671016
1A5 x 1E4	D1.3	PRJNA256991	SRS671018
1A5 x 1E4	D10.1	PRJNA256991	SRS671019
1A5 x 1E4	D11.1	PRJNA256991	SRS671021
1A5 x 1E4	D2.1	PRJNA256991	SRS671023
1A5 x 1E4	D3.1	PRJNA256991	SRS671026
1A5 x 1E4	D3.2	PRJNA256991	SRS671025

1A5 x 1E4	D4.1	PRJNA256991	SRS671027
1A5 x 1E4	D5.1	PRJNA256991	SRS671029
1A5 x 1E4	D7.1	PRJNA256991	SRS671031
1A5 x 1E4	D7.2	PRJNA256991	SRS671032
1A5 x 1E4	D7.3	PRJNA256991	SRS671033
1A5 x 1E4	D9.1	PRJNA256991	SRS671035
1A5 x 1E4	D9.2	PRJNA256991	SRS671038

Table S2 Growth rate (mm day⁻¹), temperature sensitivity and yeast/hyphae dimorphism phenotypes for the quality filtered retained progeny used in the QTL analysis for each of the two crosses.

Cross	Retained progeny for QTL analysis	Growth rate (22°C)	Growth rate (15°C)	Temperature sensitivity	Yeast/hyphae (22°C) ^a	Yeast/hyphae (15°C) ^a
3D1 x 3D7	1.1	NA	NA	NA	NA	0
3D1 x 3D7	1.2	0.406644517	0.342815475	1.186190667	0	0
3D1 x 3D7	10.1	NA	NA	NA	1	0
3D1 x 3D7	100.1	0.29786234	0.260616992	1.142912201	0	0
3D1 x 3D7	100.2	0.606077056	NA	NA	NA	NA
3D1 x 3D7	101.2	0.495770046	0.429458094	1.154408434	NA	0
3D1 x 3D7	102.1	0.250641969	0.207132414	1.210056716	0	NA
3D1 x 3D7	102.2	0.566641122	0.522758076	1.083945228	1	1
3D1 x 3D7	103.1	0.328973769	0.364346247	0.90291521	0	NA
3D1 x 3D7	104.1	0.340847502	0.280874791	1.213521159	0	0
3D1 x 3D7	104.2	0.45552374	0.406642765	1.120206184	1	NA
3D1 x 3D7	105.1	0.364083821	0.274134415	1.328121542	0	0
3D1 x 3D7	105.2	0.444067669	0.379905118	1.168890988	1	1
3D1 x 3D7	106.1	0.259157593	0.233931289	1.107836381	0	0
3D1 x 3D7	106.2	0.340098695	0.284518845	1.195346816	NA	0
3D1 x 3D7	107.1	0.32595047	0.202800106	1.607249996	0	0
3D1 x 3D7	108.1	0.308000507	0.243801121	1.263326868	0	0
3D1 x 3D7	108.2	0.488546101	0.387245709	1.261592033	1	0
3D1 x 3D7	109.1	0.361715249	0.208861372	1.73184369	NA	0
3D1 x 3D7	109.2	0.38989845	0.274274703	1.421561835	NA	0
3D1 x 3D7	11.1	0.5239504	0.504987383	1.037551468	1	1
3D1 x 3D7	11.2	NA	NA	NA	1	1
3D1 x 3D7	110.1	0.339995279	0.280525729	1.211993211	0	0
3D1 x 3D7	110.2	0.52884388	NA	NA	0	NA
3D1 x 3D7	111.2	0.372288755	0.226514091	1.643556714	0	0
3D1 x 3D7	112.1	0.357436718	0.316434035	1.129577349	NA	0
3D1 x 3D7	113.1	0.430400224	0.342025272	1.258387199	0	0
3D1 x 3D7	113.2	0.466656427	0.447454306	1.04291415	1	1
3D1 x 3D7	114.1	0.410256356	0.26417328	1.552982028	0	0
3D1 x 3D7	114.2	0.444697808	0.391397185	1.136180396	NA	NA
3D1 x 3D7	115.1	0.299606432	0.288486203	1.038546832	0	0
3D1 x 3D7	116.1	0.509011395	0.393522115	1.293475959	NA	0
3D1 x 3D7	116.2	0.340402836	0.237047467	1.43601128	0	0
3D1 x 3D7	117.1	0.330188699	0.264572657	1.248007646	0	0
3D1 x 3D7	117.2	0.347679013	0.354870972	0.979733592	0	0
3D1 x 3D7	118.1	0.456702817	0.32687023	1.397199177	1	0

3D1 x 3D7	118.2	0.524602341	0.319505549	1.641919342	1	0
3D1 x 3D7	119.1	0.606711258	0.447955528	1.354400648	1	1
3D1 x 3D7	119.2	0.462039474	0.377863365	1.222768643	1	NA
3D1 x 3D7	12.1	0.298433179	0.273393755	1.091587405	0	0
3D1 x 3D7	120.1	0.452352341	0.40480887	1.117446715	1	1
3D1 x 3D7	120.2	0.418083163	0.320159453	1.305859187	NA	0
3D1 x 3D7	121.2	0.323708547	0.292921084	1.105104976	0	0
3D1 x 3D7	122.1	0.457641653	0.403288656	1.134774425	0	0
3D1 x 3D7	123.1	NA	NA	NA	1	0
3D1 x 3D7	125.1	0.292661762	0.246035061	1.189512423	NA	0
3D1 x 3D7	126.1	0.269348948	0.160871669	1.674309401	NA	0
3D1 x 3D7	127.1	0.573611429	0.453019335	1.266196352	1	1
3D1 x 3D7	127.2	0.471723531	0.375874391	1.255003115	1	0
3D1 x 3D7	128.1	NA	NA	NA	1	0
3D1 x 3D7	128.2	0.38828956	0.387854072	1.001122815	NA	1
3D1 x 3D7	129.2	0.514236366	0.443327188	1.15994773	1	1
3D1 x 3D7	13.1	0.389389071	0.238466474	1.632888116	0	0
3D1 x 3D7	130.1	0.382400475	0.249735584	1.531221418	0	0
3D1 x 3D7	131.1	0.456644412	0.265639749	1.719036449	1	0
3D1 x 3D7	133.1	0.378417727	0.230840863	1.6393013	0	0
3D1 x 3D7	134.1	0.55729434	0.292038333	1.908291746	1	0
3D1 x 3D7	135.2	0.463539975	0.398253883	1.163930838	1	1
3D1 x 3D7	136.1	0.399781063	0.280973872	1.422840711	1	0
3D1 x 3D7	137.1	0.36404594	0.346982358	1.04917709	NA	0
3D1 x 3D7	137.2	0.542699856	0.44994951	1.206135009	1	0
3D1 x 3D7	138.1	0.402082665	0.401958453	1.000309017	0	0
3D1 x 3D7	139.2	0.443585084	0.325454957	1.362969203	0	0
3D1 x 3D7	14.1	NA	NA	NA	0	0
3D1 x 3D7	141.1	0.29981085	0.311424921	0.962706675	NA	0
3D1 x 3D7	142.1	0.45079568	0.392984466	1.14710814	NA	0
3D1 x 3D7	142.2	0.505579728	0.381804835	1.324183672	0	0
3D1 x 3D7	143.1	0.417849179	0.404679963	1.032542299	NA	0
3D1 x 3D7	144.1	0.300439613	0.225098347	1.334703771	0	0
3D1 x 3D7	145.1	0.37493814	0.24631371	1.522197609	0	0
3D1 x 3D7	145.2	0.336924835	0.367469128	0.916879294	1	0
3D1 x 3D7	146.1	0.397909751	0.340124368	1.169894863	NA	1
3D1 x 3D7	146.2	0.514117368	0.343216703	1.497938076	1	0
3D1 x 3D7	147.1	0.492488864	0.418090438	1.177948167	1	1
3D1 x 3D7	148.1	0.544643725	0.316428663	1.721221209	0	0
3D1 x 3D7	149.1	0.478869194	0.317597415	1.507786815	0	0

3D1 x 3D7	149.2	0.445530117	0.347673434	1.28146149	0	0
3D1 x 3D7	15.1	NA	NA	NA	1	1
3D1 x 3D7	15.2	NA	NA	NA	NA	1
3D1 x 3D7	150.1	0.420168626	0.33014696	1.272671498	1	0
3D1 x 3D7	150.2	0.36945829	0.372301759	0.992362462	0	0
3D1 x 3D7	151.1	0.401683888	0.379418657	1.05868249	1	1
3D1 x 3D7	152.1	0.50348707	0.307305778	1.638391163	1	0
3D1 x 3D7	152.2	0.390889258	0.26811763	1.457902111	0	0
3D1 x 3D7	154.1	0.341536595	0.277166026	1.232245526	1	1
3D1 x 3D7	154.2	0.317276337	0.215340454	1.473370804	1	0
3D1 x 3D7	155.1	0.419943575	0.333178901	1.260414669	0	0
3D1 x 3D7	156.1	0.392132136	0.367396126	1.067327901	NA	0
3D1 x 3D7	157.1	0.342072739	0.312471726	1.094731813	1	1
3D1 x 3D7	158.1	0.439130851	0.346797335	1.266246325	0	0
3D1 x 3D7	158.2	0.349774377	0.249856232	1.399902556	0	0
3D1 x 3D7	159.1	0.324485777	0.28152323	1.152607466	0	0
3D1 x 3D7	16.1	0.501428726	0.369386691	1.357462894	1	0
3D1 x 3D7	160.1	0.410992991	0.375123316	1.095621023	1	1
3D1 x 3D7	160.2	0.402491167	0.351833769	1.143981057	0	0
3D1 x 3D7	161.1	0.372262374	0.350407531	1.062369787	1	1
3D1 x 3D7	161.2	0.557502419	0.388159351	1.436272033	1	1
3D1 x 3D7	162.1	0.234813598	0.21080024	1.113915231	NA	0
3D1 x 3D7	162.2	0.516904668	0.413822062	1.249098867	1	1
3D1 x 3D7	163.1	0.326962517	0.31019746	1.054046403	1	1
3D1 x 3D7	164.1	0.252619433	0.182542799	1.38389153	0	0
3D1 x 3D7	164.2	0.464501593	0.357423508	1.299583218	NA	NA
3D1 x 3D7	165.1	0.452274844	0.363316304	1.244851493	0	0
3D1 x 3D7	165.2	0.303539309	0.221802989	1.36850865	0	0
3D1 x 3D7	166.1	0.323551442	0.223621402	1.446871541	0	0
3D1 x 3D7	167.1	0.632405527	0.497366929	1.27150699	1	1
3D1 x 3D7	167.2	0.230964725	0.18979445	1.216920332	0	0
3D1 x 3D7	168.1	0.296120964	0.286592334	1.033248028	0	0
3D1 x 3D7	169.1	0.461010853	0.386032459	1.194228212	1	NA
3D1 x 3D7	169.2	0.478700544	0.270222792	1.77150321	1	0
3D1 x 3D7	17.2	NA	NA	NA	1	0
3D1 x 3D7	170.1	0.311915878	0.286876946	1.087281087	0	0
3D1 x 3D7	170.2	0.228623499	0.228467631	1.000682229	0	0
3D1 x 3D7	171.1	0.489495978	0.408890607	1.197131874	0	NA
3D1 x 3D7	172.1	0.420417823	0.425409667	0.988265796	0	0
3D1 x 3D7	173.1	0.510624002	0.420750968	1.213601492	1	0

3D1 x 3D7	174.1	0.359584739	NA	NA	0	0
3D1 x 3D7	174.2	0.566778268	0.378334798	1.498086538	1	1
3D1 x 3D7	175.1	0.458540584	0.288761238	1.587957539	0	0
3D1 x 3D7	176.2	0.498283034	0.230816373	2.158785477	0	0
3D1 x 3D7	177.2	0.500602604	0.391623548	1.278275035	1	0
3D1 x 3D7	178.1	NA	NA	NA	NA	0
3D1 x 3D7	179.1	0.39837918	0.275893796	1.443958458	0	0
3D1 x 3D7	179.2	0.406659707	0.328415037	1.238249354	0	0
3D1 x 3D7	18.1	NA	NA	NA	1	0
3D1 x 3D7	18.2	NA	NA	NA	NA	0
3D1 x 3D7	180.1	0.521776118	0.388084283	1.344491754	0	0
3D1 x 3D7	180.2	0.605638557	0.436937405	1.386099132	1	1
3D1 x 3D7	181.1	0.633997443	0.391148877	1.620859681	1	NA
3D1 x 3D7	181.2	0.466035015	0.314369461	1.482443664	1	0
3D1 x 3D7	182.1	0.400685768	0.243544763	1.645224325	0	0
3D1 x 3D7	183.1	NA	NA	NA	NA	NA
3D1 x 3D7	184.1	NA	NA	NA	NA	NA
3D1 x 3D7	185.1	NA	NA	NA	NA	NA
3D1 x 3D7	19.1	0.448973569	0.341086443	1.316304352	0	0
3D1 x 3D7	19.2	NA	NA	NA	1	1
3D1 x 3D7	2.1	0.323729135	0.303010055	1.068377533	0	0
3D1 x 3D7	20.1	0.483606233	0.309355881	1.56326827	0	0
3D1 x 3D7	20.2	NA	0.345200266	NA	1	0
3D1 x 3D7	21.1	0.324920257	0.375530001	0.865231156	1	0
3D1 x 3D7	21.2	0.220737637	0.188915932	1.168443735	0	0
3D1 x 3D7	22.1	0.411199919	0.359527571	1.143722907	0	NA
3D1 x 3D7	22.2	0.4649716	0.28988254	1.604000022	1	0
3D1 x 3D7	23.1	0.43730722	0.307137713	1.423814796	1	0
3D1 x 3D7	23.2	0.292720682	0.347818282	0.841590845	NA	0
3D1 x 3D7	24.1	0.520438964	0.344110852	1.512416595	1	0
3D1 x 3D7	24.2	0.407494963	0.36013896	1.131493696	0	0
3D1 x 3D7	25.1	0.425862163	0.356688256	1.193933793	1	0
3D1 x 3D7	26.1	0.414454989	0.233158913	1.777564423	NA	0
3D1 x 3D7	26.2	0.402324791	0.331981523	1.211889106	0	NA
3D1 x 3D7	27.1	0.525247795	0.334705691	1.569282533	NA	1
3D1 x 3D7	28.1	0.282121185	0.231898436	1.216572178	0	0
3D1 x 3D7	29.1	0.49051787	0.391356335	1.253379147	0	0
3D1 x 3D7	3.1	0.379653696	0.478695055	0.793101355	1	1
3D1 x 3D7	3.2	NA	NA	NA	0	0
3D1 x 3D7	30.1	0.330363488	0.232745396	1.419420082	0	0

3D1 x 3D7	31.1	0.482113656	0.427593969	1.127503405	1	1
3D1 x 3D7	32.1	0.327301581	0.183961052	1.779189553	NA	0
3D1 x 3D7	33.1	0.510899625	0.429981354	1.188190186	1	0
3D1 x 3D7	34.1	0.416797179	0.400684511	1.040212855	1	1
3D1 x 3D7	34.2	0.406725654	0.216411009	1.879412952	0	0
3D1 x 3D7	35.1	0.236371387	0.196335113	1.203918054	0	0
3D1 x 3D7	35.2	0.324775929	0.351439888	0.924129389	1	NA
3D1 x 3D7	36.1	0.539581899	0.389996105	1.383557148	NA	0
3D1 x 3D7	37.1	0.348147056	0.203572278	1.710188932	NA	0
3D1 x 3D7	37.2	0.50140067	0.432774062	1.158573756	1	1
3D1 x 3D7	38.1	NA	NA	NA	NA	0
3D1 x 3D7	39.1	NA	NA	NA	NA	0
3D1 x 3D7	4.1	NA	NA	NA	0	NA
3D1 x 3D7	4.2	NA	NA	NA	0	0
3D1 x 3D7	40.1	0.527011741	0.381769104	1.380446285	1	0
3D1 x 3D7	40.2	0.452305431	0.337057779	1.34192254	NA	0
3D1 x 3D7	41.1	0.394472665	0.276371985	1.427325078	NA	0
3D1 x 3D7	41.2	0.336747816	0.254940184	1.320889513	NA	0
3D1 x 3D7	42.1	0.554500272	0.323001945	1.716708771	NA	0
3D1 x 3D7	42.2	0.475028221	0.372252405	1.276091744	1	1
3D1 x 3D7	43.1	0.327386276	0.21704424	1.508385002	0	NA
3D1 x 3D7	44.1	0.360627207	0.266495761	1.353219301	0	0
3D1 x 3D7	45.1	0.533359091	0.359497044	1.483625805	NA	0
3D1 x 3D7	46.1	0.535870106	0.262310296	2.042886285	0	0
3D1 x 3D7	46.2	0.251300151	0.262407828	0.957670175	NA	NA
3D1 x 3D7	47.1	0.145446529	NA	NA	NA	0
3D1 x 3D7	48.1	0.38319508	0.241028648	1.589832092	0	0
3D1 x 3D7	48.2	0.292327592	0.332509396	0.879155886	NA	1
3D1 x 3D7	49.1	0.298642355	0.291964741	1.022871302	0	0
3D1 x 3D7	49.2	0.515587431	0.326761446	1.577871066	NA	0
3D1 x 3D7	5.1	NA	NA	NA	1	0
3D1 x 3D7	5.2	0.452670527	0.310266849	1.458971619	NA	0
3D1 x 3D7	50.1	0.461541964	0.389908373	1.183719037	NA	0
3D1 x 3D7	51.1	0.441699394	0.358920766	1.230632041	1	0
3D1 x 3D7	51.2	0.353472475	0.20854781	1.69492298	0	0
3D1 x 3D7	52.1	0.431236575	0.386476183	1.115816691	NA	1
3D1 x 3D7	52.2	0.458100357	0.292560986	1.565828592	0	0
3D1 x 3D7	53.2	0.267015077	0.196034633	1.362081144	0	0
3D1 x 3D7	54.1	0.516776827	0.429688039	1.202679107	1	1
3D1 x 3D7	55.1	0.338883955	0.187674613	1.805699506	0	0

3D1 x 3D7	55.2	0.429475487	0.348423643	1.23262441	1	1
3D1 x 3D7	56.1	0.313012901	0.347115499	0.901754321	0	0
3D1 x 3D7	56.2	0.395890911	0.28434248	1.39230308	NA	0
3D1 x 3D7	57.1	0.371810819	0.366245543	1.015195477	1	0
3D1 x 3D7	57.2	0.445229372	0.428570178	1.038871567	1	1
3D1 x 3D7	58.1	0.31933781	0.224384226	1.423174061	0	0
3D1 x 3D7	59.1	0.469265825	0.284508588	1.649390724	0	0
3D1 x 3D7	59.2	0.363362527	0.383066965	0.948561375	0	0
3D1 x 3D7	6.1	NA	NA	NA	0	0
3D1 x 3D7	60.2	0.394385875	0.253313644	1.556907353	0	0
3D1 x 3D7	61.1	0.340059685	0.366973558	0.926659911	0	0
3D1 x 3D7	62.1	0.352628244	0.368123644	0.957907076	NA	0
3D1 x 3D7	62.2	0.46409886	0.372266194	1.246685482	NA	NA
3D1 x 3D7	63.1	0.438383552	0.38494502	1.138821205	NA	0
3D1 x 3D7	64.1	NA	NA	NA	1	NA
3D1 x 3D7	65.1	0.520553769	0.415134454	1.253940171	1	0
3D1 x 3D7	66.1	0.447594316	0.359417613	1.245332169	NA	0
3D1 x 3D7	67.1	0.418501206	0.301241879	1.389253074	1	1
3D1 x 3D7	68.1	0.492871441	0.348524668	1.414165155	0	0
3D1 x 3D7	68.2	0.50673246	0.277951241	1.823098393	0	0
3D1 x 3D7	69.1	NA	NA	NA	NA	0
3D1 x 3D7	69.2	0.420895126	0.246159948	1.709844068	0	0
3D1 x 3D7	7.1	0.444960771	0.31849397	1.397077537	1	0
3D1 x 3D7	70.1	0.379138117	0.316716484	1.197089939	1	1
3D1 x 3D7	71.2	0.329035701	0.227016042	1.449394055	0	0
3D1 x 3D7	72.1	0.385410857	0.365579346	1.054246806	1	0
3D1 x 3D7	72.2	0.310388837	0.343601136	0.903340544	1	0
3D1 x 3D7	73.1	0.407503132	0.406195464	1.003219308	0	0
3D1 x 3D7	74.1	0.383385003	0.295135431	1.299013815	0	0
3D1 x 3D7	75.1	0.442886601	0.445510323	0.99411075	1	1
3D1 x 3D7	75.2	0.392807786	0.379281016	1.035664243	0	0
3D1 x 3D7	76.1	0.591228755	0.405218454	1.459037093	1	1
3D1 x 3D7	76.2	0.369238216	0.244982351	1.507203333	1	0
3D1 x 3D7	77.1	0.313762406	0.213807134	1.467502042	0	0
3D1 x 3D7	78.1	0.356733652	0.236059554	1.511201926	NA	0
3D1 x 3D7	79.1	0.507723794	0.393345845	1.290782148	0	0
3D1 x 3D7	8.1	0.293148767	0.25462542	1.151294192	0	0
3D1 x 3D7	8.2	0.299961444	0.174344507	1.72050986	0	0
3D1 x 3D7	80.1	0.394595351	0.37769029	1.044759057	NA	NA
3D1 x 3D7	80.2	0.530960152	0.461636073	1.150170413	1	1

3D1 x 3D7	82.1	0.37657596	0.372044616	1.012179571	NA	0
3D1 x 3D7	82.2	0.395523841	0.366631265	1.078805546	1	1
3D1 x 3D7	83.1	0.350670914	0.328280394	1.068205474	NA	1
3D1 x 3D7	83.2	0.423959566	NA	NA	0	NA
3D1 x 3D7	84.1	0.521050504	0.503536267	1.034782474	1	1
3D1 x 3D7	84.2	0.336655296	0.184431285	1.825369784	0	0
3D1 x 3D7	86.2	0.43245547	0.415938885	1.039709162	NA	1
3D1 x 3D7	87.1	0.293915788	0.369674375	0.795066706	0	0
3D1 x 3D7	88.1	0.312445461	0.236081097	1.323466663	0	0
3D1 x 3D7	89.1	0.346032565	0.302494317	1.143930795	1	0
3D1 x 3D7	89.2	0.549858735	0.405568809	1.355771754	1	1
3D1 x 3D7	9.1	0.436563192	0.356605977	1.224217261	NA	0
3D1 x 3D7	90.1	0.374246936	0.352849316	1.060642374	NA	0
3D1 x 3D7	91.2	0.46762853	0.351999125	1.328493446	1	1
3D1 x 3D7	92.1	0.351174146	0.200017638	1.755715896	0	0
3D1 x 3D7	93.1	0.478761314	0.368785074	1.298212284	NA	0
3D1 x 3D7	93.2	0.362509414	0.245028668	1.479457145	0	0
3D1 x 3D7	94.1	0.240089826	0.250571754	0.958167957	NA	1
3D1 x 3D7	94.2	0.498089158	0.4220134	1.180268584	1	1
3D1 x 3D7	95.1	0.338469132	0.202023438	1.675395368	0	0
3D1 x 3D7	95.2	0.363433326	0.321335391	1.131009332	0	0
3D1 x 3D7	96.1	0.284897498	0.248544758	1.146262345	0	NA
3D1 x 3D7	96.2	0.399124867	0.391593134	1.019233568	0	0
3D1 x 3D7	97.1	0.383566078	0.291771714	1.314610225	1	1
3D1 x 3D7	97.2	0.445346525	0.404457045	1.101097213	1	0
3D1 x 3D7	98.1	0.410501087	0.309094449	1.328076542	0	0
3D1 x 3D7	99.1	NA	NA	NA	0	0
1A5 x 1E4	A1.1	0.42389102	0.362679384	1.168776167	1	0
1A5 x 1E4	A10.1	0.251383477	0.183959058	1.366518616	0	0
1A5 x 1E4	A11.1	0.456332919	0.279851799	1.630623497	1	0
1A5 x 1E4	A11.2	0.3443407	0.327693596	1.050800822	NA	0
1A5 x 1E4	A12.2	0.282652913	0.179943033	1.57079109	0	0
1A5 x 1E4	A13.1	0.318291461	0.327758192	0.97111672	0	0
1A5 x 1E4	A13.2	0.312691124	0.302783274	1.032722581	NA	0
1A5 x 1E4	A14.1	0.239268195	0.258293588	0.926341984	0	0
1A5 x 1E4	A14.2	0.4588759	0.328438145	1.397145573	0	0
1A5 x 1E4	A16.1	0.334646057	0.352733612	0.948721769	0	0
1A5 x 1E4	A16.2	0.462861083	0.398041289	1.16284691	NA	0
1A5 x 1E4	A17.1	0.228721452	0.208630269	1.096300419	0	0
1A5 x 1E4	A18.1	0.257661548	0.257869525	0.999193476	0	0

1A5 x 1E4	A18.2	0.400244089	0.302516865	1.32304719	NA	0
1A5 x 1E4	A19.1	0.26885972	0.270806248	0.992812101	0	0
1A5 x 1E4	A2.2	0.474580194	0.379367549	1.250977303	NA	0
1A5 x 1E4	A21.1	0.28550263	0.347168069	0.822375833	0	0
1A5 x 1E4	A21.2	0.337762075	0.283994745	1.189325089	0	0
1A5 x 1E4	A22.1	0.578550091	0.464638031	1.245163015	NA	0
1A5 x 1E4	A22.2	0.351458987	0.236786563	1.484286027	0	0
1A5 x 1E4	A23.1	0.32636556	0.281869657	1.157859856	1	0
1A5 x 1E4	A23.2	0.592127275	0.380808897	1.554919751	1	0
1A5 x 1E4	A24.1	0.474633636	0.3809867	1.245801064	1	0
1A5 x 1E4	A24.2	0.624202482	0.429039318	1.454884102	NA	0
1A5 x 1E4	A25.1	0.376754777	0.263400093	1.430351723	NA	0
1A5 x 1E4	A25.2	0.540761332	0.371150378	1.45698715	NA	0
1A5 x 1E4	A26.1	0.33383661	0.386013637	0.864831129	0	0
1A5 x 1E4	A26.2	0.504684095	0.318201176	1.586053521	NA	0
1A5 x 1E4	A28.1	0.321306248	0.259833168	1.236586732	0	0
1A5 x 1E4	A29.1	0.370382131	0.330691157	1.120024299	NA	0
1A5 x 1E4	A3.1	0.569628261	0.364670425	1.562035807	NA	0
1A5 x 1E4	A3.2	0.277788834	0.181500923	1.530509211	0	0
1A5 x 1E4	A30.1	0.381461862	0.251773789	1.515097593	0	0
1A5 x 1E4	A30.2	0.457597209	0.254733303	1.796377636	0	0
1A5 x 1E4	A31.1	0.537490737	0.4026851	1.334766886	NA	0
1A5 x 1E4	A32.1	0.446382216	0.328601498	1.358430255	0	0
1A5 x 1E4	A33.1	0.40494721	0.385933783	1.049266034	NA	NA
1A5 x 1E4	A33.2	0.44402163	0.320713135	1.38448221	NA	0
1A5 x 1E4	A35.2	0.345610907	0.330039708	1.047179774	NA	0
1A5 x 1E4	A36.1	0.256052511	0.234887894	1.090105187	0	0
1A5 x 1E4	A37.1	0.318231319	0.3315264	0.959897368	NA	0
1A5 x 1E4	A38.1	0.33849767	0.266598792	1.269689436	0	0
1A5 x 1E4	A39.1	0.511806618	0.38336475	1.335038286	1	NA
1A5 x 1E4	A39.2	0.417616084	0.371170791	1.125131863	0	0
1A5 x 1E4	A4.1	0.431195691	0.319703339	1.348736901	1	0
1A5 x 1E4	A40.1	0.280969577	0.264935371	1.060521198	0	0
1A5 x 1E4	A40.2	0.504500444	0.37735608	1.336934718	NA	0
1A5 x 1E4	A41.1	0.385487078	0.288406395	1.336610715	0	0
1A5 x 1E4	A42.1	NA	NA	NA	NA	NA
1A5 x 1E4	A42.2	0.457016201	0.335194616	1.363435387	NA	0
1A5 x 1E4	A43.1	0.318726494	0.391831478	0.813427485	0	0
1A5 x 1E4	A43.2	0.259209405	0.342717159	0.756336233	0	0
1A5 x 1E4	A44.1	0.40872099	0.228628237	1.787710019	NA	0

1A5 x 1E4	A44.2	0.414877958	0.369619206	1.122446969	NA	0
1A5 x 1E4	A45.1	0.602933111	0.393350364	1.532814421	1	0
1A5 x 1E4	A45.2	0.421024899	0.328114268	1.283165469	0	0
1A5 x 1E4	A46.1	0.308664405	0.370911048	0.832179054	0	0
1A5 x 1E4	A46.2	0.445130553	0.382209501	1.16462451	0	0
1A5 x 1E4	A47.1	0.386154201	0.395634374	0.976038046	0	0
1A5 x 1E4	A47.2	0.491748226	0.320508995	1.534272778	0	0
1A5 x 1E4	A48.1	0.4915612	0.391750641	1.254780845	0	0
1A5 x 1E4	A49.1	0.640315675	0.336143926	1.904885454	1	0
1A5 x 1E4	A5.1	0.359255724	0.304913553	1.178221564	1	0
1A5 x 1E4	A50.2	0.46978444	0.375527977	1.250997179	1	0
1A5 x 1E4	A51.2	0.268945067	0.295571832	0.909914403	0	0
1A5 x 1E4	A53.2	0.420112865	0.362926534	1.157569992	0	0
1A5 x 1E4	A54.1	0.412382635	0.375899568	1.097055357	NA	0
1A5 x 1E4	A54.2	0.366687537	0.270159256	1.357301404	0	0
1A5 x 1E4	A55.1	0.431830196	0.391754045	1.102299267	0	0
1A5 x 1E4	A55.2	0.367024744	0.28450597	1.290042327	0	0
1A5 x 1E4	A57.1	0.483546888	0.421572487	1.1470077	1	0
1A5 x 1E4	A59.1	0.378523459	0.34101273	1.109998032	0	0
1A5 x 1E4	A59.2	0.428648387	0.171422502	2.500537453	0	0
1A5 x 1E4	A6.1	0.402862687	0.379133611	1.062587636	0	0
1A5 x 1E4	A60.1	0.575805037	0.377215786	1.526460607	NA	0
1A5 x 1E4	A60.2	0.49104263	0.338474017	1.450754285	NA	0
1A5 x 1E4	A62.1	NA	NA	NA	NA	NA
1A5 x 1E4	A62.2	0.312016293	0.344734171	0.905092442	0	0
1A5 x 1E4	A63.1	0.400394609	0.393268339	1.018120631	0	0
1A5 x 1E4	A63.2	0.26900977	0.292865377	0.918544117	0	0
1A5 x 1E4	A64.1	0.388969681	0.397761976	0.977895589	1	0
1A5 x 1E4	A66.1	0.271517302	0.23173355	1.171678859	1	0
1A5 x 1E4	A66.2	0.517962094	0.463963489	1.116385464	1	0
1A5 x 1E4	A8.1	0.256349924	0.256257293	1.000361476	NA	0
1A5 x 1E4	A9.1	0.265145977	0.308949364	0.858218232	NA	0
1A5 x 1E4	A9.2	0.415770034	0.392218776	1.060046228	1	0
1A5 x 1E4	B1.1	0.382522386	0.384274759	0.995439792	0	0
1A5 x 1E4	B1.3	0.358521271	0.320393704	1.119002237	1	0
1A5 x 1E4	B10.1	0.271242062	0.33574517	0.807880758	0	0
1A5 x 1E4	B10.2	0.293431417	0.269139867	1.090256232	1	0
1A5 x 1E4	B11.1	0.432230038	0.331801146	1.302677954	NA	0
1A5 x 1E4	B12.1	0.27141752	0.313468997	0.865851241	0	0
1A5 x 1E4	B13.2	0.387599256	0.330680813	1.172125027	NA	0

1A5 x 1E4	B14.1	0.349722777	0.339727873	1.029420323	NA	0
1A5 x 1E4	B15.1	NA	NA	NA	NA	0
1A5 x 1E4	B16.1	0.260482077	0.225712536	1.154043464	0	0
1A5 x 1E4	B16.2	0.611946556	0.400098582	1.529489442	NA	0
1A5 x 1E4	B17.1	0.382237907	0.33036539	1.157015589	1	0
1A5 x 1E4	B17.2	0.592456126	0.378874678	1.563725845	NA	0
1A5 x 1E4	B18.1	0.439584788	0.23950511	1.835387931	NA	0
1A5 x 1E4	B18.2	0.351547603	0.29085979	1.208649717	0	0
1A5 x 1E4	B19.1	0.324356735	0.314407681	1.031643802	0	0
1A5 x 1E4	B19.2	0.432476583	0.30964872	1.396668401	NA	0
1A5 x 1E4	B20.1	0.591483261	0.367000496	1.611668832	NA	0
1A5 x 1E4	B20.2	0.666984271	0.37426189	1.782132482	NA	0
1A5 x 1E4	B21.1	0.694985784	NA	NA	NA	NA
1A5 x 1E4	B22.1	0.387514339	0.342375112	1.131841437	1	1
1A5 x 1E4	B22.2	0.334861109	0.213731349	1.566738391	NA	NA
1A5 x 1E4	B23.1	0.362692561	0.279636018	1.297016612	NA	0
1A5 x 1E4	B24.1	0.223173795	0.218324026	1.022213629	NA	0
1A5 x 1E4	B24.2	0.303117617	0.255241353	1.187572521	0	0
1A5 x 1E4	B25.1	0.35564852	0.283558939	1.254231383	NA	0
1A5 x 1E4	B26.1	0.45685148	0.403835509	1.131281104	NA	0
1A5 x 1E4	B27.1	0.284334081	0.354464702	0.802150622	NA	0
1A5 x 1E4	B28.1	0.395353817	0.343159723	1.152098544	NA	0
1A5 x 1E4	B28.2	0.517595122	0.389041921	1.330435345	NA	0
1A5 x 1E4	B29.1	0.559914624	0.380592513	1.471165627	0	0
1A5 x 1E4	B3.1	0.42809976	0.364536883	1.174366108	NA	0
1A5 x 1E4	B30.1	0.3942933	0.390471175	1.009788495	NA	0
1A5 x 1E4	B31.1	0.420706749	0.394610374	1.066132003	0	0
1A5 x 1E4	B31.2	0.387475193	0.308753939	1.254964375	1	0
1A5 x 1E4	B32.1	0.387798733	0.351296067	1.103908553	NA	0
1A5 x 1E4	B32.2	0.426645331	0.292572626	1.458254443	NA	0
1A5 x 1E4	B33.1	0.278427219	0.261253254	1.065736844	0	0
1A5 x 1E4	B33.2	0.455820644	0.426092443	1.069769371	NA	0
1A5 x 1E4	B34.2	0.289778891	0.273289097	1.060338277	0	0
1A5 x 1E4	B35.1	0.38660161	0.336327987	1.149477964	NA	0
1A5 x 1E4	B35.2	0.357964155	0.252442084	1.418005067	NA	0
1A5 x 1E4	B37.1	0.410030766	0.38026785	1.078268292	NA	0
1A5 x 1E4	B37.3	0.541580364	0.400935258	1.35079256	NA	0
1A5 x 1E4	B38.1	0.495741013	0.411513586	1.204677149	NA	0
1A5 x 1E4	B39.1	0.272078076	0.271040304	1.003828848	NA	0
1A5 x 1E4	B39.2	0.302679961	0.215693998	1.403284112	NA	0

1A5 x 1E4	B4.1	0.319435216	0.233008276	1.370917899	NA	0
1A5 x 1E4	B4.2	0.379751744	0.426901168	0.889554239	0	0
1A5 x 1E4	B40.2	0.409757481	0.370582418	1.105712146	0	0
1A5 x 1E4	B41.1	0.446220986	NA	NA	NA	0
1A5 x 1E4	B42.1	0.687387663	0.44944767	1.529405332	NA	0
1A5 x 1E4	B42.2	0.215998931	0.267457314	0.807601511	NA	0
1A5 x 1E4	B42.3	0.461921337	0.498389503	0.926827982	NA	0
1A5 x 1E4	B43.1	0.378550568	0.311443699	1.215470306	0	0
1A5 x 1E4	B44.1	0.320554276	NA	NA	NA	0
1A5 x 1E4	B45.1	0.335350916	0.2648959	1.265972465	0	0
1A5 x 1E4	B45.2	0.504787709	0.467384804	1.080025932	0	0
1A5 x 1E4	B46.1	0.310822876	0.275243398	1.129265509	NA	0
1A5 x 1E4	B46.2	0.229986552	0.233814064	0.983630104	0	0
1A5 x 1E4	B48.1	0.29264465	0.316896989	0.923469329	NA	0
1A5 x 1E4	B48.2	0.318880289	0.31156541	1.023477828	NA	0
1A5 x 1E4	B49.1	0.375098915	0.274101126	1.368469078	NA	0
1A5 x 1E4	B50.1	0.372543261	0.308098732	1.209168435	0	0
1A5 x 1E4	B50.2	0.356871334	0.309730636	1.152199017	NA	0
1A5 x 1E4	B51.1	0.2865592	0.263306044	1.088312275	NA	0
1A5 x 1E4	B7.1	0.441524194	0.310778284	1.420704779	0	0
1A5 x 1E4	B9.1	0.388076879	0.327660156	1.184388375	0	0
1A5 x 1E4	B9.2	0.3356923	0.214551335	1.564624614	0	0
1A5 x 1E4	C1.1	0.432597317	0.351288601	1.231458453	NA	0
1A5 x 1E4	C1.2	0.46463921	0.415818806	1.117407878	0	0
1A5 x 1E4	C10.1	0.253193442	0.275350523	0.919531365	0	0
1A5 x 1E4	C11.1	0.570766355	0.430379908	1.326191918	NA	0
1A5 x 1E4	C12.1	NA	0.371032301	NA	NA	1
1A5 x 1E4	C12.2	NA	NA	NA	NA	0
1A5 x 1E4	C13.1	0.405008922	0.332558047	1.217859337	NA	0
1A5 x 1E4	C14.1	0.403262522	0.276885674	1.456422486	1	0
1A5 x 1E4	C16.1	0.390116101	0.344992121	1.130797132	1	0
1A5 x 1E4	C16.2	0.294618519	0.289426727	1.017938191	NA	0
1A5 x 1E4	C16.3	0.329717866	0.369853357	0.89148269	NA	0
1A5 x 1E4	C17.1	0.307872943	0.303365507	1.0148581	0	0
1A5 x 1E4	C19.1	0.213914607	0.238220212	0.897970014	NA	0
1A5 x 1E4	C2.1	0.379828995	0.326815482	1.162212367	NA	0
1A5 x 1E4	C2.2	0.321288213	0.351534742	0.913958637	1	0
1A5 x 1E4	C20.1	0.245802458	0.231775234	1.060520805	0	0
1A5 x 1E4	C20.2	0.346505576	0.333519589	1.038936203	NA	0
1A5 x 1E4	C21.1	0.247097394	0.239383171	1.032225417	0	0

1A5 x 1E4	C21.2	0.284299515	0.366426949	0.775869558	NA	0
1A5 x 1E4	C22.1	0.319873715	0.294155419	1.087430979	1	0
1A5 x 1E4	C22.2	0.490701018	0.397504829	1.234452974	NA	NA
1A5 x 1E4	C23.1	0.272671233	0.255494537	1.067229211	NA	0
1A5 x 1E4	C23.2	0.287086826	0.300653547	0.9548759	0	0
1A5 x 1E4	C24.1	0.402372242	0.426437014	0.943567816	NA	0
1A5 x 1E4	C24.2	0.576562203	0.409959746	1.406387357	NA	1
1A5 x 1E4	C25.1	0.364605001	0.325801625	1.119101235	0	0
1A5 x 1E4	C26.1	0.380704312	0.233686764	1.629122272	NA	0
1A5 x 1E4	C27.1	0.298382347	0.359416908	0.830184502	NA	0
1A5 x 1E4	C27.2	0.318402863	0.276751135	1.150502468	NA	0
1A5 x 1E4	C28.1	0.334834761	0.366761219	0.912950289	NA	0
1A5 x 1E4	C28.2	0.393579236	0.37551746	1.048098365	NA	0
1A5 x 1E4	C29.2	0.263373246	0.308524497	0.853654244	0	0
1A5 x 1E4	C3.1	0.450342755	0.360190148	1.250291707	NA	0
1A5 x 1E4	C3.2	0.479869527	0.377916795	1.269775604	NA	0
1A5 x 1E4	C30.1	0.298591256	0.219368861	1.361137831	0	0
1A5 x 1E4	C30.2	0.489414965	0.348960397	1.402494291	1	0
1A5 x 1E4	C31.1	0.641071887	0.397009264	1.614752969	0	0
1A5 x 1E4	C32.1	0.385113527	0.251060085	1.533949643	NA	0
1A5 x 1E4	C32.2	0.442475151	0.384068587	1.152073264	NA	0
1A5 x 1E4	C33.1	0.461942042	0.316552873	1.459288735	NA	0
1A5 x 1E4	C33.2	0.445796042	0.366630297	1.215927994	NA	0
1A5 x 1E4	C34.1	0.379336104	0.265420384	1.429189798	NA	0
1A5 x 1E4	C34.2	0.374423532	0.36203636	1.034215269	0	0
1A5 x 1E4	C35.1	0.345372987	0.235666089	1.465518389	0	0
1A5 x 1E4	C36.1	0.380475944	0.398623462	0.954474537	NA	0
1A5 x 1E4	C38.1	0.608329291	0.325955147	1.866297547	1	0
1A5 x 1E4	C38.2	0.357069125	0.380880439	0.937483496	NA	0
1A5 x 1E4	C4.1	0.485477118	0.324838513	1.494518348	NA	NA
1A5 x 1E4	C4.2	0.476445811	0.321821066	1.480468067	NA	0
1A5 x 1E4	C41.1	0.408065693	0.363733647	1.12188052	NA	0
1A5 x 1E4	C41.2	0.321687218	0.252873232	1.272128393	0	0
1A5 x 1E4	C42.1	0.513820959	0.413692893	1.242034776	NA	0
1A5 x 1E4	C42.2	0.353700643	0.261138686	1.354455168	0	0
1A5 x 1E4	C44.1	0.297223713	0.285722869	1.040251744	0	0
1A5 x 1E4	C44.2	0.434520491	0.332774729	1.305749666	NA	NA
1A5 x 1E4	C45.1	0.384032004	0.360932591	1.063999245	NA	0
1A5 x 1E4	C45.2	0.542947948	0.472436761	1.14925	1	NA
1A5 x 1E4	C48.1	0.415893986	0.35882016	1.159059698	0	0

1A5 x 1E4	C48.2	0.382822785	0.39279022	0.974624023	NA	0
1A5 x 1E4	C49.1	NA	0.234822998	NA	NA	0
1A5 x 1E4	C5.1	0.545894135	0.42484691	1.284919632	NA	0
1A5 x 1E4	C5.2	0.216355801	0.226209962	0.95643799	0	0
1A5 x 1E4	C51.1	0.279214673	0.300993547	0.927643387	NA	0
1A5 x 1E4	C51.2	0.654413053	NA	NA	NA	0
1A5 x 1E4	C52.1	0.41038619	0.278175267	1.475279217	0	0
1A5 x 1E4	C53.1	0.585122504	0.458321239	1.276664607	1	0
1A5 x 1E4	C54.1	0.592299004	0.387549916	1.528316688	0	0
1A5 x 1E4	C55.1	0.288298353	0.187989901	1.533584265	0	0
1A5 x 1E4	C55.2	0.341476136	0.366796677	0.930968455	0	0
1A5 x 1E4	C56.1	0.455979148	0.383264187	1.189725427	NA	0
1A5 x 1E4	C56.2	0.277264886	0.284182511	0.97565781	0	0
1A5 x 1E4	C57.1	0.315168619	0.372526377	0.846030344	NA	0
1A5 x 1E4	C57.2	0.236857646	0.243307182	0.973492211	0	0
1A5 x 1E4	C59.2	0.339492565	0.265109892	1.280572982	NA	0
1A5 x 1E4	C6.1	0.31267625	0.323470384	0.966630226	0	0
1A5 x 1E4	C60.1	0.282001689	0.231195167	1.219755986	NA	0
1A5 x 1E4	C60.2	0.362149298	0.386195534	0.937735591	NA	NA
1A5 x 1E4	C61.1	0.320097108	0.388496566	0.823938064	0	0
1A5 x 1E4	C61.2	NA	0.427193126	NA	NA	0
1A5 x 1E4	C62.1	0.519775835	0.432244467	1.202504311	NA	0
1A5 x 1E4	C62.2	0.343364504	0.253285485	1.355642248	0	0
1A5 x 1E4	C63.1	0.306490213	0.252376028	1.214418881	0	0
1A5 x 1E4	C7.1	0.387162566	0.352736429	1.097597338	0	0
1A5 x 1E4	C7.2	0.492069977	0.361661979	1.360579784	NA	0
1A5 x 1E4	C8.1	0.272404406	NA	NA	0	0
1A5 x 1E4	CR4_A1.1	0.207601154	0.185565937	1.118746021	0	0
1A5 x 1E4	CR4_A2.1	0.331058545	0.351216309	0.942605843	0	0
1A5 x 1E4	CR4_A2.2	0.453603857	0.348886809	1.300146194	NA	0
1A5 x 1E4	CR4_A3.1	0.495287112	0.391407362	1.265400604	NA	0
1A5 x 1E4	CR4_A3.2	0.436238914	0.356938954	1.22216673	0	0
1A5 x 1E4	CR4_A4.1	0.373954122	0.292714892	1.277537059	0	0
1A5 x 1E4	D1.1	0.26972111	0.350891486	0.768673851	0	0
1A5 x 1E4	D1.2	0.436173951	0.328811139	1.326518174	1	0
1A5 x 1E4	D1.3	0.359702963	0.246712935	1.457981778	0	0
1A5 x 1E4	D10.1	0.420091693	0.271009922	1.550097096	0	0
1A5 x 1E4	D11.1	0.488915673	0.37717436	1.296259039	NA	0
1A5 x 1E4	D2.1	0.360484584	0.332175316	1.085223876	0	0
1A5 x 1E4	D3.1	0.309732762	0.225744091	1.372052582	NA	0

1A5 x 1E4	D3.2	0.333057061	0.269678045	1.235017335	1	0
1A5 x 1E4	D4.1	0.29938525	0.290278097	1.031373891	0	0
1A5 x 1E4	D5.1	0.427181204	0.394776861	1.082082682	0	0
1A5 x 1E4	D7.1	0.570777621	0.437198746	1.305533525	NA	0
1A5 x 1E4	D7.2	0.214350928	0.240356491	0.891804199	0	0
1A5 x 1E4	D7.3	0.364082728	0.384653042	0.94652242	0	0
1A5 x 1E4	D9.1	0.603564131	0.433779699	1.391407049	1	0
1A5 x 1E4	D9.2	0.32088736	0.363785951	0.882077385	1	0

^a The yeast/hyphae dimorphism phenotype was scored as a binary phenotype, with a value of '0' representing yeast-like growth and a value of '1' representing hyphal growth.

Table S3 Positions and effects of all QTLs associated with the yeast/hyphae dimorphism in cross 3D1 x 3D7.

Trait	Chromosome	Estimated position of peaking marker (cM)	Estimated position of peaking marker (kb)	LOD score at peak	P-value	Mean 3D1 allele (growth rate/temperature sensitivity)	Mean 3D7 allele (growth rate/temperature sensitivity)	Mean difference	Allele effect ^a	Percentage of variance explained by QTL (%)	Estimated position of proximal marker (kb) ^b	Estimated position of distal marker (kb) ^b	Bayes confidence interval length (kb)
Yeast/hyphae (22°C)	3	234.05	2281	8.89	<0.001	0.233	0.682	0.449	3D7	18.3	2036	3094	1058
Yeast/hyphae (22°C)	7	115.35	1070	3.42	0.036	0.306	0.583	0.277	3D7	7.5	943	1601	657
Yeast/hyphae (22°C)	11	81.06	571	11.15	<0.001	0.721	0.227	0.494	3D1	21.5	447	657	211
Yeast/hyphae (15°C)	1	30.52	284	4.5	0.003	0.339	0.1	0.239	3D1	8.3	262	343	81
Yeast/hyphae (15°C)	3	178.38	1730	10.15	<0.001	0.055	0.409	0.354	3D7	17.8	1709	1775	66
Yeast/hyphae (15°C)	11	77.83	535	4.86	0.001	0.358	0.102	0.256	3D1	9	437	647	210

^a 3D1 indicates that the 3D1 parent allele provided a higher phenotypic mean than the 3D7 parent allele. 3D7 indicates that the 3D7 parent allele provided a higher phenotypic mean than the 3D1 parent allele.

^b Markers flanking the 95% Bayes confidence interval of the associated QTL.

Table S4 Summary of genes affected by sequence variation within each Bayes confidence interval for cross 3D1 x 3D7 for the QTLs associated with the yeast/hyphae dimorphism, excluding genes containing no sequence variation or with synonymous SNPs only.

Trait	Chromosome	Estimated position of peaking marker (kb)	LOD score at peak	P-value	Estimated position of proximal marker (kb) ^a	Estimated position of distal marker (kb) ^a	Bayes confidence interval length (kb)	Number of sequence variations ^b	Number of genes ^b	Number of genes affected by sequence variations ^b	Percentage of total genes affected by sequence variations (%) ^b	Number of sequence variation affected genes with unknown function ^b	Percentage of total sequence variation affected genes with unknown function (%) ^b
Yeast/hyphae (22°C)	3	2281	8.89	< 0.001	2036	3094	1058	1310	351	266	76	108	41
Yeast/hyphae (22°C)	7	1070	3.42	0.036	943	1601	657	687	209	149	71	60	40
Yeast/hyphae (22°C)	11	571	11.15	< 0.001	447	657	211	161	68	43	63	16	37
Yeast/hyphae (15°C)	1	284	4.5	0.003	262	343	81	100	23	15	65	5	33
Yeast/hyphae (15°C)	3	1730	10.15	< 0.001	1709	1775	66	80	21	15	71	4	27
Yeast/hyphae (15°C)	11	535	4.86	0.001	437	647	210	151	68	43	63	20	47

^a Markers flanking the 95% Bayes confidence interval of the associated QTL.

^b Numbers refer to within the 95% Bayes confidence interval of the associated QTL.

Table S5 Positions and effects of all QTLs associated with the yeast/hyphae dimorphism in cross 1A5 x 1E4.

Trait	Chromosome	Estimated position of peaking marker (cM)	Estimated position of peaking marker (kb)	LOD score at peak	P-value	Mean 1A5 allele (growth rate/temperature sensitivity)	Mean 1E4 allele (growth rate/temperature sensitivity)	Mean difference	Allele effect ^a	Percentage of variance explained by QTL (%)	Estimated position of proximal marker (kb) ^b	Estimated position of distal marker (kb) ^b	Bayes confidence interval length (kb)
Yeast/hyphae (22°C)	7	196.28	971	4.24	0.005	0.095	0.413	0.318	1E4	13.3	424	1138	714
Yeast/hyphae (22°C)	11	66.72	524	4.79	0.001	0.446	0.099	0.347	1A5	14.9	410	606	196

^a 1A5 indicates that the 1A5 parent allele provided a higher phenotypic mean than the 1E4 parent allele. 1E4 indicates that the 1E4 parent allele provided a higher phenotypic mean than the 1A5 parent allele.

^b Markers flanking the 95% Bayes confidence interval of the associated QTL.

Table S6 Summary of genes affected by sequence variation within each Bayes confidence interval for the cross 1A5 x 1E4 QTLs associated with the yeast/hyphae dimorphism, excluding all genes containing no sequence variation or with only synonymous SNPs.

Trait	Chromosome	Estimated position of peaking marker (kb)	LOD score at peak	P-value	Estimated position of proximal marker (kb) ^a	Estimated position of distal marker (kb) ^a	Bayes confidence interval length (kb)	Number of sequence variations ^b	Number of genes ^b	Number of genes affected by sequence variations ^b	Percentage of total genes affected by sequence variations (%) ^b	Number of sequence variation affected genes with unknown function ^b	Percentage of total sequence variation affected genes with unknown function (%) ^b
Yeast/hyphae (22°C)	7	971	4.24	0.005	424	1138	714	897	206	157	76	69	44
Yeast/hyphae (22°C)	11	524	4.79	0.001	410	606	196	240	65	48	74	18	38

^a Markers flanking the 95% Bayes confidence interval of the associated QTL.

^b Numbers refer to within the 95% Bayes confidence interval of the associated QTL.

Table S7 Summary of genes affected by sequence variation within each Bayes confidence interval for the cross 3D1 x 3D7 QTLs associated with temperature sensitivity, excluding all genes containing no sequence variation or with synonymous SNPs only.

Trait	Chromosome	Estimated position of peaking marker (kb)	LOD score at peak	P-value	Estimated position of proximal marker (kb) ^a	Estimated position of distal marker (kb) ^a	Bayes confidence interval length (kb)	Number of sequence variations ^b	Number of genes ^b	Number of genes affected by sequence variations ^b	Percentage of total genes affected by sequence variations (%) ^b	Number of sequence variation affected genes with unknown function ^b	Percentage of total sequence variation affected genes with unknown function (%) ^b
Growth rate (15°C)	2	1805	4.89	0.001	837	1833	996	1260	307	236	77	88	37
Growth rate (22°C)	2	858	3.98	0.010	478	1826	1347	1670	424	309	73	115	37
Growth rate (15°C)	3	2175	4.77	0.001	1570	3095	1526	1724	499	377	76	144	38
Growth rate (22°C)	3	3078	4.97	0.002	2781	3107	326	511	109	88	81	41	47
Growth rate (15°C)	7	1115	3.95	0.008	943	1205	262	389	88	75	85	28	37
Growth rate (15°C)	10	634	6.00	< 0.001	616	651	35	70	16	14	88	4	29
Temperature sensitivity	10	644	11.80	< 0.001	631	651	20	32	8	6	75	1	17
Growth rate (15°C)	11	592	7.56	< 0.001	401	668	267	227	87	60	69	22	37
Growth rate (22°C)	11	538	10.38	< 0.001	435	592	157	133	54	35	65	17	49

^a Markers flanking the 95% Bayes confidence interval of the associated QTL.

^b Numbers refer to within the 95% Bayes confidence interval of the associated QTL.

Table S8 Summary of genes affected by sequence variation within each Bayes confidence interval for the cross 1A5 x 1E4 QTLs associated with temperature sensitivity, excluding all genes containing no sequence variation or with synonymous SNPs only.

Trait	Chromosome	Estimated position of peaking marker (kb)	LOD score at peak	P-value	Estimated position of proximal marker (kb) ^a	Estimated position of distal marker (kb) ^a	Bayes confidence interval length (kb)	Number of sequence variations ^b	Number of genes ^b	Number of genes affected by sequence variations ^b	Percentage of total genes affected by sequence variations (%) ^b	Number of sequence variation affected genes with unknown function ^b	Percentage of total sequence variation affected genes with unknown function (%) ^b
Growth rate (15°C)	1	5371	3.52	0.035	144	5655	5511	7686	1862	1382	74	490	35
Temperature sensitivity	1	2216	5.66	<0.001	2076	2324	248	298	92	60	65	22	37
Temperature sensitivity	2	1428	4.31	0.005	396	3516	3120	3888	978	723	74	288	40
Growth rate (22°C)	2	1372	3.71	0.023	1122	1829	707	909	218	165	76	66	40
Temperature sensitivity	4	1188	4.26	0.006	421	1863	1442	1717	436	311	71	135	43
Growth rate (22°C)	4	1312	6.77	<0.001	508	1728	1220	1372	355	256	72	111	43
Growth rate (15°C)	5	1909	4.81	0.002	1420	2786	1366	1502	388	286	74	100	35
Growth rate (15°C)	8	1506	6.77	<0.001	364	1802	1437	1587	457	327	72	121	37
Growth rate (22°C)	8	388	5.51	0.001	275	443	168	266	46	38	83	16	42

^a Markers flanking the 95% Bayes confidence interval of the associated QTL.

^b Numbers refer to within the 95% Bayes confidence interval of the associated QTL.

Table S9 Genes within the chromosome 1 QTL confidence interval associated with the yeast/hyphae (15°C) dimorphism containing ≤ 30 candidate genes for cross 3D1 x 3D7, excluding genes with no sequence variation or with only synonymous SNPs.

Protein ID ^a	Gene ontology name	Gene ontology biological process	Gene ontology cellular component	Gene ontology molecular function	Number of Non-Syn SNPs ^b	Number of other sequence variations ^{b,c}	Additional information	Highest RPKM mean ^d	RPKM Stdev
88629	nucleic acid binding	NotAvailable	NotAvailable	NotAvailable	1 (M)	3 upstream (m)	/	0.1 (56dpi)	0.1
88630	proteolysis	NotAvailable	NotAvailable	NotAvailable	10 (M)	0	/	2.7 (13dpi) *	1.3
98146	peroxisomal membrane	NotAvailable	NotAvailable	zinc ion binding	4 (M)	0	/	33.5 (13dpi)	9.5
64902	phosphogluconate dehydrogenase (decarboxylating) activity	pentose-phosphate shunt; D-gluconate metabolic process	NotAvailable	NADP binding; phosphogluconate dehydrogenase (decarboxylating) activity	4 (M)	0	/	39.5 (56dpi) *	5.1
32213 ^{# °}	ATP binding	transmembrane transport; ATP catabolic process	integral to membrane	ATPase activity, coupled to transmembrane movement of substances; ATP binding	10 (M)	0	ABC transporter, ABC-C family, MRP type. TC3-A.1.208. These transporters mainly transport conjugated compounds and can be involved in metal resistance	5.3 (7dpi)	1
64907	NotAvailable	NotAvailable	NotAvailable	NotAvailable	9 (M)	1 UTR5 Prime (m)	/	1.9 (13dpi)	1.1
64910	NotAvailable	transmembrane transport	integral to membrane	NotAvailable	1 (M)	1 upstream (m), 2 UTR5 Prime (m)	/	35.7 (13dpi)	4
16140	hydrolase activity	NotAvailable	NotAvailable	hydrolase activity	4 (M)	0	/	4.3 (13dpi)	1.9
88639	NotAvailable	NotAvailable	NotAvailable	NotAvailable	1 (M)	0	/	0 (No Specific Day)	0

88641	NotAvailable	NotAvailable	NotAvailable	NotAvailable	0 (M)	1 downstream (m), 1 intron (m)	/	0 (No Specific Day)
88642 °	NotAvailable	NotAvailable	NotAvailable	NotAvailable	2 (M)	1 downstream (m), 4 intron (m), 1 splice site donor (H)	/	0 (No Specific Day)
88643	NotAvailable	NotAvailable	NotAvailable	NotAvailable	6 (M)	1 upstream (m), 1 intron (m)	/	0 (No Specific Day)
88644 °	protein kinase activity	protein phosphorylation; serine family amino acid metabolic process	NotAvailable	ATP binding; protein serine/threonine kinase activity	13 (M)	1 intron (m), 1 splice site acceptor (H)	Ca2+/calmodulin-dependent protein kinase	0.02 (56dpi)
64915	monooxygenase activity	oxidation-reduction process	NotAvailable	monooxygenase activity; oxidoreductase activity, acting on paired donors, with incorporation or reduction of molecular oxygen nucleoside-triphosphatase activity; ATP binding	4 (M)	1 intron (m)	/	65.6 (7dpi) *
31554	nucleotide binding	NotAvailable	NotAvailable	triphosphatase activity; ATP binding	7 (M)	4 intron (m)	/	3.2 (13dpi) *

^a A # Indicates the QTL peak is positioned closest to this gene or within the gene. A ° Indicates candidate genes with a higher likelihood of contributing to the yeast/hyphae dimorphism compared to unmarked candidate genes.

^b The letter within brackets following the number of a specific sequence polymorphisms refers to the likely impact of the sequence polymorphism according to SnpEff. H=high, M=moderate, L=low, m=modifier.

^c Other sequence variations include codon change plus insertion/deletion, codon insertion/deletion, codon insertion/deletions, 100 bp upstream or downstream, frameshift, intron, splice site acceptor/donor, start gained/lost, stop gained/lost, untranslated regions (UTR).

^d A * Indicates significant changes in transcript abundances over time in planta.

Table S10 Genes within the chromosome 3 yeast/hyphae (15°C) dimorphism QTL confidence interval containing ≤ 30 candidate genes for cross 3D1 x 3D7, excluding genes with no sequence variation or with only synonymous SNPs.

Protein ID ^a	Gene ontology name	Gene ontology biological process	Gene ontology cellular component	Gene ontology molecular function	Number of Non-Syn SNPs ^b	Number of other sequence variations ^{b,c}	Additional information	Highest RPKM mean ^d	RPKM Stdev
108612	NotAvailable	NotAvailable	NotAvailable	metal ion binding; oxidoreductase activity, acting on paired donors, with incorporation or reduction of molecular oxygen, 2-oxoglutarate as one donor, and incorporation of one atom each of oxygen into both donors; organic cyclic compound binding	5 (M)	1 codon insertion (M), 3 intron (m)	/	55.6 (7dpi)	6.4
38733	NotAvailable	oxidation-reduction process	NotAvailable	oxidation-reduction process	9 (M)	0	/	5.4 (7dpi)	3.4
103731	translation initiation factor activity	translational frameshifting; peptidyl-lysine modification to hypusine; positive regulation of translational termination; positive regulation of translational elongation; regulation of translational initiation	ribosome;	translation initiation factor activity; translation elongation factor activity; ribosome binding	1 (M)	1 upstream (m), 2 intron (m), 1 UTR5 Prime (m)	/	812.1 * (13dpi)	41.3

56726	sugar:hydrogen symporter activity	transmembrane transport; carbohydrate transport	integral to membrane	substrate-specific transmembrane transporter activity	2 (M)	1 intron (m)	/	13 (56dpi)	0.8
38371 [#]	metalloendopeptidase activity	proteolysis;	NotAvailable	metal ion binding; metalloendopeptidase activity	4 (M)	1 downstream (m), 1 intron (m)	Peptidase M3A and M3B, thimet/oligopeptidase F	68.6 (13dpi)	24.9
91716	NotAvailable	NotAvailable	NotAvailable	NotAvailable	3 (M)	3 intron (m)	/	117.2 [*] (13dpi)	10.7
103733	NotAvailable	NotAvailable	NotAvailable	NotAvailable	0 (M)	1 downstream (m), 1 UTR3 Prime (m), 1 UTR5 Prime (m)	/	8.5 [*] (56dpi)	1
108617	lipid metabolic process	retinol metabolic process; lipid catabolic process; glycerolipid metabolic process	NotAvailable	retinyl-palmitate esterase activity; triglyceride lipase activity	5 (M)	1 upstream (m), 1 intron (m), 1 UTR5 Prime (m)	/	82 (13dpi)	9
103740	metabolic process	NotAvailable	NotAvailable	NotAvailable	0 (M)	2 upstream (m)	/	61.2 (7dpi)	39.9
108619	NotAvailable	NotAvailable	NotAvailable	NotAvailable	4 (M)	2 UTR3 Prime (m)	/	53.9 [*] (56dpi)	6.6
56742 [°]	Rho guanyl-nucleotide exchange factor activity	regulation of Rho protein signal transduction; regulation of GTPase activity	intracellular;	Rho guanyl-nucleotide exchange factor activity; phospholipid binding	0 (M)	1 downstream (m)	pleckstrin like protein and citron like protein maybe with hypothetical rho1 gdp-gtp exchange activity	25.1 [*] (13dpi)	2.4
39671	NotAvailable	oxidation-reduction process	NotAvailable	flavin adenine dinucleotide binding; N,N-dimethylaniline monooxygenase activity; NADP binding	3 (M)	0	/	12 (56dpi)	1.4
69847	amino acid transport	amino acid transmembrane transport	integral to membrane	amino acid transmembrane transporter	0 (M)	3 upstream (m), 1 intron (m), 1 UTR3 Prime (m)	/	50.4 (13dpi)	12.9

	activity							
79974 °	NotAvailable	NotAvailable	NotAvailable	NotAvailable	0 (M)	1 upstream (m), 2 frame shift (H),	3.3 (7dpi) *	3.7
91725	NotAvailable	GTP catabolic process	NotAvailable	NotAvailable	8 (M)	1 downstream (m), 2 upstream (m),	6.2 (7dpi) *	2

^a A # Indicates the QTL peak is positioned closest to this gene or within the gene. A ° Indicates candidate genes with a higher likelihood of contributing to the yeast/hyphae dimorphism compared to unmarked candidate genes.

^b The letter within brackets following the number of a specific sequence polymorphism refers to the likely impact of the sequence polymorphism according to SnpEff. H=high, M=moderate, L=low, m=modifier.

^c Other sequence variations include codon change plus insertion/deletion, codon insertion/deletion, 100 bp upstream or downstream, frameshift, intron, splice site acceptor/donor, start gained/lost, stop gained/lost, untranslated regions (UTR).

^d A * Indicates significant changes in transcript abundances over time in planta.

Table S1.1 Positions and effects of all QTLs associated with temperature sensitivity in cross 3D1 x 3D7.

Trait	Chromosome	Estimated position of peaking marker (cM)	Estimated position of peaking marker (kb)	LOD score at peak	P-value	Mean 3D1 allele (growth rate/temperature sensitivity)	Mean 3D7 allele (growth rate/temperature sensitivity)	Mean difference	Allele effect ^a	Percentage of variance explained by QTL (%)	Estimated position of proximal marker (kb) ^b	Estimated position of distal marker (kb) ^b	Bayes confidence interval length (kb)
Growth rate (15°C)	2	189.12	1805	4.89	0.001	0.301	0.347	0.046	3D7	9.2	837	1833	996
Growth rate (22°C)	2	114.07	858	3.98	0.01	0.384	0.433	0.049	3D7	7.4	478	1826	1348
Growth rate (15°C)	3	217.16	2175	4.77	0.001	0.303	0.349	0.046	3D7	9	1570	3095	1525
Growth rate (22°C)	3	289.38	3078	4.97	0.002	0.384	0.438	0.054	3D7	9.2	2781	3107	326
Growth rate (15°C)	7	121.17	1115	3.95	0.008	0.304	0.345	0.041	3D7	7.5	943	1205	262
Growth rate (15°C)	10	102.13	634	6	<0.001	0.297	0.346	0.049	3D7	10	616	651	35
Temperature sensitivity	10	106.13	644	11.8	<0.001	1.416	1.199	0.217	3D1	16.6	631	651	20
Growth rate (15°C)	11	83.06	592	7.56	<0.001	0.355	0.3	0.055	3D1	12.5	401	668	267
Growth rate (22°C)	11	78.07	538	10.38	<0.001	0.452	0.376	0.076	3D1	17.9	435	592	157

^a 3D1 indicates that the 3D1 parent allele provided a higher phenotypic mean than the 3D7 parent allele. 3D7 indicates that the 3D7 parent allele provided a higher phenotypic mean than the 3D1 parent allele.

^b Markers flanking the 95% Bayes confidence interval of the associated QTL.

Table S12 Summary of allele effects of peaking markers modeled upon growth rate and the yeast/hyphae dimorphism in cross 3D1 x 3D7 and 1A5 x 1E4.

Trait ^a	Chromosome	Cross	Mean 3D1/1A5 allele (growth rate/dimorphism)	Mean 3D7/1E4 allele (growth rate/dimorphism)	Mean difference	Allele effect ^b	Percentage of variance explained by QTL (%)
Yeast/hyphae (22°C) ^s	7	3D1 x 3D7	0.306	0.583	0.277	3D7	7.5
Growth rate (22°C) ^t	7	3D1 x 3D7	0.393	0.424	0.031	3D7	3.1
Growth rate (15°C) ^s	10	3D1 x 3D7	0.297	0.346	0.049	3D7	10
Yeast/hyphae (15°C) ^t	10	3D1 x 3D7	0.114	0.303	0.189	3D7	4.4
Yeast/hyphae (22°C) ^s	7	1A5 x 1E4	0.095	0.413	0.318	1E4	13.3
Growth rate (22°C) ^t	7	1A5 x 1E4	0.378	0.406	0.028	1E4	1.9
Yeast/hyphae (22°C) ^s	11	1A5 x 1E4	0.446	0.099	0.347	1A5	14.9
Growth rate (22°C) ^t	11	1A5 x 1E4	0.414	0.373	0.041	1A5	4

^a A superscript 's' after the trait name indicates the source phenotype for the peaking marker, which was modeled upon the target phenotype (indicated by a superscript 't') within the same chromosome and cross.

^b 3D1/1A5 indicates that the 3D1/1A5 parent allele provided a higher phenotypic mean than the 3D7/1E4 parent allele. 3D7/1E4 indicates that the 3D7/1E4 parent allele provided a higher phenotypic mean than the 3D1/1A5 parent allele.

Table S13 Positions and effects of all QTLs associated with temperature sensitivity in cross 1A5 x 1E4.

Trait	Chromosome	Estimated position of peaking marker (cM)	Estimated position of peaking marker (kb)	LOD score at peak	P-value	Mean 1A5 allele (growth rate/temperature sensitivity)	Mean 1E4 allele (growth rate/temperature sensitivity)	Mean difference	Allele effect ^a	Percentage of variance explained by QTL (%)	Estimated position of proximal marker (kb) ^b	Estimated position of distal marker (kb) ^b	Bayes confidence interval length (kb)
Growth rate (15°C)	1	702.5	5371	3.52	0.035	0.312	0.345	0.033	1E4	6.2	144	5655	5511
Temperature sensitivity	1	368.54	2216	5.66	<0.001	1.281	1.127	0.154	1A5	9.9	2076	2324	248
Temperature sensitivity	2	193.42	1428	4.31	0.005	1.265	1.129	0.136	1A5	7.7	396	3516	3120
Growth rate (22°C)	2	188.41	1372	3.71	0.023	0.418	0.365	0.053	1A5	6.5	1122	1829	707
Temperature sensitivity	4	222.25	1188	4.26	0.006	1.129	1.264	0.135	1E4	7.6	421	1863	1442
Growth rate (22°C)	4	234.9	1312	6.77	<0.001	0.357	0.427	0.07	1E4	11.6	508	1728	1220
Growth rate (15°C)	5	244.14	1909	4.81	0.002	0.311	0.348	0.037	1E4	7.5	1420	2786	1366
Growth rate (15°C)	8	181.03	1506	6.77	<0.001	0.304	0.349	0.045	1E4	11.5	364	1802	1437
Growth rate (22°C)	8	51.59	388	5.51	0.001	0.357	0.421	0.064	1E4	9.6	275	443	168

^a 1A5 indicates that the 1A5 parent allele provided a higher phenotypic mean than the 1E4 parent allele. 1E4 indicates that the 1E4 parent allele provided a higher phenotypic mean than the 1A5 parent allele.

^b Markers flanking the 95% Bayes confidence interval of the associated QTL.

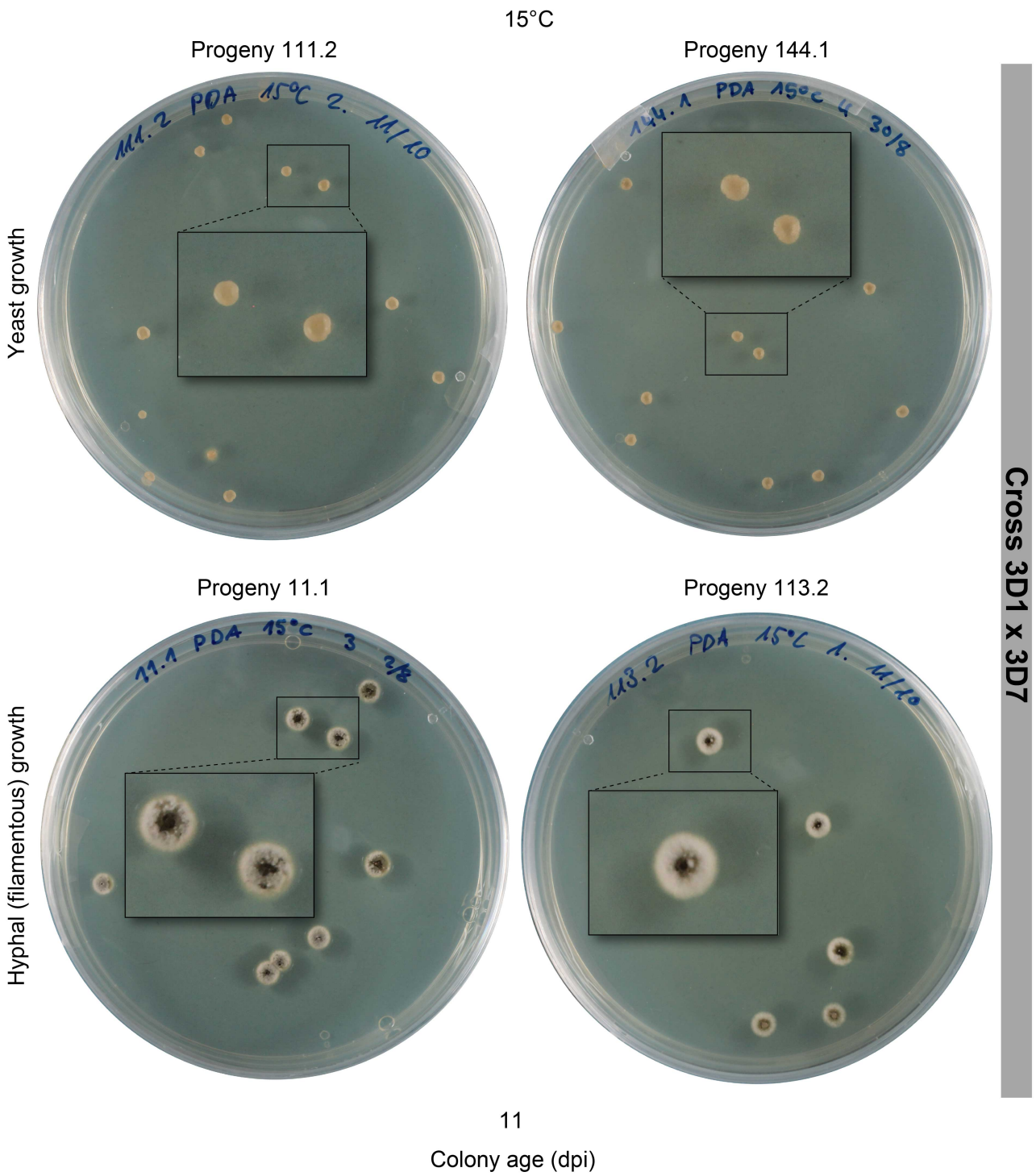


Figure S1 Examples of yeast-like growth morphology and hyphal (filamentous) growth morphology among progeny from cross 3D1 x 3D7 at 15°C and 11 dpi.

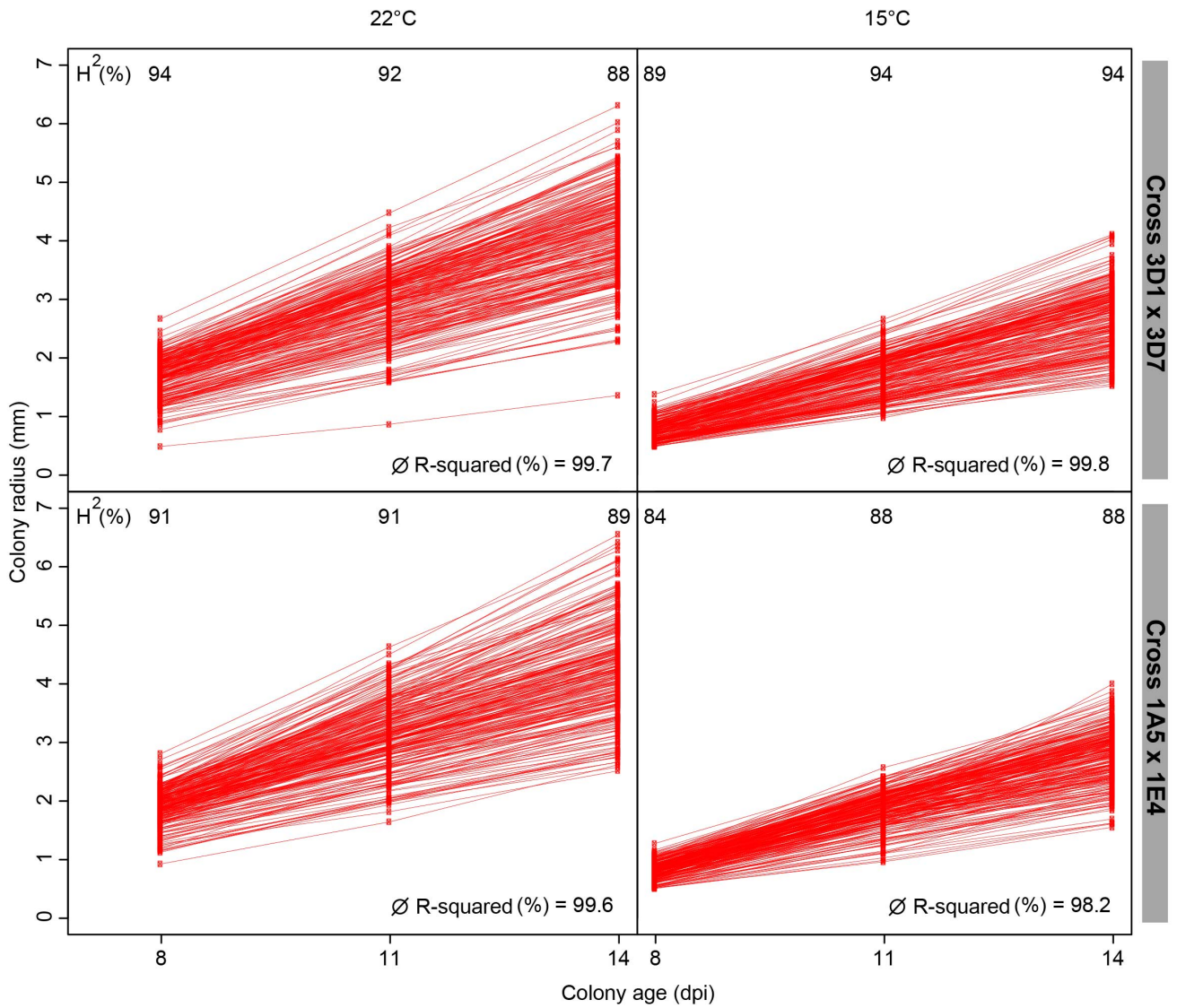


Figure S2 Norms of reaction for both crosses across the two treatments (22°C and 15°C). Broad-sense heritability (H^2) values for colony average area are indicated for each colony age and treatment. Average linear model R squared (r^2) values are shown for each treatment.

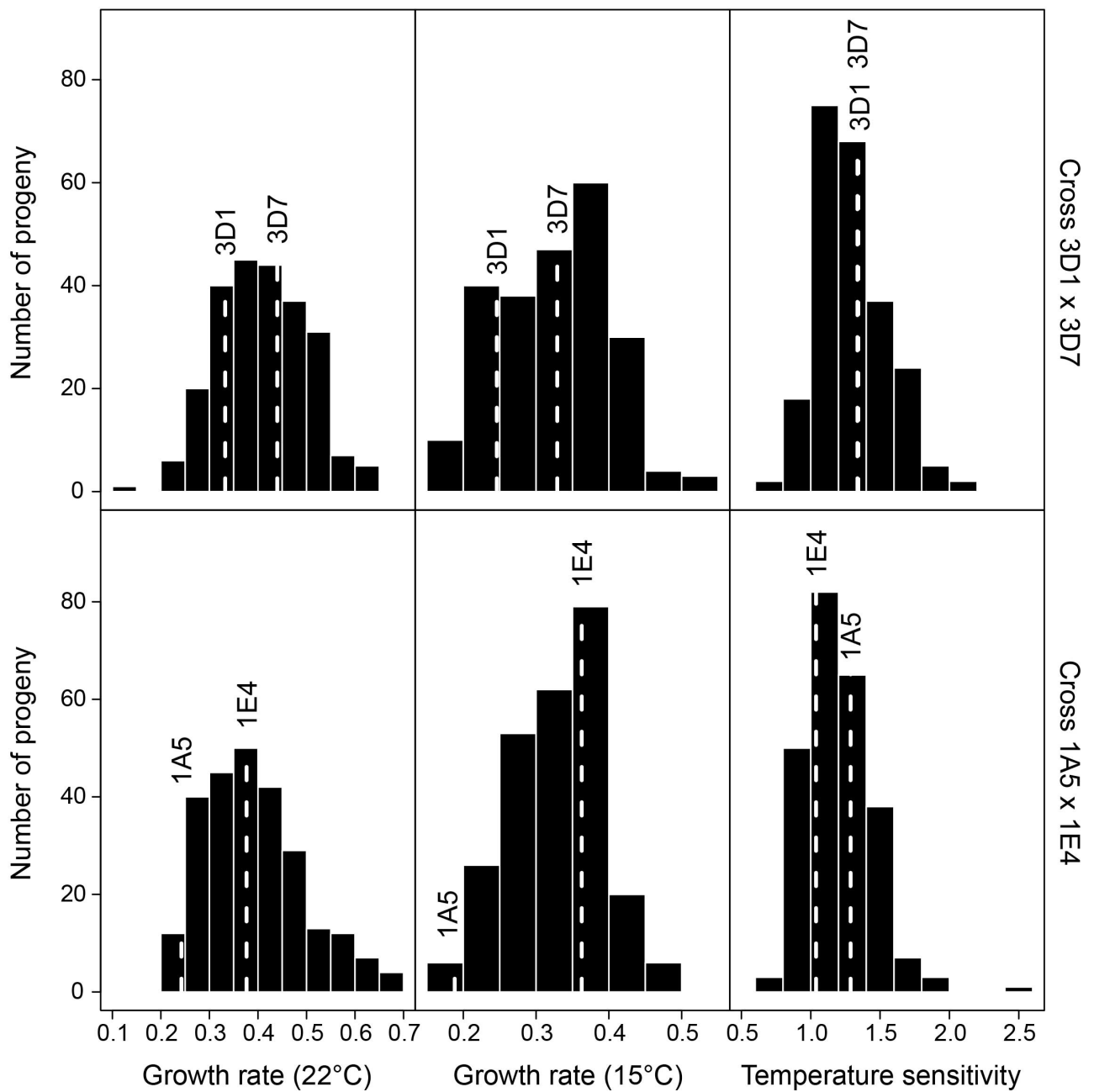


Figure S3 The distributions of growth rate and temperature sensitivity in both crosses. Positions of the parental phenotypes within each distribution are indicated by white dashed lines with corresponding parental names above their phenotypes.

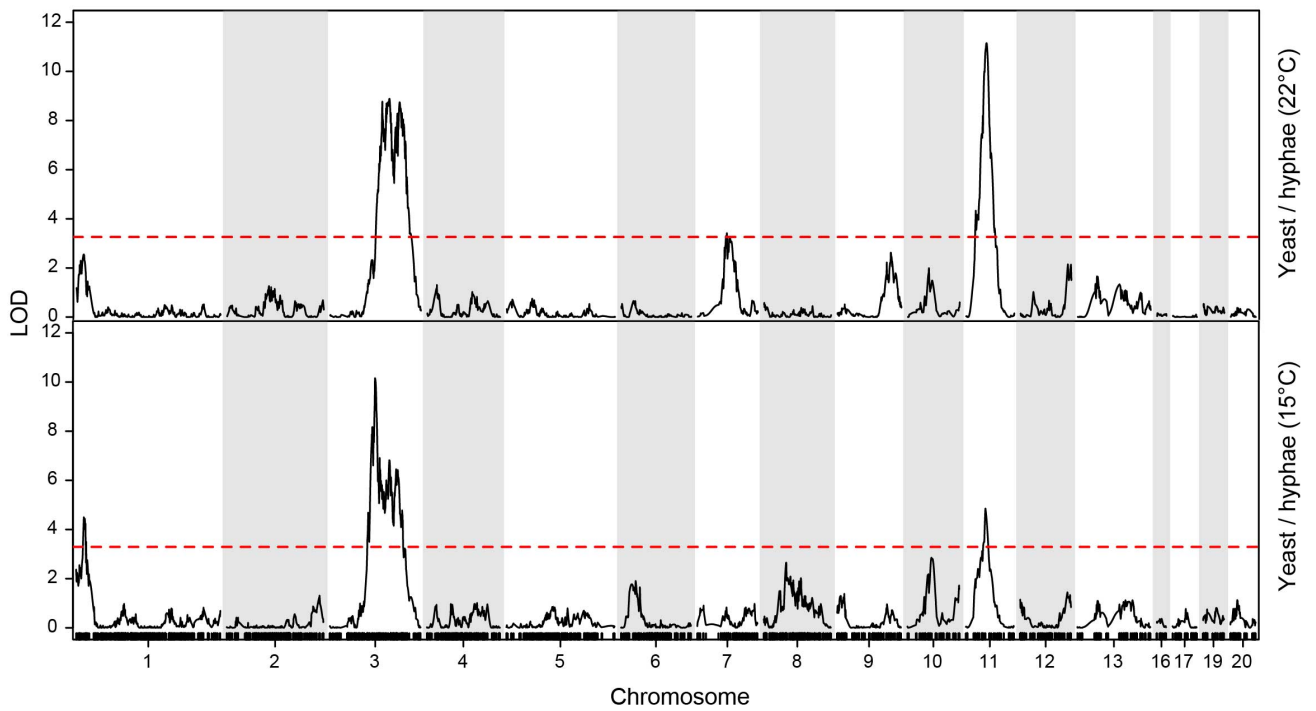


Figure S4 LOD plots from single marker interval mapping (SIM) analysis over all chromosomes for the yeast/hyphae dimorphism phenotype at 15°C and 22°C for cross 3D1 x 3D7. The dashed horizontal red line represents the significance threshold ($p = 0.05$) obtained using 1000 genome-wide permutations.

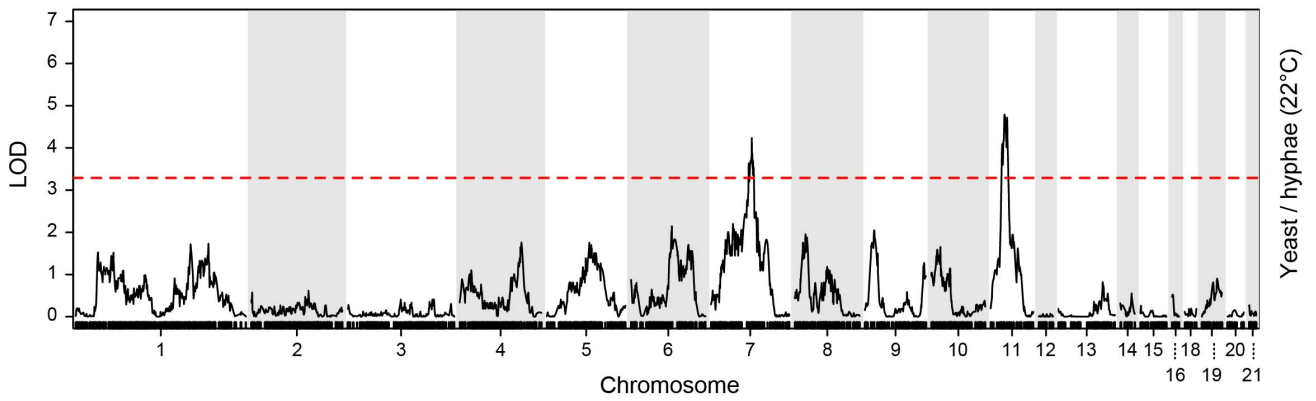


Figure S5 LOD plots from single marker interval mapping (SIM) analysis over all chromosomes for the binary yeast/hyphae dimorphism phenotype at 15°C and 22°C for cross 1A5 x 1E4. The dashed horizontal red line represents the significance threshold ($p = 0.05$) obtained using 1000 genome-wide permutations.

Temperature sensitivity versus fungicide sensitivity

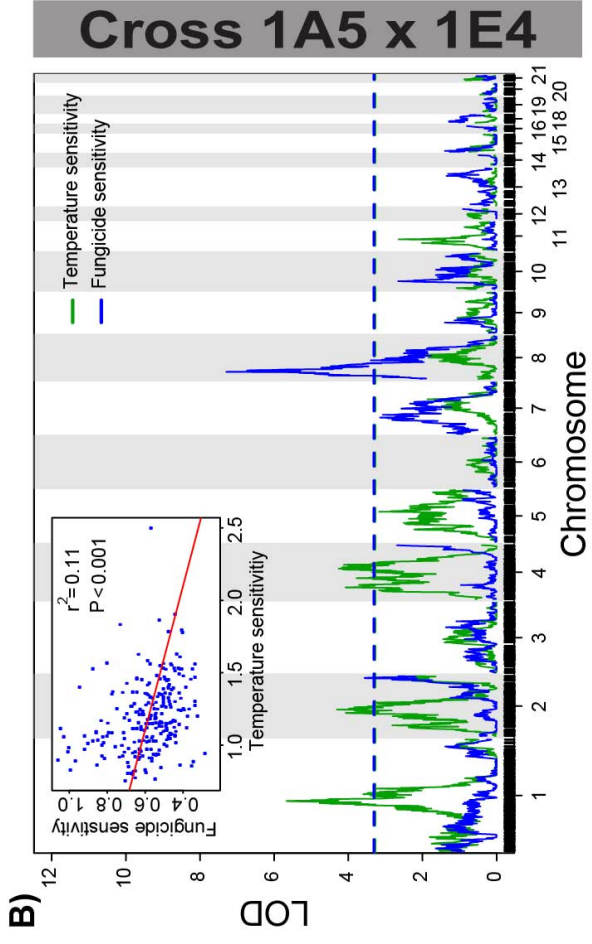
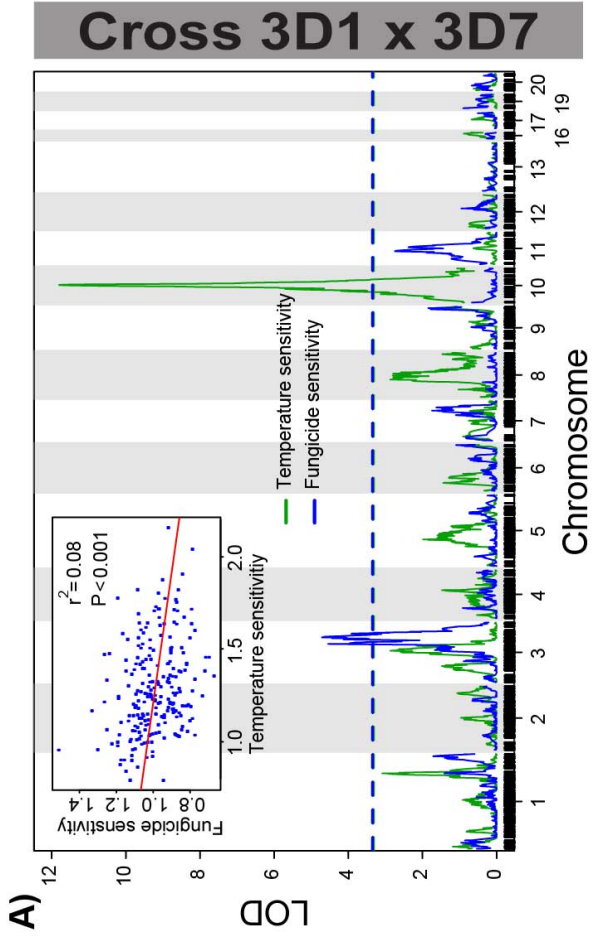


Figure S6 Pleiotropic effects between temperature and fungicide sensitivity (Panel A and B) were not observed in either cross. Each panel shows a full genome scan LOD overlap plot based on single marker interval mapping (SIM) analysis, with traits separated by colors (green = temperature sensitivity trait, blue = fungicide sensitivity trait). Horizontal lines in the LOD plots represent the color-coded significance thresholds ($p = 0.05$) obtained with 1000 genome-wide permutations. Each panel includes the corresponding linear correlation plot amongst the two traits.

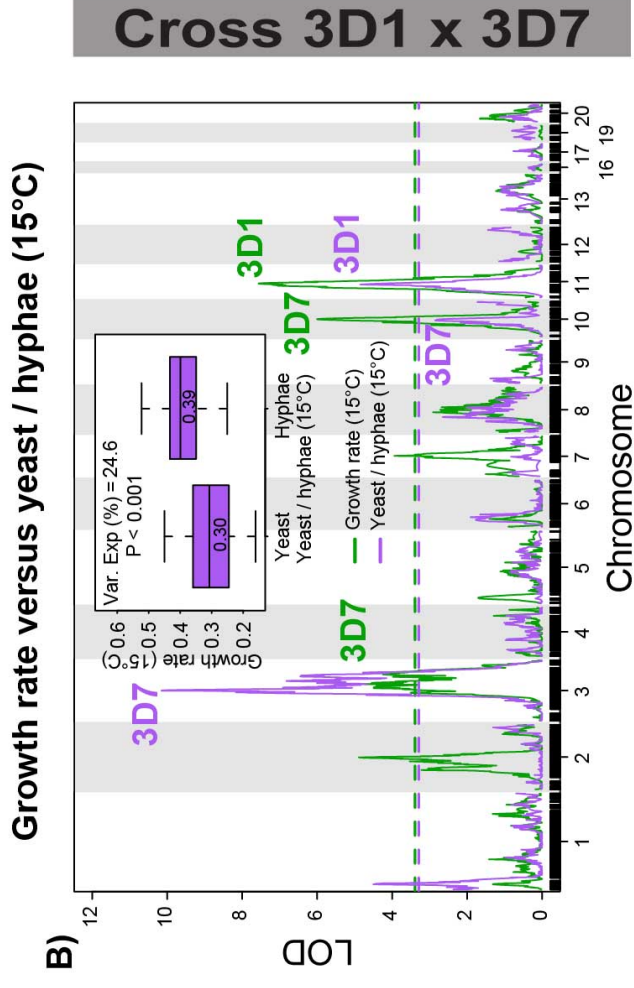
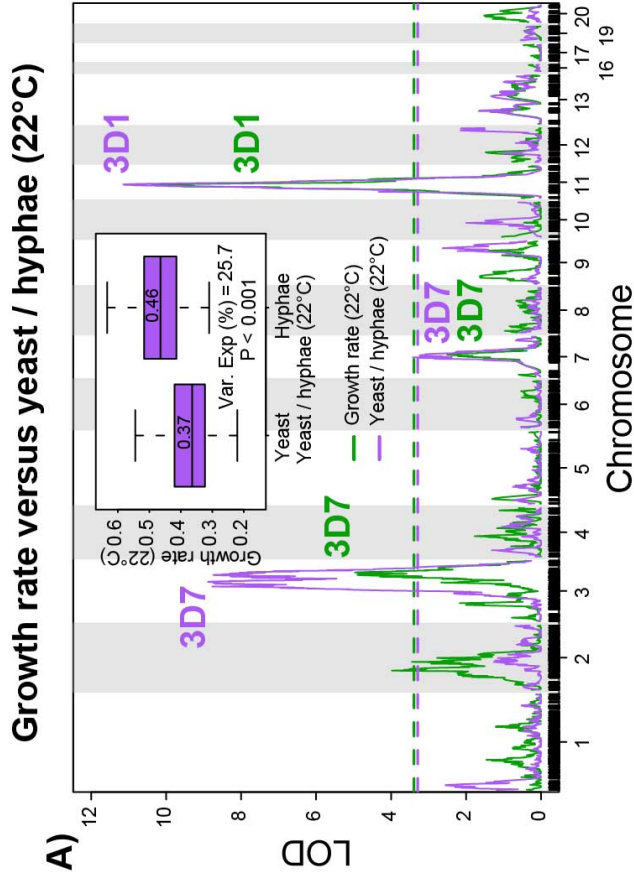


Figure S7 Evidence for pleiotropy amongst the yeast/hyphae dimorphism and growth rate phenotypes for the chromosome 3, 7, 10 and 11 QTLs in cross 3D1 x 3D7 (Panel A = 22°C / Panel B = 15°C). Each panel shows a full genome scan LOD overlap plot based on single marker interval mapping (SIM) analysis, with traits separated by colors (green = growth rate at 15°C/22°C, purple = yeast/hyphae dimorphism trait). Horizontal lines in the LOD plots represent the color-coded significance thresholds ($p = 0.05$) obtained with 1000 genome-wide permutations. Each panel includes a corresponding box plot for the two traits. Mean growth rate values are presented either above or below the median line. The name above each QTL peak indicates which parental allele provided the higher phenotypic mean. Allele effects for non-significant, but visible pleiotropic peaks for either of the phenotypes were obtained by modeling the peaking marker of the significant peak for either of the phenotypes upon the corresponding opposite phenotype. For each pleiotropic peak the allele providing faster growth also contributes to a more hyphal phenotype (Panels A and B).

Growth rate versus yeast / hyphae (22°C)

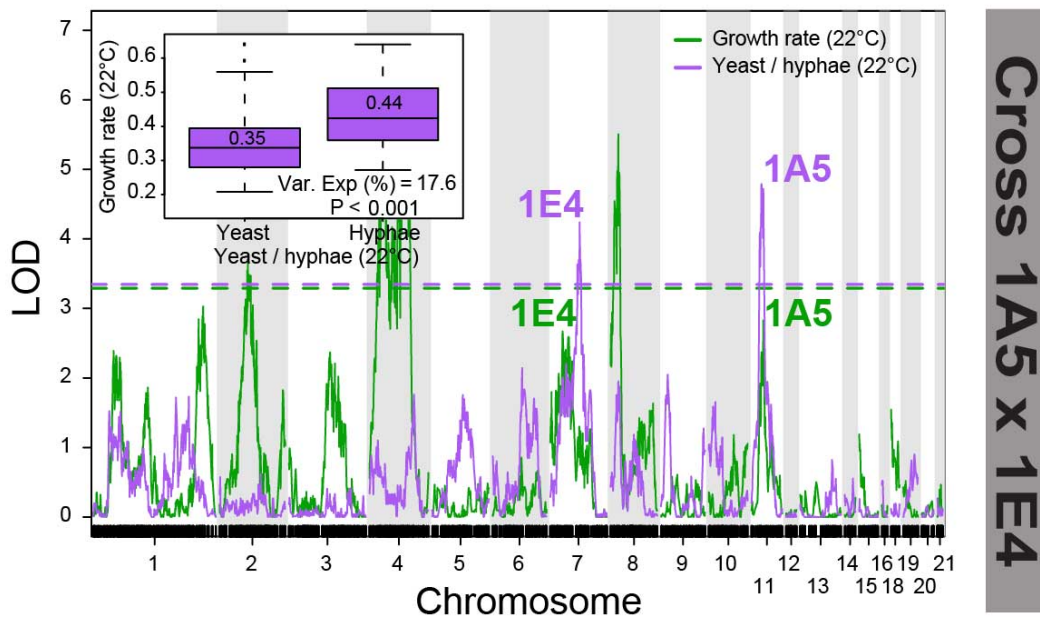


Figure S8 Evidence for pleiotropy amongst the yeast/hyphae dimorphism and growth rate phenotypes at 22°C for the chromosome 7 and 11 QTL in cross 1A5 x 1E4. The figure shows a full genome scan LOD overlap plot based on single marker interval mapping (SIM) analysis, with traits separated by colors (green = growth rate at 15°C/22°C, purple = yeast/hyphae dimorphism trait). Horizontal lines in the LOD plots represent the color-coded significance thresholds ($p = 0.05$) obtained with 1000 genome-wide permutations. In the box plot for the two traits, mean growth rate values are presented either above or below the median line. The name above each QTL peak indicates which parental allele provided the higher phenotypic mean. Allele effects for non-significant, but visible pleiotropic peaks for either of the phenotypes were obtained by modeling the peaking marker of the significant peak for either of the phenotypes upon the corresponding opposite phenotype. For each pleiotropic peak the allele providing faster growth also contributes to a more hyphal phenotype.